Mathematics of Climate Change and Mosquito-borne Disease Dynamics

by

Kamaldeen O. Okuneye

A Dissertation Presented in Partial Fulfillment
of the Requirements for the Degree
Doctor of Philosophy

Approved July 2018 by the
Graduate Supervisory Committee:

Abba B. Gumel, Chair
Yang Kuang,
John Nagy,
Hal Smith,
Horst Thieme.

ARIZONA STATE UNIVERSITY

August 2018

ABSTRACT

The role of climate change, as measured in terms of changes in the climatology of geophysical variables (such as temperature and rainfall), on the global distribution and burden of vector-borne diseases (VBDs) remains a subject of considerable debate. This dissertation attempts to contribute to this debate *via* the use of mathematical (compartmental) modeling and statistical data analysis. In particular, the objective is to find suitable values and/or ranges of the climate variables considered (typically temperature and rainfall) for maximum vector abundance and consequently, maximum transmission intensity of the disease(s) they cause.

Motivated by the fact that understanding the dynamics of disease vector is crucial to understanding the transmission and control of the VBDs they cause, a novel weather-driven deterministic model for the population biology of the mosquito is formulated and rigorously analyzed. Numerical simulations, using relevant weather and entomological data for *Anopheles* mosquito (the vector for malaria), show that maximum mosquito abundance occurs when temperature and rainfall values lie in the range $[20 - 25]^{\circ}$C and $[105 - 115]$ mm, respectively.

The *Anopheles* mosquito ecology model is extended to incorporate human dynamics. The resulting weather-driven malaria transmission model, which includes many of the key aspects of malaria (such as disease transmission by asymptomatically-infectious humans, and enhanced malaria immunity due to repeated exposure), was rigorously analyzed. The model which also incorporates the effect of diurnal temperature range (DTR) on malaria transmission dynamics shows that increasing DTR shifts the peak temperature value for malaria transmission from 29°C (when DTR is 0°C) to about 25°C (when DTR is 15°C).

Finally, the malaria model is adapted and used to study the transmission dynamics of chikungunya, dengue and Zika, three diseases co-circulating in the Americas caused

by the same vector (*Aedes aegypti*). The resulting model, which is fitted using data from Mexico, is used to assess a few hypotheses (such as those associated with the possible impact the newly-released dengue vaccine will have on Zika) and the impact of variability in climate variables on the dynamics of the three diseases. Suitable temperature and rainfall ranges for the maximum transmission intensity of the three diseases are obtained.

ACKNOWLEDGMENTS

Firstly, I would like to express my sincere gratitude to my advisor Professor Abba B. Gumel of the School of Mathematical and Statistical Sciences (SoMSS), Arizona State University (ASU), for the continuous support of my Ph.D study and related research. I am grateful for his comments, motivation, and immense knowledge. His guidance helped me in all the time of research and writing of this thesis. I would also like to thank the rest of my thesis committee members: Professor Yang Kuang, Professor John Nagy, Professor Hal Smith and Professor Horst Thieme, for their insightful comments, suggestions and encouragement. My sincere thanks also goes to Ms. Joelle Park (Graduate Program Coordinator, SoMSS, ASU) for her continued support and kindness.

I am also very grateful to Dr. Ahmed Abdelrazec (former postdoctoral fellow in our group) and Dr. Steffen Eikenberry (SoMSS, ASU) for their support, kindness and collaboration. I am thankful to Professor Jorge Velasco-Hernandez (Matemáticas Aplicadas y Biomatemáticas, UNAM, Mexico) for his support, encouragement and collaboration. In particular, I am grateful for the incidence data he shared for chikungunya, dengue and Zika from Mexico. I wish to extend my gratitude to my fellow doctoral students for their cooperation and of course friendship. My sincere thanks also goes to Mariam Salifu (McGill University, Canada), Mr. AbdulHamid and Mrs. Kudirat Salihs, for always been there for me.

Finally, I am profoundly grateful to my family: my parents (my father, Professor Rafiu O. Okuneye and my mother, Mrs. Kudirat O. Okuneye) and to my brothers and sisters (Taofik, Qasim, Ganiyat, Khadijah, Musediq, Shamsudeen, Azizat, AbdulKareem, Kabeerah, Suad, Sumaya and Rauda) for their invaluable support, love and inspiration throughout the duration of my graduate program.

TABLE OF CONTENTS

CHAPTER Page

CHAPTER Page

CHAPTER Page

List of Tables

Table Page

Table Page

List of Figure

Figure Page

Chapter 1

INTRODUCTION

1.1 Vector-borne Diseases (VBDs)

VBDs are infectious diseases caused by pathogens such as viruses, bacteria or protozoa. They are transmitted to humans by infected (transmitting) biological agents, called vectors. Vectors of human diseases are, in most cases, species of arthropods, such as mosquitoes and ticks that are able to transmit the pathogens. Arthropod-borne viruses (arboviruses) constitute the largest class of vector-borne human pathogens with over 500 arboviruses described, and 20% of which are known to cause human disease (Gray and Banerjee, 1999; Gubler, 1998; Jacobson, 1997; Lemon et al., 2008). VBDs account for about 17% of infectious diseases around the world (and over 50% of the world's population remains at risk of infection with at least one type of vector-borne pathogen) (Gratz, 1999; Lemon et al., 2008).

VBDs can be classified into two categories, namely emerging (newly-emerging) or re-emerging. Emerging (or newly-emerging) diseases are infections that have newly appeared in the population, or have existed but are rapidly increasing in disease incidence or geographic range (Morens et al., 2004; Morse, 2001). Kilbourne (1996) and Morse (2001) states that a disease is recognized as "new" when its symptoms are distinct from any disease that has previously existed and, they are usually caused by preexisting zoonotic agents. Typical examples of such VBDs include human ehrlichiosis, dengue hemorrhagic fever, Zika virus etc (Gratz, 1999; Morens et al., 2004; Morse, 2001). Re-emerging VBDs are diseases that were under control through the use of vector habitat modification and insecticides, but have re-emerged in recent times, and

are spreading (including in geographical areas in which they have not been previously found) (Gratz, 1999). This category of VBDs are the most abundant form of VBDs, some of which are believed to have existed since 16th – 18th century (Gratz, 1999). Example of these VBDs includes malaria, yellow fever, plaque, dengue, chikungunya, Leishmaniasis, Lyme disease, trench fever, etc. Following the re-emergence of these diseases, many, especially malaria and dengue, have spread beyond their previously known geographical range, leading to major global health problems. In terms of human morbidity and mortality, malaria and dengue are the most important of these reemerging VBDs (Gratz et al., 1996; Halstead, 1992; Morse, 2001). However, it is important to note that both newly-emerging and re-emerging VBDs are of public health importance, and require continuous research and development of effective control methods to prevent outbreaks (and eventually eradicate them). In this thesis, major emphasis will be on mosquito-borne VBDs as they account for over 80% of all VBDs (WHO, 2015, 2016).

1.2 Mosquito and Mosquito-borne Diseases (MBDs)

Mosquitoes are small biting insects that constitute of the family *Culicidae*. There are about 3,500 mosquito species in the world (grouped into 41 *genera*) (CDC; Harbach, 2013). Mosquito species, such as *Anopheles*, *Aedes aegypti*, *Aedes albopictus* and *Culex*, play significant roles as vectors of some major infectious diseases of humans, such as malaria, yellow fever, chikungunya, West Nile virus, dengue fever, Zika virus and other arboviruses. These diseases are responsible for several million deaths and hundreds of millions of cases annually (Miller et al., 1994; Schofield and Grau, 2005; WHO, 1994, 2009, 2015, 2016). These diseases are transmitted from human-to-human *via* an effective bite from an infected adult female mosquito.

1.2.1 Life-Cycle of the Mosquito

The life-cycle of the mosquito is completed *via* four distinct stages, namely: eggs, larva, pupa and adult stages, with the first three largely aquatic. A female mosquito can lay about 100–300 eggs *per* oviposition, and this process is temperature dependent (Mordecai et al., 2013; Paaijmans et al., 2007; Parham and Michael, 2010; Parham et al., 2012). The eggs are laid at a convenient breeding site, usually a swamp or humid area in the aquatic environment (the *Anopheles species* typically lays their eggs on the surface of the water) and after about 2 – 3 days, they hatch into larva. Larvae develop through four *instar* stages (CDC). At the end of each larval stage, the larvae molt, shedding their skins to allow for further growth (the larvae feed on microorganisms and organic matter in the water). During the fourth molt, the larvae mature into pupae (the whole process of maturation from larvae to pupae takes 4–10 days). The pupae then develop into adult mosquitoes in about 2–4 days.

The duration of the entire life-cycle of the mosquito, from egg laying to the emergence of an adult mosquito, varies between 7 and 20 days, depending on the ambient temperature of the breeding site (typically a swamp or humid area) and the mosquito species involved (for instance, *Culex tarsalis*, a common mosquito in California (USA), might go through its life cycle in 14 days at 70°F and take only 10 days at 80°F) (Ngwa, 2006). Adult mosquitoes usually mate within a few days after emerging from the pupal stage, after which they go questing for bloodmeal (required to produce eggs) (Harbach, 2013). While adult male mosquitoes feed on plant liquids such as nectar, honeydew, fruit juices and other sources of sugar for energy, female mosquitoes, in addition to feeding on sugar sources (for energy), feed on the blood of human and other animals solely to acquire the proteins needed for eggs development (Harbach, 2013). Once a bloodmeal is taken, the female mosquito moves to a

convenient breeding site where it lays its eggs. The chances of survival of the female adult mosquitoes depend on temperature and humidity, as well as their ability to successfully obtain a bloodmeal while avoiding host defenses (Mordecai et al., 2013; Paaijmans et al., 2007; Parham and Michael, 2010; Parham et al., 2012).

1.2.2 Mosquito Gonotrophic Cycle

At the adult stage, after initially emerging from the pupal stage and mating, the female mosquito lifecycle is then defined by the gonotrophic cycle (Greek "offspring feeding"), whereby the fertilized female mosquito takes mammalian bloodmeals to nourish egg development and then deposits them on the surface of appropriate waters, and classically divided into three stages (Detinova et al., 1962):

1. Stage I: Search for suitable host and the taking of a bloodmeal.
2. Stage II: Digestion of bloodmeal and egg maturation (this process is highly temperature dependent).
3. Stage III: Search for and oviposition into a suitable body of water.

Like in the case of the development of immature mosquitoes, the rate at which stage II (egg development) progresses depends on ambient (air) temperature, increasing up to around 30 °C, leveling off, and possibly sharply declining at very high temperature (Lardeux et al., 2008). Mosquito survival likewise peaks in the mid–20s (°C), and is impaired at both low and high temperatures (Lardeux et al., 2008).

The lifecycle of the *Anopheles* mosquito lifecycle is depicted in Figure 1.1.

1.3 Transmission and Global Distribution of MBDs

The major factors leading to the emergence and abundance of new MBDs and the re-emergence of previously endemic MBDs (and, in addition, the distribution of the

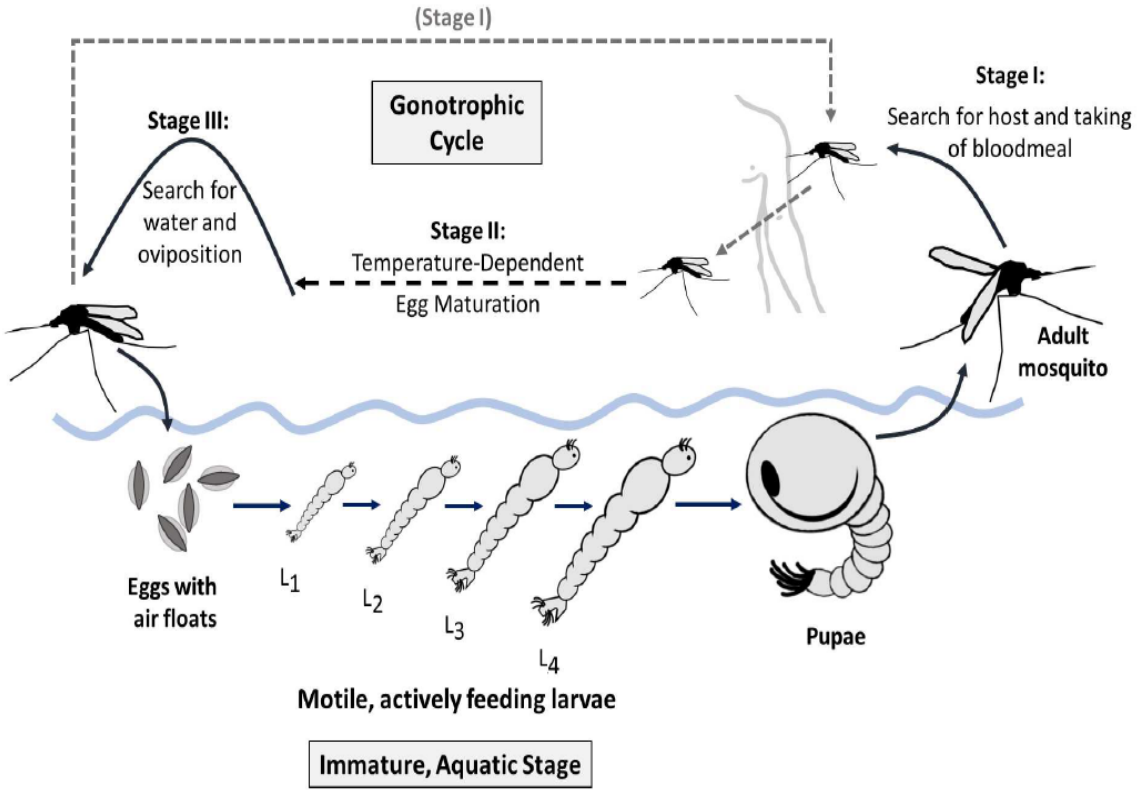

Figure 1.1: *Anopheles* mosquito lifecycle. Immature mosquitoes pass through aquatic egg, larvae, and pupae stages, with the actively feeding larvae divided into four instar stages. Adult female mosquitoes pass through the gonotrophic cycle, by which bloodmeals nourish the development of new eggs.

corresponding transmitting mosquitoes) worldwide are associated with ecological, demographic and societal changes that have led to increased vector population densities (Gratz, 1999; Gratz et al., 1996; Gubler, 1998; Morens et al., 2004). These factors include constructions of dams and irrigation systems, deforestation, change in landscape and agricultural practices, global shipping transport and most especially, increased human travel globally, leading to possible introduction of infectious humans into areas where the specific disease (they carry) have not been recorded (however, "if the area into which an infection is introduced has no suitable vectors, then the introduc-

tion remains a medical problem only for the individual patient and physician (Gratz, 1999)").

Furthermore, climate change has played a significant role in the increased population and survival of vectors of MBDs. Several studies such as those by Beck-Johnson et al. (2013, 2017); Caminade et al. (2014); Christiansen-Jucht et al. (2015); Gething et al. (2010); Hay et al. (2002); Imbahale et al. (2011); Lafferty and Mordecai (2016); Mordecai et al. (2013); Negev et al. (2015); Ogden and Lindsay (2016); Paaijmans et al. (2007); Parham and Michael (2010); Parham et al. (2012) and Watson et al. (1996), have shown that the ecology of vectors of MBDs (and pathogen of the diseases) tends to adjust continually to environmental changes in multifaceted ways. In this section, the two most important re-emerging MBDs (namely, malaria and dengue), and two emerging MBDs (Zika and chikungunya virus), will be briefly discussed.

1.3.1 Malaria

Malaria is transmitted to humans by the bite of female *Anopheles* mosquitoes that are infected with the protozoan parasites of the genus *Plasmodium* (Mordecai et al., 2013; Parham et al., 2012). Despite the existence of effective preventative measures and treatment, malaria remains, possibly, the most serious infectious disease of humans, as it is endemic in over 100 countries, with about 40% of the world's population at risk, causing up to 300-600 million cases and over 500,000 deaths annually (Miller et al., 1994; Schofield and Grau, 2005; WHO, 2016). Further, over 90% of malaria-induced morbidity and mortality are heavily concentrated in resource-poor areas of sub-Saharan Africa (especially among pregnant woemn and children under the age of five) (WHO, 2015, 2016) (Figure 1.2).

There are five *Plasmodium* species that infect humans, namely, *P. falciparum*, *P. vivax*, *P. ovale*, *P. malariae*, and *P. knowlesi* (Schofield and Grau, 2005; Smith

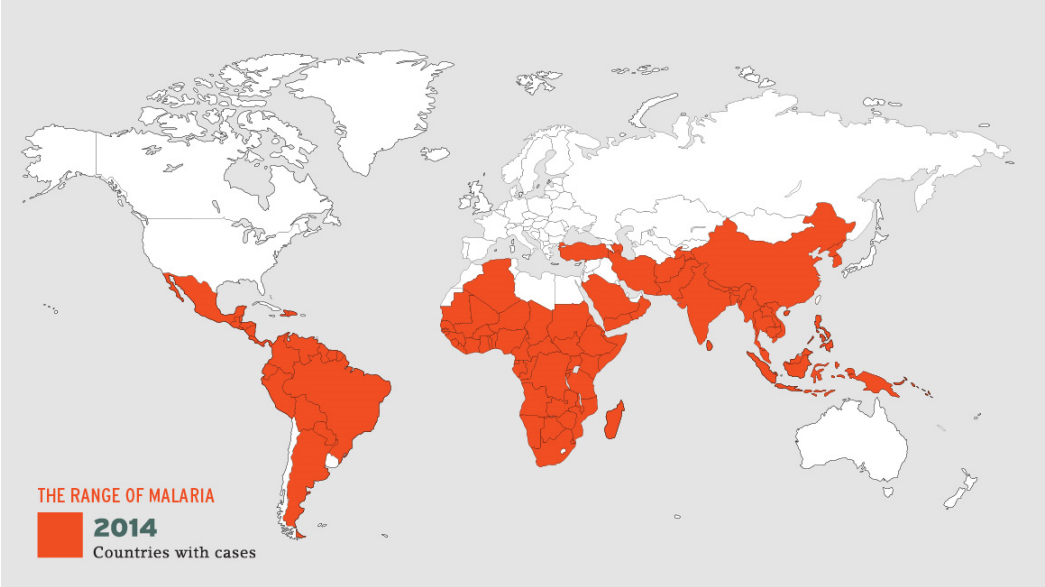

Figure 1.2: Worldwide distribution of malaria in 2014. Source: American Museum of Natural History. Website: https://www.amnh.org/explore/science-topics/disease-and-eradication/countdown-to-zero/malaria.

et al., 2000). Of these specie types, *P. falciparum* is the major cause of morbidity and mortality in sub-Saharan Africa and throughout most of the tropical regions (Schofield and Grau, 2005; Smith et al., 2000), while on the other hand, *P. ovale* also concentrated in sub-Saharan Africa and in some islands in the western Pacific (Collins and Jeffery, 2005; Faye et al., 1998), is rare and relatively less dangerous than *P. falciparum*. Malaria infections causes by *P. vivax* is also a common cause of acute febrile illness and can also lead to severe disease and death Anstey et al. (2012); Baird (2007); Schofield and Grau (2005). Although, less fatal than *P. falciparum*, *P. vivax* is predominant in Asia and South America, where it accounts for about 65% of all malaria cases (it is also found in some regions of Africa) (Anstey et al., 2012; Baird, 2007; Lindsay and Hutchinson, 2006; Schofield and Grau, 2005; Vogel, 2013; WHO, 2015, 2016). Malaria caused by *P. malariae*, is not as dangerous as that produced by

P. falciparum or *P. vivax* and is found most commonly in malaria endemic regions sub-Saharan Africa and southeast Asia Schofield and Grau (2005); Westling et al. (1997); White (2008). Discovered by Knowles and Gupta (1932) after successfully transmitting a monkey malaria parasite to humans, *P. knowles* was referred to as "The Fifth Human Malaria Parasite" by White (2008). *P. knowlesi* infection has been found in Malaysia (particularly on the island of Borneo) and some regions of Southern Asia (Schofield and Grau, 2005; White, 2008).

Mosquito Sprogonic Cycle

Plasmodium parasites are complex pathogens capable of completing a life-cycle both inside the female *Anopheles* mosquito and the human host (Coleman et al., 2007; Cowman et al., 2016; Whitten et al., 2006). *Plasmodium* sporozoites are injected into the host *dermis* during a blood feed by an infected mosquito. Once the sporozoites enter the host, they infect hepatocytes (the liver cells), and this is followed by the asexual cycle in the blood (Coleman et al., 2007; Cowman et al., 2016; Whitten et al., 2006) (Figures 1.3).

Sexual forms that develop during the blood stage are ingested by a feeding (susceptible) mosquito (during stage I of the gonotrophic cycle), this initiates the *sporogonic* (or extrinsic) cycle, by which the gametocytes emerge as extracellular male and female gametes in the mosquito's midgut. Mating occurs by fusion of micro (male) and macro (female) to form a zygote which then transform into a ookinete that migrates through the mosquito midgut epithelium and encysts to become an oocyst where asexual sporogenic replication occurs (Cowman et al., 2016; Whitten et al., 2006). "Motile sporozoites are released into the hemocoel by oocyst rupture and pass into salivary glands where they can be injected into the next human host through feeding on bloodmeal" (Cowman et al., 2016) (Figures 1.3 and 1.4). It is important to

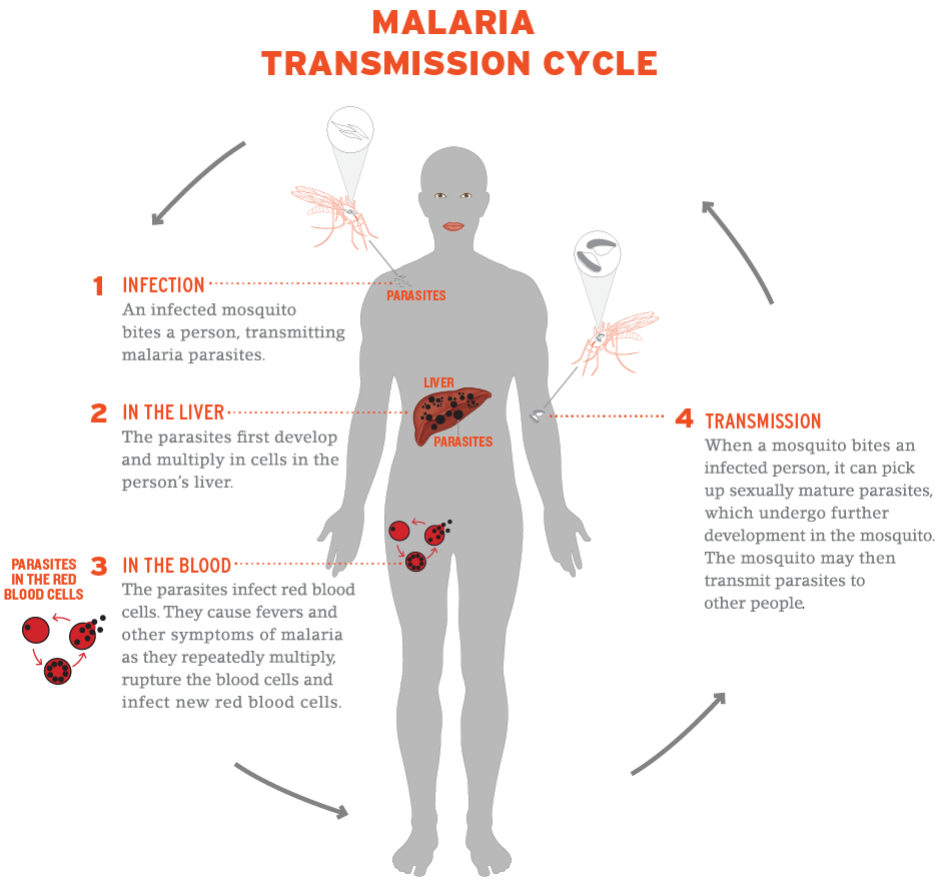

Figure 1.3: Malaria transmission cycle. Source: American Museum of Natural History.

note that, as with other developmental processes, the sporogonic cycle also generally progresses more rapidly at higher temperatures (Detinova et al., 1962).

Malaria incubation period in an individual varies by the infecting species, immune status of patient and number of parasites transmitted (Detinova et al., 1962; Schofield and Grau, 2005). Moreover, for patients infected with *P. falciparum* and *P. vivax*, the incubation period takes about 7–30 days, unlike infection with *P. malariae* which may take several months to show symptoms (Schofield and Grau, 2005). Symptoms of malaria include fever, headache, chills and vomiting, and if left untreated, *P.*

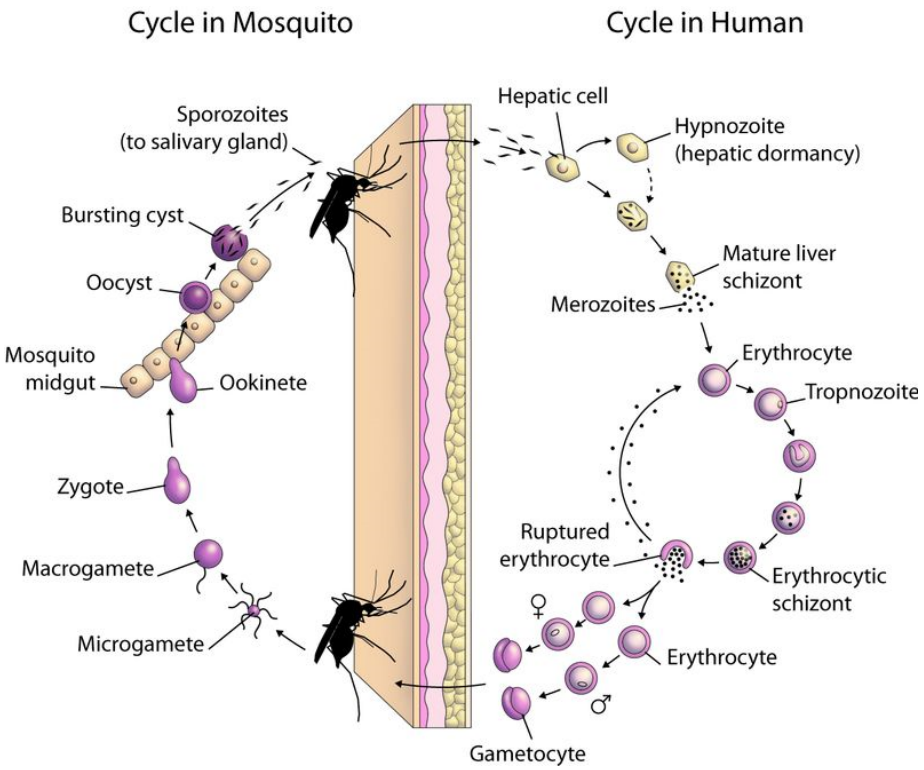

Figure 1.4: Life cycle of the *Plasmodium* parasite. Obtained from Epidemiology of Infectious Diseases, Johns Hopkins Bloomberg School of Public Health. Creative Commons BY-NC-SA. Website: http://ocw.jhsph.edu.

falciparum malaria can progress to severe illness and death (WHO, 2015, 2016). In areas of high malaria transmission, and in non-immune individuals (usually children under the age of five), infections are more clinically overt (asymptomatic), and can become severe or life threatening usually in the form of metabolic acidosis (which leads to respiratory distress), cerebral malaria and severe malarial anaemia (Schofield and Grau, 2005). Moreover, adaptive immune responses in the human (acquired after recovery from malaria) provide partial, but incomplete, protection against pathogen replication and limit the clinical impact of infection (Miller et al., 1994; Schofield and Grau, 2005).

Control Strategies Against Malaria: Global Efforts

Concerted global efforts were embarked upon by numerous public health agencies globally to combat the threat of VBDs (WHO, 2009, 2016) In 1955, the Global Malaria Eradication Programme (GMEP) was launched by World Health Organization (WHO) with the primary objective of eradicating malaria worldwide, by providing drugs (chloroquine; for prevention and treatment of malaria) and DDT chemical (for mosquito control). The success of the GMEP program saw a dramatic decline in incidence of malaria in endemic countries such as in India (from an estimated 110 million in 1955 to less than 1 million in 1968) and Sri Lanka (from an estimated 2.8 million cases in 1946 to a reported 18 cases in 1966). Between 1955 and 2015, 27 countries have been certified as malaria-free countries by the WHO (that is, the countries that reported zero indigenous cases of malaria) (WHO, 2016). Furthermore, in 1998, WHO, the World Bank, the United Nations Development Programme (UNDP) and the United Nations Children's Fund (UNICEF) created the Roll Back Malaria initiative with the aimed of reducing malaria mortality on the African continent by 50% by the year 2010. However, malaria transmission still remain largely uncontrolled (or poorly controlled) in Africa and other parts of Asia and Latin America, and until recently, malaria has resurfaced in some countries where a high level of control had been achieved (Gratz, 1999; WHO, 2016).

1.3.2 Dengue Fever

Dengue fever (DF) is caused by a virus (Dengue virus: DENV) of the *Flavivirus* genus, *Flaviviridae* family and it is transmitted to humans through bites of infected female adult *Aedes* mosquitoes. It is one of the most prevalent VBDs, affecting about 50–100 million people annually (and causing over 22,000 deaths), especially among children

under the age of 15, and it remains endemic in over 100 countries (and approximately 2.5 billion people live in dengue endemic countries) (Gubler, 1998; Packard, 2016; Rigau-Pérez et al., 1998; Simmons et al., 2012; Undurraga et al., 2017; WHO, 2009). DF is an acute illness when left untreated and can lead to severe case of dengue called

Figure 1.5: Countries and areas at risk of dengue transmission. Source: WHO (2009).

the dengue haemorrhagic fever (DHF) or dengue shock syndrome (DSS), which are more common after a secondary infection with dengue virus (Gibbons and Vaughn, 2002; Rigau-Pérez et al., 1998). DF and DHF/DSS were attributed to the "*break-bone*" fever in Philadelphia, 1780 (Gubler, 1998; Packard, 2016), due to its severe symptoms, which includes, headache, muscle pain, marked muscle, rash and joint pains plasma leakage resulting in shock, accumulation of serosal fluid sufficient to cause respiratory distress (or both), severe bleeding and organ impairment, and, in some cases, death (Gubler, 1998; Kalayanarooj et al., 1997; Simmons et al., 2012). DHF and DSS are the leading cause of hospital admission and death among children in Asia (Gubler, 1989; Rigau-Pérez et al., 1998; WHO, 2009).

DF and DHF/DSS can be caused by any of four viral serotypes, namely, DENV-1, DENV-2, DENV-3, DENV-4, which are closely related antigenically (Edelman, 2005; Gibbons and Vaughn, 2002; Gubler, 1998; Undurraga et al., 2017; WHO, 2009), with all four predominantly present in tropical and sub-tropical regions of Asia and Africa (where the *Aedes* mosquitoes are widely distributed). Infection with one serotype enhance long-term protective immunity to reinfection with the serotype but the individual remains susceptible (or gain only a short-term immunity) to all other serotypes (Edelman, 2005; Gibbons and Vaughn, 2002; Gubler, 1998; Innis, 1995; Sabin, 1952; WHO, 2009). In addition, an important characteristic of DF and DHF/DSS is its properties of antibody-dependent enhancement (ADE), whereby dengue infection becomes more severe in individual who have acquired dengue antibodies after recovering from a previous dengue infection (Edelman, 2005; Halstead, 1988; Kliks et al., 1989; Sullivan, 2001).

Dengue-related epidemics were first reported in the medical literature in 1779 and 1780 Rigau-Pérez et al. (1998). Moreover, the co-circulation of multiple dengue virus serotypes and increased epidemic activities was recorded in South-east Asia during World war II, which emerged as a major public-health problem in most countries of South-east Asia due to uncontrolled growth of cities. Specifically, the first epidemic of DHF occured in Manila, Philippines in 1953 and the disease remained localized in South-east Asia through the 1970s (Gubler, 1989, 1998; Rigau-Pérez et al., 1998). However, by 1997, with the introduction of new virus strains and serotypes, DF and DHF/DSS epidemics had spread into several other countries including India, Pakistan and Sri Lanka and this is largely as a result of immigration, population growth, unplanned and uncontrolled urbanization, increased air travel, the lack of effective mosquito control and adequate public-health infrastructure (Gubler, 1998; Rigau-Pérez et al., 1998) (Figure 1.5).

Control Strategies Against Dengue Disease

Current efforts to reduce dengue transmission is focused on the vector control, especially using combinations of chemical and biological targeting of *Aedes* mosquitoes and management of breeding sites. In addition, control effort have also been emphasized on public-health programs that promotes and encourages communal understanding of the vector specie and the disease, to enhance community vector control and practice of personal protection (Gubler, 1989; Gubler and Clark, 1994; Rosenbaum et al., 1995; WHO, 1994; Winch et al., 1992). However, these substantial vector control efforts have not stopped the rapid emergence and global spread of DENV. Recently, a new vaccine for DENV (*Dengvaxia*® (CYD-TDV), by Sanofi Pasteur) has been released in 2015 (and has been approved in 11 countries in 2016) (Vannice et al., 2016).

The efficacy of the tetravalent *Dengvaxia* vaccine varies by serotypes (71.6% for serotype 3; 76.9% for serotype 4; 54.7% for serotype 1 and 43.0% for serotype 2) 256. However, the ADE property of the DENV plays an important factor for the development of dengue vaccine as "ADE suggest that dengue vaccines must induce protective neutralizing antibodies to all 4 serotypes simultaneously, rather than sequentially, to avoid enhancement of dengue illness after subsequent infection" (Edelman, 2005). As a result, the manufacturer (Sanofi) issued a press release in 2017 stating that "for individuals who have not been previously infected by dengue virus, vaccination should not be recommended" (Halstead, 2018).

1.3.3 Zika virus

Similar to DENV, Zika virus (ZIKV) is a member of the family *Flaviviridae*, and genus *Flavivirus* (ZIKV has a closer phylogenetical relation to dengue than to any other *flavivirus* (Cao-Lormeau et al., 2016)). It is transmitted to humans by an infected

female adult *Aedes* mosquitoes. ZIKV was first detected in 1947 in the Zika region of Uganda (Dick et al., 1952). It later spread to Senegal (West Africa) in 1991 and to the South Pacific around 1960 (Duffy et al., 2009; Macnamara, 1954; Yakob and Walker, 2016). It is known that from 1951–1991, ZIKV-reported activity was rather sporadic (Kindhauser et al., 2016). However, ZIKV epidemic episodes appeared in Micronesia, the French Polinesia, with outbreaks occurring in the Yap Islands (2007), where, although no hospitalizations, hemorrhagic manifestations, or deaths due to Zika virus were reported, 73% of Yap residents (3 years of age or older) were estimated to have been infected with Zika virus (Cao-Lormeau et al., 2016; Duffy et al., 2009; Kindhauser et al., 2016; Oehler et al., 2014). ZIKV has also been reported in Easter Island, New Caledonia and Cook Islands in 2014 (Kindhauser et al., 2016). In 2014, the virus appeared in Brazil, mainly as a result of human migration from the French Polinesia (Corsica, 2015; Duffy et al., 2009; Musso et al., 2014; Pyke et al., 2014). The Pan American Health Organization (PAHO) reports, as of May 12, 2016, about 272 cases in Mexico, 711 cases in Central America, 1,742 cases in Latin Caribbean states, 4,195 in Andean states, 1034 cases in Brazil and 709 cases in non Latin Caribbean states [177].

Countries with past and current ZIKV transmission with locally-acquired cases comprise largely of geographical areas of the Americas, Central and West Africa and Southeast Asia, including many archipielagos of the South Pacific (Fauci and Morens, 2016). Fauci and Morens (2016) reported that ZIKV was originally a zoonotic disease in Central Africa, with a tendency to follow *Aedes*-transmitted chikungunya epizootics and epidemics. This has been the case in the Americas recently, where outbreaks of chikungunya were reported in 2015 followed ZIKV outbreaks in 2016 (Cohen, 2016). There are concerns that ZIKV may adapt to *Aedes albopictus* in the American continent Fauci and Morens (2016), a mosquito species with wide distri-

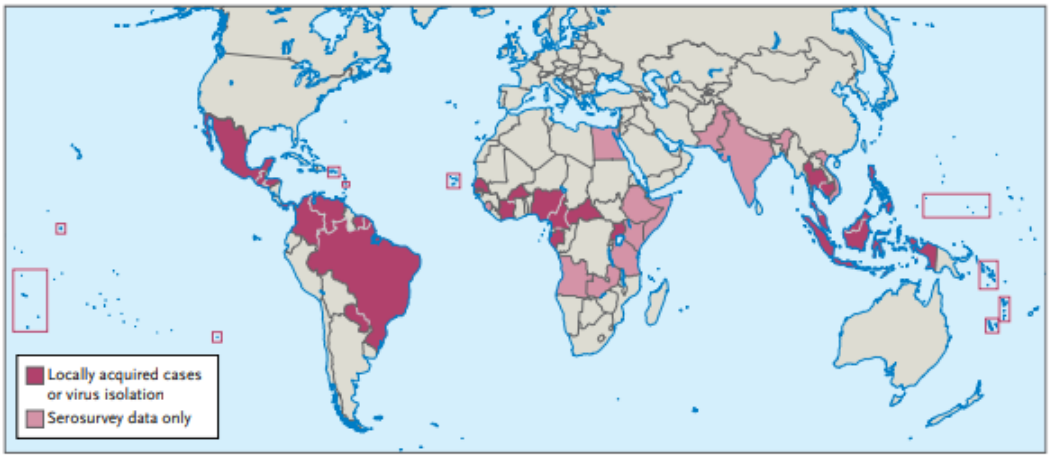

Figure 1.6: Countries with Past or Current Evidence of Zika Virus Transmission (as of December 2015). Source: Fauci and Morens (2016).

bution in the United States. This poses an important threat for ZIKV epidemics in the United States. Consequently, the CDC has taken preventive measures CDC (2016). It is known that the primary mode of ZIKV transmission between humans is through the bite of female *Aedes aegypti* mosquitoes, although other non-vector means of transmission (such as *via* sexual intercourse, blood transfusion, perinatal transmission from mother to foetus) may exist (Besnard et al., 2014; Foy et al., 2011; Petersen, 2016). It is further known that ZIKV has been isolated from semen from 90 to 188 days after symptoms onset (Petersen, 2016). Transmission from women-to-men (sexually) has also been reported to date [45].

Although, Zika and other arboviral infections like dengue or chikungunya are clinically different, the symptoms of ZIKV infection is often mistaken with these diseases (Cao-Lormeau et al., 2016; Oehler et al., 2014). These symptoms include, arthralgia (i.e., pains in small joints of hands and feet), with possible swollen joints, myalgia, retro ocular headaches, conjunctivitis, and cutaneous maculopapular rash, digestive troubles (abdominal pain, diarrhoea, constipation) (Duffy et al., 2009; Heang et al.,

2012; Oehler et al., 2014; Simpson, 1964). Severe cases, such as neurologic complications, have also been recorded in patients (Oehler et al., 2014; Simpson, 1964). Currently, there is no specific vaccine for the preventive treatment of ZIKV infection (Rather et al., 2017; Singh et al., 2018). The current strategies to prevent ZIKV infection include the use of biological or chemical control measures for vector population, as well as use of drugs and personal protection. Moreover, the possibility of other modes of transmission need to be checked and kept under control, especially, by adopting appropriate precautions during sexual intercourse, blood transfusion and organ transplantation. Several ongoing research is currently focused on the development of the ZIKV vaccine (Rather et al., 2017; Singh et al., 2018).

1.3.4 Chikungunya

Chikungunya virus (CHIKV), an emerging arbovirus associated with several recent large-scale epidemics (Tsetsarkin et al., 2007), is transmitted to humans through the bite of an infectious adult female *Aedes* mosquito (the same mosquitoes that transmit DENV and ZIKV) (Jeandel et al., 2004; Powers and Logue, 2007; Tsetsarkin et al., 2007). Moreover, the CHIKV is in the family *Alphavirus* in the family *Togaviridae* (serologically, CHIKV is most closely related to O'nyong-nyong virus) (Pialoux et al., 2007; Powers and Logue, 2007). CHIKV was first isolated in Tanzania in 1953 (Pialoux et al., 2007; Powers and Logue, 2007; Robinson, 1955; Ross, 1956). Initially diagnosed as DENV, serological and antigenic characterization of the isolates indicated that it was an *alphavirus* (and not a *flavivirus*) (Casals and Whitman, 1965; Spence and Thomas, 1959).

Between the 1960s and 1990s, possibly due to increased rate of infected travelers, CHIKV had spread or was isolated repeatedly from several countries in Central and Southern Africa including Sudan, Uganda, Democratic Republic of Congo, the Central

African Republic, Malawi, Zimbabwe, Kenya and South Africa (Pialoux et al., 2007; Powers and Logue, 2007). CHIKV occurs in western African countries including Senegal, Benin, the Republic of Guinea, Cote d'Ivoire and Nigeria (Diallo et al., 1999; Fagbami, 1977; Kuniholm et al., 2006; Moore et al., 1974; Muyembe-Tamfum et al., 2003; Pialoux et al., 2007; Powers and Logue, 2007). CHIKV outbreaks was also reported in other countries such as Burma, Thailand, Cambodia, Vietnam, India, Sri Lanka, and the Philippines (Ligon, 2006; Mackenzie et al., 2001; Pialoux et al., 2007).

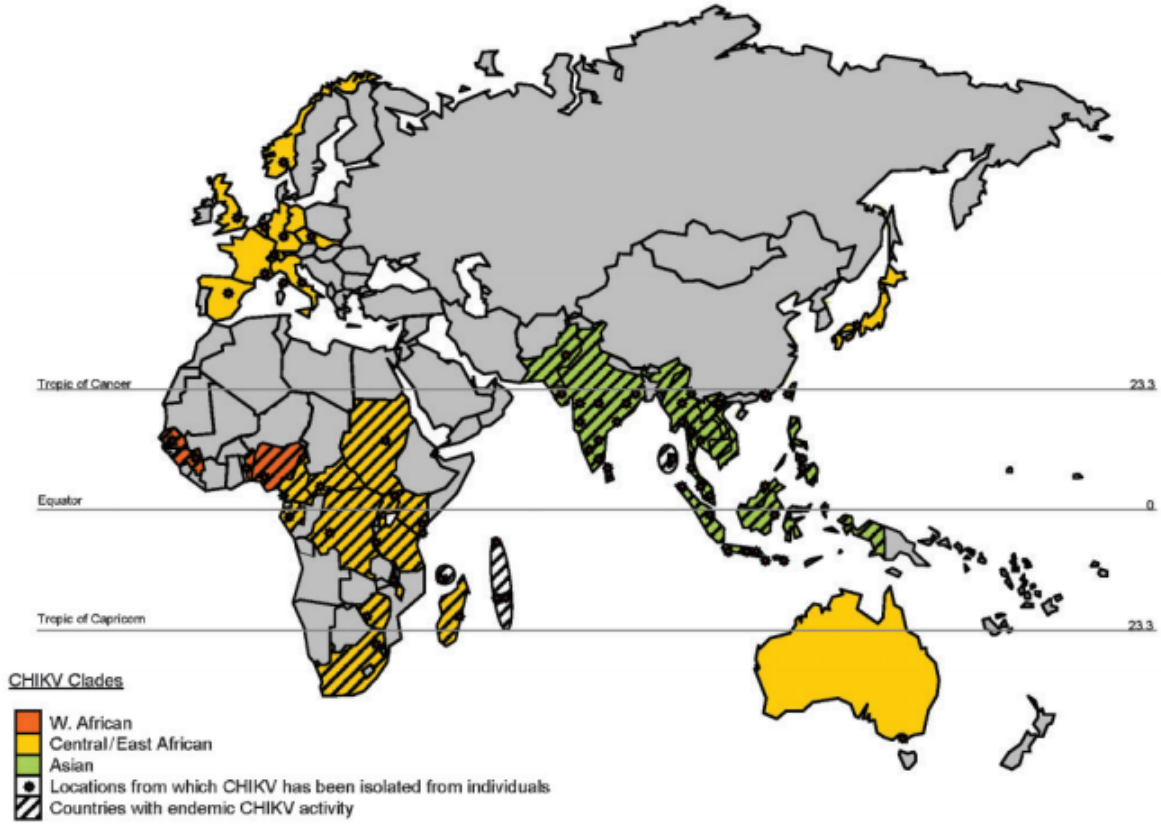

Figure 1.7: Worldwide distribution of Chikungunya virus. Source: Powers and Logue (2007).

The primary transmitting vector of CHIKV is the *Aedes aegypti* mosquito, which

is responsible for about 1.4 million reported CHIKV cases in India in 2006 (Jeandel et al., 2004; Pialoux et al., 2007; Powers and Logue, 2007; Ravi, 2006; Saxena et al., 2006; Yergolkar et al., 2006). However, CHIKV epidemic reported on Réunion island in 2005–2006 where there were approximately 266,000 cases (about 34% of the total island population), was reported to be transmitted by *Aedes albopictus*, ("the Asian tiger mosquito": a mosquito species endemic to Réunion and other islands in the Indian ocean) (Charrel et al., 2007; Enserink, 2006; Pialoux et al., 2007; Powers and Logue, 2007; Zeller, 1998). The word "chikungunya" originated from Tanzania (from

(a) *Aedes aegypti*.

(b) *Aedes albopictus*.

Figure 1.8: *Aedes aegypti* is predominant in India and it is responsible for over 1.4 million CHIKV reported cases in India, 2006, while *Aedes albopictus* is predominant on Réunion island and it is responsible for approximately 266,000 CHIKV cases. Source: Public Health Image Library.

the Makonde language), and means "that which bends up" (Charrel et al., 2007). This meaning is attributed to the major symptoms/features of both the acute and chronic phases CHIKV infections, which include intense pain caused by pressure on peripheral small joints, usually, in the ankles, wrists and phalanges (CHIKV has also been reported to affect large joints) Pialoux et al. (2007); Robinson (1955); Saxena et al. (2006). Other symptoms may include headache, muscle pain, joint swelling, or rash

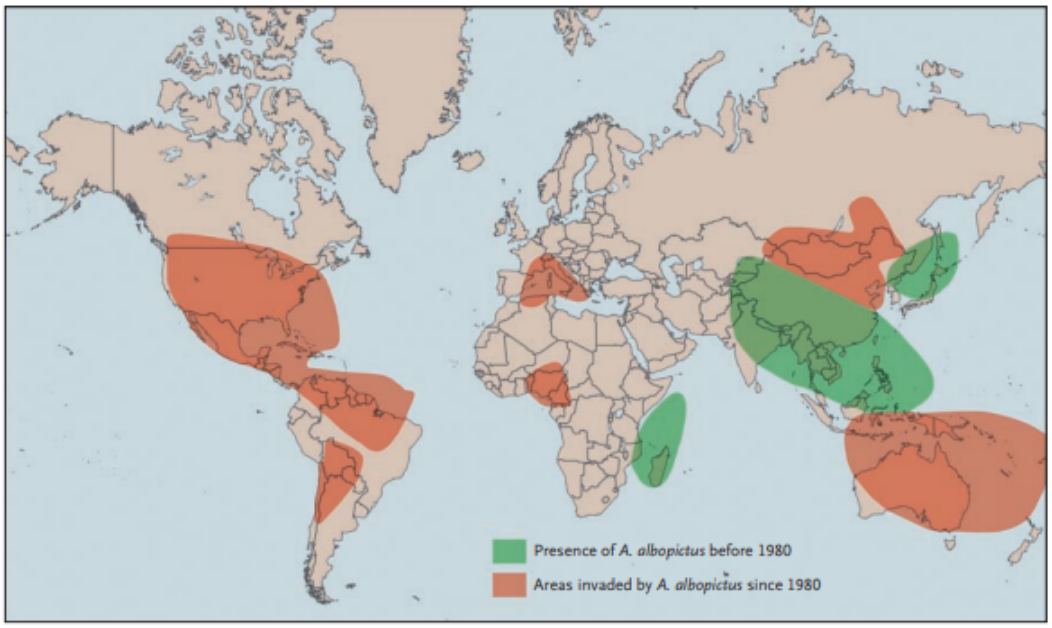

Figure 1.9: World Distribution of the *Aedes albopictus* Mosquito. Source: Charrel et al. (2007).

(Charrel et al., 2007; Pialoux et al., 2007; Powers and Logue, 2007). Non-vector CHIV transmission, especially, peripartum mother-to-infant CHKV transmission, have also been reported Charrel et al. (2007). Although CHIKV rarely affects children, people at risk include newborns (less than 3 months old), older adults ($\geq$50 years, with the highest rates observed in the 51–55 year age-group), pregnant women and people with medical conditions such as high blood pressure, diabetes, or heart disease (Pialoux et al., 2007; Ravi, 2006). Incubation period is about 2–12 days and, within 2 to 5 days of infection, conjunctivitis and a rash are common while arthralgias (joints pain) can persist for weeks to months (Pialoux et al., 2007; Powers and Logue, 2007; Ravi, 2006). There is currently no commercial vaccine for CHIKV, and the most common (and best) control strategies for CHIKV includes individual protection against mosquito bites and vector control (usually following the same model as for dengue) (Pialoux

et al., 2007).

1.4 Climate Change

The Earth's climate is rapidly changing, mainly as a result of increases in greenhouse gases (especially carbon dioxide (CO_2) and methane) caused by human (anthropogenic) activities (mostly in the developed countries), predominantly as a result of burning fossil fuels through industrialization, deforestation, and other changes in land-use (Boden; Siegenthaler et al., 2005; Stern, 2006) (Figures 1.10 and 1.11). The

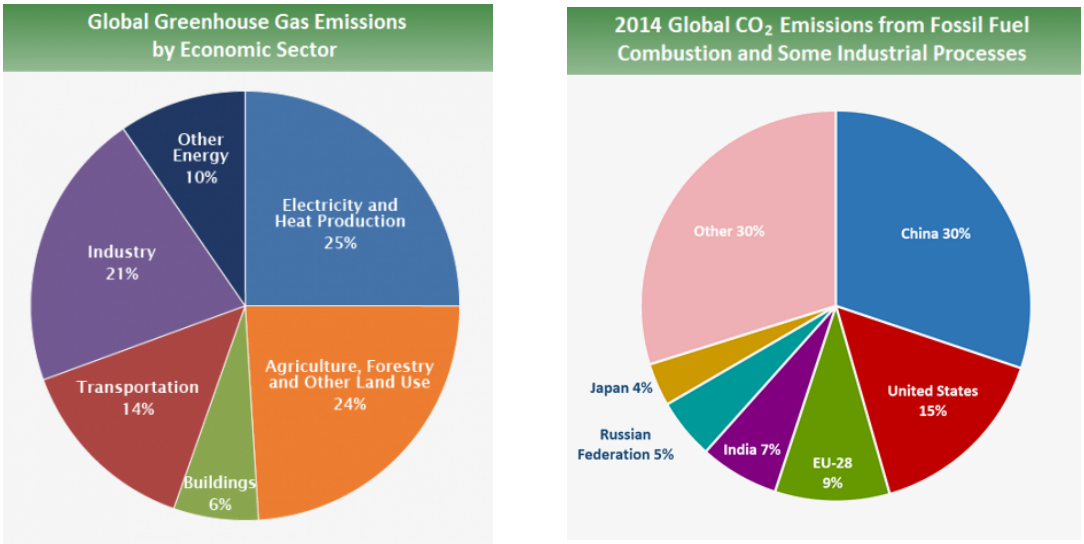

(a) Emission by economic sectors.

(b) Emission by countries.

Figure 1.10: Greenhouse gas emissions by sector and by country. Source: United States Environmental Protection Agency.

evidence that the rising levels of greenhouse gases will have an effect on the climate variabilities (such as temperature, rainfall, etc.) is "the greenhouse effect" phenomenon which is the increased amount of infrared radiation (heat energy) trapped by the atmosphere (Siegenthaler et al., 2005; Stern, 2006). The signs and effects of climate changes can be seen in many physical and biological systems. For instance,

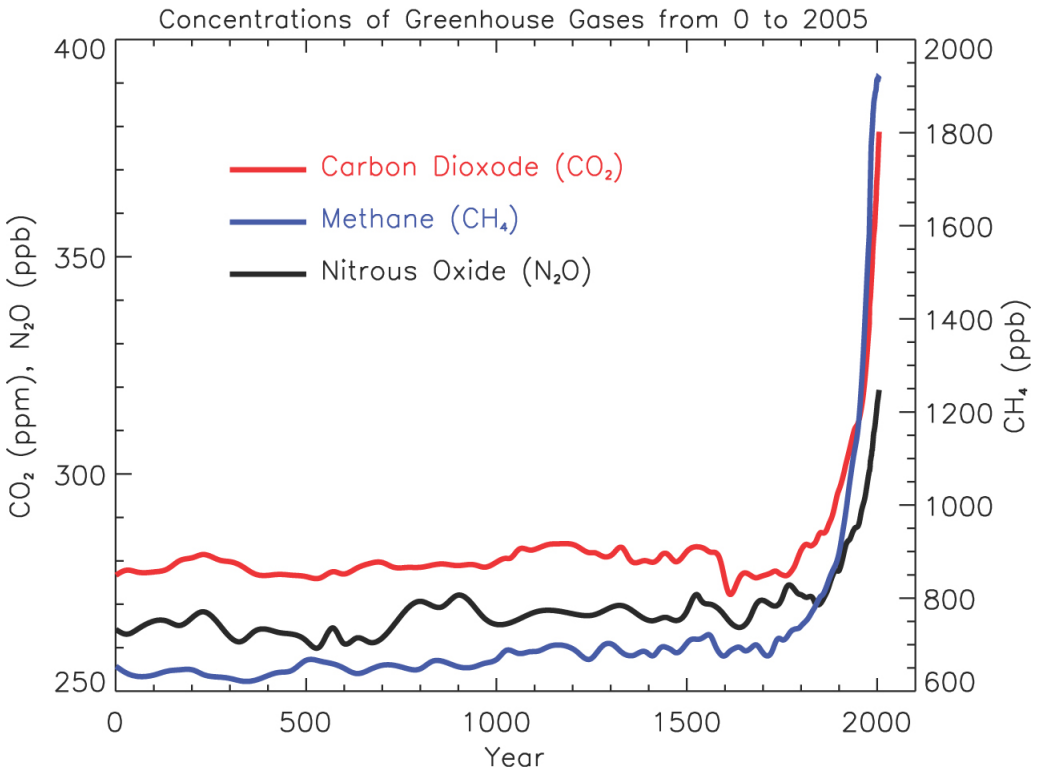

Figure 1.11: Atmospheric concentrations of important greenhouse gases over the last 2,000 years. Increases since about 1750 are attributed to human activities in the industrial era. The uncertainty on each of these is up to 10%. Source: IPCC (2001).

many species have been observed to be moving poleward for the past 30 – 40 years to search for water and favorable weather condition necessary for breeding (Parmesan and Yohe, 2003; Root et al., 2005). Moreover, the major concern of climate change is its consequences on human health as it threatens the basic elements of life for people around the world, especially, affecting access to water, food, health, and use of land and the environment in general. The increasing temperatures, especially in regions at the higher latitudes, changes in precipitation pattern, have resulted into severe storm flood in some areas and leaving some areas more drought prone (generally, causing extreme weather events such as severe storms, extreme heat and heavy rainfall, etc). (Ogden and Lindsay, 2016; Watson et al., 1996).

Another major sign of global climate change is the changing seasonal events, and one which is of major concern to human health is its effect on the ecology and physiology on vectors of infectious disease, most specifically, mosquitoes. Climate change alters biological features of the vectors, such as survival, development and reproduction rates of the vector (and their associated pathogens), usually leading to increasing the abundance of vectors (Mordecai et al., 2013; Negev et al., 2015; Ogden and Lindsay, 2016; Parham and Michael, 2010; Parham et al., 2012). For instance, mosquito egg laying have been observed to occur 2 – 3 days earlier each decade in many Northern Hemisphere temperate regions (Parmesan and Yohe, 2003; Root et al., 2005). Furthermore, the production of adults vectors (and subsequently, the intensity of disease transmission) is dependent on the longevity of the aquatic stages of the mosquitoes, thus, directly impacted by temperature of the water in which they occur (Bayoh and Lindsay, 2004; Parham et al., 2012).

1.4.1 Effect of Climate Variability on Mosquitoes and Mosquito-borne Diseases

Climate change is a complex phenomenon. So also is the transmission dynamics of MBDs and the ecological and behavioral features of the mosquitoes. Two main climate variables (temperature and rainfall) will be discussed in this section. This is because, while temperature is considered to be the main climate variable affecting the biology and ecology of the transmitting vectors, rainfall is essential for availability of breeding sites for majority of the transmitting vectors (Bi et al., 2003; Mordecai et al., 2013; Negev et al., 2015; Ogden and Lindsay, 2016; Parham and Michael, 2010; Parham et al., 2012).

1. **Effect of temperature**:

   Temperature directly impacts the ecology and physiology of disease vectors, for instance, Bayoh and Lindsay (2003); Bayoh (2001); Bayoh and Lindsay (2004);

Bi et al. (2003); Mordecai et al. (2013); Paaijmans et al. (2007); Parham et al. (2012) have all shown (using both field and laboratory experimental data) that temperature affects the survival, development and mortality rates (as well as the oviposition rate) of both adult and immature mosquitoes. Especially, under laboratory conditions, Bayoh and Lindsay (2004) used groups of 30 *Anopheles* mosquitoes, to show a critical relationship between temperature and the life cycle of the insect. They indicated that "larvae developed into adults at temperatures ranging from $[16-34]^{\circ}$C and larval survival was shortest at $[10-12]^{\circ}$ C and $[38-40]^{\circ}$C, and longest at $[14-20]^{\circ}$C". It was also stated that "within the temperature range at which adults were produced, larval mortality was highest at the upper range $[30-32]^{\circ}$C, with death (rather than adult emergence) representing over 70% of the terminal events". Furthermore, temperature has also been considered as a major factor of the pathogen development (Detinova et al., 1962). For instance, Detinova et al. (1962) showed, using laboratory data, that the minimum temperature for development of *P. falciparum* and *P. vivax* in the mosquito host is about 18°C and 15°C, respectively.

2. **Effect of rainfall**:

   Rainfall is an essential climate variable. It is the most influential factor leading to the abundance of mosquitoes, as it is necessary for the creation of breeding sites (Bi et al., 2003; Parham et al., 2012). By conducting a time-series analysis, using monthly climatic variables and monthly incidence of malaria data in Shuchen County, China, for the period 1980–1991, Bi et al. (2003) showed that monthly amount of precipitation were positively correlated with the monthly incidence of malaria. Moreover, extreme climate conditions such as excessive rainfall, leading to flood, (and prolonged absence of water) are not favorable

for the survival and maturation of the larvae (as a result of washing away of larvae at breeding habitats/sites), thereby, affecting the longevity of immature mosquitoes and reducing the population of adult mosquitoes (Agusto et al., 2015; Imbahale et al., 2011; Paaijmans et al., 2007, 2010c; Parham et al., 2012). However, due to poor drainage system, especially in disease-endemic regions, excess rainfall leave behind stagnant water on yards or lawns, thus, creating more favorable breeding sites for mosquitoes, which in-turn could leads to increased persistence of MBDs.

1.5 Research Objectives

Early studies raised and demonstrated the possibility of significant impacts of climate change on MBDs. For instance, while Martens et al. (1995) showed the correlation of climate change on the incidence on malaria, Patz et al. (1998) studied the impact of climate change on dengue. However, some studies, such as those by Reiter (2001) and Reiter et al. (2004) have countered these opinions with claims such as the lack of accuracy in results. Thus, the precise role of climate change on the spread of MBDs remains a subject of considerable debate within the scientific community. Consequently, this dissertation seeks to contribute to this global effort, by providing a realistic insight into the effect of, and mitigating the impact of, climate change on effectively combating MBDs endemic areas (and, subsequently, globally). This dissertation work addresses three main research themes, namely:

1. Develop a new mathematical modeling framework for realistically assessing the impact of anthropological climate change on the population dynamics (and ecology) of mosquito and the corresponding disease transmission dynamics in the chosen study area.

2. Determine the qualitative features of realistic models for assessing the impact

of climate change on the dynamics of malaria vector and disease (in particular, the distribution of vectors and malaria transmission intensity).

3. Use the developed models to determine suitable temperature ranges for maximum local mosquito abundance and transmission intensity of the disease(s) they cause.

1.6 Outline of the Dissertation

To achieve the goals of this dissertation, the following outline will be used. In Chapter 2, a new mathematical (compartmental) model for assessing the impact of two climate variables (rainfall and temperature) on the population biology of the mosquito is designed. Malaria transmission is strongly influenced by environmental temperature, notably by impacting the life-cycles of the female *Anopheles* mosquitoes and the *Plasmodium* parasite in these vectors. In Chapter 3, a new non-autonomous model, that explicitly accounts for the stages of the temperature-dependent *Anopheles* gonotrophic cycle as well as the temperature-dependent *Plasmodium* sporogonic cycle, is designed and used to assess the impact of temperature variability on the transmission dynamics of malaria in a population.

In Chapter 4, a new mathematical model is designed to gain qualitative and quantitative insight into the transmission dynamics of three disease viruses: DENV, CHIKV and ZIKV, that co-circulate in a given region, owing to the fact that they share the same transmitting vector (*Aedes* mosquito) but have some variations in transmission modes. In addition, the model is used to the evaluate the efficacy of the *Dengvaxia* vaccine (and its possibility of ADE on ZIKV). The model is further extended to incorporate the effect of temperature and rainfall variability on the population biology of *Aedes* mosquitoes, to gain insight into the effect of these climate

variables on transmission dynamics of the three diseases in the region of study. Conclusions derived from the dissertation are discussed in Chapter 5.

Chapter 2

MATHEMATICAL ANALYSIS OF A WEATHER-DRIVEN MODEL FOR THE POPULATION ECOLOGY OF MOSQUITOES

2.1 Introduction

As stated in Chapter 1, mosquito-borne diseases (MBDs) account for over 80% of all vector-borne diseases (VBDs). Understanding mosquito population dynamics (i.e., abundance and distribution of mosquitoes, as well as the relationship between the mosquitoes and the local environment) is very crucial to gaining realistic insight into the epidemiology of the diseases they cause and, subsequently, crucial to the design of effective strategies for combating the spread of the MBDs in human populations (Mordecai et al., 2013; Ngwa, 2006; Ngwa et al., 2010; Parham et al., 2012). This chapter presents a new deterministic weather-driven model for the population biology of the mosquito.

2.2 Literature Review of Mathematical Modeling of Mosquito Ecology

A number of population biology models have designed and used to assess the role of environmental variables on mosquito populations. These models are typically designed using a process-based approach, incorporating established biological and entomological features that affect the mosquito vital rates (such as the egg oviposition rate, adult (and immature) survival rate of adult mosquitoes and the development rate of immature mosquitoes) (Ermert et al., 2011; Hoshen and Morse, 2004; Martens, 2013; Parham et al., 2012). In particular, process-based models have been used to assess the impact of seasonality on the distribution of various mosquito species, such

as *Anopheles* mosquitoes (the vector for malaria) (Beck-Johnson et al., 2013, 2017; Cailly et al., 2012; Christiansen-Jucht et al., 2015; Mordecai et al., 2013; Parham et al., 2012), *Aedes* mosquitoes (the vector for DENV, CHIKV and ZIKV) (Lana et al., 2014; Liu-Helmersson et al., 2016; Tran et al., 2013; Yang et al., 2009, 2011), and *Culex* mosquitoes (the vector of West Nile virus) (Abdelrazec and Gumel, 2017; Ahumada et al., 2004; Ewing et al., 2016; Mulatti et al., 2014; Wang et al., 2011). These models also allow for the determination of parameters that influence the life-cycle and distribution of the mosquito species (Ahumada et al., 2004; Cailly et al., 2012; Mulatti et al., 2014; Parham et al., 2012; Tran et al., 2013; Yang et al., 2011).

Parham et al. (2012) formulated a mathematical model to establish the relationships between key aspects of mosquito ecology (and abundance) and environmental variables (such as in rainfall, temperature, wind speed and cloudiness). Parham et al. (2012) suggested that, while rainfall plays a major role in the development of mosquito breeding sites and typically correlates with vector abundance and malaria prevalence, the survival of adult *Anopheles* mosquitoes is strongly sensitive to temperature. Their model was fitted using longitudinal vector abundance data from Tanzania (in an area where no vector controls are applied; thus, suggesting that recent malaria reductions in certain areas of Africa is due to changing environmental conditions affecting vector populations). Moreover, the model designed by Parham et al. (2012) did not explicitly include the four stages of the larvae (and three distinct gonotrophic stages of the adult female mosquitoes).

Furthermore, Abdelrazec and Gumel (2017) used a stage-structured deterministic model to assess the effect on rainfall and temperature on the population dynamics of the female *Culex* mosquito subject to two forms of egg oviposition rate (namely, the Verhulst-Pearl logistic and Maynard-Smith-Slatkin functions). Their model, which incorporates density-dependent larval mortality (to account for larval competition for

nutrients), exhibits a Hopf bifurcation under certain conditions (they further showed that increased density-dependent competition in larval mortality reduces the likelihood of such bifurcation). Numerical simulations of their model, using mosquito surveillance and weather data from the Peel region of Ontario, Canada, showed a peak mosquito abundance for temperature and rainfall values in the range $[20-25]^{\circ}$C and [15–35] mm, respectively.

2.3 Formulation of Weather-driven Model for Mosquito Population Dynamics

The purpose of this chapter is to design a new stage-structured model for the population dynamics of *Anopheles* mosquitoes, which extends earlier published models in the literature for this setting. The model to be designed, which takes the form of a deterministic system of non-autonomous nonlinear differential equations, will be used to study the effect of variability in temperature and rainfall on the population dynamics of adult female *Anopheles* mosquitoes in a certain region.

The model is developed by splitting the total immature mosquito population at time t (denoted by $I_M(t)$) into mutually-exclusive compartments for eggs ($E(t)$), four larval instars ($L_i(t);\ i = 1, 2, 3, 4$) and pupae ($P(t)$), so that $I_M(t) = E(t) + \sum_{i=1}^{4} L_i(t) + P(t)$. Similarly, the population of adult female *Anopheles* mosquitoes at time t ($A_M(t)$) is sub-divided into mutually-exclusive compartments for the class of unfertilized adult female vectors not questing for bloodmeal and fertilized female mosquitoes that have laid eggs at the breeding site ($V(t)$), the class of fertilized, but not producing, adult female mosquitoes questing for bloodmeal ($W(t)$), and the class of fertilized, well-nourished with blood, and reproducing adult female mosquitoes ($U(t)$), so that $A_M(t) = U(t)+V(t)+W(t)$. Let N represents the amount of nutrients for the larvae (assumed to be constant or uniformly available at the breeding sites). The model is given by the following deterministic system of nonlinear differential

equations (Okuneye et al., 2018a):

$$\frac{dE}{dt} = \psi_U(T_A)\Big(1 - \frac{U}{K_U}\Big)_+ U - \big[\sigma_E(R, T_W) + \mu_E(T_W)\big]E,$$

$$\frac{dL_1}{dt} = \sigma_E(R, T_W)E - \big[\sigma_{L_1}(N, R, T_W) + \mu_L(T_W) + \delta_L L\big]L_1,$$

$$\frac{dL_i}{dt} = \sigma_{L_{(i-1)}}(N, R, T_W)L_{(i-1)} - \big[\sigma_{L_i}(N, R, T_W) + \mu_L(T_W) + \delta_L L\big]L_i \ ; i = 2, 3, 4,$$

$$\frac{dP}{dt} = \sigma_{L_4}(N, R, T_W)L_4 - \big[\sigma_P(R, T_W) + \mu_P(T_W)\big]P, \tag{2.3.1}$$

$$\frac{dV}{dt} = f\sigma_P(R, T_W)P + \gamma_U U - \frac{\eta_V H}{H + F}V - \mu_A(T_A)V,$$

$$\frac{dW}{dt} = \frac{\eta_V H}{H + F}V - [\tau_W H + \mu_A(T_A)]\,W,$$

$$\frac{dU}{dt} = \alpha\tau_W HW - [\gamma_U + \mu_A(T_A)]\,U,$$

where $L = \sum_{i=1}^{4} L_i$ and $r_+ = \max\{0, r\}$, with $r > 0$. The notation r_+ is used to ensure the nonnegativity of the logistic term $\left(1 - \frac{U}{K_U}\right)$ (since the negativity is not ecologically realistic). In the model (2.3.1), $R = R(t)$, $T_A = T_A(t)$, and $T_W = T_W(t)$ denote mean monthly rainfall (precipitation), air (ambient) temperature and (surface) water temperature at time t, respectively. Typically, a sinusoidal function, such as

$$T(t) = T_0\left[1 + T_1\,\cos\left(\frac{2\pi}{365}(\omega t + \theta)\right)\right], \tag{2.3.2}$$

(where T_0 is the mean annual temperature, T_1 captures variation about the mean, and ω and θ represent, respectively, the periodicity and phase shift of the function)

is used to model local fluctuations (Agusto et al., 2015) in air and surface water temperature (and similar appropriate time-dependent functions are used to account for rainfall and water temperature variability (Abdelrazec and Gumel, 2017; Okuneye and Gumel, 2017); Figure 2.1 depicts sinusoidal fluctuations in temperature and precipitation (based on the Garki project data (Dietz et al., 1974))). Thus, the

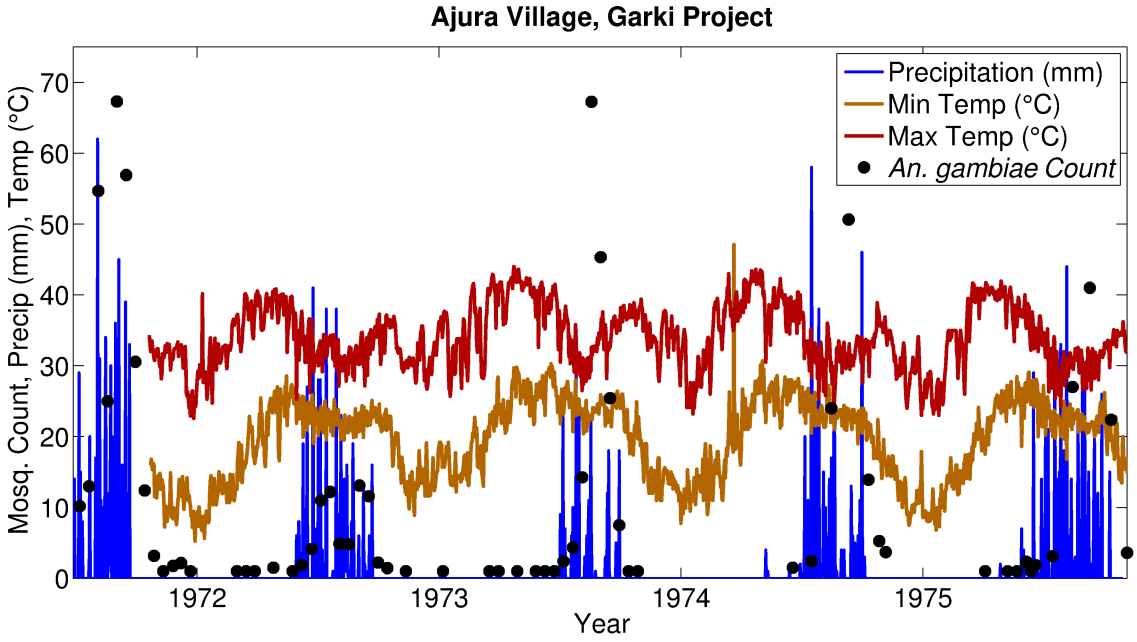

Figure 2.1: Sinusoidal pattern of temperature and rainfall variable over time. Data was extracted from The Garki Project http://garkiproject.nd.edu/.

functions $T_A(t), T_W(t)$ and $R(t)$ are assumed to be continuous, bounded, positive and ω-periodic. Furthermore, the parameters $\psi_U(T_A), \sigma_E(R, T_W)$, $\sigma_{L_i}(N, R, T_W)$ (for $i = 1, 2, 3, 4$), $\sigma_P(R, T_W)$, $\mu_E(T_W)$, $\mu_L(T_W)$, $\mu_P(T_W)$ and $\mu_A(T_A)$ in the model (2.3.1) are non-negative, ω-periodic, continuous and bounded functions defined on $[0, \infty)$. Since temperature and rainfall are functions of time t, it follows that the temperature- and rainfall-dependent parameters of the model (2.3.1) are also functions of time t. Hence, the model (2.3.1) is *non-autonomous*. However, when fixed rainfall and tem-

perature values are used (e.g., when mean daily or monthly temperature values are used) in the model, as against the time-varying case using the function of the form (2.3.2), then the model (2.3.1) is *autonomous* (and standard dynamical systems tools can generallybe used forits rigorous qualitative analysis).

The term $\psi_U(T_A)\left(1-\frac{U}{K_U}\right)_+$ represents the density-dependent eggs oviposition rate (where $\psi_U(T_A)$ is the temperature-dependent egg deposition rate and K_U is the environmental carrying capacity of the breeding sites of adult female mosquitoes). Eggs hatch into the first larval instar stage at a rainfall- and temperature-dependent rate $\sigma_E(R,T_W)$. Larvae in Stage i mature into Stage $i+1$ at a rate $\sigma_{L_i}(N,R,T_W)$ $(i=1,2,3)$, which is assumed to depend on temperature, rainfall and the amount of available nutrients. Larvae in Stage 4 (L_4 class) mature into pupae at a nutrient-, rainfall- and temperature-dependent rate $\sigma_{L_4}(N,R,T_W)$. It should be emphasized that the maturation rates for the larval stages ($\sigma_{L_j};\ j=1,2,3,4$) are dependent on nutrient, water temperature and rainfall because, while nutrients are needed for the growth and development of the larvae, rainfall is required for availability of breeding sites and habitats and favorable temperature values improve the prospect for the development of the larvae (Berkelhamer and Bradley, 1989; Imbahale et al., 2011; Paaijmans et al., 2007, 2010c; Van Handel, 1988). However, extreme climate conditions, such as excessive rainfall, washes out the larval breeding sites (such as small stagnant water on yards or lawn) and excessively hot or low temperatures are not favorable to the survival and maturation of the larvae (Agusto et al., 2015; Imbahale et al., 2011; Paaijmans et al., 2007, 2010c).

Pupae mature into adult female mosquitoes of type V at a rainfall- and temperature-dependent rate $f\sigma_P(R,T_W)$ (where f accounts for the proportion of the new adult mosquitoes that are female). These adult female mosquitoes quest for bloodmeal at the human habitat at a rate η_V (and become adult female mosquitoes of type W)

(Ngwa, 2006). The term $\frac{H}{H+F}$ accounts for the preference of human blood, as opposed to that of other animals (Hirsch et al., 1985; Ngwa et al., 2010) (where H is the population density of humans that are accessible to the mosquitoes (local to the breeding sites of the mosquitoes) and F is a positive constant representing a constant alternative food source for the adult female mosquitoes) (Ngwa, 2006).

At the human habitat, adult female mosquitoes of type W interact with humans according to standard mass action law, at a constant rate τ_W (Ngwa, 2006; Ngwa et al., 2010). This interaction can be successful with probability $\alpha \in [0, 1]$, so that questing mosquitoes successfully obtain bloodmeals and become vectors of type U (at the rate $\alpha\tau_W$) which, in turn, return to become adult female mosquitoes of type V at a rate γ_U after laying eggs. Furthermore, the parameters $\mu_E(T_W)$, $\mu_L(T_W)$, $\mu_P(T_W)$, $\mu_A(T_A)$ represent, respectively, the temperature-dependent natural death rate for eggs, larvae, pupae and adult female mosquitoes, and δ_L is the density-dependent larval mortality rate (accounting for intra and inter-species larval competition for resources and space). A flow diagram of the model (2.3.1) is depicted in Figure 2.2, and the variables and parameters of the model are described in Table 2.1.

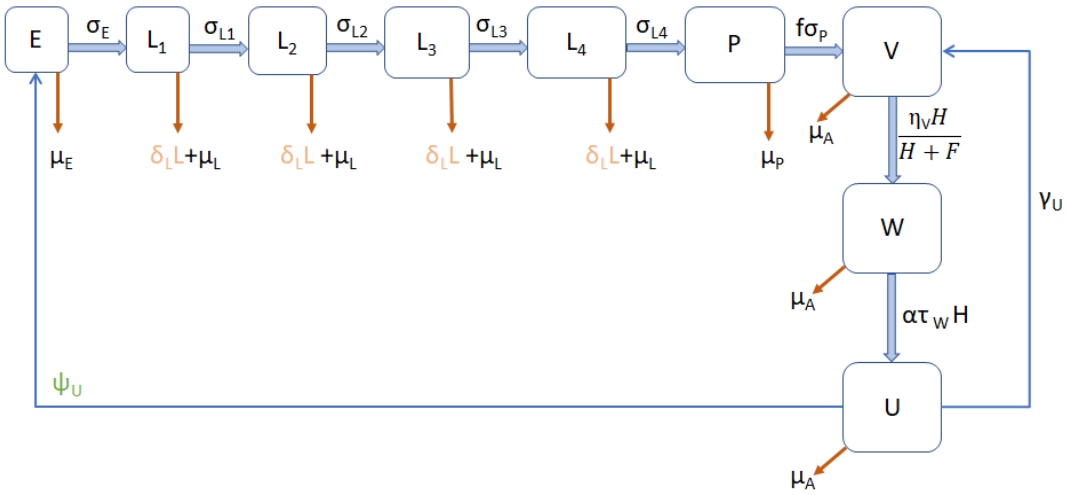

Figure 2.2: Flow diagram of the model (2.3.1).

Variables	Description
E	Population of female eggs
L_i	Population of female larvae at Stage i (for $i = 1, 2, 3, 4$)
P	Population of female pupae
V	Population of fertilized female mosquitoes that have laid eggs at the breeding site (including unfertilized female mosquitoes not questing for bloodmeal)
W	Population of fertilized, but non-reproducing, female mosquitoes questing for bloodmeal
U	Population of fertilized, well-nourished with blood, and reproducing female mosquitoes
Parameters	**Description**
ψ_U	Egg oviposition rate
σ_E (σ_P)	Maturation rate of eggs (pupae)
σ_{L_i}	Maturation rate of larvae from larval stage i to stage $i+1$ (with $i = 1, 2, 3$)
f	Proportion of new mosquitoes that are adult female mosquito
μ_E, μ_L, μ_P, μ_A	Natural mortality rate of eggs, larvae, pupae and adult female mosquitoes, respectively
δ_L	Density-dependent larval mortality rate
τ_W	Constant mass action contact rate between adult female mosquitoes of type W and humans
α	Probability of successfully taking a bloodmeal
γ_U	Rate of return of adult female mosquitoes of type U to the mosquitoes breeding site
η_V	Rate at which adult female mosquitoes of type V visit human habitat sites
H	Constant population density of humans at human habitat sites
F	Constant alternative source of bloodmeal for adult female mosquitoes
K_U	Environmental carrying capacity of adult female mosquitoes

Table 2.1: Description of the state variables and parameters of the model (2.3.1).

2.3.1 Formulation of Thermal Response Functions

Air and Water Temperature

Several (field) studies have shown (and applied) a rather linear relation between air ($T_A(t)$) and water ($T_W(t)$) temperatures (Christiansen-Jucht et al., 2015; Fry and Watt, 1957; McCombie, 1959; Parham et al., 2012). For instance, by studying the effects of weather on the bass populations in South Bay and neighboring waters in Manitoulin Island, Fry and Watt (1957) showed that the daily rate of change in water temperature was a linear function of the difference between the air and water temperatures. Furthermore, by analyzing meteorological and hydrographic records collected at South Bay, Ontario, over a period of nine years, McCombie (1959) showed that the relation between water and air temperature can be expressed as linear regressions (Figure 2.3). Moreover, Christiansen-Jucht et al. (2015) indicated that the best fitting models predict a difference between environmental air and water temperature of approximately 7°C. Similarly, some studies (Paaijmans et al., 2008a), Parham et al. (2012) and Huang et al. (2006) reported that the difference between mean daily water and air temperatures is typically around $[3-6]$°C, depending on factors such as breeding site dimensions, microclimate and weather conditions. Although some other studies have suggested a non-linear relationship between the two temperature (see, for instance, the review paper by Eikenberry and Gumel (2018)), this dissertation will use a linear relationship between the two temperatures. In particular, we will use the relation $T_W = T_A + \Delta T$; where $\Delta T \geq 0$ is (to a first approximation) assumed to capture all the thermodynamic processes taking place at the breeding sites.

The functional forms of the thermal response (rainfall- and temperature-dependent) functions of the model (2.3.1) are formulated based on using available laboratory data, as follows.

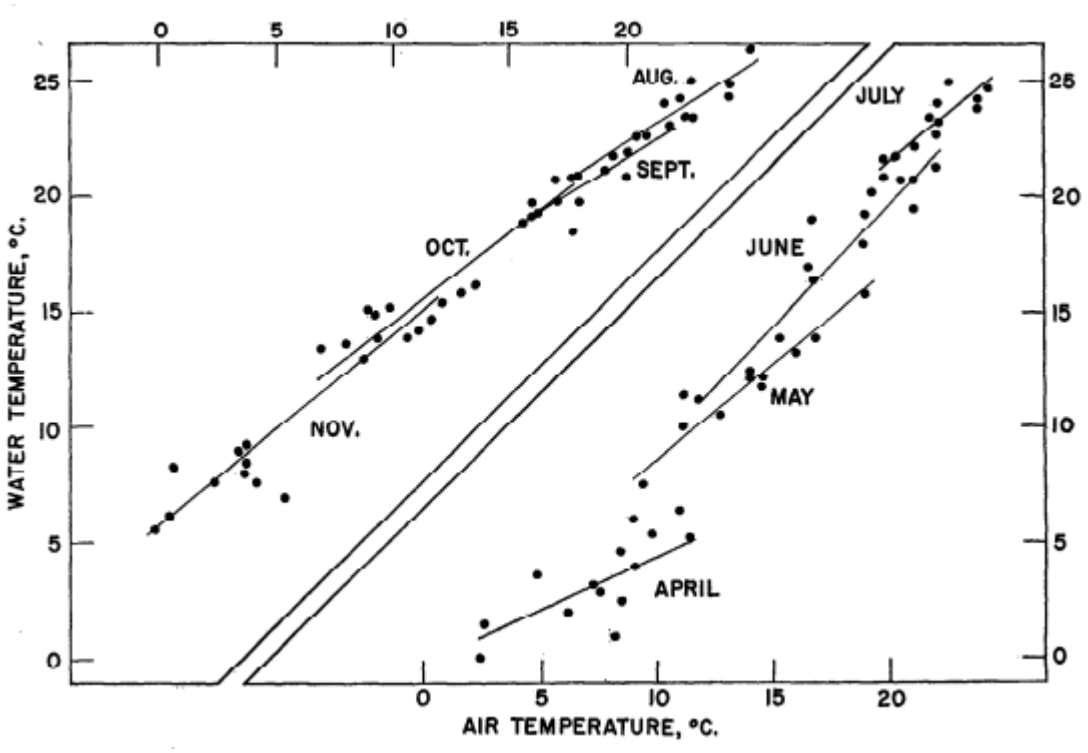

Figure 2.3: "The relation between the monthly means of the air and surface water temperatures at Lake Mendota". Source: McCombie (1959).

Survival Rate of Adult Female Mosquitoes ($\mu_M(T_A)$)

The mean survival times for adult *Anopheles gambiae* ($\mu_M(T_A)$) under laboratory conditions are taken from Bayoh (2001), whose reported survival under constant ambient temperatures from 5 to 40°C (5°C intervals), and for a range of relative humidities. We use the survival curve in Bayoh (2001) for 60% relative humidity, and fit a quadratic polynomial, such that (Figure 2.4A) (Okuneye et al., 2018b):

$$\frac{1}{\mu_M(T_A)} = \max\big(-11.8239 + 3.3292T_A - 0.0771T_A^2,\ 0.1\big).$$

Egg Oviposition Rate ($\psi_U(T_A)$)

Most *Anopheles* mosquitoes deposit individual eggs directly onto the water surface or scatter them across the water as the adult female mosquito hovers above the

oviposition site. The number of eggs laid *per* oviposition event, ψ_U, may vary from 10 to 150 for *Anopheles gambiae* (Afrane et al., 2005; Takken et al., 1998), but is typically about 40 to 85 under field conditions (Afrane et al., 2005). The *per-capita* rate of deposition of eggs ($\psi_U(T_A)$), defined using the quadratic function used in Mordecai et al. (2013), is given by (Figure 2.4B) (Okuneye et al., 2018a):

$$\psi_U(T_A) = -0.153T_A^2 + 8.61T_A - 97.7.$$

Survival Rate of Immature Mosquitoes ($\mu_i(T_W)$, $i = E, L, P$)

Using larval survival times reported by Bayoh and Lindsay (2004), we fit the per-capita death rate (inverse of survival time) of the immature mosquitoes ($\mu_E,\ \mu_L$, and μ_P) fairly well using the following fourth-order polynomial (for $i = E,\ L,\ P$) (Figure 2.4C) (Okuneye et al., 2018b):

$$\mu_i(T_W) = 8.929 \times 10^{-6}T_W^4 - 9.271 \times 10^{-4}T_W^3 + 3.536 \times 10^{-2}T_W^2 - 0.5814T_W + 3.509.$$

Maturation Rate of Eggs and Pupae ($\sigma_E(T_W, R)$, $\sigma_P(T_W, R)$)

Eggs hatch into larvae in $1 - 3$ days, and while this is a rainfall-and temperature-dependent process, most eggs hatch by the third day regardless (Dao et al., 2006). Therefore, as a first approximation, the maturation rate for eggs (σ_E) is assumed to be constant, and in the range $0.33 - 1$ day^{-1}. Similarly, pupae hatch within a few days (Bayoh and Lindsay, 2003). Thus, it is assumed that $\sigma_P = 0.33 - 1$ day^{-1}, with all temperature-dependence manifested at the larval stage of development.

Maturation Rate of Larvae ($\sigma_{Li}(N, R, T_W),\ i = 1, 2, 3, 4$)

Larval development is formulated using the relations derived by Parham et al. (2012) Parham and Michael (2010) and Bayoh and Lindsay (2003). Following Parham et al.

(2012), the *per-capita* maturation rate of larvae in Stage j is given by:

$$\sigma_{L_j}(N, R, T_W) = \sigma_{L_j}(N)\sigma_{L_j}(R)\sigma_{L_j}(T_W), \tag{2.3.3}$$

where the nutrient-dependent function $\sigma_{L_j}(N)$ is defined as:

$$\sigma_{L_j}(N) = e_j N,$$

with e_j representing the rate of nutrients intake for larvae in Stage j. Following Parham and Michael (2010) (Supplemental Material), the rainfall-dependent daily probability of survival of larvae is given by:

$$\sigma_{L_j}(R) = R(R_{I_M} - R)(4p_{Mj}/R_{I_M}^2),\ j = 1, 2, 3, 4, \tag{2.3.4}$$

where p_{Mi} is the peak daily survival probability of larvae in Stage j and $R_{I_M} > R(t) > 0$, for all time t, is the maximum rainfall threshold in the community. Furthermore, water temperature-dependent larval development ($\sigma_{L_j}(T_W)$) is formulated using the unimodal relation derived by Bayoh and Lindsay (2003), where the overall time from egg to adult mosquito, denoted by $\mathcal{D}_{EA}(T_W)$, is given by (Okuneye et al., 2018b):

$$\mathcal{D}_{EA}(T_W) = \left(a + bT_W + ce^{T_W} + de^{-T_W}\right)^{-1}, \tag{2.3.5}$$

with $a = -0.05$, b $= 0.005$, c $= -2.139 \times 10^{-16}$, and $d = -2.81357 \times 10^5$ (it is further assumed, based on survival data in Bayoh and Lindsay (2003), that development ceases below 16.1 °C and beyond about 33.9 °C. That is, it is assumed that for $j = 1, 2, 3, 4$, $\sigma_{L_j} = 0$ for $T_W < 16.1$ °C or $T_W > 39.1$ °C). Furthermore, it is assumed that all four larval instar stages are equal in duration, so that (Figure 2.4D) (Okuneye et al., 2018b):

$$\sigma_{L_j}(T_W) = 4\left(\mathcal{D}_{EA}(T_W) - \frac{1}{\sigma_E} - \frac{1}{\sigma_P}\right)^{-1} \text{ for } j = 1, 2, 3, 4.$$

It should be stated that, in line with Parham et al. (2012), the definition of $\sigma_{L_j}(R, T_W) = \sigma_{L_j}(N)\sigma_{L_j}(R)\sigma_{L_j}(T_W)$, emphasizes the assumed independence among temperature, rainfall and nutrient resources.

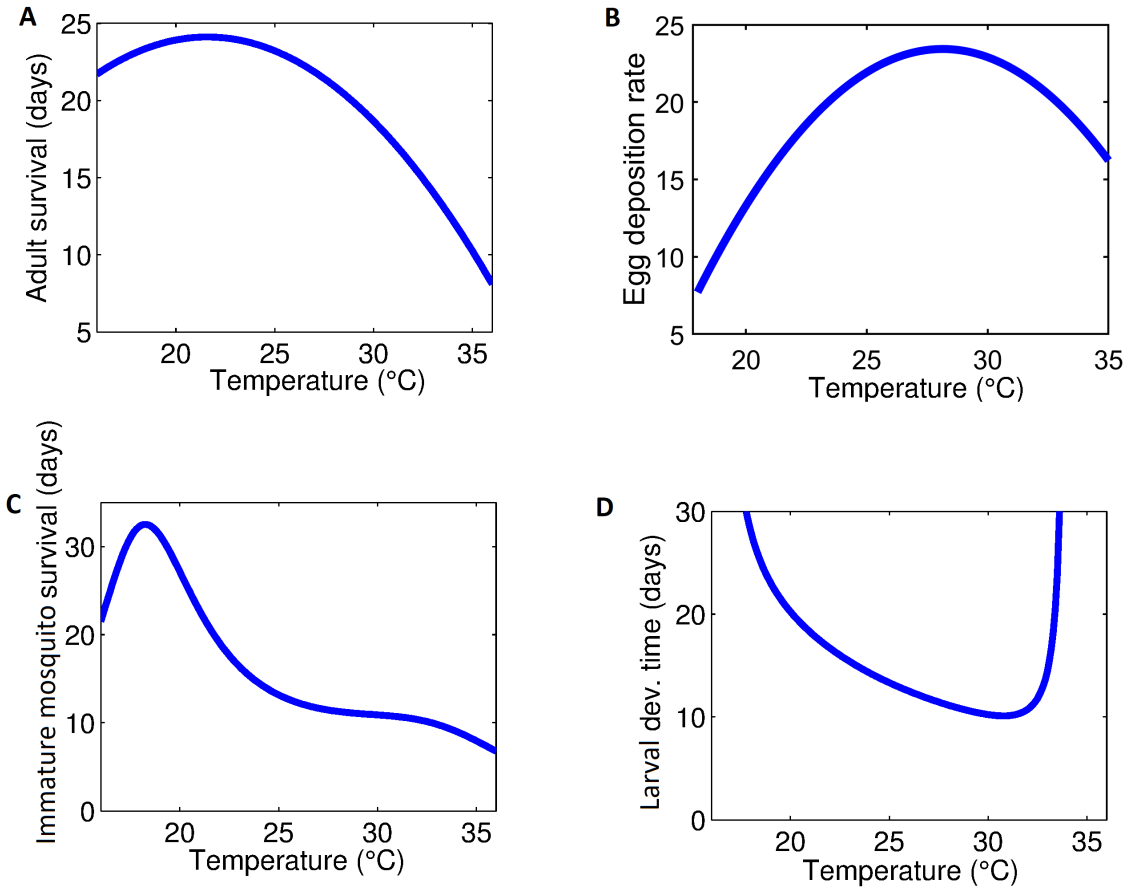

Figure 2.4: Profile of temperature-dependent parameters of the model (2.3.1): (a) Survival time of adult mosquitoes, $(\mu_A(T_A))$ (b) Mosquito egg deposition rate, $(\psi_U(T_A))^{-1}$ (c) Survival time of larvae, $(\mu_L(T_W))^{-1}$ and (d) total time for larvae development as a function of temperature $(\sigma_{L_j}(T_W))$.

2.3.2 Basic Properties

Model Invariant Region

The basic properties of the non-autonomous model (2.3.1) will now be explored.

Definition 2.3.1. For each of the time-dependent (i.e., temperature- and rainfall-dependent) parameters, the following quantities hold:

$$a^* = \sup_{t\geq 0} a(t), \quad a_* = \inf_{t\geq 0} a(t) \tag{2.3.6}$$

Lemma 2.3.1. *For any $\phi \in \Omega = \mathbb{R}^9_+$, the model* (2.3.1) *has a unique non-negative solution through ϕ, and solutions are ultimately bounded and uniformly bounded.*

Proof. Following Lou and Zhao (2010), define, for all $\phi \in \Omega$,

$$G(t,\phi) = \begin{bmatrix} \psi_U(t)\left[1-\dfrac{\phi_9}{K_U}\right]_+ \phi_9 - \big[\sigma_E(t)+\mu_E(t)\big]\phi_1 \\ \sigma_E(t)\phi_1 - \big[\sigma_{L_1}(t)+\mu_L(t)+\delta_L\phi_L\big]\phi_2 \\ \sigma_{L_{(i-2)}}(t)\phi_{(i-1)} - \big[\sigma_{L_{(i-1)}}(t)+\mu_L(t)+\delta_L\phi_L\big]\phi_i;\ i=3,4,5 \\ \sigma_{L_4}(t)\phi_5 - \big[\sigma_P(t)+\mu_P(t)\big]\phi_6 \\ f\sigma_P(t)\phi_6 + \gamma_U\phi_9 - \dfrac{\eta_V H}{H+F}\phi_7 - \mu_A(t)\phi_7 \\ \dfrac{\eta_V H}{H+F}\phi_7 - \big[\tau_W H+\mu_A(t)\big]\phi_8 \\ \alpha\tau_W H\phi_8 - \big[\gamma_U+\mu_A(t)\big]\phi_9 \end{bmatrix},$$

with $\phi_L = \sum_{i=2}^{5}\phi_i$. Thus, for all $\phi \in \Omega$, the function $G(t,\phi)$ is continuous and Lipschitzian (with respect to ϕ in each compact set in $\mathbb{R}\times\Omega$) (Lou and Zhao, 2010). Hence, there is a unique solution of system (2.3.1) through $(0,\phi)$. It should be noted that $G_i(t,\phi) \geq 0$ whenever $\phi \geq 0$ and $\phi_i = 0$ (Lou and Zhao, 2010). Thus, it follows

from Theorem A.4 in Thieme (2003) that the region Ω is positively-invariant with respect to the model (2.3.1).

Consider, next, the first equation of the model (2.3.1). It follows from the boundedness of the logistic term, and Definition 2.3.1, that:

$$\frac{dE}{dt} \leq \psi_U^* \frac{K_U^4}{4} - (\sigma_{E*} + \mu_{E*})E,$$

so that $\limsup_{t\to\infty} E(t) \leq \dfrac{\psi_U^* K_U^2}{4(\sigma_{E*} + \mu_{E*})} = \overline{E}$. In addition, for any $\varepsilon > 0$, there exists $t_1 \in \mathbb{N}$ such that $E(t) \leq \overline{E} + \varepsilon$, whenever $t \geq t_1$. Furthermore, it follows, by substituting $\overline{E} + \varepsilon$ into the second equation of the model (2.3.1), that

$$\frac{dL_1}{dt} = \sigma_E(t)E - (\sigma_{L_1} + \mu_L + \delta_L L)L_1 \leq \sigma_E^*(\overline{E} + \varepsilon) - (\sigma_{L_1*} + \mu_{L*})L_1, \ t \geq t_1, \tag{2.3.7}$$

so that $L_1(t) \leq \dfrac{\sigma_E^*(\overline{E} + \varepsilon)}{\sigma_{L_1*} + \mu_{L*}} = \overline{L}_1$. Using similar approach, the following bounds can be established for the remaining immature mosquito compartments: $L_j(t) \leq \overline{L}_j$ (for $j = 2, 3, 4$) and $P(t) \leq \overline{P}$.

Furthermore, considering the compartments for adult female mosquitoes in the model (2.3.1) (given by the seventh, eighth and ninth equations of the model), the rate of change of the total adult mosquito population ($A_M(t)$) is given by:

$$\frac{dA_M}{dt} = f\sigma_P(t)P - \mu_A(t)A_M - (1-\alpha)\tau_W HW \leq f\sigma_P^*\overline{P} - \mu_{A*}A_M.$$

Thus, $A_M(t) \leq \dfrac{f\sigma_P^*\overline{P}}{\mu_{A*}} = \overline{A}_M$. Hence, the solutions of the model (2.3.1) are ultimately and uniformly bounded. □

Since the region Ω is positively-invariant, the existence, uniqueness, and continuation results hold for the system (hence, it is sufficient to consider the dynamics of the flow generated by model (2.3.1) in the region Ω (Hethcote, 2000)).

2.4 Analysis of Autonomous Version of the Model

In this section, the autonomous (i.e., no explicit temperature and rainfall effects, or fixed (mean) values of these climate variables are used in the model) version of model (2.3.1) will be analyzed. The objective is to determine whether or not the autonomous version exhibits dynamical features not present in the original non-autonomous model. This special case, obtained by setting each of the rainfall- and temperature-dependent parameters of the model (2.3.1) to a constant (i.e., $\sigma_E(t) = \sigma_E$, $\sigma_P(t) = \sigma_P$, $\sigma_{L_i}(t) = \sigma_{L_i}$, $\mu_E(t) = \mu_E$, $\mu_L(t) = \mu_L$, $\mu_A(t) = \mu_A$), is given by:

$$\begin{aligned}
\frac{dE}{dt} &= \psi_U \left(1 - \frac{U}{K_U}\right)_+ U - (\sigma_E + \mu_E)\, E, \\
\frac{dL_1}{dt} &= \sigma_E E - (\sigma_{L_1} + \mu_L + \delta_L L)\, L_1, \\
\frac{dL_i}{dt} &= \sigma_{L_{(i-1)}} L_{(i-1)} - (\sigma_{L_i} + \mu_L + \delta_L L)\, L_i\,; \quad i = 2, 3, 4, \\
\frac{dP}{dt} &= \sigma_{L_4} L_4 - (\sigma_P + \mu_P)\, P, \\
\frac{dV}{dt} &= f\sigma_P P + \gamma_U U - \big(\eta_V^* + \mu_A\big) V, \\
\frac{dW}{dt} &= \eta_V^* V - (\tau_W^* + \mu_A)\, W, \\
\frac{dU}{dt} &= \alpha\tau_W^* W - (\gamma_U + \mu_A)\, U,
\end{aligned} \tag{2.4.1}$$

where, now, $L = \sum_{i=1}^{4} L_i$, $\eta_V^* = \dfrac{\eta_V H}{H + F}$ and $\tau_W^* = \tau_W H$.

2.4.1 Computation of Vectorial Reproduction Number ($\mathcal{R}_M$)

The autonomous model (2.4.1) has a trivial (mosquito-free) equilibrium solution, denoted by $\mathcal{T}_0$, given by:

$$\mathcal{T}_0 = (E^*, L_1^*, L_2^*, L_3^*, L_4^*, P^*, V^*, W^*, U^*) = \big(0, 0, 0, 0, 0, 0, 0, 0, 0\big).$$

The linear stability of $\mathcal{T}_0$ is obtained by using the next generation operator method (Diekmann et al., 1990; van den Driessche and Watmough, 2002) applied the system

(2.3.1). Using the notation in van den Driessche and Watmough (2002), the non-negative matrix $\mathcal{F}$ and the non-singular matrix $\mathcal{V}$, for the new egg deposition terms and the remaining transfer terms, are, respectively, given (at the trivial equilibrium, $\mathcal{T}_0$) by:

$$\mathcal{F} = \begin{bmatrix} \mathbf{0} & \mathbf{0} & \mathcal{F}_1 \\ \mathbf{0} & \mathbf{0} & \mathbf{0} \\ \mathbf{0} & \mathbf{0} & \mathbf{0} \end{bmatrix} \text{ and } \mathcal{V} = \begin{bmatrix} \mathcal{V}_1 & \mathbf{0} & \mathbf{0} \\ \mathcal{V}_2 & \mathcal{V}_3 & \mathbf{0} \\ \mathbf{0} & \mathcal{V}_4 & \mathcal{V}_5 \end{bmatrix},$$

where $\mathbf{0}$ denotes a zero matrix of order 3, and

$$\mathcal{F}_1 = \begin{bmatrix} 0 & 0 & \psi_U \\ 0 & 0 & 0 \\ 0 & 0 & 0 \end{bmatrix}, \mathcal{V}_1 = \begin{bmatrix} C_E & 0 & 0 \\ -\sigma_E & C_1 & 0 \\ 0 & -\sigma_{L_1} & C_2 \end{bmatrix}, \mathcal{V}_2 = \begin{bmatrix} 0 & 0 & -\sigma_{L_2} \\ 0 & 0 & 0 \\ 0 & 0 & 0 \end{bmatrix},$$

$$\mathcal{V}_3 = \begin{bmatrix} C_3 & 0 & 0 \\ -\sigma_{L_3} & C_4 & 0 \\ 0 & -\sigma_{L_4} & C_P \end{bmatrix}, \mathcal{V}_4 = \begin{bmatrix} 0 & 0 & -f\sigma_P \\ 0 & 0 & 0 \\ 0 & 0 & 0 \end{bmatrix}, \mathcal{V}_5 = \begin{bmatrix} C_5 & 0 & -\gamma_U \\ -\eta_V^* & C_6 & 0 \\ 0 & -\alpha\tau_W^* & C_7 \end{bmatrix}.$$

It follows that the associated *vectorial reproduction number* of the autonomous model (2.4.1) is given by (where ρ denotes the spectral radius) (see also Ngwa (2006); Ngwa et al. (2010)).

$$\begin{aligned} \mathcal{R}_M &= \rho(\mathcal{F}\mathcal{V}^{-1}) \\ &= (\psi_U) \cdot \underbrace{\Big(\frac{\sigma_E}{\sigma_E + \mu_E}\Big)}_{\text{(a)}} \cdot \left(\underbrace{\frac{\prod_{j=1}^{4} \sigma_{L_j}}{\prod_{j=1}^{4} (\sigma_{L_j} + \mu_L)}}_{\text{(b)}} \right) \cdot \underbrace{\Big(\frac{f\sigma_P}{\sigma_P + \mu_P}\Big)}_{\text{(c)}} \cdot \underbrace{\Big(\frac{\alpha\tau_W^*\eta_V^*}{C_5C_6C_7 - \alpha\tau_W^*\eta_V^*\gamma_U}\Big)}_{\text{(d)}}, \end{aligned} \tag{2.4.2}$$

where $C_5 = \eta_V^* + \mu_A, C_6 = \tau_W^* + \mu_A,\ C_7 = \gamma_U + \mu_A$, so that $C_5C_6C_7 - \alpha\tau_W^*\eta_V^*\gamma_U > 0$.

Interpretation of Vectorial Reproduction Number ($\mathcal{R}_M$)

The threshold quantity, $\mathcal{R}_M$, measures the average number of new adult female mosquitoes (offspring) produced by one reproductive adult female mosquito during its entire reproductive period (Ngwa et al., 2010). It is the product of the egg oviposition rate (ψ_U), the fraction of eggs that survived and hatched into larvae (a), fraction of larvae that survived all four larval instar stages and matured into pupae (b), the fraction of pupae that developed into adult female mosquitoes (c) and the total average duration in the adult stage (of mosquitoes of all three types) (d).

The total duration in the adult stage can further be simplified to:

$$\frac{\alpha\tau_W^*\eta_V^*}{C_5C_6C_7-\alpha\tau_W^*\eta_V^*\gamma_U}=\Big(\frac{\eta_V^*}{C_5}\Big)\cdot\Big(\frac{\alpha\tau_W^*}{C_6}\Big)\cdot\Big[\sum_{i=0}^{n\to\infty}\Big(\frac{\gamma_U}{C_7}\cdot\frac{\eta_V^*}{C_5}\cdot\frac{\alpha\tau_W^*}{C_6}\Big)^i\Big]\cdot\Big(\frac{1}{C_7}\Big),$$

where $\frac{\eta_V^*}{C_5}$, $\frac{\alpha\tau_W^*}{C_6}$ and $\frac{\gamma_U}{C_7}$ is the fraction of adult female mosquitoes that transit from type V to type W, type W to type U, and type U to type V, respectively, and $\frac{1}{C_7}$ is the average duration in the class of the reproducing mosquitoes (U class). Furthermore, n (usually $n \leq 6$ (Delatte et al., 2009)) denotes the number of times an adult female mosquito completes (or survives) all three stages of the adult gonotrophic cycle after the first cycle (i.e., $n = 0$ means that an adult female mosquito survived all three stages only once, and $n \geq 1$ indicates that the mosquito completes the cycle more than once). The result below follows from Theorem 2 in van den Driessche and Watmough (2002).

Theorem 2.4.1. *The trivial equilibrium ($\mathcal{T}_0$) is locally-asymptotically (LAS) stable whenever $\mathcal{R}_M < 1$, and unstable if $\mathcal{R}_M > 1$.*

Furthermore, the following result holds.

Theorem 2.4.2. *$\mathcal{T}_0$ is globally-asymptotically stable (GAS) in Ω whenever $\mathcal{R}_M \leq 1$.*

Proof. Consider the Lyapunov function

$$\mathcal{K}_1 = a_0\big[a_1E + a_2L_1 + a_3L_2 + a_4L_3 + a_5L_4\big] + a_6\big[a_7P + a_8V + a_9W + a_{10}U\big],$$

where,

$$\begin{aligned} &a_0 = \alpha\tau_W^*\eta_V^*\sigma_{L_4}f\sigma_P,\ a_1 = \sigma_E\sigma_{L_1}\sigma_{L_2}\sigma_{L_3},\ a_2 = C_E\sigma_{L_1}\sigma_{L_2}\sigma_{L_3},\ a_3 = C_1C_E\sigma_{L_2}\sigma_{L_3},\\ &a_4 = C_1C_2C_E\sigma_{L_3},\ a_5 = C_1C_2C_3C_E,\ a_6 = C_1C_2C_3C_4C_E,\\ &a_7 = \alpha\tau_W^*\eta_V^*f\sigma_P,\ a_8 = C_P\eta_V^*\alpha\tau_W^*,\ a_9 = C_PC_5\alpha\tau_W^*,\ a_{10} = C_PC_5C_6 \end{aligned} \tag{2.4.3}$$

with $C_E = \sigma_E + \mu_E$, $C_P = \sigma_P + \mu_P$, $C_i = \sigma_{L_i} + \mu_L$ (for $i = 1, 2, 3, 4$), $C_5 = \eta_V^* + \mu_A$, $C_6 = \tau_W^* + \mu_A$, $C_7 = \gamma_U + \mu_A$. Thus, the Lyapunov derivative is given by:

$$\begin{aligned} \dot{\mathcal{K}}_1 &= a_0\big[a_1\dot{E} + a_2\dot{L}_1 + a_3\dot{L}_2 + a_4\dot{L}_3 + a_5\dot{L}_4\big] + a_6\big[a_7\dot{P} + a_8\dot{V} + a_9\dot{W} + a_{10}\dot{U}\big],\\ &= a_0\Bigg\{a_1\left[\psi_U\left(1 - \frac{U}{K_U}\right)_+U - C_EE\right] + a_2\big[\sigma_EE - (C_1 + \delta_LL)L_1\big] + a_3\big[\sigma_{L_1}L_1 - (C_2\\ &\quad + \delta_LL)L_2\big] + a_4\big[\sigma_{L_2}L_2 - (C_3 + \delta_LL)L_3\big] + a_5\big[\sigma_{L_3}L_3 - (C_4 + \delta_LL)L_4\big]\Bigg\} + a_6\Big[a_7\\ &\quad (\sigma_{L_4}L_4 - C_PP) + a_8\big(f\sigma_PP + \gamma_UU - C_5V\big) + a_9\big(\eta_V^*V - C_6W\big) + a_{10}\big(\alpha\tau_W^*W - C_7U\big)\Big]. \end{aligned} \tag{2.4.4}$$

Using (2.4.3) in (2.4.4), and simplifying, gives:

$$\begin{aligned} \dot{\mathcal{K}}_1 &= a_7\sigma_E\prod_{j=1}^{4}\sigma_{L_j}\left[\psi_U\left(1 - \frac{U}{K_U}\right)_+U\right] + C_EC_P\prod_{j=1}^{4}C_j\big(\eta_V^*\alpha\tau_W^*\gamma_U - C_5C_6C_7\big)U - \delta_LLS,\\ &= C_EC_PD\big(\mathcal{R}_M - 1\big)U\prod_{j=1}^{4}C_j - a_7\sigma_E\psi_U\frac{U^2}{K_U}\prod_{j=1}^{4}\sigma_{L_j} - \delta_LLS, \end{aligned} \tag{2.4.5}$$

where $S = a_0\big[a_2L_1 + a_3L_2 + a_4L_3 + a_5L_4\big]$ and $D = C_5C_6C_7 - \alpha\tau_W^*\eta_V^*\gamma_U > 0$. Thus, it follows from (2.4.5) that, for $\mathcal{R}_M \leq 1$ in Ω, the Lyapunov derivative $\dot{\mathcal{K}}_1 \leq 0$ (with $\dot{\mathcal{K}}_1 = 0$ if and only if $L_1 = L_2 = L_3 = L_4 = U = 0$). Furthermore, substituting

$L_1 = L_2 = L_3 = L_4 = U = 0$ into the model (2.4.1) gives:

$$\begin{aligned}
\frac{dE}{dt} &= -(\sigma_E + \mu_E)\, E, \\
\frac{dP}{dt} &= -(\sigma_P + \mu_P)\, P, \\
\frac{dV}{dt} &= f\sigma_P P - \left(\eta_V^* + \mu_A\right) V, \\
\frac{dW}{dt} &= \eta_V^* V - (\tau_W^* + \mu_A)\, W, \\
\frac{dU}{dt} &= \alpha\tau_W^* W.
\end{aligned} \tag{2.4.6}$$

It can be deduced from the last equation of (2.4.6) that $W = 0$. Substitution $U = W = 0$ in (2.4.6) show that $E = P = V = 0$. Thus, it follows from the LaSalle's Invariance Principle (Theorem 6.4 in LaSalle (1976)) that the maximal invariant set contained in $\{\left(E, L_1, L_2, L_3, L_4, P, V, W, U\right) \in \Omega \,|\, \dot{\mathcal{K}}_1 = 0\}$ is $\{\mathcal{T}_0\}$. Hence, the trivial equilibrium $\mathcal{T}_0$ is GAS in Ω whenever $\mathcal{R}_M \leq 1$. □

The ecological implication of Theorem 2.4.2 is that the mosquito population (both immature and mature) will be effectively controlled in (or eliminated from) the community if the associated vectorial reproduction threshold, $\mathcal{R}_M$, can be brought to (and maintained at) a value less than or equal to unity. In other words, a vector control strategy (e.g., larvaciding or adulticiding that can bring $\mathcal{R}_M$ to a value less than unity can lead to the effective control of the mosquito population in the community).

2.4.2 Existence and Asymptotic Stability of Non-trivial Equilibrium Point

The existence and stability of a non-trivial equilibrium of the autonomous model (2.4.1) is explored in this Section. Let $\mathcal{T}_1^{**} = \left(E^{**}, L_1^{**}, L_2^{**}, L_3^{**}, L_4^{**}, P^{**}, V^{**}, W^{**}, U^{**}\right)$ represents an arbitrary non-trivial equilibrium of the model (2.4.1). Solving for the

state variables of the model (2.4.1) at $\mathcal{T}_1^{**}$ gives

$$E^{**} = \frac{\psi_U}{C_E}\left(1 - \frac{U^{**}}{K_U}\right)U^{**},\ E^{**} = \frac{1}{\sigma_E}\big(C_1 + \delta_L L^{**}\big)L_1^{**},\ L_1^{**} = \frac{1}{\sigma_{L_1}}\big(C_2 + \delta_L L^{**}\big)L_2^{**},$$
$$L_2^{**} = \frac{1}{\sigma_{L_2}}\big(C_3 + \delta_L L^{**}\big)L_3^{**},\ L_3^{**} = \frac{1}{\sigma_{L_3}}\big(C_4 + \delta_L L^{**}\big)L_4^{**},\ L_4^{**} = \frac{C_P D U^{**}}{\alpha\tau_W^*\eta_V^*\sigma_P\sigma_{L_4}},$$
$$P^{**} = \frac{DU^{**}}{\alpha\tau_W^*\eta_V^*\sigma_P},\ V^{**} = \frac{C_6C_7U^{**}}{\alpha\tau_W^*\eta_V^*},\ W^{**} = \frac{C_7U^{**}}{\alpha\tau_W^*},\ U^{**} = \frac{\alpha\tau_W^*\eta_V^*\sigma_P\sigma_{L_4}L_4^{**}}{C_PD}. \tag{2.4.7}$$

where $D = C_5C_6C_7 - \alpha\tau_W^*\eta_V^*\gamma_U > 0$. It follows from (2.4.7) that

$$L_j^{**} \ = \ \frac{\big(C_{j+1} + \delta_L L^{**}\big)L_{j+1}^{**}}{\sigma_{L_j}};\ j = 1, 2, 3. \tag{2.4.8}$$

It can be shown, by multiplying the second, third, fourth and fifth equations of (2.4.7), and substituting the first and sixth equations of (2.4.7) into the resulting equation (and simplifying), that:

$$\alpha\tau_W^*\eta_V^*\psi_U\sigma_E\sigma_P\left(1 - \frac{U^{**}}{K_U}\right)\prod_{j=1}^{4}\sigma_{L_j} \ = \ C_EC_PD\prod_{i=1}^{4}\big(C_i + \delta_L L^{**}\big). \tag{2.4.9}$$

Substituting the equation for U^{**} in (2.4.7) into (2.4.9), and simplifying, gives (it can be shown that $L_4^{**} > 0$)

$$L_4^{**} = \frac{K_UC_PD}{\alpha\tau_W^*\eta_V^*\sigma_P\sigma_{L_4}}\left[1 - \frac{C_EC_PD\prod_{i=1}^{4}\big(C_i + \delta_L L^{**}\big)}{\alpha\tau_W^*\eta_V^*\psi_U\sigma_E\sigma_P\prod_{j=1}^{4}\sigma_{L_j}}\right]. \tag{2.4.10}$$

Furthermore, substituting the expressions for L_i $(i = 1, 2, 3)$, given in (2.4.8), into $L^{**} = \sum_{i=1}^{4} L_i^{**}$ gives,

$$L^{**} = \frac{L_4^{**}}{\prod_{j=1}^{3}\sigma_{L_j}}\left[\prod_{j=1}^{3}\sigma_{L_j} + \prod_{j=1}^{2}\sigma_{L_j}\big(C_4 + \delta_L L^{**}\big) + \sigma_{L_1}\prod_{i=3}^{4}\big(C_i + \delta_L L^{**}\big) + \prod_{i=2}^{4}\big(C_i + \delta_L L^{**}\big)\right]. \tag{2.4.11}$$

Finally, substituting Equation (2.4.10) into (2.4.11), and simplifying, shows that the non-trivial equilibria of the model (2.4.1) satisfy the following polynomial:

$$b_7(L^{**})^7 + b_6(L^{**})^6 + b_5(L^{**})^5 + b_4(L^{**})^4 + b_3(L^{**})^3 + b_2(L^{**})^2 + b_1(L^{**}) + b_0 = 0, \tag{2.4.12}$$

where the coefficients b_i $(i = 0, \ldots, 7)$ are constants, and are given in Appendix A1. It follows from the expressions of b_i $(i = 0, \ldots, 7)$ in Appendix A1 that:

(i) The coefficients b_i $(i = 0, \ldots, 7) > 0$ whenever $\mathcal{R}_M < 1$. Thus, no positive solution exists whenever $\mathcal{R}_M < 1$. Furthermore, when $\mathcal{R}_M = 1$, the coefficients b_i $(i = 1, \ldots, 7) > 0$ and $b_0 = 0$ (thus, the polynomial has no positive roots for the case when $\mathcal{R}_M = 1$).

(ii) The polynomial (2.4.12) has at least one positive root whenever $\mathcal{R}_M > 1$ (using the Descartes' Rule of Signs).

These results are summarized below.

Theorem 2.4.3. *The model* (2.4.1) *has at least one non-trivial (non-zero) equilibrium whenever* $\mathcal{R}_M > 1$*, and no non-trivial equilibrium whenever* $\mathcal{R}_M \leq 1$*.*

Furthermore, it is worth stating that, for the special case of the autonomous model (2.4.1) with no density-dependent larval mortality (i.e., $\delta_L = 0$), the coefficients b_i $(i = 2, \ldots, 7) = 0$ and $b_1 = 1$. Thus, in this special case with $\delta_L = 0$, the polynomial (2.4.12) reduces to $L^{**} + b_0 = 0$, so that (where Q_1 and X_6 are defined in Appendix A1)

$$L^{**} = \left(1 - \frac{1}{\mathcal{R}_M}\right) Q_1 X_6. \tag{2.4.13}$$

Thus, in the absence of density-dependent larval mortality (i.e., $\delta_L = 0$), the autonomous model (2.4.1) has a unique non-trivial equilibrium (denoted by $\mathcal{T}_1 = (E^{**}, L_1^{**},$

$L_2^{**}, L_3^{**}, L_4^{**}, P^{**}, V^{**}, W^{**}, U^{**})$) whenever $\mathcal{R}_M > 1$ (the components of this unique equilibrium can be obtained by substituting (2.4.13) into (2.4.7)).

Theorem 2.4.4. *The model* (2.4.1) *with* $\delta_L = 0$ *has a unique non-trivial equilibrium whenever* $\mathcal{R}_M > 1$*, and no non-trivial equilibrium otherwise.*

Asymptotic Stability of Non-trivial Equilibrium Point: Special Case

Consider the special case of the autonomous model (2.4.1) in the absence of density-dependent mortality rate for larvae (i.e., $\delta_L = 0$), so that the model (2.4.1) has a unique non-trivial equilibrium ($\mathcal{T}_1$) whenever $\mathcal{R}_M > 1$. Linearizing the autonomous model (2.4.1), with $\delta_L = 0$, at $\mathcal{T}_1$ gives:

$$\mathcal{J}(\mathcal{T}_1) = \begin{bmatrix} -C_E & 0 & 0 & 0 & 0 & 0 & 0 & 0 & \psi_U\left(\frac{2}{\mathcal{R}_M} - 1\right) \\ \sigma_E & -C_1 & 0 & 0 & 0 & 0 & 0 & 0 & 0 \\ 0 & \sigma_{L_1} & -C_2 & 0 & 0 & 0 & 0 & 0 & 0 \\ 0 & 0 & \sigma_{L_2} & -C_3 & 0 & 0 & 0 & 0 & 0 \\ 0 & 0 & 0 & \sigma_{L_3} & -C_4 & 0 & 0 & 0 & 0 \\ 0 & 0 & 0 & 0 & \sigma_{L_4} & -C_P & 0 & 0 & 0 \\ 0 & 0 & 0 & 0 & 0 & f\sigma_P & -C_5 & 0 & \gamma_U \\ 0 & 0 & 0 & 0 & 0 & 0 & \eta_V^* & -C_6 & 0 \\ 0 & 0 & 0 & 0 & 0 & 0 & 0 & \alpha\tau_W^* & -C_7 \end{bmatrix},$$

where, $C_E = \sigma_E + \mu_E, C_P = \sigma_P + \mu_P, C_i = \sigma_{L_i} + \mu_L$ (for $i = 1, 2, 3, 4), C_5 = \eta_V^* + \mu_A, C_6 = \tau_W^* + \mu_A, C_7 = \gamma_U + \mu_A$. The eigenvalues of $\mathcal{J}(\mathcal{T}_1)$ satisfy:

$$\begin{aligned} P_9(\lambda) = \lambda^9 + A_8\lambda^8 + A_7\lambda^7 + A_6\lambda^6 + A_5\lambda^5 + A_4\lambda^4 + A_3\lambda^3 + A_2\lambda^2 + A_1\lambda \\ + CD(\mathcal{R}_M - 1), \end{aligned} \tag{2.4.14}$$

where $C = C_E C_P \prod_{j=1}^{4} C_j$, $D = C_5 C_6 C_7 - \alpha \tau_W^* \eta_V^* \gamma_U$ and A_i $(i = 1, \ldots, 8)$ are positive constants given in Appendix A2.

It is convenient to re-write the polynomial (2.4.14) as

$$P_9(\lambda) = F(\lambda)G(\lambda) + CD\big(\mathcal{R}_M - 2\big), \tag{2.4.15}$$

where,

$$F(\lambda) = (\lambda + C_E)(\lambda + C_P)(\lambda + C_1)(\lambda + C_2)(\lambda + C_3)(\lambda + C_4), \tag{2.4.16}$$

$$G(\lambda) = \lambda^3 + (C_5 + C_6 + C_7)\lambda^2 + (C_5 C_6 + C_5 C_7 + C_6 C_7)\lambda + D, \tag{2.4.17}$$

so that,

$$F(\lambda)G(\lambda) = \lambda^9 + A_8\lambda^8 + A_7\lambda^7 + A_6\lambda^6 + A_5\lambda^5 + A_4\lambda^4 + A_3\lambda^3 + A_2\lambda^2 + A_1\lambda + CD. \tag{2.4.18}$$

The asymptotic stability of $\mathcal{T}_1$ will be explored using the properties of *Bézout* matrices (Hershkowitz, 1992). It is, first of all, convenient to recall the following four results:

Theorem 2.4.5. (Routh-Hurwitz (Hershkowitz, 1992)). *Let A be an $n \times n$ complex matrix, and let E_k be the sum of all principal minors of A of order k, $k \in < n >$. Let $\Omega(A)$ be the $n \times n$ Hurwitz matrix of A and assume that $\Omega(A)$ is real. Then A is stable if and only if all leading principal minors of $\Omega(A)$ are positive.*

Definition 2.4.1. (Bézout Matrix (Hershkowitz, 1992)). Let $a(x)$ and $b(x)$ be two polynomials with real coefficients of degree n and m respectively, $n \geq m$. The *Bézoutiant* defined by $a(x)$ and $b(x)$ is the bilinear form

$$\frac{a(x)b(y) - a(y)b(x)}{x - y} = \sum_{i,k=0}^{n-1} b_{ik} x^i y^k.$$

The symmetric matrix $(b_{ik})_0^{n-1}$ associated with this bilinear form is called the *Bézout matrix* and is denoted by $B_{a,b}$. Each entry $b_{i,j}$ of $B_{a,b}$ can be computed separately by

the entry formula

$$b_{i,j} = \sum_{k=\max(0,i-j)}^{\min(i,n-1-j)} \left(b_{i-k}a_{j+1+k} - a_{i-k}b_{j+1+k}\right) \text{ for all } i,j \leq n.$$

Theorem 2.4.6. (Liénard-Chipart (Hershkowitz, 1992)) *Let* $f(x) = x^n - a_n x^{n-1} - \ldots - a_1$ *be a polynomial with real coefficients, and let* $a_{n-1} = -1$. *Define the polynomials*

$$h(u) = -a_1 - a_3 u - \cdots,$$

$$g(u) = -a_2 - a_4 u - \cdots.$$

The polynomial $f(x)$ *is negative stable if and only if the Bézout matrix* $B_{h,g}$ *is positive definite and* $a_i < 0$ *for all* $i \in < n >$.

Theorem 2.4.7. (Sylvester's Criterion (George, 1991)) *A real, symmetric matrix is positive definite if and only if all its principal minors are positive.*

We claim the following result.

Lemma 2.4.1. *The polynomial* $F(\lambda)G(\lambda)$, *defined by Equations* (2.4.16), (2.4.17) *and* (2.4.18), *is Hurwitz stable (i.e., all its roots have negative real part).*

Proof. It follows from the equation for $F(\lambda)$ in (2.4.16) that all roots of $F(\lambda)$ are negative. Furthermore, consider $G(\lambda) = 0$ from (2.4.17). That is,

$$G(\lambda) = \lambda^3 + (C_5 + C_6 + C_7)\lambda^2 + (C_5C_6 + C_5C_7 + C_6C_7)\lambda + D = 0.$$

Using the Routh-Hurwitz Criterion (Theorem 2.4.5), the principal minors, Δ_k ($k = 1, 2, 3$), of the associated Hurwitz matrix for $G(\lambda)$ are:

$$\Delta_1 = C_5 + C_6 + C_7 > 0,$$

$$\Delta_2 = (C_5 + C_6 + C_7)(C_5C_6 + C_5C_7) + C_6C_7(C_6 + C_7) + \alpha\tau_W^*\eta_V^*\gamma_U > 0,$$

$$\Delta_3 = (C_5C_6C_7 - \alpha\tau_W^*\eta_V^*\gamma_U)\Delta_2 > 0.$$

Thus, all the roots of $G(\lambda)$ have negative real part. Hence, all nine roots of $F(\lambda)G(\lambda)$ have negative real part. $\square$

Remark 2.4.1. *It follows from Lemma 2.4.1 and Theorem 2.4.6 that the corresponding Bézout matrix of $F(\lambda)G(\lambda)$ is positive-definite (Hershkowitz, 1992).*

Remark 2.4.2. *Consider $P_9(\lambda) = F(\lambda)G(\lambda) + CD(\mathcal{R}_M - 2)$. Then, $P_9(\lambda) \leq F(\lambda)G(\lambda)$ whenever $1 < \mathcal{R}_M \leq 2$. Thus, it follows from Lemma 2.4.1 that all nine roots of $P_9(\lambda)$ have negative real part whenever $1 < \mathcal{R}_M \leq 2$ (hence, $\mathcal{T}_1$ is LAS whenever $1 < \mathcal{R}_M \leq 2$).*

Furthermore, consider the characteristic polynomial $P_9(\lambda)$ given in (2.4.14). Let $A_0 = CD(\mathcal{R}_M - 1)$, where $C = C_E C_P \prod_{j=1}^{4} C_j$, $D = C_5 C_6 C_7 - \alpha \tau_W^* \eta_V^* \gamma_U$,

$$P_9(\lambda) = \lambda^9 + A_8\lambda^8 + A_7\lambda^7 + A_6\lambda^6 + A_5\lambda^5 + A_4\lambda^4 + A_3\lambda^3 + A_2\lambda^2 + A_1\lambda + A_0.$$

To apply Theorem 2.4.6, let

$$h(u) = A_0 + A_2u + A_4u^2 + A_6u^3 + A_8u^4,\ g(u) = A_1 + A_3u + A_5u^2 + A_7u^3 + u^4.$$

Thus, it follows from Definition 2.4.1 that the corresponding *Bézout matrix* of $P_9(\lambda)$, denoted by $B_{h,g}(P_9)$, is given by $B_{h,g}(P_9) =$

$$\begin{bmatrix} A_1A_2 - A_0A_3 & A_1A_4 - A_0A_5 & A_1A_6 - A_0A_7 & A_1A_8 - A_0 \\ A_1A_4 - A_0A_5 & A_3A_4 - A_2A_5 + A_1A_6 - A_0A_7 & A_3A_6 - A_2A_7 + A_1A_8 - A_0 & A_3A_8 - A_2 \\ A_1A_6 - A_0A_7 & A_3A_6 - A_2A_7 + A_1A_8 - A_0 & A_5A_6 - A_4A_7 + A_1A_8 - A_2 & A_5A_8 - A_4 \\ A_1A_8 - A_0 & A_3A_8 - A_2 & A_5A_8 - A_4 & A_7A_8 - A_6 \end{bmatrix}.$$

Sylvester's Criterion (Theorem 2.4.7) can be used to obtain the necessary and sufficient conditions for $B_{h,g}(P_9)$ to be positive-definite. First of all, it is evident that $B_{h,g}(P_9)$ is symmetric. It then suffices to show that the k^{th} leading principal minor of $B_{h,g}(P_9)$ is positive (i.e., to show that the determinant of the upper-left $k \times k$ submatrix of $B_{h,g}(P_9)$ is positive). It is convenient to introduce the following notations:

(i) $b_{i,j}^{(J)} : 0 \leq i,j \leq 3, J \in \{FG,\, P_9\}$ are the entries of the corresponding *Bézout matrix* of the polynomial $F(\lambda)G(\lambda)$ (denoted by $B_{h,g}(FG)$) and $P_9(\lambda)$ (clearly, $B_{h,g}(FG) = B_{h,g}(P_9)$ when $A_0 = CD$).

(ii) $\Delta_k^{(P_9)}$ is the k^{th} leading principal minor of *Bézout matrix* $B_{h,g}(P_9)$.

Therefore, $B_{h,g}(P_9)$ can be re-written (in terms of the entries of the positive-definite *Bézout matrix*, $B_{h,g}(FG)$. That is, in terms of $b_{i,j}^{(FG)}$) as

$$B_{h,g}(P_9) = \begin{bmatrix} b_{0,0}^{(FG)} - CD(\mathcal{R}_M - 2)A_3 & b_{0,1}^{(FG)} - CD(\mathcal{R}_M - 2)A_5 & b_{0,2}^{(FG)} - CD(\mathcal{R}_M - 2)A_7 & b_{0,3}^{(FG)} - CD(\mathcal{R}_M - 2) \\ b_{1,0}^{(FG)} - CD(\mathcal{R}_M - 2)A_5 & b_{1,1}^{(FG)} - CD(\mathcal{R}_M - 2)A_7 & b_{1,2}^{(FG)} - CD(\mathcal{R}_M - 2) & b_{1,3}^{(FG)} \\ b_{2,0}^{(FG)} - CD(\mathcal{R}_M - 2)A_7 & b_{2,1}^{(FG)} - CD(\mathcal{R}_M - 2) & b_{2,2}^{(FG)} & b_{2,3}^{(FG)} \\ b_{3,0}^{(FG)} - CD(\mathcal{R}_M - 2) & b_{3,1}^{(FG)} & b_{3,2}^{(FG)} & b_{3,3}^{(FG)} \end{bmatrix}.$$

It follows from Remark 2.4.2 that the *Bézout matrix*, $B_{h,g}(P_9)$, is a positive definite matrix for $1 < \mathcal{R}_M \leq 2$. Furthermore, the *Bézout matrix*, $B_{h,g}(P_9)$, can be re-written as (after row-column operations)

$$B_{h,g}(P_9) = \begin{bmatrix} \Delta_1^{(P_9)} & b_{0,1}^{(P_9)} & b_{0,2}^{(P_9)} & b_{0,3}^{(P_9)} \\ 0 & \dfrac{\Delta_2^{(P_9)}}{\Delta_1^{(P_9)}} & b_{1,2}^{(P_9)} - \dfrac{b_{0,1}^{(P_9)} b_{0,3}^{(P_9)}}{b_{0,0}^{(P_9)}} & b_{1,3}^{(P_9)} - \dfrac{b_{0,1}^{(P_9)} b_{0,4}^{(P_9)}}{b_{0,0}^{(P_9)}} \\ 0 & 0 & \dfrac{\Delta_3^{(P_9)}}{\Delta_2^{(P_9)}} & B_1 \\ 0 & 0 & 0 & \dfrac{\Delta_4^{(P_9)}}{\Delta_3^{(P_9)}} \end{bmatrix}, \tag{2.4.19}$$

where $B_1 = B_1\big(b_{i,j}^{(P_9)}\big)$ $0 \leq i,j \leq 3$. However, since the k^{th} leading principal minor of a triangular matrix is the product of its diagonal elements up to row k, Sylvester's Criterion is equivalent to finding conditions for which all the diagonal elements of *Bézout matrix*, $B_{h,g}(P_9)$, in (2.4.19) are all positive (i.e., finding the conditions for which $\Delta_k^{(P_9)}$ are positive for all $k = 1, 2, 3, 4$) (Porphyre et al., 2005). For example, it

can be verified that the first leading principal minor of the matrix $B_{h,g}(P_9)$, given by

$$\begin{aligned}\Delta_1^{(P_9)} &= A_1A_2 - C_EC_P(C_5C_6C_7 - \alpha\tau_W^*\eta_V^*\gamma_U)(\mathcal{R}_M - 1)A_3\prod_{j=1}^{4}C_j \\ &= b_{0,0}^{(FG)} - C_EC_P(C_5C_6C_7 - \alpha\tau_W^*\eta_V^*\gamma_U)(\mathcal{R}_M - 2)A_3\prod_{j=1}^{4}C_j,\end{aligned}$$

is positive whenever the following inequality holds:

$$\mathcal{R}_M < 2 + \frac{b_{0,0}^{(FG)}}{C_EC_P(C_5C_6C_7 - \alpha\tau_W^*\eta_V^*\gamma_U)A_3\prod_{j=1}^{4}C_j} = 2 + Z_1,$$

where, $b_{0,0}^{(FG)} = A_1A_2 - C_EC_P(C_5C_6C_7 - \alpha\tau_W^*\eta_V^*\gamma_U)A_3\prod_{j=1}^{4}C_j > 0$ is the first leading principal minor of $B_{h,g}(FG)$ and Z_1 is the positive constant such that $\Delta_1^{(P_9)}$ is positive whenever $\mathcal{R}_M < 2 + Z_1$. Similarly, we obtain constants $Z_k = Z_k\big(b_{i,j}^{(FG)}\,(0 \leq i,j \leq 3),\, A_i\,(1 \leq i \leq 9), C, D\big)$ such that the k^{th} principal minor $\Delta_k^{(P_9)}$ is positive whenever $\mathcal{R}_M < 2 + Z_k$, for each $k = 2,3,4$ (i.e., Z_i $(i = 1,2,3,4)$, is the constant such that $\mathcal{R}_M < 2 + Z_i$ makes the determinant of the associated matrix of minors of matrix (2.4.19) to be positive). Therefore, the result below follows (from the above derivations and Remark 2.4.2).

Theorem 2.4.8. *Consider the model* (2.4.1) *with* $\delta_L = 0$. *The unique non-trivial equilibrium* $(\mathcal{T}_1)$ *is LAS in* $\Omega \setminus \{\mathcal{T}_0\}$ *whenever*

$$1 < \mathcal{R}_M < \mathcal{R}_M^C = 2 + \min\left\{Z_k : \Delta_k^{(P_9)} > 0 \text{ for all } k = 1,2,3,4\right\},$$

and unstable whenever $\mathcal{R}_M > \mathcal{R}_M^C$.

The two results above (Theorem 2.4.4 and Theorem 2.4.8) show that the condition $\mathcal{R}_M > 1$ defines the existence of a unique non-trivial equilibrium $\big(\mathcal{T}_1\big)$ of the special case of the model (2.4.1) with $\delta_L = 0$ (which is LAS if $1 < \mathcal{R}_M < \mathcal{R}_M^C$). Thus, it can be deduced that, to maintain a non-trivial mosquito population, each reproducing

adult female mosquito (of type U) must produce at least one egg during its entire reproductive life period (see also Ngwa (2006)). In other words, an increase in adult female mosquitoes of type $U(t)$ leads to a corresponding increase in the number of eggs laid in the population ($E(t)$. We claim the following result.

2.4.3 Hopf Bifurcation Analysis

Consider the special case of the autonomous model (2.4.1) with $\delta_L = 0$ and $\mathcal{R}_M > 1$ (so that $\mathcal{T}_1$ exists, by Theorem 2.4.4). Hopf bifurcation can occur (at a fixed value of a chosen bifurcation parameter) when the Jacobian of this special case of the system (2.4.1) with $\delta_L = 0$, evaluated at $\mathcal{T}_1$, has a pair of purely imaginary eigenvalues (i.e.,, when the polynomial $P_9(\lambda)$ given by (2.4.14), has a pair of purely imaginary roots). The rank and signature of the *Bézout matrix*, $B_{h,g}(P_9)$, can be used to evaluate the number of roots with negative real parts. The direct effect of the characteristic polynomial P_9 having a pair of purely imaginary eigenvalues is that the rank of the *Bézout matrix*, $B_{h,g}(P_9)$, is reduced by exactly one (Parks, 1977). From the stability point of view, this possibility represent the existence of a boundary (Hopf bifurcation) (Parks, 1977). To prove the existence of Hopf bifurcation, it also suffices to verify the transversality condition (Chow et al., 1994).

Let ψ_U be a bifurcation parameter. Solving for ψ_U from $\mathcal{R}_M = \mathcal{R}_M^C$ gives

$$\psi_U = \psi_U^* = \frac{C_E C_P\big(C_5C_6C_7 - \alpha\tau_W^*\eta_V^*\gamma_U\big)(2+Z_4)\prod_{j=1}^{4} C_j}{\alpha\tau_W^*\eta_V^*\sigma_E\sigma_P\prod_{j=1}^{4}\sigma_{L_j}},$$

where Z_4 is as defined in Theorem 2.4.8.

Theorem 2.4.9. *Consider the autonomous model* (2.4.1) *with* $\delta_L = 0$. *A Hopf bifurcation occurs at* $\psi_U = \psi_U^*$.

Proof. To prove Theorem 2.4.9, it is sufficient to establish the transversality condition [49]. Let $\psi_U = \psi_U^*$ (and all other parameters of the model (2.4.1) are fixed). Then, $\mathcal{R}_M = \mathcal{R}_M^C = 2 + Z_4$. Since $Z_4 < Z_i$ ($i = 1, 2, 3$), it follows from Theorem 2.4.8 that $\Delta_i^{(P_9)} > 0$ for $i = 1, 2, 3$. Furthermore, $\Delta_4^{(P_9)}$ can be re-written as (where $B = \sigma_E \sigma_P \prod_{j=1}^{4} \sigma_{L_j}$, $C = C_E C_P \prod_{j=1}^{4} C_j$, $D = C_5 C_6 C_7 - \alpha \tau_W^* \eta_V^* \gamma_U$)

$$\Delta_4^{(P_9)} = \begin{vmatrix} b_{0,0}^{(FG)} - (\alpha\tau_W^*\eta_V^*\psi_U B - 2CD)A_3 & b_{0,1}^{(FG)} - (\alpha\tau_W^*\eta_V^*\psi_U B - 2CD)A_5 & b_{0,2}^{(P_9)} & b_{0,3}^{(P_9)} \\ b_{1,0}^{(FG)} - (\alpha\tau_W^*\eta_V^*\psi_U B - 2CD)A_5 & b_{1,1}^{(FG)} - (\alpha\tau_W^*\eta_V^*\psi_U B - 2CD)A_7 & b_{1,2}^{(P_9)} & b_{1,3}^{(P_9)} \\ b_{2,0}^{(FG)} - (\alpha\tau_W^*\eta_V^*\psi_U B - 2CD)A_7 & b_{2,1}^{(FG)} - (\alpha\tau_W^*\eta_V^*\psi_U B - 2CD) & b_{2,2}^{(P_9)} & b_{2,3}^{(P_9)} \\ b_{3,0}^{(FG)} - (\alpha\tau_W^*\eta_V^*\psi_U B - 2CD) & b_{3,1}^{(P_9)} & b_{3,2}^{(P_9)} & b_{3,3}^{(P_9)} \end{vmatrix}.$$

Hence, $\Delta_4^{(P_9)}(\psi_U) = 0$ if and only if $\psi_U = \psi_U^*$. Furthermore, it can be verified that

$$\left.\frac{d\Delta_4^{(P_9)}(\psi_U)}{d\psi_U}\right|_{\psi_U=\psi_U^*} = \mathrm{Tr}\left(\left.\mathrm{Adj}(B_{h,g}(P_9)(\psi_U))\right|_{\psi_U=\psi_U^*} \left.\frac{dB_{h,g}(P_9)(\psi_U)}{d\psi}\right|_{\psi_U=\psi_U^*}\right) \neq 0,$$

where 'Tr' and 'Adj' denote, respectively, the trace and adjoint of a matrix. Similarly, let μ_A be a bifurcation parameter (and all other parameters of the model (2.4.1) are fixed). Thus,

$$\left.\frac{d\Delta_4^{(P_9)}(\mu_A)}{d\psi}\right|_{\mu_A=\mu_A^*} = \mathrm{Tr}\left(\left.\mathrm{Adj}(B_{h,g}(P_9)(\mu_A))\right|_{\mu_A=\mu_A^*} \left.\frac{dB_{h,g}(P_9)(\mu_A)}{d\mu_A}\right|_{\mu_A=\mu_A^*}\right),$$

for all $\Delta_4^{(P_9)}(\mu_A^*) = 0$. It can be verified that $\left.\frac{d\Delta_4^{(P_9)}(\mu_A)}{d\psi}\right|_{\mu_A=\mu_A^*} \neq 0$. □

Theorem 2.4.9 shows that sustained oscillations are possible, with respect to the special case of the autonomous model (2.4.1) with $\delta_L = 0$, whenever $\mathcal{R}_M = \mathcal{R}_M^C$. This result, which is numerically illustrated in Figure 2.6 (a), is in line with that reported in Abdelrazec and Gumel (2017) using a simple mosquito dynamics population model that does not incorporate vector gonotrophic cycle. It is worth mentioning that, in the proof of Theorem 2.4.9, two bifurcation parameters (ψ_U and μ_A) were considered. The reason is, that the transversality condition may fail at some points if only one

parameter is used (Chow et al., 1994). The nature of the Hopf bifurcation property of the model (2.4.1) is investigated numerically. The results obtained, depicted in Figure 2.6 (b), show convergence of the solutions to a stable limit cycle.

2.4.4 Numerical Illustrations

In this section, a bifurcation diagram for the special case of the autonomous model (2.4.1) with $\delta_L = 0$, which summarizes the main results obtained in Section 2.4, will be generated in the $\mu_A - \psi_U$ plane as follows:

(i) Solving for ψ_U from $\mathcal{R}_M = 1$ gives the following equation for ψ_U^l (depicted in Figure 2.7):

$$l: \quad \psi_U = \psi_U^l = \frac{C_E C_P \big(C_5 C_6 C_7 - \alpha \tau_W^* \eta_V^* \gamma_U\big) \prod_{j=1}^{4} C_j}{\alpha \tau_W^* \eta_V^* \sigma_E \sigma_P \prod_{j=1}^{4} \sigma_{L_j}}.$$

(ii) Solving for ψ_U from $\Delta_4^{(P_9)} = 0$ (and fixing all parameters of the models (using their values as in Figure 2.5), except the parameters, μ_A and ψ_U) give the following curve $\Delta_4^{(P_9)} = 0$:

$$\mathcal{H}: \quad \psi_U = \psi_U^* = \frac{C_E C_P \big(C_5 C_6 C_7 - \alpha \tau_W^* \eta_V^* \gamma_U \big[2 + Z_4(\mu_A)\big]}{\alpha \tau_W^* \eta_V^* \sigma_E \sigma_P \prod_{j=1}^{4} \sigma_{L_j}},$$

where, $C_E = \sigma_E + \mu_E$, $C_P = \sigma_P + \mu_P$, $C_i = \sigma_{L_i} + \mu_L$ (for $i = 1, 2, 3, 4$), $C_5 = \eta_V^* + \mu_A$, $C_6 = \tau_W^* + \mu_A$, $C_7 = \gamma_U + \mu_A$. The curves l and $\mathcal{H}$ (depicted in Figure 2.7) divide the $\mu_A - \psi_U$ plane into three distinct regions, namely $\mathcal{D}_1$, $\mathcal{D}_2$ and $\mathcal{D}_3$, given by:

$$\mathcal{D}_1 = \big\{(\mu_A, \psi_U): \, 0 < \psi_U \leq \psi_U^l; \, \mu_A > 0\big\},$$

$$\mathcal{D}_2 = \big\{(\mu_A, \psi_U): \, \psi_U^l < \psi_U < \psi_U^*; \, \mu_A > 0\big\},$$

$$\mathcal{D}_3 = \big\{(\mu_A, \psi_U): \, \psi_U > \psi_U^*; \, \mu_A > 0\big\}.$$

The regions can be described as follows (see also Table 2.2):

(i) *Region* $\mathcal{D}_1$: In this region, $\mathcal{R}_M \leq 1$. Hence, in this region (note that $\delta_L = 0$), the trivial equilibrium ($\mathcal{T}_0$) is globally-asymptotically stable (in line with Theorem 2.4.2).

(ii) *Region* $\mathcal{D}_2$: Here, $1 < \mathcal{R}_M < \mathcal{R}_M^C$. Thus, the model has two equilibria, namely the unstable trivial equilibrium ($\mathcal{T}_0$) and the locally-asymptotically stable non-trivial equilibrium ($\mathcal{T}_1$). The model undergoes a Hopf bifurcation whenever $\mathcal{R}_M = \mathcal{R}_M^C$.

(iii) *Region* $\mathcal{D}_3$: In this region, $\mathcal{R}_M > \mathcal{R}_M^C$. Thus, the model has the unstable trivial equilibrium ($\mathcal{T}_1$), unstable non-trivial equilibrium and a stable limit cycle.

Threshold Condition	$\mathcal{T}_0$	$\mathcal{T}_1$	Existence of Stable Limit Cycle
$\mathcal{R}_M \leq 1$	GAS	No	No
$1 < \mathcal{R}_M < \mathcal{R}_M^C$	Unstable	LAS	No
$\mathcal{R}_M > \mathcal{R}_M^C$	Unstable	Unstable	Yes

Table 2.2: Stability properties of the solutions of the autonomous model (2.4.1).

It is worth mentioning that, for the fixed values of the parameters used in Figure 2.5, the associated bifurcation point of the model (2.4.1) with $\delta_L = 0$ is $\psi_U = \psi_U^* = 107.889493160695073$ (so that, $\Delta_2 = 0$). This is equivalent to $\mathcal{R}_M = \mathcal{R}_M^C = 4.5573$. Therefore, for this particular set of parameter values, the non-trivial equilibrium ($\mathcal{T}_1$) is LAS for $1 < \mathcal{R}_M < 4.5573$, and unstable whenever $\mathcal{R}_M > 4.5573$.

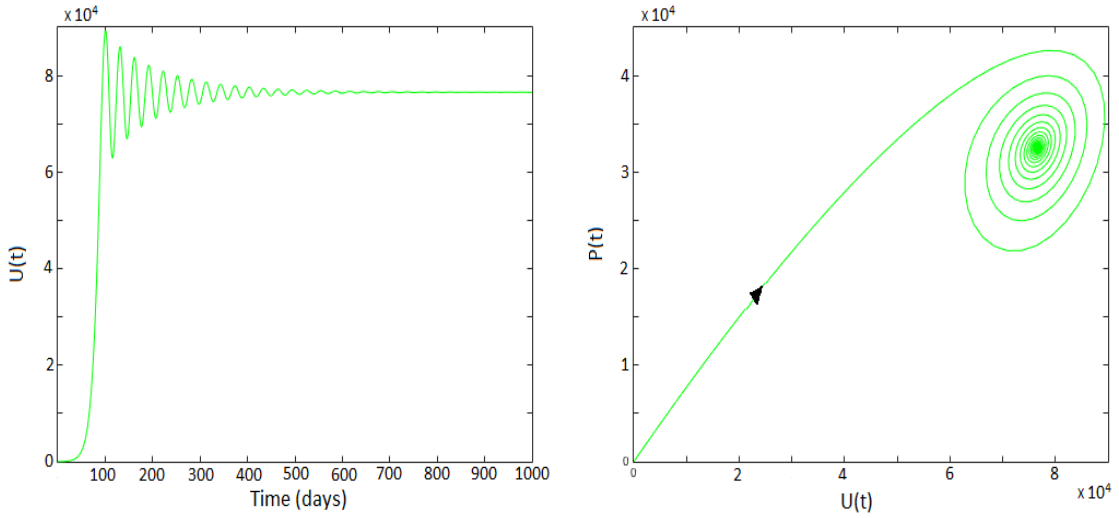

(a) $t - U$ plane (b) a stable $\mathcal{T}_1$

Figure 2.5: Simulations of the autonomous model (2.4.1), showing: (a) total number of adult female mosquitoes of type $U(t)$ as a function of time. (b) phase portrait of $U(t) - P(t)$ showing stable non-trivial equilibrium $\mathcal{T}_1$. The parameter values used are: $\psi_U = 100.91$, $K_U = 10^5$, $\sigma_E = 0.84$, $\mu_E = 0.05$, $\sigma_{L_1} = 0.15$, $\sigma_{L_2} = 0.11$, $\sigma_{L_3} = 0.24$, $\sigma_{L_4} = 0.5$, $\mu_L = 0.34$, $\delta_L = 0$, $K_L = 10^7$, $f\sigma_P = 0.8$, $\mu_P = 0.17$, $\gamma_U = 0.3$, $\eta_V^* = 0.4$, $\tau_W^* = 16$, $\alpha = 0.86$ and $\mu_A = 0.12$ (so that, $\mathcal{R}_M = 4.2625 < \mathcal{R}_M^C = 4.5573$).

2.4.5 Sensitivity Analysis

The autonomous model (2.4.1) contains 17 parameters, and uncertainties in the estimates of their values used in the numerical simulations of the model are expected to arise (Cariboni and Saltelli, 2007; Wu et al., 2013). Thus, it is instructive to assess the impact of such uncertainties on the overall numerical simulation results obtained. The effect of these uncertainties, as well as the determination of the parameters that have the greatest influence on the mosquitoes dispersal dynamics (with respect to a given response function), will be carried out using an uncertainty and sensitivity analysis (Blower and Dowlatabadi, 1994; Marino et al., 2008; McKay et al., 1979;

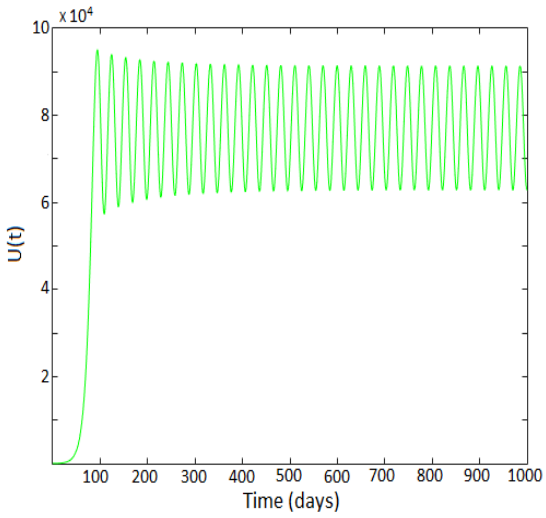

(a) $t - U$ plane

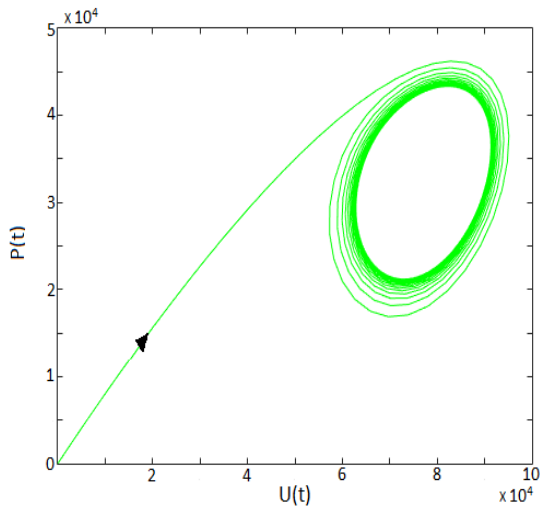

(b) a stable limit cycle

Figure 2.6: Simulations of the autonomous model (2.4.1), showing: (a) total number of adult female mosquitoes of type $U(t)$ as a function of time. (b) phase portrait of $U(t) - P(t)$ showing a stable limit cycle. The parameter values used are as given in the simulations for Figure 2.5, with $\psi_U = 110.91$ (so that, $\mathcal{R}_M = 4.6849 > \mathcal{R}_M^C = 4.5573$).

McLeod et al., 2006). In particular, following Blower and Dowlatabadi (1994), the Latin Hypercube Sampling (LHS) and Partial Rank Correlation Coefficients (PRCC) will be used for the autonomous model (2.4.1). The PRCC method of sensitivity analysis is an efficient and reliable sampling-based method that determines the sensitivity of an output state variable to an input parameter as a linear correlation. This method provides a measure of monotonicity between parameters and model output after removing the linear effects of all parameters except the parameter of interest (Blower and Dowlatabadi, 1994; Marino et al., 2008; Wu et al., 2013). PRCC is usually combined with LHS, which is a stratified Monte Carlo sampling method that divides each parameter's range into equal intervals and randomly draws one sample from each interval (only once) (Blower and Dowlatabadi, 1994; Helton and Davis,

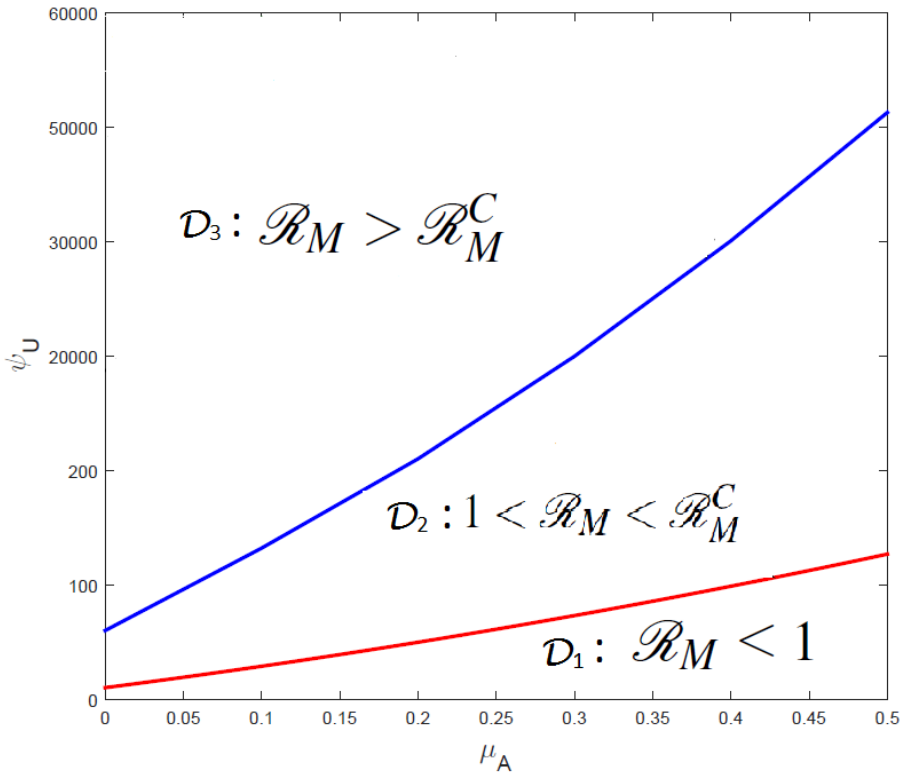

Figure 2.7: Bifurcation curves in the $\mu_A - \psi_U$ plane for the autonomous model (2.4.1).

2003; Wu et al., 2013). LHS is computationally-efficient, requiring fewer simulations than other Monte Carlo sampling approach (Helton and Davis, 2003; Wu et al., 2013). The combined LHS-PRCC procedure generally involves the following steps (Wu et al., 2013):

(i) Generating LHS of the parameter space.

(ii) Obtaining model output for each set of sampled parameters.

(ii) Ranking parameter and output values and replacing their original values with their ranks.

(iv) Calculating the PRCC for each input parameter.

The PRCC method is implemented on the model (2.4.1) using the range and baseline values of the parameters tabulated in Table 2.3. Appropriate response functions are chosen for these analyses. For instance, using the population of adult female mosquitoes of type U as the response function, it is shown in Table 2.4 that the top three PRCC-ranked parameters of the autonomous version of the model are the probability of adult female mosquito of type W successfully taking a bloodmeal (α), the natural mortality rate of adult female mosquitoes (μ_A) and the natural mortality rate of female larvae (μ_L).

Similarly, using the population of adult female mosquitoes of type V as the response function, the top three PRCC-ranked parameters are the natural mortality rate of female larvae (μ_L), the deposition rate of female eggs (ψ_U) and the maturation rate of female larvae from Stage 1 to Stage 2 (σ_{L_1}). Furthermore, using the population of female larvae in stage 4 (L_4) and population of female pupae (P) as the response functions, it is shown that the same top three PRCC-ranked parameters appeared as in the case when the population of adult female mosquitoes of type V is chosen as the response function for both cases. However, using the vectorial reproduction number of the autonomous version of the model ($\mathcal{R}_M$) as the response function, the top three PRCC-ranked parameters are the natural mortality rate of female larvae (μ_L), the deposition rate of female eggs (ψ_U) and the natural mortality rate of adult female mosquitoes (μ_A).

In summary, the sensitivity analyses conducted in this chapter led to the identification of five model parameters that significantly influence the population dynamics and dispersal of the mosquito, namely:

(a) the probability of adult female mosquito of type W successfully taking a bloodmeal (α);

(b) the natural mortality rate of adult female mosquitoes (μ_A);

(c) the natural mortality rate of female larvae (μ_L);

(d) the deposition rate of female eggs (ψ_U);

(e) the maturation rate of female larvae (σ_{L_i}).

The specific effect of each of the aforementioned influential parameters ($\alpha, \psi_U, \sigma_{L_i}, \mu_L$ and μ_A) on the population dynamics of the mosquito and the reproduction threshold ($\mathcal{R}_M$) are tabulated in Table 2.5.

Parameters	Baseline Value	Range	Reference
ψ_U	50/day	$(10-100)$/day	[9; 60; 131; 140; 213]
K_U	40000	$(50-3\times10^6)$	[9; 131; 213]
σ_E	0.84/day	$(0.33-1)$/day	[60]
μ_E	0.05/day	$(0.01-0.07)$/day	[60]
σ_{L_1}	0.095/day	$(0.05-0.15)$/day	[72]
σ_{L_2}	0.11/day	$(0.06-0.17)$/day	[72]
σ_{L_3}	0.13/day	$(0.08-0.19)$/day	[72]
σ_{L_4}	0.16/day	$(0.08-0.23)$/day	[72]
μ_L	0.34/day	$(0.15-0.48)$/day	[60]
δ_L	0.04/ml	$(0.02-0.06)$/ml	[60]
f	0.5	$(0.45-0.55)$	[72]
σ_P	0.8/day	$(0.3-1)$/day	[60]
μ_P	0.17/day	$(0.12-0.21)$/day	[72]
γ_U	0.89/day	$(0.30-1)$/day	[166; 167]
η_V^*	0.8/day	$(0.46-0.92)$/day	[166; 167]
τ_W^*	16	$(12-20)$	[166]
α	0.86	$(0.75-0.95)$	[166]
μ_A	0.05/day	$(0.041-0.203)$/day	[9; 48; 131; 168; 213]

Table 2.3: Values and ranges of the parameters of the autonomous model (2.4.1).

Parameters	U Class	V Class	L_4 Class	P Class	$\mathcal{R}_M$
ψ_U	**+0.6863**	**+0.8509**	**+0.9083**	**+0.8958**	**+0.88**
K_U	+0.1174	+0.1783	+0.1952	+0.2218	–
σ_E	+0.0066	+0.1099	−0.0959	+0.0046	+0.031
μ_E	−0.1118	+0.0045	−0.0326	−0.0291	−0.082
σ_{L1}	+0.4598	**+0.6525**	**+0.6896**	**+0.7019**	**+0.63**
σ_{L2}	+0.4366	**+0.6337**	**+0.6817**	**+0.6543**	**+0.60**
σ_{L3}	+0.3224	+0.5714	+0.2781	+0.5779	+0.49
σ_{L4}	+0.4213	**+0.6473**	+0.0914	+0.2447	+0.55
f	+0.0223	+0.0437	+0.0014	+0.0747	+0.032
μ_L	**-0.7842**	**-0.9103**	**-0.9193**	**-0.9427**	**-0.96**
δ_L	−0.1121	−0.0679	−0.0807	−0.0699	–
K_L	+0.0472	+0.0173	+0.0869	−0.1206	–
σ_P	+0.0621	−0.3878	+0.1045	+0.0088	+0.093
μ_P	−0.1031	−0.1578	−0.0648	+0.0171	−0.051
γ_U	−0.0948	−0.2255	−0.2908	−0.2934	−0.25
η_V^*	+0.2278	+0.1773	+0.2047	+0.2521	+0.16
τ_W^*	**-0.6390**	+0.0956	−0.0123	+0.0523	−0.026
α	**+0.9284**	+0.5431	**+0.6106**	**+0.6224**	+0.55
μ_A	**-0.8597**	−0.2584	−0.5379	−0.3373	**-0.69**

Table 2.4: PRCC values for the parameters of the autonomous model (2.4.1) using total number of adult mosquitoes of type U, adult mosquitoes of type V, fourth instar larvae (L_4), pupae (P), and $\mathcal{R}_M$ as output. The parameters that have the most influence on the dynamics of the model with respect to each of the six response functions are highlighted in bold font. "Notation: a line (−) indicates the associated model parameter does not appear in the expression for $\mathcal{R}_M$".

2.5 Analysis of Non-autonomous Model

In this section, the full non-autonomous model (2.3.1) will be analyzed.

2.5.1 Computation of Vectorial Reproduction Ratio

The *vectorial reproduction ratio*, associated with the non-autonomous model (2.3.1), will be computed using the operator theory approach in Bacaér (2007, 2009, 2011); Bacaér and Abdurahman (2008); Bacaér and Guernaoui (2006); Bacaér and Ouifki (2007); Wang and Zhao (2008). The next generation matrices $F(t)$ and $V(t)$, associated with the non-autonomous model (2.3.1) (linearized at the trivial equilibrium $\mathcal{T}_0$), are given, respectively, by:

$$F(t) = \begin{bmatrix} \mathbf{0} & \mathbf{0} & F_1(t) \\ \mathbf{0} & \mathbf{0} & \mathbf{0} \\ \mathbf{0} & \mathbf{0} & \mathbf{0} \end{bmatrix} \text{ and } V(t) = \begin{bmatrix} V_1(t) & \mathbf{0} & \mathbf{0} \\ V_2(t) & V_3(t) & \mathbf{0} \\ \mathbf{0} & V_4(t) & V_5(t) \end{bmatrix},$$

where,

$$F_1(t) = \begin{bmatrix} 0 & 0 & \psi_U(t) \\ 0 & 0 & 0 \\ 0 & 0 & 0 \end{bmatrix}, V_1(t) = \begin{bmatrix} C_E(t) & 0 & 0 \\ -\sigma_E(t) & C_1(t) & 0 \\ 0 & -\sigma_{L_1}(t) & C_2(t) \end{bmatrix},$$

$$V_2(t) = \begin{bmatrix} 0 & 0 & -\sigma_{L_2}(t) \\ 0 & 0 & 0 \\ 0 & 0 & 0 \end{bmatrix}, V_3(t) = \begin{bmatrix} C_3(t) & 0 & 0 \\ -\sigma_{L_3}(t) & C_4(t) & 0 \\ 0 & -\sigma_{L_4}(t) & C_P(t) \end{bmatrix},$$

$$V_4(t) = \begin{bmatrix} 0 & 0 & -f\sigma_P(t) \\ 0 & 0 & 0 \\ 0 & 0 & 0 \end{bmatrix}, V_5 = \begin{bmatrix} C_5(t) & 0 & -\gamma_U \\ -\eta_V^* & C_6(t) & 0 \\ 0 & -\alpha\tau_W^* & C_7(t) \end{bmatrix},$$

with, $C_E(t) = \sigma_E(t) + \mu_E(t)$, $C_j(t) = \sigma_{L_j}(t) + \mu_L(t)$ (for $i = 1, 2, 3, 4$), $C_P = \sigma_P(t) + \mu_P(t)$, $C_5(t) = \eta_V^* + \mu_A(t)$, $C_6(t) = \tau_W^* + \mu_A(t)$, $C_7(t) = \gamma_U + \mu_A(t)$.

The linearized version of the model (2.3.1), at $\mathcal{T}_0$, can be expressed as

$$\frac{dx(t)}{dt} = \big[F(t) - V(t)\big]x(t),$$

where $x(t) = \big(E(t), L_1(t), L_2(t), L_3(t), L_4(t), P(t), V(t), W(t), U(t)\big)$. Following Wang and Zhao (2008), let $Y(t, s)$, $t \geq s$, be the evolution operator of the linear ω-periodic system $\dfrac{dy}{dt} = -V(t)y$. Thus, for each $s \in \mathbb{R}$, the associated 9×9 matrix $Y(t, s)$ satisfies Wang and Zhao (2008)

$$\frac{dY(t, s)}{dt} = -V(t)Y(t, s) \ \forall \ t \geq s, \ Y(s, s) = I_{9\times 9},$$

where $I_{9\times 9}$ is the 9×9 identity matrix.

Suppose that $\phi(s)$ (ω-periodic in s) is the initial distribution of new eggs. Thus, $F(s)\phi(s)$ is the rate of generation (hatching) of new eggs in the breeding habitat at time s. Since $t \geq s$, it follows that $Y(t, s)F(s)\phi(s)$ represents the distribution of new eggs at time s, and became adult at time t. Hence, the cumulative distribution of new eggs at time t, produced by all adult female mosquitoes ($\phi(s)$) introduced at a prior time $s = t$, is given by

$$\Psi(t) = \int_{-\infty}^{t} Y(t, s)F(s)\phi(s)\, ds = \int_{0}^{\infty} Y(t, t - a)F(t - a)\phi(t - a)\, da.$$

Let $\mathbb{C}_\omega$ be the ordered Banach space of all ω-periodic functions from $\mathbb{R}$ to $\mathbb{R}^9$, which is equipped with maximum norm and positive cone $\mathbb{C}_\omega^+ = \big\{\phi \in \mathbb{C}_\omega : \phi(t) \geq 0, \forall \ t \in \mathbb{R}\big\}$ [251]. Define a linear operator $L : \mathbb{C}_\omega \to \mathbb{C}_\omega$

$$(L\phi)(t) = \int_{0}^{\infty} Y(t, t - a)F(t - a)\phi(t - a)\, da \ \forall \ t \in \mathbb{R}, \phi \in \mathbb{C}_\omega.$$

The vectorial reproduction ratio of the model (2.3.1) ($\mathcal{R}_{Mt}$) is then given by the spectral radius of the linear operator L, (i.e., $\mathcal{R}_{Mt} = \rho(L)$).

Lemma 2.5.1. *The model* (2.3.1) *further satisfies Assumptions* $A1 - A7$ *in Wang and Zhao (2008).*

The proof of Lemma 2.5.1 is given in Appendix B. Thus, the following result follows from Lemma 2.5.1 and Theorem 2.2 in Wang and Zhao (2008).

Theorem 2.5.1. *The trivial equilibrium* ($\mathcal{T}_0$)*, of the non-autonomous model* (2.4.1)*, is LAS in* Ω *if* $\mathcal{R}_{Mt} < 1$*, and unstable if* $\mathcal{R}_{Mt} > 1$.

Furthermore, the following result holds.

Theorem 2.5.2. *The trivial equilibrium* ($\mathcal{T}_0$) *of the non-autonomous model* (2.3.1) *is GAS in* Ω *whenever* $\mathcal{R}_{Mt} < 1$.

Proof. Consider the non-autonomous model (2.3.1) with $\mathcal{R}_{Mt} < 1$. Using the fact that $U(t) \geq 0$ for all t (Lemma 2.3.1) and $\psi_U \left(1 - \frac{U(t)}{K_U}\right)_+ U(t) \leq \psi_U U(t)$ it then follows that the non-autonomous model (2.3.1) can be re-written as

$$\begin{aligned}
\frac{dE}{dt} &\leq \psi_U U - C_E(t)E, \\
\frac{dL_1}{dt} &\leq \sigma_E(t)E - C_1(t)L_1, \\
\frac{dL_i}{dt} &\leq \sigma_{L_{(j-1)}}(t)L_{(j-1)} - C_j(t)L_j \ ; \ i = 2, 3, 4, \\
\frac{dP}{dt} &= \sigma_{L_4}(t)L_4 - C_P(t)P, \\
\frac{dV}{dt} &= \sigma_P(t)P + \gamma_U U(t) - C_5(t)V, \\
\frac{dW}{dt} &= \eta_V^* V - C_6(t)W, \\
\frac{dU}{dt} &= \alpha\tau_W^* W - C_7(t)U.
\end{aligned} \tag{2.5.1}$$

The expressions in (2.5.1), with equalities used in place of the inequalities, can be re-written in terms of the next generation matrices $F(t)$ and $V(t)$, as follows

$$\frac{dX(t)}{dt} = [F(t) - V(t)]X(t). \tag{2.5.2}$$

It follows, from Lemma 2.1 in Zhang and Zhao (2007), that there exists a positive and bounded ω-periodic function, $x(t) = \big(\bar{E}, \bar{L}_1, \bar{L}_2, \bar{L}_3, \bar{L}_4, \bar{P}, \bar{V}, \bar{W}, \bar{U}\big)(t)$, such that

$$X(t) = e^{\theta t}x(t), \text{ with } \theta = \frac{1}{\omega}\ln\rho\big[\phi_{F-V}(\omega)\big],$$

is a solution of the linearized system (2.5.1). Furthermore, it follows from Theorem 2.2 in Wang and Zhao (2008) that $\mathcal{R}_{Mt} < 1$ if and only if $\rho\big[\phi_{F-V}(\tau)\big] < 1$. Hence, θ is a negative constant. Thus, $X(t) \to 0$ as $t \to \infty$. Thus, the unique trivial solution of the linear system (2.5.1), given by $X(t) = 0$, is globally-asymptotically stable (Lou and Zhao, 2010; Safi et al., 2012)]. For any non-negative initial solution $(E, L_1, L_2, L_3, L_4, P, V, W, U)(0))^T$ of the system (2.5.2), there exists a sufficiently large $Q^* > 0$ such that

$$((E, L_1, L_2, L_3, L_4, P, V, W, U)(0))^T \leq Q^* \left((\bar{E}, \bar{L}_1, \bar{L}_2, \bar{L}_3, \bar{L}_4, \bar{P}, \bar{V}, \bar{W}, \bar{U})(0)\right)^T.$$

Thus, it follows, by comparison theorem (Lakshmikantham and Leela, 1969; Smith, 1996), that

$$\big(E(t), L_1(t), L_2(t), L_3(t), L_4(t), P(t), V(t), W(t), U(t)\big) \leq Q^* X(t) \text{ for all } t > 0,$$

where $Q^*X(t)$ is also a solution of (2.5.2). Hence,

$$\big(E(t), L_1(t), L_2(t), L_3(t), L_4(t), P(t), V(t), W(t), U(t)\big) \to \big(0, 0, \ldots, 0\big), \text{ as } t \to \infty.$$

□

The epidemiological implication of Theorem 2.5.2 is that the mosquito population (both immature and mature) can be effectively controlled (or eliminated) if the associated vectorial reproduction threshold, $\mathcal{R}_{Mt}$, can be brought to (and maintained at) a value less than unity. Thus, any vector control strategy that can reduce $\mathcal{R}_{Mt}$ to a value less than unity can lead to the effective control of the mosquito population in the community.

2.5.2 Existence of Non-trivial Positive Periodic Solution

In this section, the possibility of the existence of a non-trivial positive periodic solution for the non-autonomous model (2.3.1) will be explored using uniform persistence theory (Lou and Zhao, 2010; Smith, 1996; Thieme, 1993; Zhao et al., 2017; Zhi-Fen et al., 2006). Using notations in Lou and Zhao (2010), it is convenient to define the following sets (X, X_0 and ∂X_0):

$$X = \Omega,$$

$$X_0 = \big\{\phi = (\phi_1, \phi_2, \phi_3, \phi_4, \phi_5, \phi_6, \phi_7, \phi_8, \phi_9) \in X : \phi_i(0) > 0 \text{ for all } i \in \{1, 2, \ldots, 9\}\big\},$$

$$\partial X_0 = X \setminus X_0 = \big\{\phi \in X : \phi_i(0) = 0 \text{ for some } i \in \{1, 2, \ldots, 9\}\big\}.$$

Theorem 2.5.3. *Consider the non-autonomous model* (2.3.1) *Let* $\mathcal{R}_{Mt} > 1$. *The model has at least one positive periodic solution, and there exists a* $\varphi > 0$ *such that any solution* $u(t, \phi)$ *of the model with initial data* $\phi \in X_0$ *satisfies*

$$\liminf_{t\to\infty}(E, L_1, L_2, L_3, L_4, P, V, W, U)(t) \geq (\varphi, \varphi, \varphi, \varphi, \varphi, \varphi, \varphi, \varphi, \varphi).$$

Proof. The proof is based on using uniform persistent theory. Following Lou and Zhao (2010), let $u(t, \phi)$ be the unique solution of the model (2.3.1), with $u(0, \phi) = \phi$. Let $\Phi(t)\psi = u(t, \psi)$ and let $\mathcal{P} : X \to X$ be the Poincaré map associated with the model (2.3.1). That is, $\mathcal{P}(\phi) = u(\omega, \phi)$ for all $\phi \in X$. Then, using similar approach as in Lemma 2.3.1, it can be seen X_0 is a positively invariant set. Hence, since the solutions of model (2.3.1) are uniformly (ultimately) bounded, $\mathcal{P}$ is point dissipative (Lou and Zhao, 2010). It then follows from Theorem 1.1.2 in Zhao et al. (2017) that $\mathcal{P}$ admits a global attractor in X. Thus, it suffices to show that model (2.3.1) is

uniformly-persistent with respect to $(X_0, \partial X_0)$. It is convenient to define:

$$\begin{aligned} K_\partial &= \big\{\phi \in \partial X_0 : \mathcal{P}^n(\phi) \in \partial X_0 \text{ for } n \geq 0\big\}, \\ D_1 &= \big\{\phi \in X : \phi_i = 0 \text{ for all } i = 1, \ldots, 9\big\}, \\ \partial X_0 \setminus D_1 &= \big\{\phi \in X : \phi_i \geq 0 \text{ for some } i \in [1, 9]\big\}. \end{aligned} \tag{2.5.3}$$

We claim the following result.

Lemma 2.5.2. $K_\partial = D_1$.

Proof. This result can be proved by, first of all, seeing that for any $\psi \in D_1$, $u_i(t, \psi) = 0$ for all $i = 1, \ldots, 9$, (hence, $D_1 \subset K_\partial$). Furthermore, for any $\psi \in \partial X_0 \setminus D_1$, we can choose $\psi_i(0) > 0$ for all $i = 1, \ldots, 9$, so that $u(t, \psi) \in X_0$. This implies that, for any $\psi \in \partial X_0 \setminus D_1$, there exists some n, with $n\omega > t_0$, such that $\mathcal{P}^n(\psi) \notin \partial X_0$. Hence, $K_\partial \subset D_1$. □

Thus, it follows from Lemma 2.5.2 that $\mathcal{A} := \{\mathcal{T}_0\}$ is a compact and isolated invariant set for the Poincaré map P in K_∂ and $\cup_{\phi \in K_\partial} \omega(\phi) = \mathcal{A}$ (Lou and Zhao, 2010). Furthermore, $\mathcal{A}$ does not form a cycle in K_∂ (and, hence, not in ∂X_0). In addition, it follows from the proof of Theorem 3.2 (*Claim* 2) in Lou and Zhao (2010) that there exists an $\epsilon > 0$ such that

$$\limsup_{t \to \infty} |\Phi(n\omega)\phi - \mathcal{T}_0| \geq \epsilon \text{ for all } \phi \in X_0.$$

Thus, $\mathcal{A}$ is a compact, and an isolated invariant set for $\mathcal{P}$ in X and $W^s(\mathcal{A}) \cap X_0 = \emptyset$ where $W^s(\mathcal{A})$ is the stable manifold of $\mathcal{A}$ for $\mathcal{P}$ (Lou and Zhao, 2010). Hence, every trajectory in K_∂ converges to $\mathcal{A}$, and $\{\mathcal{A}\}$ is acyclic in K_∂ (Zhao et al., 2017). It then follows from Theorem 1.3.1 in Zhao et al. (2017) that $\mathcal{P}$ is uniformly persistent with respect to X_0. Thus, it follows from Theorem 3.1.1 in Zhao et al. (2017) that the periodic semiflow $\Phi(t) : X \to X$ is also uniformly persistent to X (Lou and Zhao,

2010) where $\Phi(t)\psi = u_t(\psi)$. It then follows from Theorem 4.5 in Magal and Zhao (2005) (see also Theorem 4.6 in Thieme (1992) and Theorem 3.1 in Zhao (2008)) that the autonomous model (2.3.1) admits a positive ω-periodic solution $\mathcal{T}_1^* = \Phi(t)\phi^*$ with $\phi^* \in X_0$.

It follows, from Theorem 4.5 in Magal and Zhao (2005) (see also Theorem 2.1 in Zhao (1995)), that $\mathcal{P} : X_0 \to X_0$ has a compact global attractor, denoted by $\mathcal{A}_0$. Hence, $\mathcal{A}_0$ is invariant for $\mathcal{P}$ (that is, $\mathcal{A}_0 = \mathcal{P}(\mathcal{A}_0) = \Phi(\omega)A_0$). Furthermore, let $\mathcal{A}_0^* := \bigcup_{t\in[0,\omega]} \Phi(t)\mathcal{A}_0$. Then, $\psi_i(0) > 0$ for all $\psi \in \mathcal{A}_0^*$, $i = 1, \ldots, 9$. Since X_0 is invariant, it follows that $\Phi(t)X_0 \subset X_0$. Thus, $\mathcal{A}_0^* \subset X_0$ and $\limsup_{t\to\infty} d(\Phi(t)\phi, \mathcal{A}_0^*) = 0$ for all $\phi \in X_0$ (Lou and Zhao, 2010; Zhao, 1995). Also, it follows, by the continuity of $\Phi(t)\phi$ for $(t, \phi) \in [0, \infty) \times X_0$ and the compactness of $[0, \tau] \times \mathcal{A}_0$, that $\mathcal{A}_0^*$ is compact in X_0 (Lou and Zhao, 2010; Zhao, 1995). Thus, $\inf_{\phi\in\mathcal{A}_0^*} d(\phi, \partial X_0) = \min_{\phi\in\mathcal{A}_0^*} d(\phi, \partial X_0) > 0$ (Lou and Zhao, 2010; Zhao, 1995). Consequently, there exists $\varphi > 0$ such that

$$\liminf_{t\to\infty} \min\big(E(t,\phi), L_1(t,\phi), L_2(t,\phi), L_3(t,\phi), L_4(t,\phi), P(t,\phi), V(t,\phi), W(t,\phi), U(t,\phi)\big)$$
$$= \liminf_{t\to\infty} d(\phi, \partial X_0) \geq \varphi, \text{ for all } \phi \in X_0.$$

In particular, $\liminf_{t\to\infty} \min(\Phi(t)\phi^*) \geq \varphi$. Hence, $u_i(t, \phi) > 0$, $i = 1, \ldots, 9$ for all $t \geq 0$. □

The ecological implication of Theorem 2.5.3 is that the mosquito population will persist in the community if $\mathcal{R}_{Mt} > 1$. The theoretical results obtained in Theorems (2.5.1), (2.5.2) and (2.5.3) show that the two models (2.3.1) and (2.4.1) have the same dynamics with respect to the elimination or persistence of the mosquito population in the community. In other words, adding the effect of local climate variability on the autonomous model (2.4.1) does not alter its dynamics with respect to the asymptotic stability of its steady-state solutions.

2.6 Numerical Simulations

The non-autonomous model (2.3.1) will now be simulated to assess the effect of the two climate variables (temperature and rainfall) on the population dynamics of adult mosquitoes in a community. Suitable functional forms for the temperature- and rainfall-dependent functions, relevant to *Anopheles* mosquitoes as defined in Section 2.3.1, will be used in the simulations. For these simulations, water temperature (T_W) is taken to be defined by $T_W = T_A + 3°\text{C}$. Furthermore, the simulations are carried out using the parameter values in Table 2.3 (with a fixed nutrient value of $N = 100,000$).

The combined effect of mean monthly temperature and rainfall is assessed by simulating the model (2.3.1) using various mean monthly temperature and rainfall values in the range $[16-40]°\text{C}$ and $[90-120]$ mm, respectively (the temperature ranges for most tropical and sub-tropical regions of the world lie within this temperature range (Belda et al., 2014)). The results obtained for this general settings (as measured in terms of the total number of adult female mosquitoes), depicted in Figure 2.8, show that the total mosquito population (of a typical community with the aforementioned temperature and rainfall ranges) is maximized when the mean monthly temperature and rainfall values lie in the range $[20-25]°\text{C}$ and $[105-115]$ mm, respectively.

Furthermore, simulations were carried out using weather (temperature and rainfall) data for three cities in Africa, namely, KwaZulu-Natal, South-Africa (Southern Africa); Lagos, Nigeria (Western Africa) and Nairobi, Kenya (Eastern Africa) (see profiles Tables 2.6, 2.7 and 2.8, respectively). While the peak mosquito abundance for KwaZulu-Natal (Figure 2.9a) and Lagos (Figure 2.9b) occur when the temperature and rainfall values lie in the range $[22-25]°\text{C}$, $[98-121]$ mm (occurring during the months of January, March, April, November and December) and $[24-27]°\text{C}$ $[113-255]$ mm (occurring during the months of May, July, August, September and

October) respectively, the peak mosquito abundance for Nairobi (Figure 2.9c) occurs for temperature and rainfall ranges $[20.5 - 21.5]^{\circ}$C and $[50 - 120]$ mm (occurring during the months of January, February, March and April).

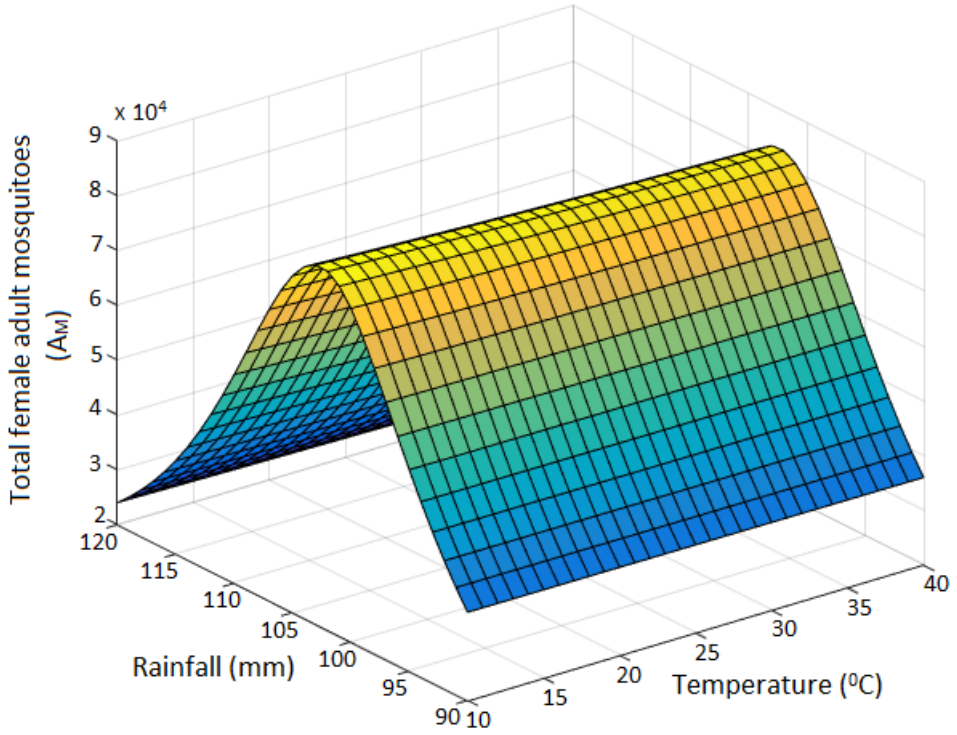

Figure 2.8: Simulation of the model (2.3.1), using parameter values in Table 2.3, showing the total number of adult female mosquitoes (A_M) for various values of mean monthly temperature and rainfall values in the range $T_A\,(T_W) \in [16 - 40]^{\circ}$C and $R \in [90 - 120]$ mm.

2.7 Summary of Results

In this chapter, a new mathematical model for the population biology of the mosquito (the world's deadliest animal, which accounts for 80% of vector-borne diseases of

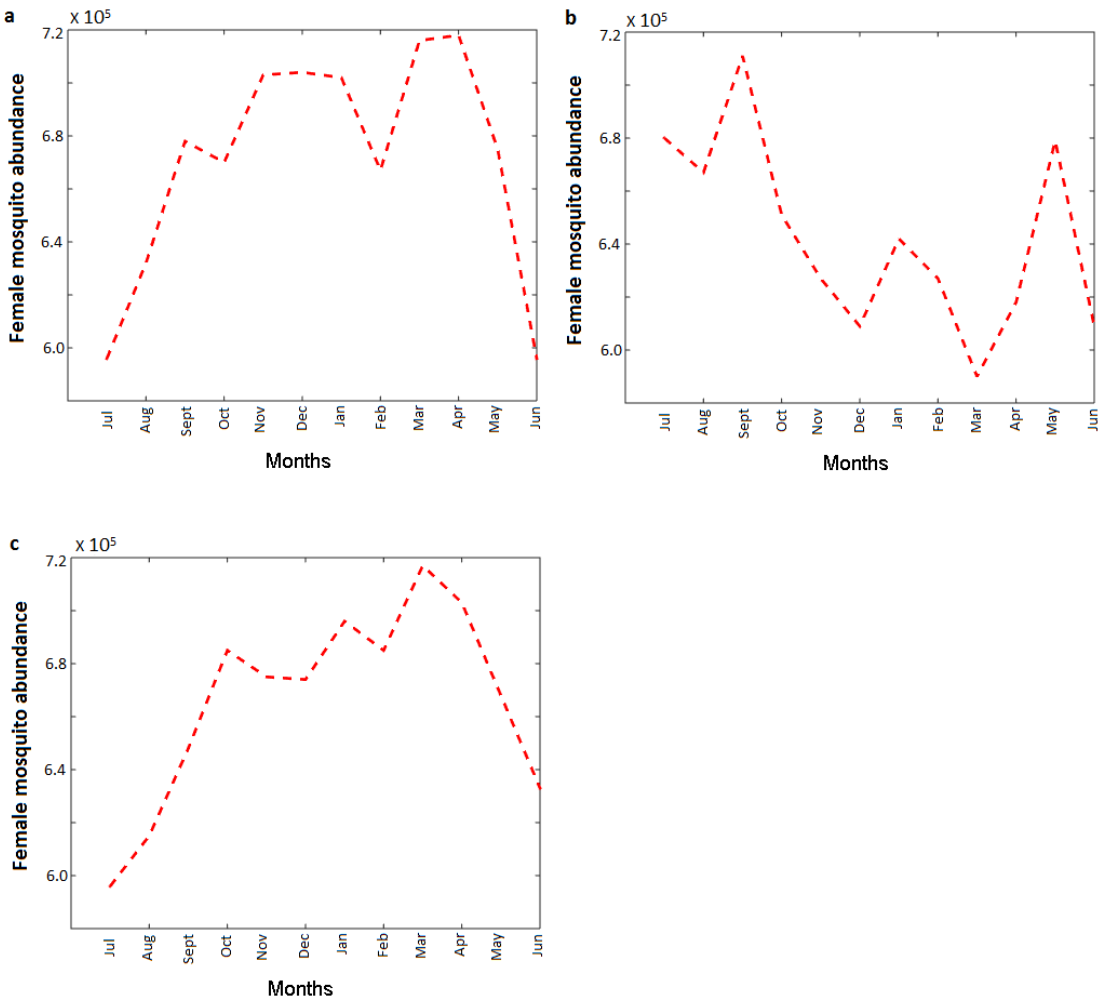

Figure 2.9: Simulation of non-autonomous model (2.3.1), showing the total number of adult female mosquitoes (A_M) for three cities in sub-Saharan Africa: (a) KwaZulu-Natal, South-Africa ($R_{I_M} = 200$ mm); (b) Lagos, Nigeria ($R_{I_M} = 400$ mm); (c) Nairobi, Kenya ($R_{I_M} = 200$ mm).

humans) is presented. Some of the notable features of the model include:

(i) incorporating four developmental stages of the mosquito larvae (i.e., the four instar larval stages, L_1, L_2, L_3, L_4);

(ii) including density-dependence for the eggs oviposition process given by the lo-

gistic term $\left(\psi_U\left(1-\frac{U}{K_U}\right)\right)$ and larval mortality rates (i.e., $\delta_L \neq 0$);

(iii) including the gonotrophic cycle of the adult female mosquitoes (i.e., compartments U, V and W).

The model, which takes the form of a non-autonomous deterministic system of non-linear differential equations, is used to assess the impact of temperature and rainfall on the population dynamics of the mosquito. The main findings, with regards the theoretical analysis and numerical simulations of the model, include:

(i) The trivial equilibrium of the autonomous version of the model (given by Equation (2.4.1)) is globally-asymptotically stable whenever the associated vectorial reproduction number ($\mathcal{R}_M$) is less than unity. For the case when $\mathcal{R}_M$ exceeds unity, it was shown that the model has at least one non-trivial equilibrium. Furthermore, the autonomous model has a unique non-trivial equilibrium for the special case with no density-dependent larval mortality (i. e., $\delta_L = 0$). Using the properties of Bèzout matrices, it is shown that this unique non-trivial equilibrium is shown to be locally-asymptotically stable under certain conditions. Furthermore, the equilibrium bifurcates into a stable limit cycle *via* a Hopf bifurcation.

(ii) Uncertainty and sensitivity analysis of the autonomous version of the model shows that the top five parameters that have the most influence on the dynamics of the model (with respect to various response functions) are the probability of adult female mosquito of type W successfully taking a bloodmeal (α), the natural mortality rate of adult female mosquitoes (μ_A), the natural mortality rate of female larvae (μ_L), the deposition rate of female eggs (ψ_U) and the maturation rate of female larvae from Stage 1 to Stage 2 (σ_{L_1}). Hence, this

study suggests that the population of adult mosquito in a community can be effectively-controlled using mosquito-reduction strategies, as well as personal protection against mosquito bites.

(iii) The trivial periodic solution of the non-autonomous model (2.3.1) is shown to be locally-asymptotically stable, whenever the spectral radius of a certain linear operator (denoted by $\mathcal{R}_{Mt}$) is less than unity. Furthermore, it is shown, using uniform persistence theory, that the non-autonomous model (2.3.1) has at least one positive periodic solution whenever $\mathcal{R}_{Mt} > 1$.

Numerical simulations of the non-autonomous model (2.3.1), using the functional forms of the temperature- and rainfall-dependent parameters of the model given in Section 2.3.1 and parameter values associated with the population dynamics of the *Anopheles species* of mosquitoes (which causes malaria in humans), show the following:

(i) For mean monthly temperature and rainfall values in the range $[10, 40]^{\circ}$C and $[90 - 120]$ mm, respectively, peak mosquito abundance is attained when temperature and rainfall values lie in the range $[20 - 25]^{\circ}$C and $[105 - 115]$ mm, respectively.

(ii) For mean monthly temperature and rainfall data for three cities in Africa, namely, KwaZulu-Natal, South-Africa; Lagos, Nigeria and Nairobi, Kenya (Tables 2.6, 2.7 and 2.8), it is shown that the peak mosquito abundance for KwaZulu-Natal (Figure 2.9a) and Lagos (Figure 2.9b) occur when the mean temperature and rainfall values lie in the range $[22 - 25]^{\circ}$C, $[98 - 121]$ mm (these ranges are typically recorded during the months of January, March, April, November and December) and $[24 - 27]^{\circ}$C, $[113 - 255]$ mm (occurring during the months of May, July, August, September and October) respectively. Similarly, the peak

mosquito abundance for Nairobi (Figure 2.9c) occur when the mean temperature and rainfall values lie in the range $[20.5 - 21.5]^{\circ}$C and $[50 - 120]$ mm (recorded during the months of January, February, March and April). Thus, the results of these simulations can be used, in each of the three chosen cities, to determine a more suitable time to intensify mosquito control strategies (i.e., corresponding to the time periods when the aforementioned temperature and rainfall are recorded in each of the three chosen cities).

Control measure by model (2.4.1)	Effect on population dynamics of mosquitoes	Effect on vectorial reproduction number $\mathcal{R}_M$	Environmental interpretation
Significant reduction in the value of α: (probability of successfully taking a blood meal)	Significant decrease in the population size of adult mosquitoes of type U	Significant decrease in the value of $\mathcal{R}_M$	Personal protection against mosquito bite plays an important role in minimizing the size of mosquito population in the community.
Significant reduction in the value of ψ_U: (deposition rate of female eggs)	Significant decrease in the population size of all three adult mosquito compartments	Significant decrease in the value $\mathcal{R}_M$	The removal of mosquito breeding (egg laying) sites, such as removal of stagnant waters, is an effective control measure against the mosquito population.
Significant reduction in the value of σ_{L_i} (maturation rate of female larvae) and significant increase of μ_L (natural mortality rate of female larvae)	Significant decrease in the population size of all three adult mosquito compartments	Significant decrease in the value $\mathcal{R}_M$	The removal of mosquito breeding sites and use of larvicides are effective control measures against the mosquito population.
Significant increase in the value of μ_A: (natural mortality rate of adult female mosquitoes)	Significant decrease in the population size of adult mosquitoes of type U	Significant decrease in the value of $\mathcal{R}_M$	The use of insecticides and insecticides treated bednets (ITNs) are important control measures against the mosquito population.

Table 2.5: Control measures suggested by the sensitivity analysis of the model (2.4.1).

Month	Jul	Aug	Sept	Oct	Nov	Dec	Jan	Feb	Mar	Apr	May	Jun
Temperature (°C)	17.5	18.5	20	21.0	22.5	22.0	25	25	25.5	22.5	20	17.5
Rainfall (mm)	48.2	32.3	65.2	107.1	121	118.3	124	142.2	113	98.1	35.4	34.7

Table 2.6: Monthly mean temperature (in ^{0}C) and rainfall (in mm) for KwaZulu-Natal, South Africa [1].

Month	Jul	Aug	Sept	Oct	Nov	Dec	Jan	Feb	Mar	Apr	May	Jun
Temperature (°C)	25.5	25	24	25.5	26	26.5	25.5	26	27	27.5	27	26.5
Rainfall (mm)	255	115	162	113	57	15	20	55	80	150	210	320

Table 2.7: Monthly mean temperature (in ^{0}C) and rainfall (in mm) for Lagos, Nigeria [2].

Month	Jul	Aug	Sept	Oct	Nov	Dec	Jan	Feb	Mar	Apr	May	Jun
Temperature (°C)	17.5	18	19	20.5	20	19.5	20.5	20.5	21.5	20.5	19.5	18.5
Rainfall (mm)	14.5	29.8	21.3	36.7	151	79.1	73.9	48.8	89.2	119.9	129.4	15.8

Table 2.8: Monthly mean temperature (in ^{0}C) and rainfall (in mm) for Nairobi, Kenya [4].

Chapter 3

WEATHER-DRIVEN MALARIA TRANSMISSION MODEL WITH GONOTROPHIC AND SPOROGONIC CYCLES

3.1 Introduction

Malaria is a complex disease (with complex vector-host-parasite dynamics), and realistically modeling its transmission dynamics (especially when climate effects are taken into account) is inherently complex. Consequently, realistically modeling of malaria transmission dynamics subject to variability in local climate variables will require the use of a reasonably complex model. Therefore, while the focus of this chapter is on the design of a model that incorporates these complexities (hence, more realistic), comparison will be made with simplified versions of the model (to determine what features of the complex model may, or may not, be safely relaxed, without compromising the model's ability to capture the disease dynamics, or observed data, reasonably well). In other words, the main aim of this chapter is to design a realistic model for malaria transmission dynamics, which is reasonably tractable enough for mathematical analysis and computation. In particular, a new malaria model that incorporates crucial aspects of malaria transmission dynamics, such as the aquatic structure (i.e., the dynamics of immature mosquitoes), mosquito gonotrophic and sporogonic cycles and increased malaria immunity in humans due to recovery from past exposure, will be developed.

The model to be designed is based on subdividing the total human population at time t (denoted by $N_H(t)$) into mutually-exclusive compartments of wholly-susceptible ($S_H(t)$) humans, uninfected humans with reduced susceptibility to malaria

infection due to recovery from prior malaria infection ($W_H(t)$), exposed (infected but not yet infectious) humans without immunity to malaria (i.e., exposed and malaria-naive humans) ($E_{HN}(t)$), exposed humans with partial immunity to malaria due to recovery from prior infection ($E_{HR}(t)$), symptomatic and infectious humans ($I_H(t)$), asymptomatically-infectious humans ($A_H(t)$) and recovered ($R_H(t)$) humans. Thus, $N_H(t) = S_H(t) + W_H(t) + E_{HN}(t) + E_{HR}(t) + I_H(t) + A_H(t) + R_H(t)$. Similarly, the total mosquito population at time t (denoted by $N_V(t)$) is sub-divided into sub-populations of immature (aquatic stages) mosquitoes (denoted by $A_M(t)$) and adult female mosquitoes (denoted by $N_M(t)$), so that $N_V(t) = A_M(t) + N_M(t)$. The total immature mosquito population at time t is sub-divided into compartments for eggs ($E(t)$), four larval (instar) stages ($L_1(t), L_2(t), L_3(t), L_4(t)$) and pupae ($P(t)$), so that $A_M(t) = E(t) + L_1(t) + L_2(t) + L_3(t) + L_4(t) + P(t)$. The female mosquito lifecycle is defined by the gonotrophic cycle (Greek for "offspring feeding"), classically divided into the following three stages Detinova et al. (1962); Mala et al. (2014):

1. Stage I: Search for suitable host and the taking of a bloodmeal.
2. Stage II: Digestion of bloodmeal and egg maturation.
3. Stage III: Search for, and oviposition into, a suitable body of water (breeding site).

Vectors in Stages I, II and III at time t are denoted by $X(t)$, $Y(t)$ and $Z(t)$, respectively. Vectors in each of these compartments are further subdivided into susceptible ($S_X(t), S_Y(t), S_Z(t)$), exposed ($E_X(t), E_Y(t), E_Z(t)$) and infected ($I_X(t), I_Y(t), I_Z(t)$) vectors (where the exposed vector classes are included to account for the vector sporogonic cycle). Thus,

$$N_M(t) = S_X(t) + E_X(t) + I_X(t) + S_Y(t) + E_Y(t) + I_Y(t) + S_Z(t) + E_Z(t) + I_Z(t).$$

3.2 Literature Review: Mathematical Modeling of Malaria Transmission Dynamics

Malaria is one of the earliest diseases that has been subject to extensive mathematical inquiry, dating back to the pioneering works of Sir Ronald Ross (who discovered the malaria lifecycle) in the early 1900s (Ross et al., 1916), and its extensions in the early 1950s by the highly influential British malariologist George Macdonald Macdonald et al. (1957). Since these seminal works, numerous mathematical models have been introduced to study malaria transmission. Since the 1990s, numerous authors (e.g., Agusto et al. (2015); Christiansen-Jucht et al. (2015); Paaijmans et al. (2010c); Parham et al. (2012); Yang et al. (2009)) have turned to modeling to quantify the impact of weather and climate on malaria transmission, mainly focusing on temperature and rainfall, and how anthropogenic climate change might be expected to affect (potential) disease burden, especially in tropical Africa.

The models used to gain insight into the likely impact of anthropogenic (man-made) climate change on malaria transmission dynamics and control are typically statistical (using data and statistical approaches to correlate some climate variables with malaria incidence) or mechanistic (accounting for the detailed dynamic nonlinear processes involved in disease transmission, also sometimes referred to as "process-based") in nature. These models have (generally) reached divergent conclusions, with some predicting a large *expansion* in the continental land area suitable for transmission (Caminade et al., 2014; Martens, 1999; Tanser et al., 2003) and in the number of people at risk of malaria (Martens, 1999; Pascual and Bouma, 2009; Patz et al., 1996), while others predict only modest poleward (and altitudinal) *shifts* in the burden of disease, with little net effect (Gething et al., 2010; Hay et al., 2002; Rogers and Randolph, 2000), and the issue remains unresolved thus far. In other words, the current related debate within the ecology community is on poleward-expansion of

malaria from tropical latitudes *vs.* poleward-shift-with-no-net-expansion in malaria cases. Similarly, malaria burden may expand into equatorial highland areas, such as those of eastern Africa, with uncertain changes at lower altitude (Bhattacharya et al., 2006; Gething et al., 2010; Lafferty, 2009; Lafferty and Mordecai, 2016; Pascual and Bouma, 2009; Rogers and Randolph, 2000).

It is now generally believed that, in the context of malaria for example (and if non-climatic human factors are not taken into account), climate warming will lead to poleward expansion of malaria from tropical latitudes (Gething et al., 2010; Rogers and Randolph, 2000). Additionally, models differ regarding the expected optimum temperature for transmission (Mordecai et al., 2013) (in particular, Mordecai et al. (2013) showed that models which use monotonic functions for the vector and parasite temperature-dependent vital rates, may have over-estimated the optimal temperature range for malaria transmission). Although, most of the above modeling studies used constant or mean monthly temperature in their formulation, recent studies have shown that a more realistic approach is to incorporate daily (diurnal) temperature fluctuations in the model (Beck-Johnson et al., 2013, 2017; Paaijmans et al., 2010a).

The parasite sporogonic and vector gonotrophic cycles are clearly central to malaria transmission dynamics and should be incorporated into mathematical models of malaria transmission for such dynamics (Detinova et al., 1962; Eikenberry and Gumel, 2018). To explicitly account for the effect of the gonotrophic cycle on malaria transmission, Ngonghala et al. (2012) considered a mathematical model for the dynamics of malaria transmission that includes the gonotrophic cycle of the adult female mosquitoes and its interaction with the human population. The model by Ngonghala et al. (2012) does not incorporate the vector sporogonic cycle (i.e., it assumes that newly-infected mosquito is instantaneously capable of transmitting infection without necessarily completing the sporogonic cycle). To establish the epidemiological effec-

tiveness of malaria vectors and its implications on malaria incidence in human host populations, it is necessary to incorporate the duration of the temperature-dependent gonotrophic and sporogony cycles of the transmitting vector (Detinova et al., 1962).

The model to be designed in this chapter extends the previous (autonomous) model by Ngonghala et al. (2012), which has only two classes of (susceptible and infectious) mosquitoes for each stage of the gonotrophic cycle, to include the sporogonic cycle (i.e., have three classes of susceptible, exposed and infectious mosquitoes) for each stage of the gonotrophic cycle of the adult female mosquitoes. This allows for a comprehensive (and a more realistic) modeling, and a quantitative understanding of the effect of temperature-dependent gonotrophic and sporogonic cycles on malaria transmission dynamics. Furthermore, the model to be designed considers disease transmission to vectors by asymptomatically-infectious humans, reduced malaria susceptibility in humans due to recovery from prior malaria infection, the possibility of progression from a symptomatically infected to asymptomatically infected state, and the complete loss of partial immunity in humans.

3.3 Weather-driven Model for Malaria Transmission Dynamics

The model is designed by monitoring the temporal dynamics of the mosquito (immature and adult) and human populations, as follows.

3.3.1 Dynamics of Immature Mosquitoes

The population of mosquito eggs is generated at the logistic rate:

$$\psi_E \varphi_Z \left(1 - \frac{E}{K_E}\right)_+ (S_Z + E_Z + I_Z),$$

where ψ_E is the number of eggs laid *per* oviposition, φ_Z is the rate at which female mosquitoes transition from Stage III to Stage I of the gonotrophic cycle (i.e. the rate of

oviposition for mosquitoes in Stage III) and K_E is the environmental carrying capacity of eggs (as in Chapter 2, the notation $r_+ = \max\{0, r > 0\}$ is used to ensure the non-negativity of the logistic term). The parameters $\mu_i(T_W)$ and η_i $(i = E, L, P)$ represent the temperature-*dependent* and temperature-*independent* death rates, respectively, for immature mosquitoes of type i, where the latter may be due to processes such as predation, anthropogenic vector control measures, etc. Density-dependent larval mortality occurs at a rate $k_L L$ (where $L = L_1 + L_2 + L_3 + L_4$). Furthermore, $\sigma_E(T_W)$ is the temperature-dependent hatching rate of eggs into larvae, $\sigma_{Lj}(T_W)(j = 1, 2, 3)$ is the temperature-dependent progression rate of larvae from Stage j to Stage $j + 1$ and $\sigma_P(T_W)$ is the temperature-dependent rate at which pupae mature into adult mosquitoes.

Based on the above formulation and assumptions, the equations for the dynamics of the immature *Anopheles* mosquitoes are given by (Okuneye et al., 2018b):

$$\begin{aligned}
\frac{dE}{dt} &= \psi_E \varphi_Z \left(1 - \frac{E}{K_E}\right)_+ (S_Z + E_Z + I_Z) - \big[\sigma_E(T_W) + \eta_E + \mu_E\big] E, \\
\frac{dL_1}{dt} &= \sigma_E(T_W) E - \big[\sigma_{L_1}(T_W) + \eta_L + k_L L + \mu_L(T_W)\big] L_1, \\
\frac{dL_j}{dt} &= \sigma_{L_{(j-1)}}(T_W) L_{j-1} - \big[\sigma_{Lj}(T_W) + \eta_L + k_L L + \mu_L(T_W)\big] L_j,\ j = 2, 3, 4, \\
\frac{dP}{dt} &= \sigma_{L_4}(T_W) L_4 - \big[\sigma_P(T_W) + \eta_P + \mu_P\big] P.
\end{aligned} \tag{3.3.1}$$

3.3.2 Dynamics of Adult Female Mosquitoes: Gonotrophic and Sporogonic Cycles

We first note that only mosquitoes in Stage I of the gonotrophic cycle (i.e., of type X in our formulation, regardless of infection status) will bite humans (i.e., only mosquitoes

in classes S_X, E_X and I_X will bite humans). Furthermore, it is convenient to define the quantity

$$\mathcal{G}_H = \frac{I_H + A_H}{N_H}, \tag{3.3.2}$$

as the proportion of infectious humans in the community.

The equations for the dynamics of the adult mosquitoes (taking into account the gonotrophic and sporogonic cycles) are given by (Okuneye et al., 2018b):

$$\begin{aligned}
\frac{dS_X}{dt} &= f\sigma_P(T_W)P + \varphi_Z S_Z - \big[b_H p_H + \eta_M + \mu_M(T_A)\big]S_X,\\
\frac{dE_X}{dt} &= \varphi_Z E_Z - \big[b_H p_H + \kappa_M(T_A) + \eta_M + \mu_M(T_A)\big]E_X,\\
\frac{dI_X}{dt} &= \varphi_Z I_Z + \kappa_M(T_A)E_X - \big[b_H p_H + \eta_M + \mu_M(T_A)\big]I_X,\\
\frac{dS_Y}{dt} &= b_H p_H(1-\beta_V)\mathcal{G}_H S_X + b_H p_H(1-\mathcal{G}_H)S_X - \big[\theta_Y(T_A) + \eta_M + \mu_M(T_A)\big]S_Y,\\
\frac{dE_Y}{dt} &= b_H p_H \beta_V \mathcal{G}_H S_X + b_H p_H E_X - \big[\theta_Y(T_A) + \kappa_M(T_A) + \eta_M + \mu_M(T_A)\big]E_Y,\\
\frac{dI_Y}{dt} &= \kappa_M(T_A)E_Y + b_H p_H I_X - \big[\theta_Y(T_A) + \eta_M + \mu_M(T_A)\big]I_Y,\\
\frac{dS_Z}{dt} &= \theta_Y(T_A)S_Y - \big[\varphi_Z + \eta_M + \mu_M(T_A)\big]S_Z,\\
\frac{dE_Z}{dt} &= \theta_Y(T_A)E_Y - \big[\varphi_Z + \kappa_M(T_A) + \eta_M + \mu_M(T_A)\big]E_Z,\\
\frac{dI_Z}{dt} &= \theta_Y(T_A)I_Y + \kappa_M(T_A)E_Z - \big[\varphi_Z + \eta_M + \mu_M(T_A)\big]I_Z,
\end{aligned} \tag{3.3.3}$$

where f is the fraction of new adult mosquitoes that are females, $\sigma_P(T_W)$ and φ_Z are as defined above, b_H is the *percapita* biting rate of adult female mosquitoes (during Stage I of the gonotrophic cycle) and p_H is the probability that female mosquitoes (in Stage I) successfully take a bloodmeal from humans. Stage II of the gonotrophic cycle progresses at rate $\theta_Y(T_A)$, and is thus the transition rate from the Y to Z mosquito class. The parameters $\mu_M(T_A)$ and η_M represent, respectively, the natural temperature-dependent and temperature-independent adult mosquito death rates, with the latter possibly related to predation, accidents, or human vector control

measures. Parasites mature in exposed mosquitoes at a temperature-dependent rate $\kappa_M(T_A)$. The parameter β_V is the transmission probability from infectious human to a susceptible mosquito and the quantity $\mathcal{G}_H$ is as defined in Equation (3.3.2).

3.3.3 Human Dynamics

The equations for the dynamics of the human populations are given as (Okuneye et al., 2018b):

$$\begin{aligned}
\frac{dS_H}{dt} &= \Pi_H - \lambda_H(N_V, N_H)S_H + \rho_H W_H - \mu_H S_H, \\
\frac{dW_H}{dt} &= \xi_H R_H - (1-\epsilon)\lambda_H(N_V, N_H)W_H - (\rho_H + \mu_H)W_H, \\
\frac{dE_{HN}}{dt} &= \lambda_H(N_V, N_H)S_H - (\gamma_{HN} + \mu_H)E_{HN}, \\
\frac{dE_{HR}}{dt} &= (1-\epsilon)\lambda_H(N_V, N_H)W_H - (\gamma_{HR} + \mu_H)E_{HR}, \\
\frac{dI_H}{dt} &= r\gamma_{HN}E_{HN} + q\gamma_{HR}E_{HR} - (\alpha_H + \nu_H + \mu_H + \delta_H)I_H, \\
\frac{dA_H}{dt} &= (1-r)\gamma_{HN}E_{HN} + (1-q)\gamma_{HR}E_{HR} + \nu_H I_H - (\alpha_{HA} + \mu_H + \delta_{HA})A_H, \\
\frac{dR_H}{dt} &= \alpha_H I_H + \alpha_{HA}A_H - (\xi_H + \mu_H)R_H,
\end{aligned} \tag{3.3.4}$$

where Π_H is the recruitment rate (by birth or immigration) and λ_H is the force of infection of susceptible humans (by infectious adult female mosquitoes of type X),

given by

$$\lambda_H = b_H \beta_H p_H \frac{I_X}{N_H},$$

where b_H is the effective *per capita* biting rate of adult female mosquitoes during the first stage (X) of the gonotrophic cycle and β_H is the probability of infection of susceptible humans *per* bite by an infectious mosquito. Furthermore, μ_H is the natural death rate of humans and ξ_H is the rate at which initially-recovered humans progress to the partially-immune class. It is assumed that individuals who recovered from malaria acquire partial protective immunity against further infection (and move to the W_H class) (Doolan et al., 2009). The parameter $0 < \epsilon < 1$ accounts for reduced susceptibility to infection, *per se*, among individuals in the W_H class; those humans who are infected from the W_H class transition to the exposed class E_{HR}, and are more likely to then become asymptomatic than those exposed from the malaria-naive state (E_{HN}). Partially immune individuals eventually lose immunity at rate ρ_H (to become wholly-susceptible again).

The parameter γ_{HR} (γ_{HN}) models the transition out of the exposed E_{HR} (E_{HN}) class, a proportion r (q) of which develops clinical symptoms of malaria (and moves to the I_H class), while the remaining proportion, $1-r$ ($1-q$), becomes asymptomatically-infectious (and moves to the A_H class); it is assumed that susceptible mosquitoes in Stage I of the gonotrophic cycle can acquire malaria infection by biting both symptomatic and asymptomatically infected humans (I_H and A_H classes) (Laishram et al., 2012). Symptomatic humans progress to the asymptomatic class A_H at a rate ν_H. Infectious humans in the I_H (A_H) recover at a rate α_H (α_{HA}) and die due to malaria at rate δ_H (δ_{HA}). The flow diagram of the model is depicted in Figure 3.1, and the state variables of the model are described in Table 3.1.

The model $\{(3.3.1), (3.3.3), (3.3.4)\}$ includes numerous key aspects of malaria dis-

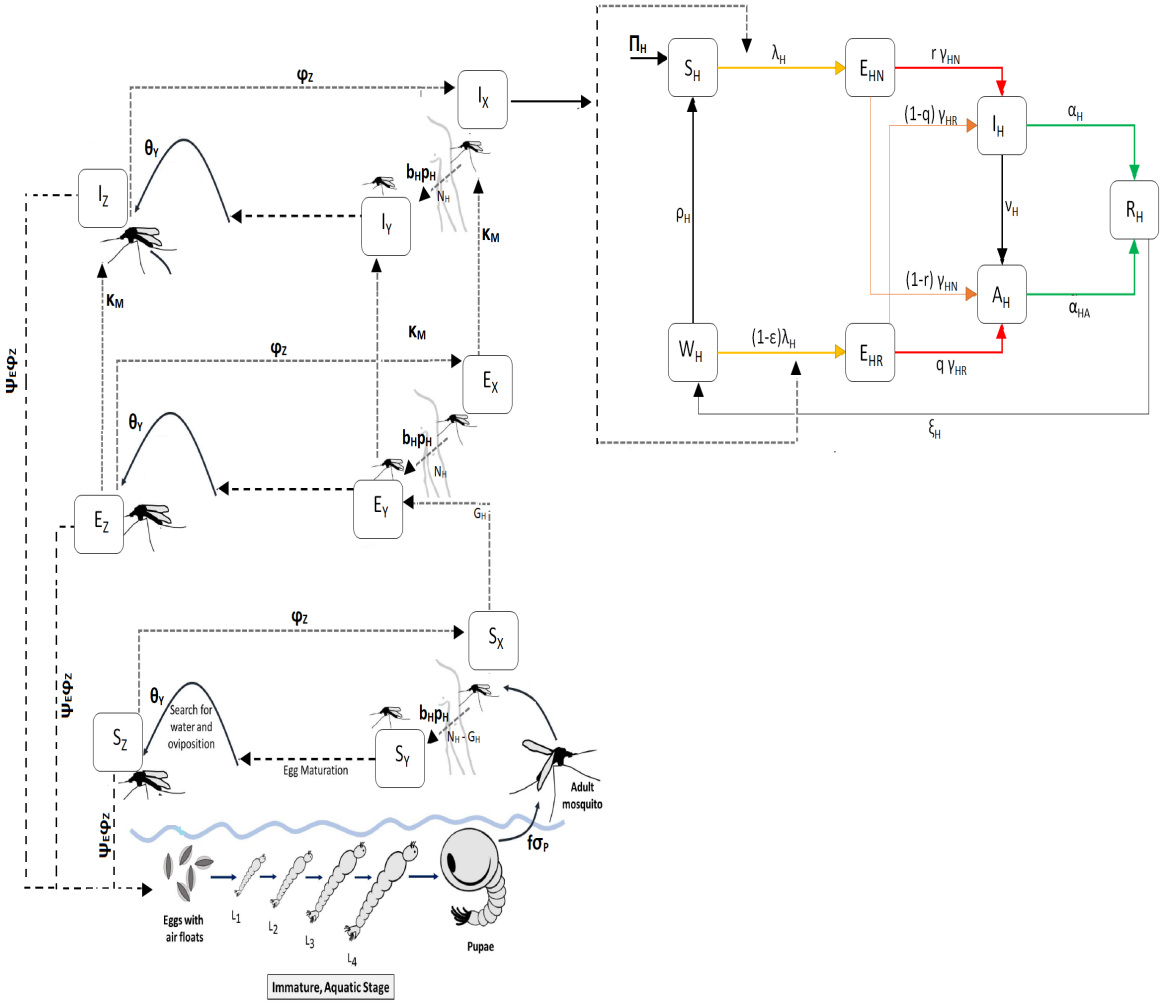

Figure 3.1: Flowchart of model $\{(3.3.1), (3.3.3), (3.3.4)\}$.

ease (e.g., mosquito life-cycle, density-dependent larval mortality, reduced susceptibility due to prior infection and climate change effects). Hence, it can be used to realistically assess the impacts of microclimate on malaria dynamics and control.

Formulation of Thermal-response Functions

In this section, only the thermal response function associated with the gonotrophic and sporogonic cycle will be discussed (other thermal response functions related immature and adult mosquitoes have been described in Section 2.3.1).

Variables	Description
E	Population of eggs
L_j	Population of larvae at Stage j (with $j = 1, 2, 3, 4$)
P	Population of pupae
S_X, E_X, I_X	Population of susceptible, exposed, and infectious female mosquitoes in gonotrophic Stage I, respectively
S_Y, E_Y, I_Y	Population of susceptible, exposed, and infectious female mosquitoes in gonotrophic Stage II, respectively
S_Z, E_Z, I_Z	Population of susceptible, exposed, and infectious, exposed, infectious adult female mosquitoes in gonotrophic Stage III, respectively
S_H	Population of wholly-susceptible humans
W_H	Population of susceptible humans with reduced malaria susceptibility due to prior recovery from malaria
E_{HN}	Population of exposed humans without prior immunity (i.e., exposed and malaria-naive humans)
E_{HR}	Population of exposed humans with partial malaria immunity due to recovery from prior immunity infection
I_H	Population of symptomatically-infectious humans
A_H	Population of asymptomatically-infectious humans
R_H	Population of recovered humans

Table 3.1: Description of state variables of the model $\{(3.3.1), (3.3.3), (3.3.4)\}$.

Plasmodium's Sporogonic Cycle

Mosquito sporogony is modeled as follows. The transition rate from the exposed to infectious mosquito class ($\kappa_M(T_A)$) is the inverse of the mean sporogonic cycle

duration (in days). The Moshkovsky formula (Detinova et al., 1962) is used, such that:

$$\frac{1}{\kappa_M(T_A)} = \frac{D}{T_A - T_{min}},$$

where $D = 111$ and $T_{min} = 16°\text{C}$ (Detinova et al., 1962). We assume that, above some temperature, T_{max}, sporogony ceases (i.e., $\kappa_M(T_A) = 0$), with $T_{max} = 40$ °C. That is (Okuneye et al., 2018b),

$$\kappa_M(T_A) = \begin{cases} \dfrac{T_A - 16}{111}, & \text{if } 16°\text{C} < T_A < 40°\text{C}, \\ 0, & \text{if } T_A \leq 16°\text{C},\ T_A \geq 40°\text{C}. \end{cases}$$

Adult Female Mosquito Gonotrophic Cycle

Mosquito gonotrophy is modeled as follows. The rate at which mosquitoes complete Stage II of the gonotrophic cycle (i.e., the transition from the Y to Z compartments) is given by Moshkovky's formula (Detinova et al., 1962):

$$\theta_Y(T_A) = \begin{cases} \dfrac{T_A - 9.9}{36.5}, & \text{if } 9.9°\text{C} < T_A < 40°\text{C}, \\ 0, & \text{if } T_A \leq 9.9°\text{C},\ T_A \geq 40°\text{C}. \end{cases}$$

Mosquitoes are assumed to bite once every gonotrophic cycle, which is subdivided into three stages, progressing at rates b_H, φ_Z, and θ_Y, respectively. Therefore, the overall biting rate (the inverse of the gonotrophic cycle length Mordecai et al. (2013)), in days^{-1}, is given as (Mordecai et al., 2013):

$$\Gamma = \left(\frac{1}{b_H} + \frac{1}{\varphi_Z} + \frac{1}{\theta_Y}\right)^{-1}.$$

It should be noted that Γ is temperature-dependent, since it is a function of θ_Y. Thus, no biting occurs when temperatures are extreme (i.e., when $T(t) \leq 9.9°\text{C}$ and $T(t) \geq 40°\text{C}$).

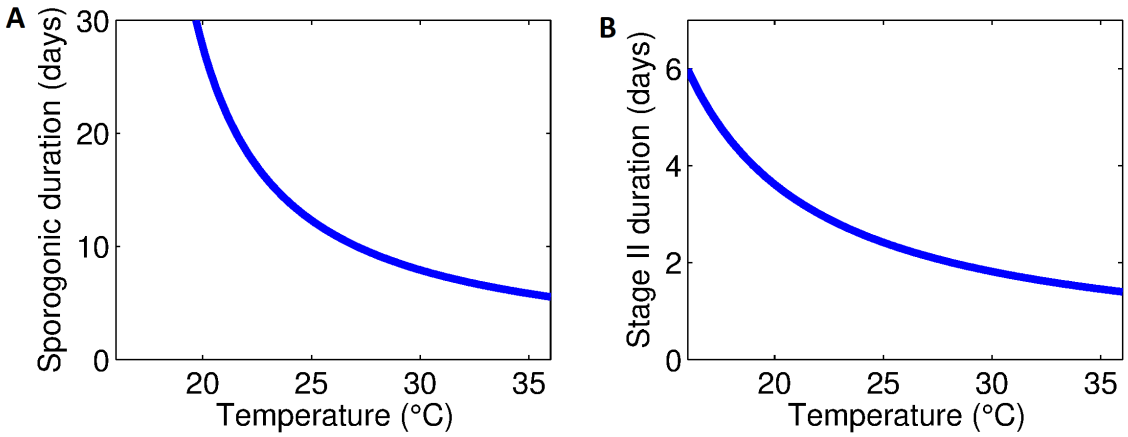

Figure 3.2: (A) Sporogonic cycle duration in adult female mosquitoes, $(\kappa_M(T_A))^{-1}$ (B) Duration of Stage II of the gonotrophic cycle.

3.3.4 Basic Properties

Model Invariant Region

Lemma 3.3.1. *Each component of the solution of the model* $\{(3.3.1), (3.3.3), (3.3.4)\}$, *subject to non-negative initial conditions, remains nonnegative and bounded for all* $t > 0$.

Proof. Since the functions on the right-hand side of the model $\{(3.3.1), (3.3.3), (3.3.4)\}$ (denoted by $Q(t, \phi)$, where $\phi \in \mathbb{R}^{22}_+$) is continuous and Lipschitzian at $t = 0$, then for each non-negative initial condition, the model has a unique and non-negative solution in $\mathbb{R}^{22}_+$. In addition, using similar approach as in Section 2.3.2, it should be noted that $Q_i(t, \phi) \geq 0$ whenever $\phi \geq 0$ and $\phi_i = 0$ (Lou and Zhao, 2010). Hence, it follows from Theorem A.4 in Thieme (2003) that the region $\mathbb{R}^{22}_+$ is positively-invariant with respect to the model $\{(3.3.1), (3.3.3), (3.3.4)\}$.

The boundedness of the solutions of the model $\{(3.3.1), (3.3.3), (3.3.4)\}$ is shown as follows:

(i) *Immature and adult mosquito compartments*:

Since $\left(1-\frac{E}{K_E}\right)_+ \geq 0$, then $E(t) \leq K_E$ for all t. Thus, using Definition 2.3.1, it can be deduced from the second equation of (3.3.1) (i.e., using the equation for the first larval instar stage, L_1) that,

$$\frac{dL_1}{dt} = \sigma_E(t)E - [\sigma_{L_1}(t) + \eta_L + k_L L + \mu_L(t)]L_1 \ \leq \ \sigma_E^* K_E - (\sigma_{L_{1*}} + \eta_L + \mu_{L*})L_1,$$

so that $\limsup_{t\to\infty} L_1(t) \leq \frac{\sigma_E^* K_E}{\sigma_{L_{1*}} + \eta_L + \mu_{L*}} = \overline{L}_1$. Similarly, the following bounds are obtained: $\limsup_{t\to\infty} L_j(t) \leq \overline{L}_j$, (for $j = 2, 3, 4$) and $\limsup_{t\to\infty} P(t) \leq \overline{P}$.

Furthermore, the equation for the rate of change of the total adult mosquitoes population ($N_V(t)$) is given by:

$$\frac{dN_V}{dt} = f\sigma_P(t)P - [\eta_M + \mu_M(t)]N_V \ \leq \ f\sigma_P^* \overline{P} - (\eta_M + \mu_{M*})N_V.$$

from which it follows that $\limsup_{t\to\infty} N_V(t) \leq \frac{f\sigma_P^* \overline{P}}{\eta_M + \mu_{M*}} = \overline{N}_V$.

(ii) *Human compartments*

The equation for the rate of change of the total human population ($N_H(t)$):

$$\frac{dN_H}{dt} = \Pi_H - \mu_H N_H(t) - \delta_{HA} A_H(t) - \delta_H I_H(t) \ \leq \ \Pi_H - \mu_H N_H(t),$$

so that $N_H(t) = \frac{\Pi_H}{\mu_H} + \left[N_H(0) - \frac{\Pi_H}{\mu_H}\right] e^{-\mu_H t}$. Thus, $N_H \leq \frac{\Pi_H}{\mu_H}$ if $N_H(0) \leq \frac{\Pi_H}{\mu_H}$. In addition, if $N_H(0) > \frac{\Pi_H}{\mu_H}$, then $N_H(t) \to \frac{\Pi_H}{\mu_H}$ as $t \to \infty$. That is, $\limsup_{t\to\infty} \leq \frac{\Pi_H}{\mu_H}$.

□

It is convenient to define the set of variables $\mathcal{B}$ by:

$$\mathcal{B} = (S_H, W_H, E_{HN}, E_{HR}, I_H, A_H, R_H, E, L_1, L_2, L_3, L_4, P, S_X, E_X, I_X, S_Y, E_Y, I_Y, S_Z, E_Z, I_Z). \tag{3.3.5}$$

Consider the region:

$$\Omega = \big\{\mathcal{B}(t) \in \mathbb{R}^{22}_{+} : N_H(t) \leq \frac{\Pi_H}{\mu_H},\, 0 \leq E(t) < K_E,\, 0 \leq L_j(t) \leq \overline{L}_j\,(j = 1, 2, 3, 4),$$
$$0 \leq P(t) \leq \overline{P}, 0 \leq N_V(t) \leq \overline{N}_V\big\}.$$

Thus, it follows from Lemma 3.3.1 that Ω is positively-invariant for the model $\{(3.3.1), (3.3.3), (3.3.4)\}$. Hence, it is sufficient to consider the dynamics of the model in Ω (Hethcote, 2000).

3.4 Analysis of Autonomous Version of the Model

As in Chapter 2, it is instructive to, first of all, to gain insight into the dynamics of the autonomous version of the model $\{(3.3.1), (3.3.3), (3.3.4)\}$. Setting the temperature-dependent parameters of the model to constants give the following autonomous version of the model $\{(3.3.1), (3.3.3), (3.3.4)\}$ (denoted as the "autonomous

model"; the parameters of the model (3.4.1) are described in Table 3.2):

$$
\begin{aligned}
\frac{dE}{dt} &= \psi_E \varphi_Z \left(1 - \frac{E}{K_E}\right)_+ (S_Z + E_Z + I_Z) - (\sigma_E + \eta_E + \mu_E)E, \\
\frac{dL_1}{dt} &= \sigma_E E - (\sigma_{L_1} + \eta_L + k_L L + \mu_L)L_1, \\
\frac{dL_j}{dt} &= \sigma_{L_{(j-1)}} L_{j-1} - (\sigma_{Lj} + \eta_L + k_L L + \mu_L)L_j,\ j = 2, 3, 4, \\
\frac{dP}{dt} &= \sigma_{L_4} L_4 - (\sigma_P + \eta_P + \mu_P)P,
\end{aligned}
$$

$$
\begin{aligned}
\frac{dS_X}{dt} &= f\sigma_P P + \varphi_Z S_Z - (b_H p_H + \eta_M + \mu_M)S_X, \\
\frac{dE_X}{dt} &= \varphi_Z E_Z - (b_H p_H + \kappa_M + \eta_M + \mu_M)E_X, \\
\frac{dI_X}{dt} &= \varphi_Z I_Z + \kappa_M E_X - (b_H p_H + \eta_M + \mu_M)I_X, \\
\frac{dS_Y}{dt} &= b_H p_H (1 - \beta_V)\mathcal{G}_H S_X + b_H p_H (1 - \mathcal{G}_H)S_X - (\theta_Y + \eta_M + \mu_M)S_Y, \\
\frac{dE_Y}{dt} &= b_H p_H \beta_V \mathcal{G}_H S_X + b_H p_H E_X - (\theta_Y + \kappa_M + \eta_M + \mu_M)E_Y, \\
\frac{dI_Y}{dt} &= \kappa_M E_Y + b_H p_H I_X - (\theta_Y + \eta_M + \mu_M)I_Y, \\
\frac{dS_Z}{dt} &= \theta_Y S_Y - (\varphi_Z + \eta_M + \mu_M)S_Z, \\
\frac{dE_Z}{dt} &= \theta_Y E_Y - (\varphi_Z + \kappa_M + \eta_M + \mu_M)E_Z, \\
\frac{dI_Z}{dt} &= \theta_Y I_Y + \kappa_M E_Z - (\varphi_Z + \eta_M + \mu_M)I_Z,
\end{aligned}
\tag{3.4.1}
$$

$$
\begin{aligned}
\frac{dS_H}{dt} &= \Pi_H - b_H \beta_H \frac{I_X}{N_H} S_H + \rho_H W_H - \mu_H S_H, \\
\frac{dW_H}{dt} &= \xi_H R_H - (1 - \epsilon) b_H \beta_H \frac{I_X}{N_H} W_H - (\rho_H + \mu_H)W_H, \\
\frac{dE_{HN}}{dt} &= b_H \beta_H \frac{I_X}{N_H} S_H - (\gamma_{HN} + \mu_H)E_{HN}, \\
\frac{dE_{HR}}{dt} &= (1 - \epsilon) b_H \beta_H \frac{I_X}{N_H} W_H - (\gamma_{HR} + \mu_H)E_{HR}, \\
\frac{dI_H}{dt} &= r\gamma_{HN} E_{HN} + q\gamma_{HR} E_{HR} - (\alpha_H + \nu_H + \delta_H + \mu_H)I_H, \\
\frac{dA_H}{dt} &= (1 - r)\gamma_{HN} E_{HN} + (1 - q)\gamma_{HR} E_{HR} + \nu_H I_H - (\alpha_{HA} + \delta_{HA} + \mu_H)A_H, \\
\frac{dR_H}{dt} &= \alpha_H I_H + \alpha_{HA} A_H - (\xi_H + \mu_H)R_H,
\end{aligned}
$$

with $L = \sum_{j=1}^{4} L_j$ and $\mathcal{G}_H = \dfrac{I_H + A_H}{N_H}$.

Vectorial Reproduction Number ($\mathcal{R}_{MP}$)

It is convenient to define the threshold quantity:

$$\mathcal{R}_{MP} = \frac{\psi_E \varphi_Z \sigma_E \prod_{k=1}^{4} \sigma_{Lk} f \sigma_P \theta_Y b_H p_H}{\big(\sigma_E + \eta_E + \mu_E\big)\big(\sigma_P + \eta_P + \mu_P\big)\big(C_X C_Y C_Z - \theta_Y b_H p_H \varphi_Z\big) \prod_{k=1}^{4} \big(\sigma_{Lk} + \eta_L + \mu_L\big)},$$

where $C_X = b_H p_H + \eta_M + \mu_M$, $C_Y = \theta_Y + \eta_M + \mu_M$, $C_Z = \varphi_Z + \eta_M + \mu_M$ and $C_X C_Y C_Z - \theta_Y b_H p_H \varphi_Z = \big(\eta_M + \mu_M\big)\big[C_Z(C_X + \theta_Y) + b_H p_H \theta_Y\big] > 0$ (so that $\mathcal{R}_{MP} > 0$). The procedure to obtain (and interpretation of) threshold quantity ($\mathcal{R}_{MP}$) is similar to the *vectorial reproduction number* described in Chapter 2 (Section 2.4.1, Equation 2.4.2). That is, it measures the average number of new adult female mosquitoes produced by one reproductive mosquito during its entire reproductive period.

3.4.1 Existence and Asymptotic Stability of Disease-free Equilibria

For mathematical tractability, the analysis for the existence and asymptotic stability of the disease-free equilibrium of the autonomous model (3.4.1) will be carried out for the special case with no density-dependent larval mortality (i.e., $k_L = 0$).

Definition 3.4.1. Given $\mathcal{B}(t)$ as the vector of state variables defined in Equation (3.3.5), it is convenient to define

$$\mathcal{B}^{\diamond} = (S_H^{\diamond}, W_H^{\diamond}, E_{HN}^{\diamond}, E_{HR}^{\diamond}, I_H^{\diamond}, A_H^{\diamond}, R_H^{\diamond}, E^{\diamond}, L_1^{\diamond}, L_2^{\diamond}, L_3^{\diamond}, L_4^{\diamond}, P^{\diamond}, S_X^{\diamond}, E_X^{\diamond}, I_X^{\diamond}, S_Y^{\diamond}, E_Y^{\diamond}, I_Y^{\diamond}, S_Z^{\diamond}, E_Z^{\diamond}, I_Z^{\diamond}).$$

The following results follow from model (3.4.1):

(i) The model (3.4.1) has a trivial disease-free equilibrium (TDFE), where no mosquitoes exist, given by:

$$\mathcal{T}_0 = \Big(\frac{\Pi_H}{\mu_H}, 0, 0, 0, 0, 0, 0, 0, 0, 0, 0, 0, 0, 0, 0, 0, 0, 0, 0, 0, 0, 0, 0, 0\Big).$$

(ii) The model (3.4.1), with $k_L = 0$ has a unique non-trivial disease-free (mosquito-present) equilibrium (NDFE), given by,

$$\mathcal{E}_0 = \mathcal{B}^\diamond = \Big(\frac{\Pi_H}{\mu_H}, 0, 0, 0, 0, 0, 0, E^\diamond, L_1^\diamond, L_2^\diamond, L_3^\diamond, L_4^\diamond, P^\diamond, S_X^\diamond, 0, 0, S_Y^\diamond, 0, 0, S_Z^\diamond, 0, 0\Big),$$

where,

$$E_V^\diamond = K_E\Big(1 - \frac{1}{\mathcal{R}_{MP}}\Big),\ L_1^\diamond = \frac{\sigma_E}{C_{L1}}E^\diamond,\ L_j^\diamond = \frac{\sigma_{L_{j-1}}}{C_{Lj}}L_{j-1}^\diamond,\ (j = 2, 3, 4),\ P_V^\diamond = \frac{\sigma_{L_4}}{C_P}L_4^\diamond,$$
$$S_X^\diamond = \frac{1}{C_X}(f\sigma_P P^\diamond + \varphi_Z S_Z^\diamond),\ S_Y^\diamond = \frac{1}{C_Y}b_H p_H S_X^\diamond,\ S_Z^\diamond = \frac{\theta_Y b_H p_H f\sigma_P P^\diamond}{C_X C_Y C_Z - \theta_Y b_H p_H \varphi_Z}, \tag{3.4.2}$$

with $C_{Lj} = \sigma_{Lj} + \eta_L + \mu_L\,(j = 1, 2, 3, 4)$, $C_P = \sigma_P + \eta_P + \mu_P$, $C_X = b_H p_H + \eta_M + \mu_M$, $C_Y = \theta_Y + \eta_M + \mu_M$, $C_Z = \varphi_Z + \eta_M + \mu_M$ and $C_X C_Y C_Z - \theta_Y b_H p_H \varphi_Z = \big(\eta_M + \mu_M\big)\big[C_Z(C_X + \theta_Y) + b_H p_H \theta_Y\big] > 0$. This equilibrium exists if and only if $\mathcal{R}_{MP} > 1$.

Asymptotic Stability of TDFE

Theorem 3.4.1. *The TDFE of the model* (3.4.1)*, denoted by* $\mathcal{T}_0$*, is GAS in* Ω *whenever* $\mathcal{R}_{MP} \leq 1$.

The proof of Theorem 3.4.1 is given in Appendix C. It should, however, be stated that the TDFE (mosquito-free equilibrium), is ecologically unrealistic (since mosquitoes always exist in the (malaria-endemic) regions of interest).

3.4.2 Basic Reproduction Number ($\mathcal{R}_0$)

Asymptotic Stability of NDFE: Special Case

Consider the special case of the autonomous model (3.4.1) with no density-dependent larval mortality (i.e., $k_L = 0$). Furthermore, let $\mathcal{R}_{MP} > 1$ (so that the unique NDFE, $\mathcal{E}_0$, of the model (3.4.1) exists). It can be shown, using the next generation operator method Diekmann et al. (1990); van den Driessche and Watmough (2002), that the

associated reproduction number of the model (3.4.1) (denoted by $\mathcal{R}_0$) is given by:

$$\mathcal{R}_0 = \sqrt{\mathcal{R}_{HV} \times \mathcal{R}_{VH}}, \tag{3.4.3}$$

where,

$$\mathcal{R}_{HV} = b_H p_H \beta_V \frac{S_X^\diamond}{N_H^*}\left[\frac{r\gamma_{HN}}{g_1}\frac{1}{g_3} + \frac{r\gamma_{HN}}{g_1}\frac{\nu_H}{g_3}\frac{1}{g_4} + \frac{(1-r)\gamma_{HN}}{g_1}\frac{1}{g_4}\right], \tag{3.4.4}$$

and,

$$\mathcal{R}_{VH} = b_H \beta_H \frac{S_H^\diamond}{N_H^*}\frac{\kappa_M \varphi_Z \theta_Y (C_Y C_Z + C_Y g_X + g_X g_Z)}{(C_X C_Y C_Z - b_H p_H \varphi_Z \theta_Y)(g_X g_Y g_Z - b_H p_H \varphi_Z \theta_Y)}, \tag{3.4.5}$$

with $N_H^* = \dfrac{\Pi_H}{\mu_H}$, $g_1 = \gamma_{HN} + \mu_H$, $g_2 = \gamma_{HR} + \mu_H$, $g_3 = \alpha_H + \nu_H + \delta_H + \mu_H$, $g_4 = \alpha_{HA} + \delta_{HA} + \mu_H$, $C_X = b_H p_H + \eta_M + \mu_M$, $C_Y = \theta_Y + \eta_M + \mu_M$, $C_Z = \varphi_Z + \eta_M + \mu_M$, $g_X = C_X + \kappa_M$, $g_Y = C_Y + \kappa_M$, $g_Z = C_Z + \kappa_M$ and $C_X C_Y C_Z - \theta_Y b_H p_H \varphi_Z = \big(\eta_M + \mu_M\big)\big[C_Z(C_X + \theta_Y) + b_H p_H \theta_Y\big] > 0$. It is worth nothing that, at disease free equilibrium, $\dfrac{S_H^\diamond}{N_H^*} = 1$. The result below follows from Theorem 2 of van den Driessche and Watmough (2002).

Theorem 3.4.2. *The NDFE, $\mathcal{E}_0$, of the autonomous model* (3.4.1)*, with $k_L = 0$ and $\mathcal{R}_{EP} > 1$, is LAS in $\Omega \setminus \{\mathcal{T}_0\}$ if $\mathcal{R}_0 < 1$, and unstable if $\mathcal{R}_0 > 1$.*

Epidemiological Interpretation of Reproduction Threshold ($\mathcal{R}_0$)

The threshold quantity $\mathcal{R}_0$, given by Equation (3.4.3), measures the average number of new infections in humans (vectors) generated by an infectious vector (human). Its components are epidemiologically interpreted as follows.

1. *Interpretation of $\mathcal{R}_{HV}$:* The quantity $\mathcal{R}_{HV}$, given by (3.4.4), is associated with the infection of susceptible mosquitoes by infectious (asymptomatic and symptomatic) humans. It can further be expressed as:

$$\mathcal{R}_{HV} = \mathcal{R}_{I_H V} + \mathcal{R}_{A_H V}, \tag{3.4.6}$$

where,

$$\mathcal{R}_{I_HV} = b_H p_H \beta_V \frac{S_X^\diamond}{N_H^*} \frac{r\gamma_{HN}}{g_1} \frac{1}{g_3} \text{ and } \mathcal{R}_{A_HV} = b_H p_H \beta_V \frac{S_X^\diamond}{N_H^*} \left[\frac{r\gamma_{HN}}{g_1} \frac{\nu_H}{g_3} + \frac{(1-r)\gamma_{HN}}{g_1} \right] \frac{1}{g_4},$$

with $\mathcal{R}_{I_HV}$ accounting for the average number of new infectious adult female mosquitoes generated by symptomatically-infectious humans (I_H) and $\mathcal{R}_{A_HV}$ measures the average number of new infectious adult female mosquitoes generated by asymptomatically-infectious humans (A_H). In particular,

i. the quantity $\mathcal{R}_{I_HV}$ is the product of the infection rate of susceptible mosquitoes by symptomatically infected humans $\left(b_H p_H \beta_V \frac{S_X^\diamond}{N_H^*}\right)$, the probability that an exposed human survived the E_{HN} class and moved to the symptomatically-infected class (I_H) $\left(\frac{r\gamma_{HN}}{g_1}\right)$, and the average duration in the I_H class, $\left(\frac{1}{g_3}\right)$;

ii. the quantity $\mathcal{R}_{A_HV}$ is the product of infection rate of susceptible mosquito by asymptomatically infected humans $\left(b_H p_H \beta_V \frac{S_X^\diamond}{N_H^*}\right)$, the sum of the probability that an exposed human survived the E_{HN} and I_H classes and moved to the asymptomatically infected class (A_H) $\left(\frac{(1-r)r\gamma_{HN}}{g_1} + \frac{r\gamma_{HN}}{g_1}\frac{\nu_H}{g_3}\right)$, and the average duration in the A_H class $\left(\frac{1}{g_4}\right)$.

2. *Interpretation of $\mathcal{R}_{VH}$:* The threshold quantity $\mathcal{R}_{VH}$, given by (3.4.5), is associated with the infection of susceptible humans by infected mosquitoes at Stage I of the gonotrophic cycle (I_X). It can further be expressed as

$$\mathcal{R}_{VH} = b_H \beta_H \frac{S_H^\diamond}{N_H^*} \frac{1}{C_X} \big(\mathcal{R}_{V1H} + \mathcal{R}_{V2H} + \mathcal{R}_{V3H}\big), \tag{3.4.7}$$

where, $\mathcal{R}_{V1H}, \mathcal{R}_{V2H}$ and $\mathcal{R}_{V3H}$ account for all possible routes at which an exposed mosquito in Stage II of the gonotrophic cycle (E_Y) mosquito survives to become (and remain) an infected mosquito at Stage I of the gonotrophic cycle

(I_X) (i.e., the sum $\mathcal{R}_{V1H} + \mathcal{R}_{V2H} + \mathcal{R}_{V3H}$ is the probability that an exposed mosquito in E_Y class survives to become an infected mosquito in I_X class; see Appendix D for the derivation of the quantities $\mathcal{R}_{V1H}, \mathcal{R}_{V2H}$ and $\mathcal{R}_{V3H}$). It is convenient to introduce the following notations.

Definition 3.4.2. (a) $X \to Y$ means the fraction of adult mosquitoes that survives the X class and moves to the Y class;

(b) $X \to Y \to Z$ is the product of the proportions of adult mosquitoes that survived $X \to Y$ and $Y \to Z$ transmissions;

(c) $\big(\to X \to Y \to Z\big)^j = \to X \to Y \to Z \to X \to Y \to Z \to \cdots \to X \to Y \to Z$ (j times). That is, for $j = 2$, $\big(\to X \to Y \to Z\big)^2 = \to X \to Y \to Z \to X \to Y \to Z$.

(d) $\big(\to X \to Y \to Z\big)^\circ = 1$.

(i) The quantity $\mathcal{R}_{V1H}$, which accounts for the infection route (for $j, k \in \mathbb{Z}$)

$$E_Y \to E_Z \to E_X \big(\to E_Y \to E_Z \to E_X\big)^j \to I_X \big(\to I_Y \to I_Z \to I_X\big)^k,$$

is given by:

$$\mathcal{R}_{V1H} = \frac{\theta_Y}{g_Y}\frac{\varphi_Z}{g_Z} \times \sum_{j=0}^{n}\left(\frac{b_H p_H}{g_X}\frac{\theta_Y}{g_Y}\frac{\varphi_Z}{g_Z}\right)^j \times \frac{\kappa_M}{g_X} \times \sum_{k=0}^{m}\left(\frac{b_H p_H}{C_X}\frac{\theta_Y}{C_Y}\frac{\varphi_Z}{C_Z}\right)^k.$$

That is, there are two routes for an exposed mosquito in the second stage of the gonotrophic cycle (E_Y) to reach I_X class (so that it can transmit infection to a susceptible human), namely

(a) Direct route: $E_Y \to E_Z \to E_X \to I_X$ (when $n = 0$);

(b) Indirect route (i.e., E_Y fails to show symptoms the first time it become an E_X mosquito): $E_Y \to E_Z \to E_X \big(\to E_Y \to E_Z \to E_X\big)^j \to I_X$ (when $n > 0$).

This mosquito will remain in I_X where it can undergo the gonotrophic cycle (with $m > 0$) or not (with $m = 0$).

(*ii*) The quantity $\mathcal{R}_{V2H}$ which accounts for the infection route (for $j, k \in \mathbb{Z}$)

$$E_Y \to E_Z \left(\to E_X \to E_Y \to E_Z\right)^j \to I_Z \to I_X \left(\to I_Y \to I_Z \to I_X\right)^k,$$

is given by:

$$\mathcal{R}_{V2H} = \frac{\theta_Y}{g_Y} \times \sum_{j=0}^{n} \left(\frac{\varphi_Z}{g_Z}\frac{b_H p_H}{g_X}\frac{\theta_Y}{g_Y}\right)^j \times \frac{\kappa_M}{g_Z}\frac{\varphi_Z}{C_Z} \times \sum_{k=0}^{m} \left(\frac{b_H p_H}{C_X}\frac{\theta_Y}{C_Y}\frac{\varphi_Z}{C_Z}\right)^k.$$

(*iii*) The quantity $\mathcal{R}_{V3H}$ which accounts for the infection route (for $j, k \in \mathbb{Z}$)

$$E_Y \left(\to E_Z \to E_X \to E_Y\right)^j \to I_Y \to I_Z \to I_X \left(\to I_Y \to I_Z \to I_X\right)^k,$$

is given by:

$$\mathcal{R}_{V3H} = \sum_{j=0}^{n} \left(\frac{\theta_Y}{g_Y}\frac{\varphi_Z}{g_Z}\frac{b_H p_H}{g_X}\right)^j \times \frac{\kappa_M}{g_Y}\frac{\theta_Y}{C_Y}\frac{\varphi_Z}{C_Z} \times \sum_{k=0}^{m} \left(\frac{b_H p_H}{C_X}\frac{\theta_Y}{C_Y}\frac{\varphi_Z}{C_Z}\right)^k.$$

It is worth nothing that $0 \leq n, m \leq 6$, since an adult mosquito undergoes the gonotrophic cycle at most six in its lifetime Maharaj (2003). The quantity $\mathcal{R}_{VH}$ is the product of infection rate of susceptible humans by infected mosquitoes at Stage I of the gonotrophic cycle $\left(b_H \beta_H \frac{S_H^\diamond}{N_H^*}\right)$, the probability that an exposed mosquito at Stage II of the gonogtrophic cycle (E_Y) survived to become an infectious mosquito at Stage I of the gonotrophic cycle (I_X) (i.e., the sum of $\mathcal{R}_{V1H}, \mathcal{R}_{V2H}$ and $\mathcal{R}_{V3H}$), and the average duration in the I_X class $\left(\frac{1}{C_X}\right)$.

Global Asymptotic Stability of the NDFE: Special Case

The epidemiological implication of Theorem 3.4.2 is that the disease can be effectively controlled in a population if the initial sizes of the subpopulations of the model are close enough to the non-trivial disease-free equilibrium ($\mathcal{E}_0$). For such control to be

independent of the initial size of the subpopulation, a global asymptotic stability result need to be established for the NDFE ($\mathcal{E}_0$). This is done below for a special case of the model (3.4.1) with no disease-induced mortality in the human population (i.e., $\delta_H = \delta_{HA} = 0$) and no density-dependent larval mortality (i.e., $k_L = 0$).

Theorem 3.4.3. *The unique NDFE of the special case of the autonomous version of the model* (3.4.1) *with* $k_L = \delta_H = \delta_{HA} = 0$ *is GAS in* $\Omega \setminus \{\mathcal{T}_0\}$ *whenever* $\mathcal{R}_{MP} > 1$ *and* $\mathcal{R}_1 = \mathcal{R}_0\big|_{\delta_H=\delta_{HA}=0} < 1$.

Proof. Consider the special case of the autonomous model (3.4.1) with $\delta_H = \delta_{HA} = 0$ so that $N_H(t) \to N_H^* = \dfrac{\Pi_H}{\mu_H}$, as $t \to \infty$. Furthermore, let $k_L = 0$ and $\mathcal{R}_{MP} > 1$ (so that the unique NDFE, $\mathcal{E}_0$, exists) and $\mathcal{R}_1 = \mathcal{R}_0\big|_{\delta_H=\delta_{HA}=0} < 1$. Following Dumont and Chiroleu (2010), it is convenient to re-write the autonomous model (3.4.1) as:

$$\begin{aligned} \frac{dx_S}{dt} &= A_1(x)(x_S - x_{NDFE,S}) + A_{12}(x)x_I, \\ \frac{dx_I}{dt} &= A_2(x)x_I, \end{aligned} \tag{3.4.8}$$

where,

$$x_S(t) = \big(S_H(t), W_H(t), R_H(t), E(t), L_1(t), L_2(t), L_3(t), L_4(t), P(t), S_X(t), S_Y(t), S_Z(t)\big)^T,$$

$$x_I(t) = \big(E_{HN}(t), E_{HR}(t), I_H(t), A_H(t), E_X(t), I_X(t), E_Y(t), I_Y(t), E_Z(t), I_Z(t), 0, 0\big)^T,$$

$$x_{NDFE,S} = \big(S_H^\diamond, 0, 0, E^\diamond, L_1^\diamond, L_2^\diamond, L_3^\diamond, L_4^\diamond, P_V^\diamond, S_X^\diamond, S_Y^\diamond, S_Z^\diamond\big)^T, \text{ with } A_1(x) =$$

$$
\begin{bmatrix}
-\mu_H & +\rho_H & 0 & 0 & 0 & 0 & 0 & 0 & 0 & 0 & 0 & 0 \\
0 & -(\rho_H+\mu_H) & \xi_H & 0 & 0 & 0 & 0 & 0 & 0 & 0 & 0 & 0 \\
0 & 0 & -(\xi_H+\mu_H) & 0 & 0 & 0 & 0 & 0 & 0 & 0 & 0 & 0 \\
0 & 0 & 0 & -g_E-\psi_E\varphi_Z\dfrac{S_Z}{K_E} & 0 & 0 & 0 & 0 & 0 & 0 & 0 & \psi_E\varphi_Z\left(1-\dfrac{E^\diamond}{K_E}\right) \\
0 & 0 & 0 & \sigma_E & -g_{L1} & 0 & 0 & 0 & 0 & 0 & 0 & 0 \\
0 & 0 & 0 & 0 & \sigma_{L_1} & -g_{L2} & 0 & 0 & 0 & 0 & 0 & 0 \\
0 & 0 & 0 & 0 & 0 & \sigma_{L_2} & -g_{L3} & 0 & 0 & 0 & 0 & 0 \\
0 & 0 & 0 & 0 & 0 & 0 & \sigma_{L_3} & -g_{L2} & 0 & 0 & 0 & 0 \\
0 & 0 & 0 & 0 & 0 & 0 & 0 & \sigma_{L_4} & -g_P & 0 & 0 & 0 \\
0 & 0 & 0 & 0 & 0 & 0 & 0 & f\sigma_P & -C_X & 0 & 0 & 0 \\
0 & 0 & 0 & 0 & 0 & 0 & 0 & 0 & 0 & b_H p_H(1-\beta_V\mathcal{G}_H) & -C_Y & 0 \\
0 & 0 & 0 & 0 & 0 & 0 & 0 & 0 & 0 & 0 & \theta_Y & -C_Z
\end{bmatrix},
$$

$$
A_{12}(x) = \begin{bmatrix}
0 & 0 & 0 & 0 & 0 & b_H\beta_H\dfrac{S_H}{N_H} & 0 & 0 & 0 & 0 & 0 & 0 \\
0 & 0 & 0 & 0 & 0 & (1-\epsilon)b_H\beta_H\dfrac{W_H}{N_H} & 0 & 0 & 0 & 0 & 0 & 0 \\
0 & 0 & \alpha_H & \alpha_{HA} & 0 & 0 & 0 & 0 & 0 & 0 & 0 & 0 \\
0 & 0 & 0 & 0 & 0 & 0 & 0 & 0 & \psi_E\varphi_Z\left(1-\dfrac{E}{K_E}\right) & \psi_E\varphi_Z\left(1-\dfrac{E}{K_E}\right) & 0 & 0 \\
0 & 0 & 0 & 0 & 0 & 0 & 0 & 0 & 0 & 0 & 0 & 0 \\
0 & 0 & 0 & 0 & 0 & 0 & 0 & 0 & 0 & 0 & 0 & 0 \\
0 & 0 & 0 & 0 & 0 & 0 & 0 & 0 & 0 & 0 & 0 & 0 \\
0 & 0 & 0 & 0 & 0 & 0 & 0 & 0 & 0 & 0 & 0 & 0 \\
0 & 0 & 0 & 0 & 0 & 0 & 0 & 0 & 0 & 0 & 0 & 0 \\
0 & 0 & 0 & 0 & 0 & 0 & 0 & 0 & 0 & 0 & 0 & 0 \\
0 & 0 & 0 & 0 & 0 & 0 & 0 & 0 & 0 & 0 & 0 & 0 \\
0 & 0 & 0 & 0 & 0 & 0 & 0 & 0 & 0 & 0 & 0 & 0
\end{bmatrix},
$$

and, $A_2(x) =$

$$\begin{bmatrix}
-g_1 & 0 & 0 & 0 & 0 & b_H\beta_H\frac{S_H}{N_H} & 0 & 0 & 0 & 0 & 0 & 0 \\
0 & -g_2 & 0 & 0 & 0 & (1-\epsilon)b_H\beta_H\frac{W_H}{N_H} & 0 & 0 & 0 & 0 & 0 & 0 \\
r\gamma_{HN} & q\gamma_{HR} & -g_3 & 0 & 0 & 0 & 0 & 0 & 0 & 0 & 0 & 0 \\
(1-r)\gamma_{HN} & (1-q)\gamma_{HR} & \nu_H & -g_4 & 0 & 0 & 0 & 0 & 0 & 0 & 0 & 0 \\
0 & 0 & 0 & 0 & -g_X & 0 & 0 & 0 & 0 & 0 & 0 & 0 \\
0 & 0 & 0 & 0 & \kappa_M & -C_X & 0 & 0 & 0 & 0 & 0 & 0 \\
0 & 0 & b_Hp_H\beta_V\frac{S_X}{N_H} & b_Hp_H\beta_V\frac{S_X}{N_H} & b_Hp_H & 0 & -g_Y & 0 & 0 & 0 & 0 & 0 \\
0 & 0 & 0 & 0 & 0 & b_Hp_H & \kappa_M & -C_Y & 0 & 0 & 0 & 0 \\
0 & 0 & 0 & 0 & 0 & 0 & \theta_Y & 0 & -g_Z & 0 & 0 & 0 \\
0 & 0 & 0 & 0 & 0 & 0 & 0 & \theta_Y & \kappa_M & -C_Z & 0 & 0 \\
0 & 0 & 0 & 0 & 0 & 0 & 0 & 0 & 0 & 0 & 0 & 0 \\
0 & 0 & 0 & 0 & 0 & 0 & 0 & 0 & 0 & 0 & 0 & 0
\end{bmatrix},$$

where $g_1 = \gamma_{HN} + \mu_H$, $g_2 = \gamma_{HR} + \mu_H$, $g_3 = \alpha_H + \nu_H + \delta_H + \mu_H$, $g_4 = \alpha_{HA} + \delta_{HA} + \mu_H$, $C_X = b_Hp_H + \eta_M + \mu_M$, $C_Y = \theta_Y + \eta_M + \mu_M$, $C_Z = \varphi_Z + \eta_M + \mu_M$, $g_X = C_X + \kappa_M$, $g_Y = C_Y + \kappa_M$ and $g_Z = C_Z + \kappa_M$. It can be verified that the eigenvalues of $A_1(x)$ are real and non-positive. Hence, the system $\dfrac{dx_S}{dt} = A_1(x)(x_S - x_{NDFE,S})$ is GAS at $x_{NDFE,S}$ (Dumont and Chiroleu, 2010). It should be noted that the matrix $A_2(x)$ is a Metzler irreducible. Consider, next, the following bounded invariant set:

$$\begin{aligned}
\mathcal{B}_2 = \Big\{ & (S_H, W_H, R_H, E, L_1, L_2, L_3, L_4, P, S_X, S_Y, S_Z, E_{HN}, E_{HR}, I_H, A_H, E_X, I_X, E_Y, I_Y, \\
& E_Z, I_Z, 0, 0) \in \mathbb{R}^{24}_+ : N_H(t) \leq \frac{\Pi_H}{\mu_H},\ 0 \leq E(t) < K_E,\ 0 \leq L_j(t) \leq \overline{L}_j\ (j = 1, 2, 3, 4), \\
& 0 \leq P(t) \leq \overline{P}, 0 \leq N_V(t) \leq \overline{N}_V \Big\},
\end{aligned}$$

It is convenient to define

$$(\mathcal{R}_G)^2 = \frac{\overline{N}_V}{S^\diamond_X}(\mathcal{R}_1)^2 > (\mathcal{R}_1)^2.$$

Further, define a matrix $A_2(\bar{x}) = \bar{A}_2$, where $\bar{A}_2$ is an up*per*bound of the set (Dumont

and Chiroleu, 2010)

$$\mathcal{M} = \big\{A_2(x) \in \mathbb{R}^{12\times 12} : \, x(t) \in \mathcal{B}_2\big\},$$

with $\bar{x} = \big(S_H, W_H, R_H, E, L_1, L_2, L_3, L_4, P, S_X, S_Y, S_Z, E_{HN}, E_{HR}, I_H, A_H, E_X, I_X, E_Y, I_Y, E_Z, I_Z, 0, 0\big) \in \mathbb{R}^{12}_{+} \times \{0\}$. It can be verified that $\rho(\bar{A}_2) \leq 0$ if and only if $\mathcal{R}_G \leq 1$. Thus, it follows from Theorem 2.7 in Dumont and Chiroleu (2010) that, for $\mathcal{R}_{MP} > 1$ and $\mathcal{R}_1 < 1$,

$$\begin{aligned}&\big(S_H, W_H, R_H, E, L_1, L_2, L_3, L_4, P, S_X, S_Y, S_Z, E_{HN}, E_{HR}, I_H, A_H, E_X, I_X, E_Y, I_Y, E_Z,\\ &I_Z\big)(t) \to \Big(\frac{\Pi_H}{\mu_H}, 0, 0, E^{\diamond}, L_1^{\diamond}, L_2^{\diamond}, L_3^{\diamond}, L_4^{\diamond}, P^{\diamond}, S_X^{\diamond}, S_Y^{\diamond}, S_Z^{\diamond}, 0, 0, 0, 0, 0, 0, 0, 0, 0, 0\Big), \text{ as } t \to \infty,\end{aligned} \tag{3.4.9}$$

where $E, L_1, L_2, L_3, L_4, P, S_X, S_Y, S_Z$ are as defined in Equation (3.4.2). Thus, the NDFE ($\mathcal{E}_0$) of the autonomous model (3.4.1), with $\delta_H = \delta_{HA} = 0$, is GAS in $\Omega \setminus \{\mathcal{T}_0\}$ whenever $\mathcal{R}_{MP} > 1$ and $\mathcal{R}_1 < 1$. □

The epidemiological implication of Theorem 3.4.3 is that, for the special case of the autonomous version of the model (3.4.1) considered in Theorem 3.4.3, bringing (and maintaining) the threshold quantity $\mathcal{R}_1$ to a value less than unity is necessary and sufficient for the effective control (or elimination) of malaria in the population. It is worth mentioning that, as in prior models for spread of malaria and other vector-borne diseases (such as those in Castillo-Chavez and Song (2004); Forouzannia and Gumel (2014); Garba et al. (2008)), the autonomous version of the model (3.4.1) undergoes the phenomenon of backward bifurcation if the assumption on disease-induced mortality in humans is relaxed (i.e., if $\delta_H \neq 0, \delta_{HA} \neq 0$).

3.4.3 Sensitivity Analysis

As in Section 2.4.5, sensitivity analysis is carried out on the parameters of the model (3.4.1), with the basic reproduction number ($\mathcal{R}_0$) chosen as the response function. The

sensitivity analysis result obtained, tabulated in Table 3.4, show that the top PRCC-ranked parameters of the model are the aggregate (natural and biological control-related) death rate of adult female mosquitoes ($\mu_M + \eta_M$), *percapita* mosquito biting rate (b_H) and the transmission probability from infected mosquitoes to susceptible humans (β_H). These sensitivity analysis results suggest that malaria can be effectively controlled in the endemic setting considered by implementing a multi-faceted control strategy that minimizes the contact humans have with mosquitoes (i.e., minimize the parameters b_H and β_H by, for instance, using mosquito repellents and insecticide-treated bed nets) and reduces the mosquito population (i.e., increase $\mu_M + \eta_M$ by insecticide spraying and the use of insecticide-treated bed nets).

3.5 Numerical Simulations

3.5.1 Simulation of Autonomous Version of the Model

In this section, we present numerically-obtained curves relating $\mathcal{R}_0$ (for the autonomous model (3.4.1)) and temperature, across a range of fixed temperature values. We examine the effect of several key parameters on the relationship between $\mathcal{R}_0$ and temperature, namely temperature-independent adult (η_M) and immature death rates (η_E, η_L, and η_P) which may be related to the use of chemical/ biological control (e.g., the use of larvacides and adulticides), carrying capacity of eggs (K_E) which is a general measure of anopheline habitat availability, and finally infected human recovery rates (α_H and α_{HA}). For each temperature value (using a range of $14 - 40$ °C), the temperature-dependent parameters given in Section 3.3.3 are evaluated and set to a constant (i.e., $\mathcal{R}_0$ changes with temperature, but is time-invariant).

The results, depicted in Figure 3.3, show that the $\mathcal{R}_0$–temperature curves largely takes the same basic form regardless of which parameter (set) controls variations

in the $\mathcal{R}_0$–temperature curve, but with some slight variations. Most notably, the curve is extremely sensitive to temperature-independent adult *Anopheles* death, η_M, and increasing values of η_M also act to shift both the temperature range for sustained transmission and the peak temperature to higher values. Indeed, we note that when $\mathcal{R}_0$ is near one over much of its range, the temperature range where transmission is possible (i.e., $\mathcal{R}_0 > 1$) is invariable narrowed, but asymmetrically, such that higher temperatures are relatively favorable. This suggests that, in areas of marginal malaria potential, small increases in mean temperature could be more likely to increase malaria than elsewhere.

3.5.2 Simulation of Non-autonomous Model

The model $\{(3.3.1), (3.3.3), (3.3.4)\}$ is simulated to illustrate the effect of temperature on malaria transmission, with the temperature-dependent parameters determined using the expressions given in Section 3.3.3). Interestingly (and limiting ourselves to the case of constant temperature), we find that steady-state total (N_M) and infectious vector populations ($I_X + I_Y + I_Z$) are nearly linear functions of $\mathcal{R}_0$, whereas the infectious human compartments (I_H and A_H) vary hyperbolically with $\mathcal{R}_0$. This is demonstrated in Figure 3.4, and suggests that, when $\mathcal{R}_0$ is relatively small, smaller changes in $\mathcal{R}_0$, whether due to changing climate or other factors, may significantly affect the burden of disease. Whereas when the baseline $\mathcal{R}_0$ is high, disease burden, but not the infectious vector population, is insensitive to such small changes.

This pattern is further demonstrated in Figure 3.5, which shows how steady-state populations vary with temperature when $\mathcal{R}_0$ is relatively small versus large: when $\mathcal{R}_0$ is small over the temperature range where transmission is possible, infectious human populations also vary significantly, while when $\mathcal{R}_0$ is large over this temperature range, these populations are almost invariant, and the model tends to the same steady-

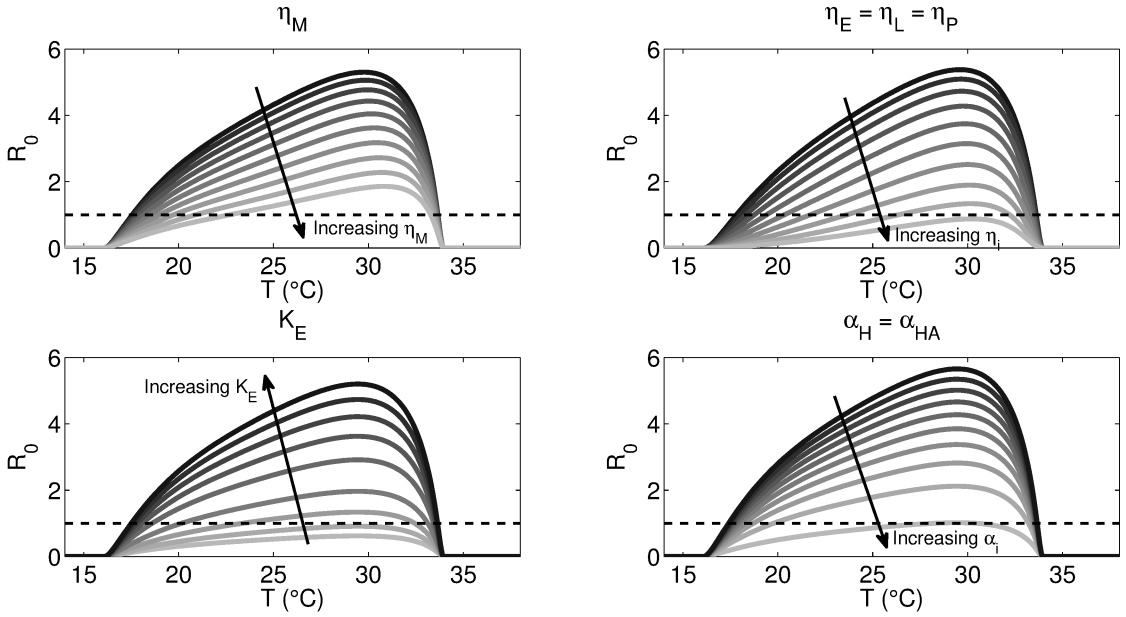

Figure 3.3: Curves for $\mathcal{R}_0$ as a function of temperature for various values of (a) adult mosquitoes death due to biological control (η_M) with $\eta_M \in [0.0079, 0.1]$, (b) immature mosquitoes death due to biological control (η_E, η_L and η_P) with $\eta_E = \eta_L = \eta_P \in [0.040, 0.79]$, (c) carrying capacity of eggs (K_E) with $K_E \in [10^3, 7 \times 10^4]$, and (d) recovery rates of infectious humans (α_A and α_{HA}) with $\alpha_H = \alpha_{HA} \in [0.33, 0.01]$. Note that, while the curves under variations in adult (η_M) and immature (η_E, η_L, η_P) mosquito mortality are similar in magnitude, η_M values are fivefold lower, and the peak of transmission potential also shifts slightly towards higher temperatures with increasing η_M. Other parameters values used are as given in Table 3.3.

state regardless. However, the infectious vector population still varies markedly with temperature even when $\mathcal{R}_0$ is large enough such that $I_H(\infty)$ and $A_H(\infty)$ do not. In all cases shown, $\mathcal{R}_0$ is modulated by K_E.

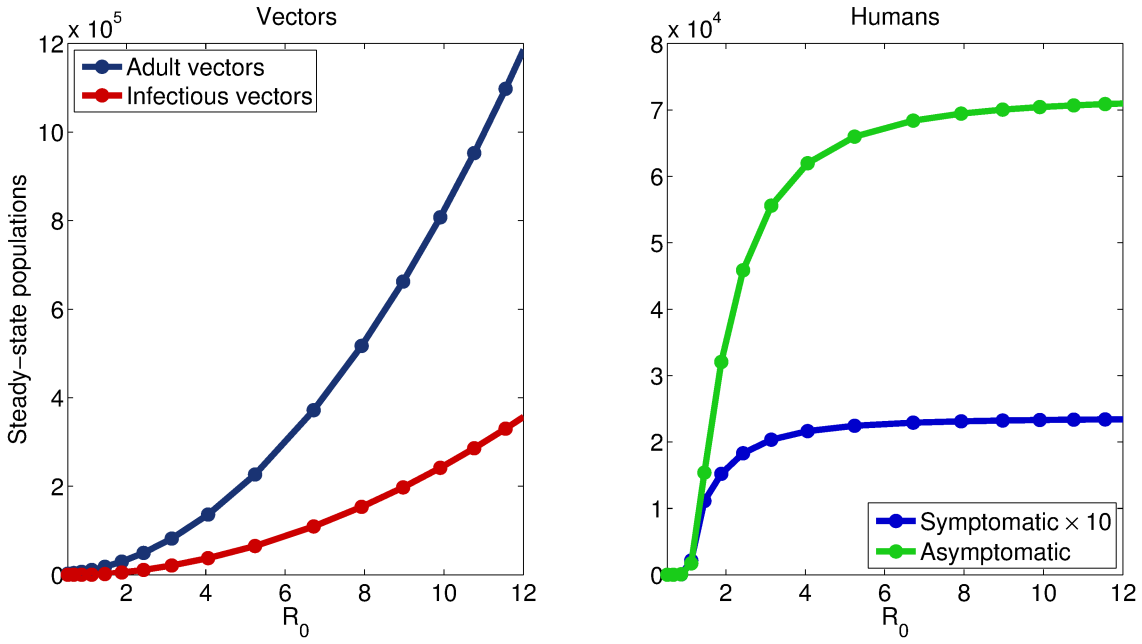

Figure 3.4: Steady-state vector (total and infectious, left panel) and infected human populations (symptomatic and asymptomatic, right panel), as a function of $\mathcal{R}_0$, when the carrying capacity K_E is used to modulate K_E (similar results are obtained when other parameters are used). Both vector populations increase somewhat super-linearly with $\mathcal{R}_0$, while a hyperbolic relationship between both infected human populations is seen, with little variation seen above $\mathcal{R}_0 > 4$. Also of note, a greater proportion of infected humans are symptomatic when $\mathcal{R}_0$ is relatively small. Parameters values used are as given in Table 3.3.

3.5.3 Effect of Diurnal Temperature Range (DTR)

While the simulations in Section 3.5.1 employ a constant ambient air and water temperature, there is increasing interest in the effect of diurnal temperature variations upon malaria transmission and climate (Beck-Johnson et al., 2017). Diurnal temperature variation is the possible fluctuation in temperature that occur during each day. This phenomenon has been shown (theoretically and experimentally) to have

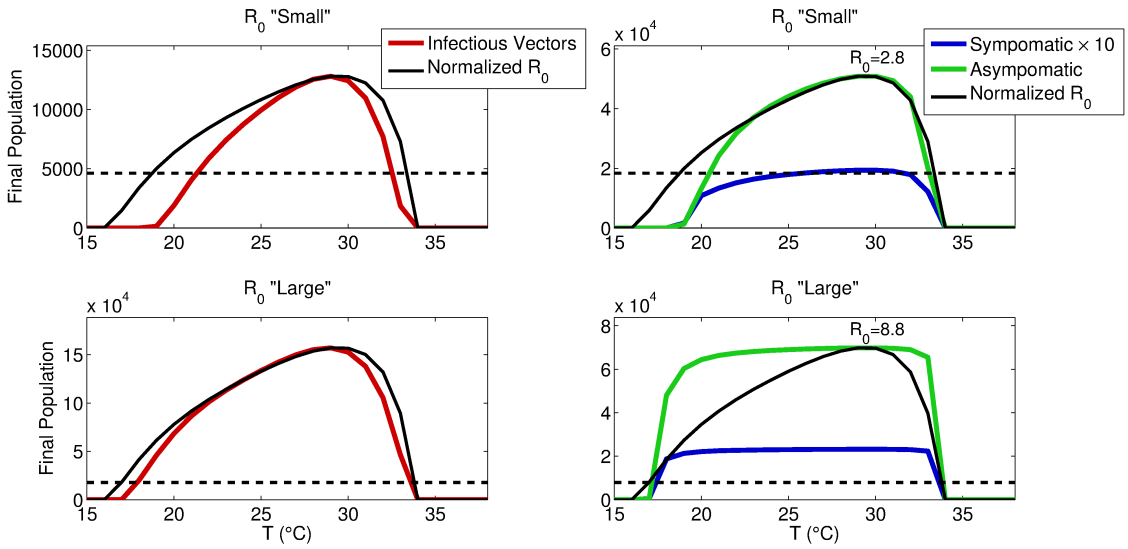

Figure 3.5: Steady-state infectious vector (left panels) and infected human populations (right panels) as a function of temperature, using either $K_E = 2 \times 10^4$ (top panels) or $K_E = 2 \times 10^5$ (bottom panels), with $\mathcal{R}_0$ normalized to the peak of either population also inscribed (the dotted line gives $\mathcal{R}_0 \equiv 1$); peak $\mathcal{R}_0$ values are also indicated in the right panels. We see that infectious vectors track $\mathcal{R}_0$ quite well regardless, whereas infected human populations are nearly invariant when $\mathcal{R}_0$ is large across most of the temperature range where transmission is possible.

important (or consequential) effect on pathogen development, vector survival (and development) and malaria transmission potential (Beck-Johnson et al., 2017; Eikenberry and Gumel, 2018; Gething et al., 2010; Paaijmans et al., 2008a,b). For instance, Paaijmans et al. (2010b) showed, experimentally, that the daily temperature fluctuations about relatively low temperatures accelerate the *Plasmodium* sporogonic duration, while fluctuations at higher temperatures leads to increased the *Plasmodium* sporogonic duration. Thus, most existing mathematical models of effect of temperature on malaria transmission dynamics that do not incorporate the effect of diurnal temperature variation may either under- or overestimated malaria potential at low and high

temperatures, respectively.

For these simulations, the following sinusoidal function will be used to simulate the model $\{(3.3.1), (3.3.3), (3.3.4)\}$ to account for the hourly fluctuations in local ambient temperature (Okuneye et al., 2018b):

$$T_A(t) = T_{A0} - \frac{\text{DTR}}{2} \sin\Big[\frac{2\pi}{24}\big(t_h + 14\big)\Big], \tag{3.5.1}$$

where in (3.5.1), T_{A0} is the mean daily air temperature, DTR captures variation about the mean (i.e., DTR is the diurnal temperature range), and t_h is the time in hours for any given day. Furthermore, near the surface of the water, air and surface water temperature are assumed equal in these simulations (i.e., $T_W(t) = T_A(t) = T(t)$) for computational tractability.

Therefore, we run the model under repeated (sinusoidal) diurnal temperature variation (given by Equation 3.5.1), with the daily temperature range (DTR) varying from 0 (constant temperature) to 15 °C, until it reaches a stable periodic solution. Average values of this periodic solution are plotted against daily mean temperature under different values of DTR in Figures 3.6 and 3.7, which differ in that K_E is 10^4 and 10^5, giving relatively low and high $\mathcal{R}_0$ values, respectively, and again shows how this affects the infected human populations. As we see, increasing DTR always shifts the temperature at which transmission peaks to a lower value, and also acts to asymmetrically narrow the temperature range over which transmission is possible: Transmission is decreased at both low and high temperature extremes, but the effect is more noticeable at the higher temperature range. Moreover, we also have found that peak transmission temperature decreases roughly linearly with DTR, from about 29.5 °C at a DTR of °0, down to 23.5 °C at a DTR of 20 °C (not shown).

Figure 3.8 shows how temperature-*independent* adult *Anopheles* mortality (η_M) interacts with both mean daily temperature and DTR. This figure shows that in-

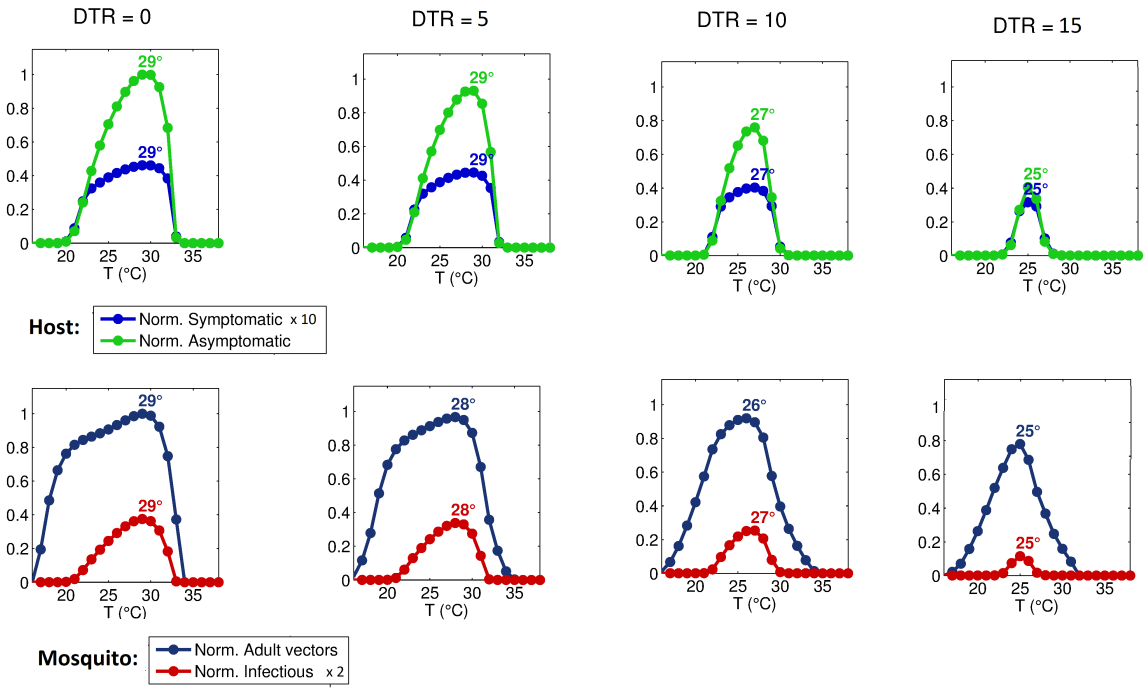

Figure 3.6: Approximate, normalized steady-state vector and infected human populations as functions of mean daily temperature, for DTRs of 0, 5, 10, and 15 °C (with daily variation about the mean given by Equation (3.5.1)). Vector populations are normalized to the maximum total population under DTR of 0, while human populations are normalized to the maximum asymptomatic population under DTR 0. All temperature-independent parameters are as in Table 3.3, except $K_E = 10^4$, giving a relatively low $\mathcal{R}_0(T)$ throughout. Increasing DTR results in both smaller vector and infected human populations, and shifts the temperature for peak transmission to lower values (peak temperatures for all curves are indicated in the figure).

creasing η_M tends to very slightly increase peak transmission temperatures, and disproportionately reduces the infectious vector population relative to the total vector population.

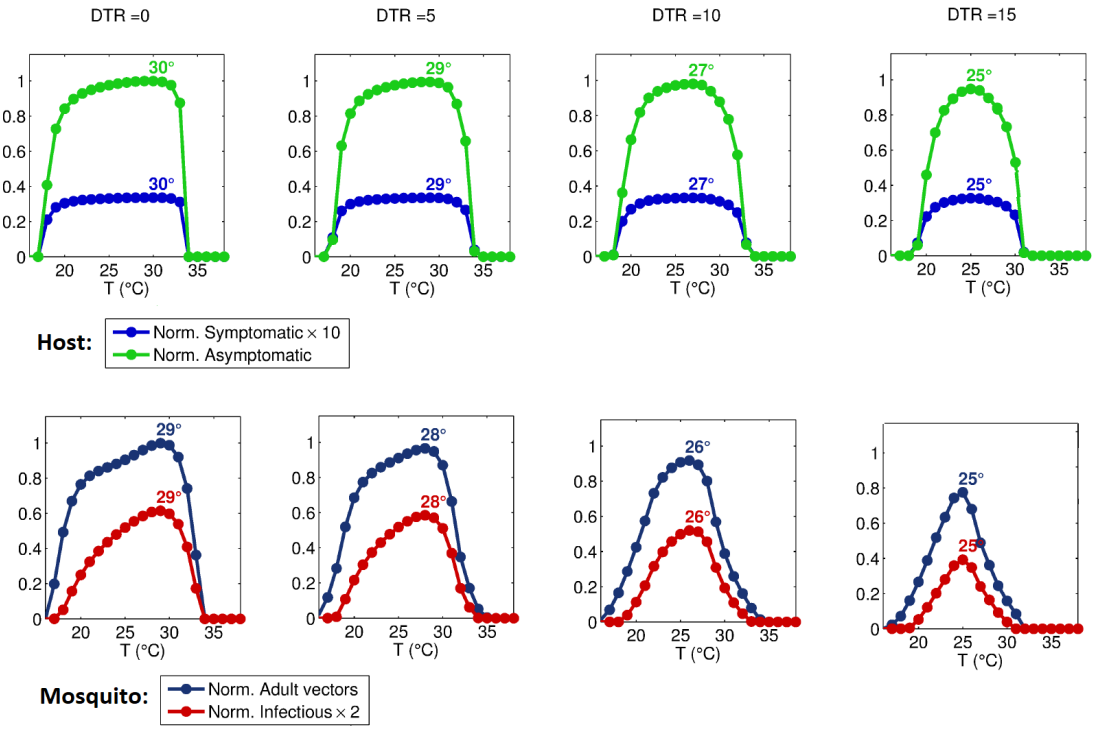

Figure 3.7: Mirroring Figure 3.6, we have approximate, normalized steady-state vector and infected human populations as functions of mean daily temperature, for DTRs of 0, 5, 10, and 15 °C, but with $K_E = 10^5$ (and other parameters *per* Table 3.3), giving a relatively high $\mathcal{R}_0(T)$ throughout. Vector and human numbers are normalized to the peak total vector and asymptomatic human population under DTR 0 °C, respectively.

Effect of Sporogony and Gonotropy

We have also formulated two slightly different versions of the full non-autonomous model, with Case (a) the model lacking an explicit representation of the gonotrophic cycle (the resulting compartments for the dynamics of the adult female mosquitoes are presented in Appendix E), and, therefore, oviposition occurs at temperature-dependent rate proportional to all adult female mosquitoes (not just those in stage

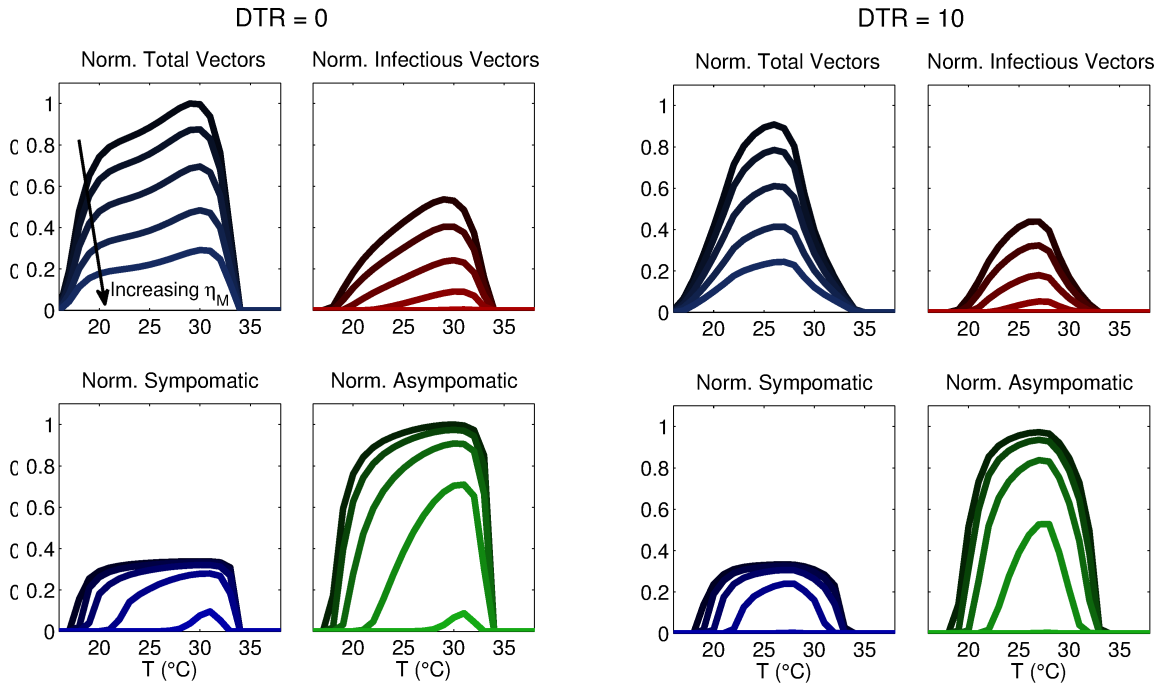

Figure 3.8: The left set of panels shows how increasing values of η_M, from 0.0079 to 0.1585 day^{-1}, affect (normalized) steady-state total adult vector, infectious vector, symptomatic human, and asymptomatic human populations as a function of daily mean temperature, when DTR is 0 °C. The right set panels gives the same populations, but under DTR = 10 °C. Lighter curves indicate larger η_M values, and all temperature-independent parameter values are given in Table 3.3. As in Figures 3.6 and 3.7, vector and human populations are always normalized to the peak total vector and peak asymptomatic human populations when DTR is 0 °C. Also note that the symptomatically infected human population size is inflated by a factor of ten for clarity.

III of the gonotrophic cycle), and Case (b) a model omitting the exposed but non-infectious mosquito compartments (i.e., the model does not account for the delay from infection to infectivity imposed by the sporogonic cycle; the resulting compartments for the dynamics of the adult female mosquitoes are presented in Appendix E). As seen

in Figure 3.9, the omission of gonotrophy has almost no effect on the temperature range across which transmission is predicted to be possible, with the omission of sporogony much more influential. It should be noted that, while (normalized) steady-state values for infected humans and adults mosquitoes are essentially unaffected by the omission of gonotrophy, its inclusion is still expected to affect model dynamics under more variable weather conditions.

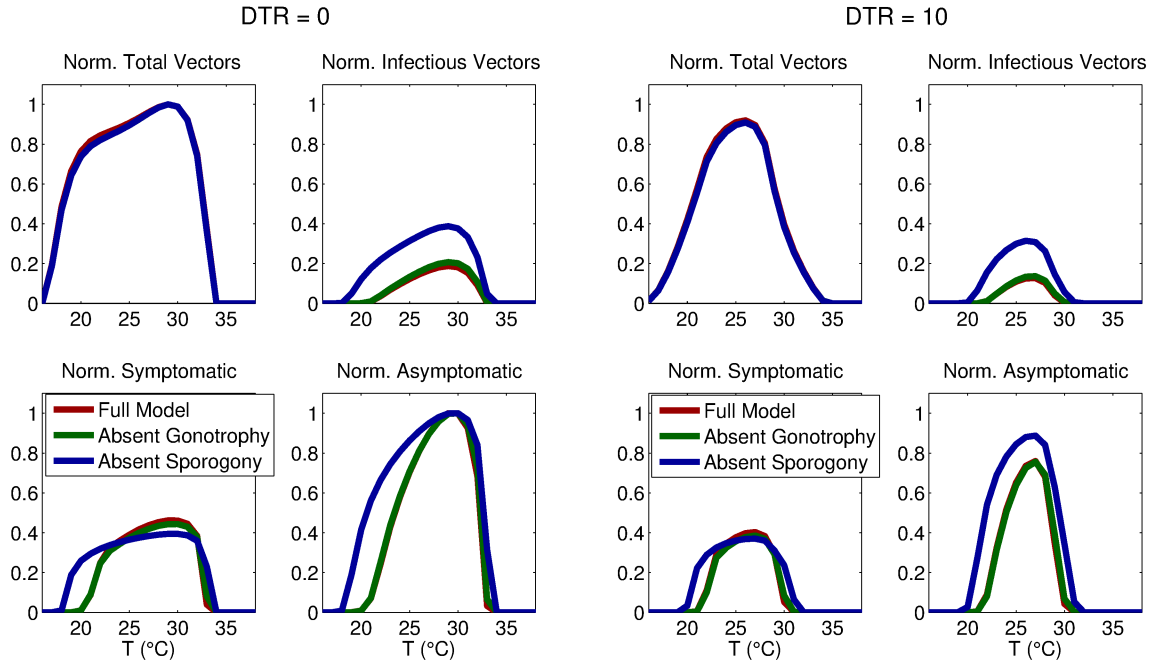

Figure 3.9: Normalized steady-state total adult vector, infectious vector, symptomatic human, and asymptomatic human populations under either the full model or versions omitting either gonotrophy or sporogony, as a function of daily mean temperature, with DTR either 0 (left panels) or 10 °C (right panels). Normalization is performed independently for each model version, with normalization performed relative to the maximum total vector and asymptomatic human populations, and with the symptomatic human compartment inflated tenfold for display purposes. All temperature-independent parameters are as given in Table 3.3, except $K_E = 10^4$.

3.6 Summary of Results

A new temperature-dependent model for assessing the population-level impact of temperature variability on the transmission dynamics of malaria in a community has been developed and rigorously analyzed. Some of the notable novel features of the model include incorporating the gonotrophic cycle of the female *Anopheles* mosquitoes and the *Plasmodium's* sporogonic cycle, as well as all aquatic stages of the immature mosquitoes. This allows for a comprehensive modeling and a quantitative understanding of the effect of the temperature-dependent gonotrophic and sporogonic cycles on malaria transmission dynamics. Furthermore, other pertinent features of malaria transmission dynamics, such as, disease transmission to vectors by asymptomatically-infectious humans, reduced malaria susceptibility in humans due to recovery from prior malaria infection, the possibilities of conversion of symptomatic humans to an asymptomatic state, and the complete loss of partial immunity in humans, are also incorporated.

The non-autonomous model $\{(3.3.1), (3.3.3), (3.3.4)\}$ has a non-trivial disease-free solution (NDFS) which exists whenever a certain *vectorial reproduction ratio* ($\mathcal{R}_{Mt}$; the spectral radius of a certain linear operator of a function of the next generation matrices of vector-only model) is greater than unity. The NDFS is shown to be globally-asymptotically stable, in the absence of disease-induced mortalities in humans (i.e., $\delta_H = \delta_{HA} = 0$), whenever the spectral radius of a certain linear operator of a function of the next generation matrices of full model (denoted by $\mathcal{R}_{0t}$) is less than unity. The model has at least one positive periodic solution whenever $\mathcal{R}_{0t} > 1$ (and the disease persists in the population in this case).

Furthermore, this study suggests (using detailed sensitivity and uncertainty analyses of the autonomous version of the model, to identify the top PRCC-ranked pa-

rameters) that effective malaria control entails a multi-faceted approach based on:

(a) minimizing the contact humans have with mosquitoes (i.e., minimizing the *percapita* mosquito biting rate and the transmission probability from infected mosquitoes by using mosquito repellents and insecticide-treated bed nets, and potentially via the use of anti-malaria drugs as intermittent preventative therapy);

(b) reducing the mosquito population (i.e., increasing death rate of mature mosquitoes by insecticide spraying, using insecticide-treated bed nets and removing stagnant waters, to prevent successfully fed adult female mosquitoes from returning close-by breeding sites);

(c) early diagnosis and treatment of malaria cases.

The aforementioned simulations suggest several interesting observations. First, there is a highly nonlinear, *hyperbolic*, relationship between $\mathcal{R}_0$, which represents the number of new infections introduced by a single case into a fully susceptible, non-immune population, and the actual asymptotic populations of infected humans (both symptomatic and asymptomatic), such that, once $\mathcal{R}_0$ is sufficiently large, disease burden is essentially unaffected by (reasonably small) changes in $\mathcal{R}_0$. This relates to the well-known epidemiology of malaria: in highly endemic areas, the population may be exposed to as many as hundreds of infectious bites *per* year, yet disease burden is essentially stable, with most clinical disease concentrated in very young children who have not yet developed a degree of immunity (Carter and Mendis, 2002). It is only in more marginal areas of malaria transmission that disease burden tends to be more unstable, where severe disease affects persons across age groups and the population has a high degree of vulnerability to epidemics (Carter and Mendis, 2002; Macdonald

et al., 1957). This is reflected in our model, in that only at relatively low $\mathcal{R}_0$ values do changes in this parameter translate nearly linearly into clinical disease.

Furthermore, this phenomenon of $\mathcal{R}_0$ relating hyperbolically to clinical disease is also manifested in our $\mathcal{R}_0$-temperature curves. When temperature-independent parameters are such that $\mathcal{R}_0$ is relatively low across the temperature range for which transmission is possible, both $\mathcal{R}_0$ and infected human populations (I_H and A_H) change appreciably with temperature. If, on the other hand, the "basal" $\mathcal{R}_0$ is high, then while $\mathcal{R}_0$ changes with temperature, I_H and A_H do not, except for a quasi-threshold phenomenon where, below about 17 and above 34 °C, I_H and A_H are zero, but almost constant within these temperature bounds. Thus, our results suggest that climate change may affect areas of high endemicity (e.g. holo- and hyperendemic areas) and areas of low endemicity or unstable transmission very differently. Within the former, which tend to be warm areas in western and central equatorial Africa, several degrees of warming will affect disease burden only if a threshold mean daily temperature (likely on the order of about 34 °C) is crossed, and then dramatically, with a sharp drop in disease burden. In the latter, which tend to be cooler areas, such as the eastern African highlands, warming temperatures may affect disease burden in a more continuous manner, with increases in $\mathcal{R}_0$ with temperature translating more directly into clinical disease. Thus, modest warming would most likely result in a net increase in overall disease potential.

Numerical simulations of the model also indicate that temperature variability is important in determining the optimum temperature ranges for malaria transmission, with increasing daily temperature range (DTR) shifting the optimum temperature for transmission down from about 29.5 °C when temperature is constant, to 23.5 °C when DTR is 20 °C, and moreover, asymmetrically contracting the temperature range where transmission is possible, such that higher temperatures are more affected, in

reasonable concordance with recent modeling work by Beck-Johnson et al. (2017).

Finally, two reduced version of the model (one omitting explicit representation of the gonotrophic cycle and the other omitting the sporogonic cycle) are also briefly considered. In the former case, normalized asymptotic mosquito and infected humans populations are hardly affected under constant weather conditions, although dynamics may still be affected when weather conditions vary (in other words, mosquito gonotrophic cycle does not seem to have major impact on malaria dynamics, and its explicit inclusion in malaria transmission models can be relaxed). The omission of sporogony, however, very strongly affects model predictions (suggesting that it is crucial to include in models for malaria transmission dynamics).

Parameters	Description
Π_H	Recruitment rate of humans
μ_H	Natural death rate of humans
ρ_H	Rate of complete loss of partial immunity (from W_H to S_H class)
b_H	*percapita* mosquito biting rate in gonotrophic Stage I
β_H	Transmission probability from infectious mosquitoes to susceptible humans
ξ_H	Rate of loss of infection-acquired immunity (from R_H to W_H)
ϵ	Modification parameter for the reduction of human susceptibility after recovery from prior infection
γ_{HR} (γ_{HN})	Progression rate of exposed humans with (without) prior immunity to infectious class
q (r)	Probability of exposed humans with (without) prior immunity showing symptoms of disease
p_H	Probability of successfully taking bloodmeal from humans
ν_H	Transition rate of symptomatic humans to asymptomatically infectious class
δ_H, δ_{HA}	Malaria-induced death rates of humans in class I_H and A_H, respectively
α_H	Recovery rate of symptomatically infectious humans
α_{HA}	Recovery rate of asymptomatically infectious humans
ψ_E	Number of eggs laid *per* oviposition
σ_E	Maturation rate of eggs
σ_{Lj}	Maturation rate of larvae from larval Stage j to Stage $j+1$ (for $j = 1, 2, 3$)
σ_P	Maturation rate of pupae
f	Proportion of adult mosquitoes that are females
$\mu_E, \mu_L, \mu_P, \mu_M$	Temperature-dependent death rates of eggs, larvae, pupae and adult mosquitoes, respectively
$\eta_E, \eta_L, \eta_P, \eta_M$	Temperature-independent death rates for eggs, larvae, pupae and adult female mosquitoes, respectively
k_L	Density-dependent mortality rate of larvae
β_V	Transmission probability from infectious humans to susceptible mosquitoes
θ_Y	Rate of progression for stage II of the gonotrophic cycle
φ_Z	Rate of oviposition for adults in stage III of the gonotrophic cycle
κ_M	Progression rate of exposed adult female mosquitoes to infectious stage
K_E	Carrying capacity of eggs

Table 3.2: Description of parameters of the autonomous model (3.4.1).

Parameters	Range	Baseline	Reference
μ_H	$1/(50 \times 365) - 1/(70 \times 365)$ day^{-1}	$1/(60 \times 365)$ day^{-1}	Derived from data
Π_H	$3 - 5$ day^{-1}	4.5 day^{-1}	Derived from data
ξ_H	$0.003 - 0.016$ day^{-1}	0.01 day^{-1}	[72]
α_H	$1/1500 - 1$ day^{-1}	1/30 day^{-1}	[117; 216; 225]
α_{HA}	$1/1500 - 1/100$ day^{-1}	1/180 day^{-1}	[117; 216; 225]
r	$0.67 - 1.0$	0.9	[72]
q	$0.01 - 0.33$	0.33	[72]
γ_{HN}	$0.09 - 0.15$ day^{-1}	1/14 day^{-1}	[72]
γ_{HR}	$0.08 - 0.13$ day^{-1}	1/14 day^{-1}	[72]
δ_H	$0.0001 - 0.0025$	0.0021	[72]
δ_{HA}	$1 \times 10^{-7} - 5.61 \times 10^{-6}$	5.61×10^{-6}	[72]
b_H	$0.5 - 4$ day^{-1}	2 day^{-1}	[61]
p_H	$0.3 - 1$	1	[120]
β_H	$0.01 - 0.50$	0.50	[141; 198; 204; 225]
ν_H	$0.001 - 0.05$	1/30	[72]
ϵ	$0.1 - 1.0$	0.5	[229]
β_V	$0.02 - 0.25$	0.15	[46; 91; 138]
ρ_H	$1/(5 \times 365) - 1/(7 \times 365)$ day^{-1}	$1/(6 \times 365)$ day^{-1}	[80]
f	$0.4 - 0.6$	0.5	[72]
σ_E	$0.33 - 1$ day^{-1}	0.5	[72]
σ_P	$0.33 - 1$ day^{-1}	0.5	[72]
η_E	$0 - 0.5$ day^{-1}	0	[72]
η_L	$0 - 0.5$ day^{-1}	0	[72]
η_P	$0 - 0.5$ day^{-1}	0	[72]
η_M	$0 - 0.5$ day^{-1}	0	[72]
φ_Z	$0.5 - 4$ day^{-1}	2 day^{-1}	[61]
ψ_E	$10 - 150$ eggs oviposition^{-1}	65 eggs oviposition^{-1}	[8; 234]
K_E	$1.0 \times 10^4 - 1.0 \times 10^6$	1.0×10^5	[72]
k_L	$0 - 0.0001$	0	[72]

Table 3.3: Ranges and baseline values for the temperature-independent parameters of the model (detailed derivation of the values of these parameters is given in Section 2.5).

Parameters	$\mathcal{R}_0$	Parameters	$\mathcal{R}_0$
Π_H	-0.18	b_H	**+0.57**
β_H	**+0.53**	p_H	$+0.067$
γ_{HN}	$+0.013$	r	-0.35
ν_H	$+0.081$	δ_H	$+0.046$
δ_{HA}	-0.034	α_H	-0.26
α_{HA}	-0.44	ψ_E	$+0.061$
σ_E	$+0.32$	σ_{L_1}	$+0.15$
σ_{L_2}	$+0.17$	σ_{L_3}	$+0.15$
σ_{L_4}	$+0.12$	σ_P	$+0.23$
f	$+0.13$	β_V	-0.42
$\mu_E + \eta_E$	$+0.15$	$\mu_L + \eta_L$	-0.15
$\mu_P + \eta_P$	-0.034	$\mu_M + \eta_M$	**-0.72**
θ_Y	$+0.22$	φ_Z	-0.29
κ_M	$+0.34$	K_E	$+0.28$

Table 3.4: PRCC values for the parameters of the model (3.4.1), using the basic reproduction number $\mathcal{R}_0$ as the response functions. The top (most-influential) parameters that affect the dynamics of the model (with respect to $\mathcal{R}_0$) are highlighted in bold font. Parameter values and ranges used are as given in Table 3.3.

Chapter 4

MATHEMATICAL ANALYSIS OF DENGUE-CHIKUNGUNYA-ZIKA TRANSMISSION: ROLE OF DENGUE VACCINE AND SEASONALITY

4.1 Introduction

Aedes aegypti is the vector for numerous diseases in humans and other (reservoir) hosts, such as chikungunya (CHIKV), dengue fever (DENV) and Zika virus (ZIKV). In this chapter, a new deterministic model is designed and used to assess the dynamics of the three diseases in a population where *Aedes* mosquitoes are abundant. The model to be designed incorporates the recently-released imperfect vaccine against dengue virus (*Dengvaxia*® vaccine by Sanofi Pasteur) as well as allow for sexual transmission of Zika. Further, the model allows for the assessment of the population-level impact of three biological hypotheses, namely a competitive dengue-chikungunya-Zika superinfection hierarchy, an antibody-dependent enhancement of dengue over Zika and that the *Dengvaxia* vaccine can induce reduced susceptibility to Zika infection in vaccinated individuals. The effect of seasonality on the dynamics of the three diseases in a population will be studied.

Three mosquito-borne viruses CHIKV, DENV and ZIKV, are currently co-circulating in the same geographical regions of the American continent (with ZIKV being the most recent of the three mosquito-borne viral diseases). Concurrent outbreaks of these three viruses have been reported in the South Pacific region Roth et al. (2014). The outbreaks distribution is interesting, since, in the South Pacific, there are islands with a single outbreak with one virus differing from the virus of the outbreak in a neighboring island. Furthermore, there are multiple outbreaks of different viruses in

a single island (for instance, DENV-1, DENV-3, ZIKV and CHIKV in New Caledonia and the islands of Kiribati (DENV-1 and DENV-3) and Fiji (DENV-1, DENV-2 and DENV-3)) (Roth et al., 2014).

Dengue, chikungunya and Zika are epidemic vector-borne diseases co-circulating in many parts of the world. There is evidence for rare occurrence of co-infections limited to certain geographical areas (mainly in Asia and Southeast Asia) and under-reporting of each of them because of the diagnostic clues which are similar in all three diseases Cardoso et al. (2017); Dupont-Rouzeyrol et al. (2015); Furuya-Kanamori et al. (2016). In particular, although such co-infections are very rare in the Americas (e.g., that of ZIKV and DENV Dupont-Rouzeyrol et al. (2015); Furuya-Kanamori et al. (2016)), the three viruses maintain their own epidemic (the current study does not include the effect of co-infections, owing to their rarity).

Furthermore, it is known that ZIKV shares up to 60% of nucleotide identity with DENV, and it has been postulated that primary infection with DENV (or other *flavivirus*) may induce antibody that cross-react with a subsequent secondary infection with ZIKV and result in increased viral burden and a cascade of deleterious immunologic and clinical events Barouch et al. (2017); Dejnirattisai et al. (2016); Durbin (2016). On the other hand, Althouse et al. (2015) pointed out that the patterns of viral abundance (referring to ZIKV, CHIKV and DENV) "could stem from processes within their mammalian hosts, including cycling of immunity, cross-immunity between viruses, and host demographics and abundance". The distribution of the mosquitoes capable of transmitting the disease is also heterogeneous. *Aedes aegypti* is present in most of the islands in the South Pacific, but at least four different species of *Aedes* are present in different regions of this area of the world.

Dengue Vaccine: *Dengevaxia*

A new vaccine for DENV (*Dengvaxia*®, by Sanofi Pasteur) has been released in 2015 (and has been approved in 11 countries in 2016) (Vannice et al., 2016). The vaccine is a tetravalent vaccine but has lower efficacy for one of the four dengue serotypes. The efficacy of the vaccine varies by serotypes (71.6% for serotype 3; 76.9% for serotype 4; 54.7% for serotype 1 and 43.0% for serotype 2) [176]. Although the precise effect of the dengue vaccine on ZIKV is not yet known, the possible practical and theoretical impact of this vaccine on ZIKV has been a subject of considerable debate. For instance, while Paul et al. (2016) described the possible consequence of the large antigenic overlap of ZIKV and DENV, (Tang et al., 2016) noted that ADE is a real concern (since the response of ZIKV to DENV antibody has not been fully investigated). Furthermore, Halstead (interview reported by Cohen (2016)) warned about the possible secondary undersigned implications that ADE and DENV vaccine may produce. Consequently, it seems plausible to explore the hypothesis that the *Dengvaxia* vaccine may have some effect on ZIKV. The model to be designed in this study will incorporate the assumption that DENV vaccine could decrease susceptibility to ZIKV.

The purpose of this chapter is to study the transmission dynamics of the three diseases in a population. In particular, the study will focus on exploring the coexistence mechanisms, among these three viral species, given that they share the same vector but have some variations in transmission modes and regional spread. This study proposes three fundamental hypotheses. The first is a superinfection hypothesis (i.e., the existence of a competitive hierarchy among the viruses involved). Superinfection has been postulated as a common mechanism for community structure (Levin and Pimentel, 1981; Nowak and May, 1994; Tilman, 1994), and has been used to

particularly explain pathogen communities sharing a common host (Castillo-Chavez and Velasco-Hernandez, 1998; Mena-Lorca et al., 2006; Nowak and May, 1994). The second hypothesis is that dengue can increase Zika dynamics *via* antibody-dependent enhancement. The third hypothesis is that the dengue vaccine can impact (reduce or increase) the susceptibility of vaccinated individuals to ZIKV infection.

4.2 Formulation of Mathematical Model

The total human population at time t, denoted by $N_H(t)$, is split into the mutually-exclusive compartments of humans who are wholly-susceptible ($S_H(t)$), vaccinated against DENV ($V_H(t)$), susceptible and partially-immuned to CHIKV due to past exposure and recovery from CHIKV ($S_{RC}(t)$), susceptible and fully-immuned to DENV due to past exposure and recovery from DENV ($S_{RD}(t)$), susceptible and partially-immuned to ZIKV due to past exposure and recovery from ZIKV ($S_{RZ}(t)$), infected with CHIKV ($Y_C(t)$), DENV ($Y_D(t)$), ZIKV ($Y_Z(t)$), recovered from CHIKV ($R_C(t)$), recovered from DENV ($R_D(t)$) and recovered from ZIKV ($R_Z(t)$), so that:

$$N_H = S_H + V_H + S_{RC} + S_{RD} + S_{RZ} + Y_C + Y_D + Y_Z + R_C + R_D + R_Z.$$

Similarly, the total population of adult female *Aedes aegypti* mosquitoes at time t, denoted by $N_V(t)$, is split into susceptible mosquitoes ($S_V(t)$) and mosquitoes infected with CHIKV ($I_C(t)$), infected with DENV ($I_D(t)$) and infected with ZIKV ($I_Z(t)$). Thus,

$$N_V(t) = S_V(t) + I_C(t) + I_D(t) + I_Z(t).$$

The model is given by the following deterministic system of nonlinear differential equations (where a prime represents differentiation with respect to time t) (Okuneye et al., 2017):

$$
\begin{aligned}
S'_H &= \mu_H N_H + \alpha_H V_H - \beta_H \frac{I_D + \theta_C I_C + \theta_Z I_Z}{N_H} S_H - \beta_S \frac{Y_Z}{N_H} S_H - (\psi_D + \mu_H) S_H, \\
V'_H &= \psi_D S_H - \beta_H \frac{\sigma_D I_D + \theta_C I_C + \sigma_Z \theta_Z I_Z}{N_H} V_H - \beta_S \sigma_Z \frac{Y_Z}{N_H} V_H - (\alpha_H + \mu_H) V_H, \\
S'_{RC} &= \xi_C R_C - \beta_H \frac{I_D + \varphi_C \theta_C I_C + \theta_Z I_Z}{N_H} S_{RC} - \beta_S \frac{Y_Z}{N_H} S_{RC} - \mu_H S_{RC}, \\
S'_{RD} &= \xi_D R_D - \beta_H \frac{\theta_C I_C + \theta_Z I_Z}{N_H} S_{RD} - \beta_S \frac{Y_Z}{N_H} S_{RD} - \mu_H S_{RD}, \\
S'_{RZ} &= \xi_Z R_Z - \beta_H \frac{I_D + \theta_C I_C + \varphi_Z \theta_Z I_Z}{N_H} S_{RZ} - \varphi_Z \beta_S \frac{Y_Z}{N_H} S_{RZ} - \mu_H S_{RZ}, \\
Y'_C &= \beta_H \theta_C \frac{I_C}{N_H} \big(S_H + V_H + \varphi_C S_{RC} + S_{RD} + S_{RZ}\big) + \eta_C \beta_H \theta_C \frac{I_C}{N_H} Y_Z - \rho_D \beta_H \frac{I_D}{N_H} Y_C \\
&\quad - (\gamma_C + \mu_H) Y_C, \qquad (4.2.1) \\
Y'_D &= \beta_H \frac{I_D}{N_H} \big(S_H + \sigma_D V_H + S_{RC} + S_{RZ}\big) + \eta_D \beta_H \frac{I_D}{N_H} Y_Z + \rho_D \beta_H \frac{I_D}{N_H} Y_C \\
&\quad - (\gamma_D + \mu_H + \delta_D) Y_D, \\
Y'_Z &= \beta_H \frac{\theta_Z I_Z}{N_H} (S_H + \sigma_Z V_H + S_{RC} + S_{RD} + \varphi_Z S_{RZ}) + \beta_S \frac{Y_Z}{N_H} \big(S_H + \sigma_Z V_H + S_{RC} \\
&\quad + S_{RD} + \varphi_Z S_{RZ}\big) - \beta_H \frac{\eta_C \theta_C I_C + \eta_D I_D}{N_H} Y_Z - (\gamma_Z + \mu_H) Y_Z, \\
R'_i &= \gamma_i Y_i - (\xi_i + \mu_H) R_i, \ (i = C,\ D,\ Z) \\
S'_V &= \Pi_V - \beta_V \frac{Y_D + \theta_C Y_C + \theta_Z Y_Z}{N_H} S_V - \mu_V S_V, \\
I'_C &= \beta_V \theta_C \frac{Y_C}{N_H} S_V - \mu_V I_C, \\
I'_D &= \beta_V \frac{Y_D}{N_H} S_V - \mu_V I_D, \\
I'_Z &= \beta_V \theta_Z \frac{Y_Z}{N_H} S_V - \mu_V I_Z.
\end{aligned}
$$

In the SIRS model (4.2.1), μ_H is the *per capita* birth/death rate of humans, β_H is the rate of acquisition of infection (effective contact rate) and β_S is the rate of male-to-female sexual transmission of ZIKV (as stated in the Introduction section, although there is evidence for sexual transmission of ZIKV from male-to-female, not significant evidence exists for female-to-male transmission (CDC, 2016; Davidson, 2016). This

fact obviates the need to incorporate sex structure in the model). Although it is plausible to expect sexual transmission of ZIKV to be important in highly-endemic areas, it (alone) cannot sustain appreciable epidemics (since the ZIKV transmission cycle is not completed by infected females to their susceptible male partners, but by the mosquito) (Davidson, 2016).

The modification parameter $0 < \theta_C < 1$ accounts for the assumption that a susceptible human is more likely to acquire DENV infection than CHIKV. This hypothesis is supported by epidemiological records in Mexico. In particular, the Mexican Health Surveillance systems (Boletín Epidemiológico SE 7, 2016) reported a cumulative total of 234 confirmed cases of DENV by Week 7, 2016. For the same week, the cumulative cases for CHIKV (which first appeared in Mexico in 2015) and DENV were only 60 and 28, respectively. In the case of ZIKV, these low numbers may be due to its recent introduction, and the fact that it is still colonizing the region (the case of CHIKV, however, is different since colonization took place during 2015). For the year 2016, the Mexican authorities reported a cumulative total of 200 CHIKV and 865 DENV cases. Furthermore, for Week 14, Boletín Epidemiológico (SE 14, 2016) reported a total of 2,109 DENV cases, 264 CHIKV cases and 224 ZIKV cases.

Susceptible humans are vaccinated against DENV at a rate ψ_D, and it is assumed that the vaccine wanes at a rate α_H. The DENV vaccine to be released and applied in Mexico is a recombinant, live-attenuated, tetravalent vaccine immunogenic for all DENV serotypes and protective for Serotypes 1, 3 and 4 (the recommended schedule is of three doses *per* child (Betancourt-Cravioto et al., 2014)). Natural death occurs in all human compartments at a rate μ_H.

Vaccinated humans receive vaccine-induced protection at a rate $\beta_H \sigma_D$, where $0 \leq 1 - \sigma_D$ is the vaccine efficacy against DENV infection for the case where the vaccine does indeed generate such protection. Furthermore, σ_D can be greater than unity for

the case when the vaccine induces immune enhancement effect, which is well known in DENV transmission dynamics (Acosta and Bartenschlager, 2016). Vaccinated individuals can also acquire CHIKV (at a rate $\theta_C\beta_H$) or ZIKV (at a rate $\theta_Z\beta_H$) infection, where, $0 < \theta_C < 1$ and $0 < \theta_Z < 1$ are the modification parameters for the assumed reduction in infectiousness of CHIKV and ZIKV, respectively, over DENV (it is possible, due to antibody-dependent enhancement, that the parameter θ_Z can exceed unity). In other words, the case $\theta_Z > 1$ represents the scenario where DENV vaccine induces an increase in ZIKV cases due to antibody-dependent enhancement (Cohen, 2016).

The parameter $0 \leq 1 - \sigma_Z$ has the same definition as σ_D (but with respect to ZIKV). It is known that, in antigen diagnostic tests, ZIKV cross-reacts with DENV (Gyurech et al., 2016); thereby producing false positives for DENV. This fact, coupled with the close phylogenetic relationship between DENV and ZIKV that triggers similar immune responses to infection, prompted us to explore the theoretical possibility that microcephaly and abortions and other neurologic abnormalities associated with ZIKV are related to immune enhancement mechanisms (Solomon et al., 2016).

As stated earlier, a DENV-CHIKV-ZIKV competitive hierarchy of the three diseases is hypothesized, with DENV more competent than CHIKV, and both more competent than ZIKV. In other words, DENV can replace CHIKV and ZIKV, *via* super-infection; and CHIKV can displace ZIKV, but not DENV *vice versa*. Using this working hypothesis, we will use the mathematical model presented above, and the available data on DENV-CHIKV-ZIKV epidemiology, to investigate the transmission dynamics of the rather new pandemic scenario of three concurrent viral infections transmitted by the same mosquito species.

Humans infected with CHIKV acquire DENV (super) infection at a rate $\rho_D\beta_H$, where $0 < \rho_D < 1$ is a modification parameter accounting for the reduced likelihood

of CHIKV-DENV super-infection, and humans infected with ZIKV acquire CHIKV (super) infection at a rate $\eta_C\theta_C\beta_H$ or DENV (super) infection at a rate $\eta_D\beta_H$, where $0 < \eta_C, \eta_D < 1$ are modification parameters accounting for the reduced likelihood of ZIKV-CHIKV or ZIKV-DENV super-infection, respectively. Humans recover from CHIKV, DENV and ZIKV infection at a rate γ_C, γ_D and γ_Z, respectively, and partially lose their infection-acquired immunity to CHIKV and ZIKV at a rate ξ_C and ξ_Z, respectively (it should be mentioned that individuals who partially lost their immunity to CHIKV or ZIKV can still acquire infection with CHIKV or ZIKV, respectively (but at a reduced rate compared to someone who is wholly susceptible to these diseases) and are wholly susceptible to the other two diseases). Individuals who recovered from prior DENV infection develop permanent immunity to DENV at a rate ξ_D (while they remain wholly susceptible to CHIKV and ZIKV).

The parameter Π_V represents the production (birth) rate of adult female *Aedes* mosquitoes. Susceptible adult female mosquitoes acquire infection at a rate β_V. Natural death occurs in all adult female mosquito compartments at a rate μ_V. It is worth mentioning that the model (4.2.1) is robust enough to allow for the assessment of the impact of the three hypotheses advanced in this study by varying the relevant parameters (ρ_D, η_C and η_D affecting the relative secondary infections strength that, in turn, affect the realized (observed) competitive hierarchy; θ_Z for the ADE hypothesis and σ_Z for the hypothesis on the impact of the DENV vaccine on ZIKV). The hierarchy hypothesis can be relaxed by setting $\rho_D = \eta_C = \eta_D = 0$. Similarly, the ADE hypothesis can be relaxed by fixing θ_Z in the interval (0,1], while the DENV vaccine hypothesis can be relaxed by setting σ_Z to unity.

The state variables and parameters of the model are described in Table 4.1 and 4.2, respectively (and a flow diagram of the model is depicted in Figure 4.1). The main assumptions made in the construction of the model are:

1. A DENV-CHIKV-ZIKV superinfection hierarchy is assumed for primary infections based upon the relative magnitude of the reproduction numbers. That is, it is assumed that in a completely naive (susceptible) population DENV is the competitively superior species, followed by CHIKV and then ZIKV (thereby presenting a scenario where DENV may take over hosts already infected with either of the other two species; while CHIKV can only take over ZIKV infected hosts and ZIKV can colonize only fully susceptible hosts).

2. Individuals with prior immunity to CHIKV and ZIKV (due to recovery from prior infection) can acquire infection with any of the three diseases (with reduced susceptibility to that particular disease, in comparison to wholly susceptible individuals). Individuals with prior immunity to DENV are permanently immune from getting DENV again (but are fully susceptible to CHIKV or ZIKV).

3. The four DENV serotypes (DENV1, DENV2, DENV3 and DENV4) are lumped into one for mathematical tractability (data shows that, for several years in the Americas, DENV epidemics are largely dominated by one DENV serotype (Carrillo-Valenzo et al., 2010)).

4. The (imperfect) *Dengvaxia* vaccine may induce a cross-reaction to ZIKV. Hence, individuals who received such a vaccine may be at risk to ZIKV infection due to the immune-enhancement effect seen in DENV (Cohen, 2016; Solomon et al., 2016).

Variable	Description
$S_H(t)$	Population of wholly-susceptible humans
$V_H(t)$	Population of susceptible humans vaccinated against DENV
$S_{Rj}(t),\ (j = C, D, Z)$	Population of susceptible humans with prior immunity to CHIKV, DENV, ZIKV, respectively
$Y_j(t),\ (j = C, D, Z)$	Population of humans infected with CHIKV, DENV, ZIKV, respectively
$R_j(t),\ (j = C, D, Z)$	Population of humans who recovered from CHIKV, DENV, ZIKV, respectively
$S_V(t)$	Population of susceptible adult female mosquitoes
$I_j(t),\ (j = C, D, Z)$	Population of adult female *Aedes* mosquitoes infected with CHIKV, DENV, ZIKV, respectively

Table 4.1: Description of the state variables of the model (4.2.1).

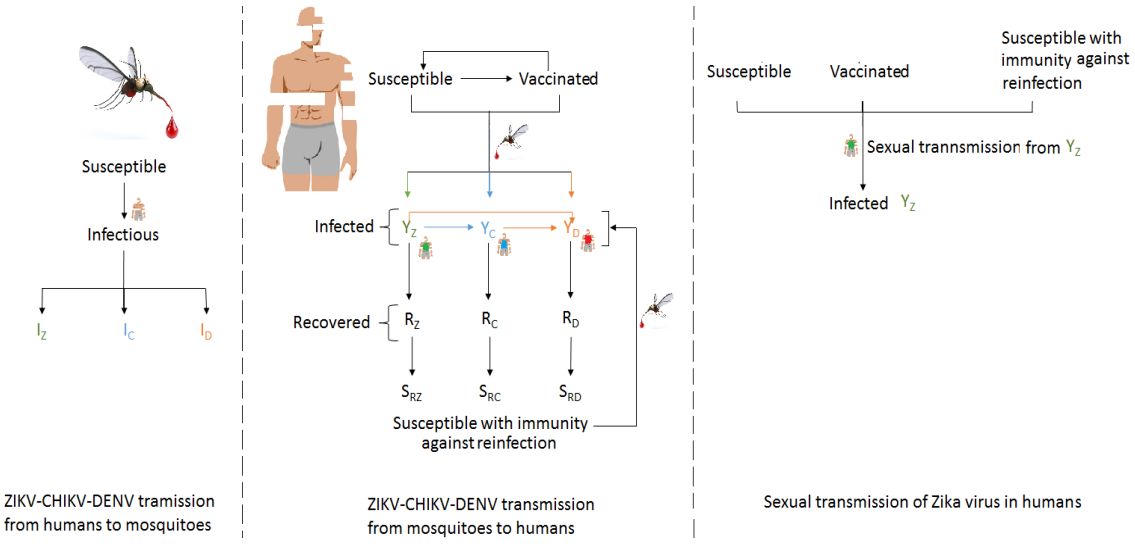

Figure 4.1: Flowchart of the model (4.2.1).

Parameters	Description	Best Range	Reference
μ_H	*Per capita* birth/death rate of humans	$1/(70 \times 365)$ day^{-1}	
β_H	Effective contact rate of susceptible humans with an infected mosquitoes	$(0.43 - 0.79)$ day^{-1}	Fitted
β_S	Sexual transmission rate of ZIKV	$(0.008 - 0.01)$ day^{-1}	Fitted
ψ_D	DENV-vaccination rate	$(0.15 - 0.48)$ day^{-1}	Fitted
α_H	Failure rate of DENV-vaccination	$(0.29 - 0.38)$ day^{-1}	Fitted
$1 - \sigma_D$	Vaccination efficacy against DENV	$0.81 - 0.88$	Fitted
$1 - \sigma_Z$	Vaccination efficacy against ZIKV	$0.74 - 0.88$	Fitted
θ_C	Modification parameter for the infectiousness of CHIKV in relation to DENV	$0.18 - 0.99$	Fitted
θ_Z	Modification parameter for the infectiousness of ZIKV in relation to DENV	$0.10 - 0.69$	Fitted
ξ_C	Rate of partial loss of natural immunity to CHIKV	$(0.032 - 0.035)$ day^{-1}	Fitted
ξ_D	Rate of acquisition of permanent natural immunity to DENV	$(0.026 - 0.035)$ day^{-1}	Fitted
ξ_Z	Rate of partial loss of natural immunity to ZIKV	$(0.029 - 0.030)$ day^{-1}	Fitted
φ_C	Modification parameter for the re-infection of CHIKV	$0.18 - 0.40$	Fitted
φ_Z	Modification parameter for the re-infection of ZIKV	$0.03 - 0.51$	Fitted
η_C	Modification parameter for super-infection of CHIKV over ZIKV	$0.14 - 0.40$	Fitted
η_D	Modification parameter for super-infection of DENV over ZIKV	$0.07 - 0.41$	Fitted
ρ_D	Modification parameter for super-infection of DENV over CHIKV	$0.02 - 0.15$	Fitted
γ_C	Recovery rate from CHIKV	$(0.15 - 0.27)$ day^{-1}	[264]
γ_D	Recovery rate from DENV	$(0.11 - 0.15)$ day^{-1}	Garba et al. (2008)
γ_Z	Recovery rate from ZIKV	$(0.09 - 0.11)$ day^{-1}	Fitted
δ_D	Disease-induced death rate for humans	0.001 day^{-1}	Garba et al. (2008)
Π_V	Birth rate of adult female mosquitoes	$5000 - 50000$ day^{-1}	Garba et al. (2008)
β_V	Effective contact rate of susceptible mosquitoes with an infected humans	$0.60 - 0.75$ day^{-1}	Garba et al. (2008)
μ_V	*Per capita* death rate of *Aedes* mosquitoes	$(1/21 - 1/7)$ day^{-1}	Garba et al. (2008)

Table 4.2: Description, values and ranges of the parameters of the model (4.2.1).

4.2.1 Basic Properties

Theorem 4.2.1. (Invariant region) *The closed set*

$$\mathcal{D} = \Bigg\{ \big(S_H, V_H, S_{RC}, S_{RD}, S_{RZ}, Y_C, Y_D, Y_Z, R_C, R_D, R_Z, S_V, I_C, I_D, I_Z\big) \in \mathbb{R}^{15}_{+} : \\ N_H(t) \leq N_H(0),\ N_V \leq \frac{\Pi_V}{\mu_V} \Bigg\}$$

is positively-invariant and attracting for the model (4.2.1).

Proof. Adding the first eleven equations and the last four equations of the model (2.4.1) gives, respectively,

$$N_H'(t) = -\delta_D Y_D(t) \text{ and } N_V'(t) = \Pi_V - \mu_V N_V(t).$$

Since $N_V'(t) = \Pi_V - \mu_V N_V(t)$, it follows that $N_V'(t) \leq 0$ if $N_V(t) \geq \dfrac{\Pi_V}{\mu_V}$. Furthermore, it follows, using comparison theorem Lakshmikantham and Leela (1969), that

$$N_H(t) = N_H(0) \exp\Big[-\int_0^t \delta_D Y_D(s) ds\Big] \text{ and } N_V(t) = \frac{\Pi_V}{\mu_V} + \Big[N_V(0) - \frac{\Pi_V}{\mu_V}\Big] e^{-\mu_V t}.$$

In particular, $N_H(t) \leq N_H(0)$ for all $t \geq 0$ and $N_V(t) \leq \dfrac{\Pi_V}{\mu_V}$ if $N_V(0) \leq \dfrac{\Pi_V}{\mu_V}$. Thus, the region $\mathcal{D}$ is positively-invariant for the model (4.2.1). Furthermore, if $N_V(0) > \dfrac{\Pi_V}{\mu_V}$, then either the solution enters $\mathcal{D}$ in finite time or $N_V(t) \to \dfrac{\Pi_V}{\mu_V}$ as $t \to \infty$. Hence, the region $\mathcal{D}$ attracts all solutions of model (2.4.1) in $\mathbb{R}^{15}_{+}$. □

By Theorem 4.2.1, the existence, uniqueness, continuation results hold for the system (hence, it is sufficient to consider the dynamics of the flow generated by the model (4.2.1) in $\mathcal{D}$ (Hethcote, 2000)).

4.3 Asymptotic Stability Disease-free Equilibrium (DFE)

4.3.1 Local Asymptotic Stability of DFE

The DFE of the model (4.2.1), denoted by $\mathcal{E}_0$, is given by (where $N_H^* = N_H(0) = S_H^* + V_H^*$)

$$\begin{aligned}\mathcal{E}_0 &= \big(S_H^*, V_H^*, S_{RC}^*, S_{RD}^*, S_{RZ}^*, Y_C^*, Y_D^*, Y_Z^*, R_C^*, R_D^*, R_Z^*, S_V^*, I_C^*, I_D^*, I_Z^*\big), \\ &= \left(\frac{(\alpha_H+\mu_H)N_H^*}{\alpha_H+\psi_D+\mu_H}, \frac{\psi_D N_H^*}{\alpha_H+\psi_D+\mu_H}, 0,0,0,0,0,0,0,0,0, \frac{\Pi_V}{\mu_V}, 0,0,0\right).\end{aligned}$$

It can be shown, using the *next generation operator* method (Diekmann et al., 1990; van den Driessche and Watmough, 2002), that the associated *reproduction number* of the model (4.2.1) (denoted by $\mathcal{R}_0$) is given by:

$$\mathcal{R}_0 = \max\big\{\mathcal{R}_C, \mathcal{R}_D, \mathcal{R}_Z\big\},$$

where,

$$\begin{aligned}\mathcal{R}_C &= \sqrt{\frac{\theta_C^2\beta_H\beta_V S_V^*}{\mu_V(\gamma_C+\mu_H)N_H^*}}, \\ \mathcal{R}_D &= \sqrt{\frac{(S_H^*+\sigma_D V_H^*)S_V^*\beta_H\beta_V}{\mu_V(\gamma_D+\mu_H+\delta_D)(N_H^*)^2}}, \\ \mathcal{R}_Z &= \frac{1}{2}\left\{\frac{\beta_S(S_H^*+\sigma_Z V_H^*)}{(\gamma_Z+\mu_H)N_H^*} + \sqrt{\left[\frac{\beta_S(S_H^*+\sigma_Z V_H^*)}{(\gamma_Z+\mu_H)N_H^*}\right]^2 + 4\frac{\theta_Z^2\beta_H\beta_V(S_H^*+\sigma_Z V_H^*)S_V^*}{\mu_V(\gamma_Z+\mu_H)(N_H^*)^2}}\right\}.\end{aligned} \tag{4.3.1}$$

The square roots in the expressions in (4.3.1) account for the two generations (vector-human-vector) needed to complete the (vector-component of the) transmission cycle of each of the three diseases.

Interpretation of $\mathcal{R}_0$

The three components of the *reproduction number* ($\mathcal{R}_0$) can be interpreted as follows.

1. **Interpretation of $\mathcal{R}_C$**:

   This threshold quantity is associated with the transmission dynamics of CHIKV (between humans and mosquitoes). It can be re-written as

$$\mathcal{R}_C = \sqrt{\mathcal{R}_{CH}\mathcal{R}_{CV}},$$

   where,

$$\mathcal{R}_{CH} = \frac{\theta_C \beta_V S_V^*}{(\gamma_C + \mu_H) N_H^*} \text{ and } \mathcal{R}_{CV} = \frac{\theta_C \beta_H}{\mu_V}.$$

   The quantity $\mathcal{R}_{CH}$ measures the human-to-vector transmission of CHIKV (i.e., the average number of new cases of CHIKV in the vector population generated by an average infected human). It is the product of the infection rate of susceptible mosquitoes by CHIKV-infected humans ($\frac{\theta_C \beta_V S_V^*}{N_H^*}$) and the average symptomatic period of CHIKV-infected humans (i.e., average duration in the Y_C class, given by $\frac{1}{\gamma_C + \mu_H}$). Similarly, the quantity $\mathcal{R}_{CV}$ accounts for the infection of susceptible humans by CHIKV-infected mosquitoes. It is the product of the infection rate of susceptible humans by CHIKV-infected mosquitoes ($\theta_C \beta_H$) and the average duration in the I_C class ($\frac{1}{\mu_V}$).

2. **Interpretation of $\mathcal{R}_D$**:

   This quantity, associated with DENV transmission between humans and mosquitoes, can be re-written as

$$\mathcal{R}_D = \sqrt{\mathcal{R}_{DH}\mathcal{R}_{DV}},$$

   where,

$$\mathcal{R}_{DH} = \frac{\beta_V S_V^*}{(\gamma_D + \mu_H + \delta_D) N_H^*} \text{ and } \mathcal{R}_{DV} = \frac{\beta_H \left(S_H^* + \sigma_D V_H^*\right)}{\mu_V N_H^*},$$

   where $\mathcal{R}_{DH}$ measures DENV transmission from DENV-infected humans to susceptible mosquitoes and $\mathcal{R}_{DV}$ accounts for DENV transmission from infected

mosquitoes to susceptible humans. The quantity $\mathcal{R}_{DH}$ is the product of the infection rate of susceptible mosquitoes by DENV-infected humans (β_V) and the average duration in the Y_D class ($\frac{1}{\gamma_D + \mu_H + \delta_D}$). Similarly, $\mathcal{R}_{DV}$ is the product of the infection rate of susceptible humans by DENV-infected mosquitoes $\left(\frac{\beta_H\left(S_H^* + \sigma_D V_H^*\right)}{N_H^*}\right)$ and the average duration in the I_D class ($\frac{1}{\mu_V}$).

3. **Interpretation of $\mathcal{R}_Z$**:

   This threshold quantity is associated with the ZIKV disease transmission between humans and mosquitoes and sexually between humans. It can be re-written as

$$\mathcal{R}_Z = \frac{1}{2}\left[\mathcal{R}_{ZSH} + \sqrt{\left(\mathcal{R}_{ZSH}\right)^2 + 4\mathcal{R}_{ZH}\mathcal{R}_{ZV}}\right],$$

   where,

$$\mathcal{R}_{ZSH} = \frac{\beta_S(S_H^* + \sigma_Z V_H^*)}{(\gamma_Z + \mu_H)N_H^*},\ \mathcal{R}_{ZH} = \frac{\theta_Z \beta_V S_V^*}{(\gamma_Z + \mu_H)N_H^*} \text{ and } \mathcal{R}_{ZV} = \frac{\theta_Z \beta_H\left(S_H^* + \sigma_Z V_H^*\right)}{\mu_V N_H^*}.$$

   The quantity $\mathcal{R}_{ZSH}$ is associated with the sexual transmission of ZIKV between humans (and it is equal to the *basic reproduction number* of ZIKV transmission in the absence of vectorial transmission). It is the product of the rate at which ZIKV is transmitted sexually to susceptible and vaccinated humans $\left(\frac{\beta_S\left(S_H^* + \sigma_Z V_H^*\right)}{N_H^*}\right)$ and the average duration in the Y_Z class ($\frac{1}{\gamma_Z + \mu_H}$). Furthermore, the threshold quantity $\mathcal{R}_{ZH}$ is associated with the infection of susceptible mosquitoes by ZIKV-infected humans. It is the product of the infection rate of susceptible mosquitoes by ZIKV-infected humans ($\beta_V \theta_Z$) and the average duration in the Y_Z class ($\frac{1}{\gamma_Z + \mu_H}$). Similarly, the threshold quantity $\mathcal{R}_{ZV}$ accounts for the infection of susceptible and vaccinated humans by ZIKV-infected mosquitoes. It is the product of the infection rate of susceptible and vaccinated humans $\left(\frac{\theta_Z \beta_H\left(S_H^* + \sigma_Z V_H^*\right)}{N_H^*}\right)$ and the average duration in the I_Z class ($\frac{1}{\mu_V}$).

It should be mentioned that the product $\mathcal{R}_{ZH}\mathcal{R}_{ZV}$ is the square of the reproduction number of ZIKV transmission in the absence of sexual transmission of ZIKV (i.e., it is the square of the vector-human-vector transmission of ZIKV. Hence, it is the square of a geometric mean).

It is worth stating that the reproduction number ($\mathcal{R}_0$) of the model is the number of secondary infections generated by a typical infected vector or host. The vector-host and host-vector cycles naturally divide the transmission process into two parts (contributing $\sqrt{\mathcal{R}_{ZH}\mathcal{R}_{ZV}}$ secondary infections into the overall $\mathcal{R}_0$). However, while either of these transmissions is happening, human sexual transmission is also going on (with a reproduction number of $\mathcal{R}_{ZSH}$ during the time host-vector transmission happens, and $\mathcal{R}_{ZSH}$ while vector-host happens). Hence, the total contribution of secondary cases during the whole vector-human cycle, in the presence of sexual human transmission, is $\sqrt{\mathcal{R}_{ZSH}^2 + \mathcal{R}_{ZH}\mathcal{R}_{ZV}}$. The square root appears because of the averaging (of transmissions) over multiple processes. It should be mentioned that $\sqrt{\mathcal{R}_{ZH}\mathcal{R}_{ZV}}$ is the reproduction number of ZIKV for vectorial transmission only (i.e., in the absence of sexual transmission). The numbers 1/2 and 4, that appeared in the expression for $\mathcal{R}_{ZSH}$, result from the averaging of the two modes of ZIKV transmission (sexual and vector-based). The result below follows from Theorem 2 of (van den Driessche and Watmough, 2002).

Theorem 4.3.1. *The DFE* ($\mathcal{E}_0$) *of the model* (4.2.1) *is locally-asymptotically stable (LAS) whenever* $\mathcal{R}_0 < 1$*, and unstable whenever* $\mathcal{R}_1 = \min\{\mathcal{R}_C, \mathcal{R}_D, \mathcal{R}_Z\} > 1$.

Target Reproduction Number ($\mathcal{R}_{ZT}$)

It is convenient to define the following quantity:

$$\mathcal{R}_{ZT} = \mathcal{R}_{ZSH} + \mathcal{R}_{ZH}\mathcal{R}_{ZV} = \frac{\beta_S\big(S_H^* + \sigma_Z V_H^*\big)}{(\gamma_Z + \mu_H)N_H^*} + \frac{\theta_Z\beta_V S_V^*}{(\gamma_Z + \mu_H)N_H^*} \cdot \frac{\theta_Z\beta_H\big(S_H^* + \sigma_Z V_H^*\big)}{\mu_V N_H^*}.$$

The formulation (or form) of the quantity $\mathcal{R}_{ZT}$ is consistent with the concept of *target reproduction number* discussed in Shuai et al. (2013).

Theorem 4.3.2. $\mathcal{R}_{ZT} < 1$ (> 1) if and only if $\mathcal{R}_{\mathrm{Z}} < 1$ (> 1).

Proof. For $\mathcal{R}_Z < 1$, then

$$\begin{aligned}
\mathcal{R}_Z = \ & \frac{1}{2}\left[\mathcal{R}_{ZSH} + \sqrt{\left(\mathcal{R}_{ZSH}\right)^2 + 4\mathcal{R}_{ZH}\mathcal{R}_{ZV}}\right] < 1, \\
\iff \ & \mathcal{R}_{ZSH} + \sqrt{\left(\mathcal{R}_{ZSH}\right)^2 + 4\mathcal{R}_{ZH}\mathcal{R}_{ZV}} < 2, \\
\iff \ & \left(\mathcal{R}_{ZSH}\right)^2 + 4\mathcal{R}_{ZH}\mathcal{R}_{ZV} < \left(2 - \mathcal{R}_{ZSH}\right)^2, \\
\iff \ & \left(\mathcal{R}_{ZSH}\right)^2 + 4\mathcal{R}_{ZH}\mathcal{R}_{ZV} < 4 - 4\mathcal{R}_{ZSH} + \left(\mathcal{R}_{ZSH}\right)^2, \\
\iff \ & \mathcal{R}_{ZSH} + \mathcal{R}_{ZH}\mathcal{R}_{ZV} < 1.
\end{aligned}$$

□

Thus, from now, we define $\mathcal{R}_{0T} = \max\{\mathcal{R}_C, \mathcal{R}_D, \mathcal{R}_{ZT}\}$ as the *basic reproduction number* in terms of the *target reproduction number* for the transmission of the ZIKV. Thus (by Theorem 4.3.2), Theorem 4.3.1 can be re-written in terms of the *target reproduction number* as below:

Theorem 4.3.3. *The DFE* $(\mathcal{E}_0)$ *of the model* (4.2.1) *is LAS whenever* $\mathcal{R}_{0T} < 1$*, and unstable whenever* $\mathcal{R}_{1T} = \min\{\mathcal{R}_C, \mathcal{R}_D, \mathcal{R}_{ZT}\} > 1$.

4.3.2 Global Asymptotic Stability of DFE: Special Case

Consider the special case of the model (4.2.1) in the absence of DENV-induced mortality (i.e., $\delta_D = 0$, so that $N_H^* = N_H(0)$).

Theorem 4.3.4. *The DFE,* $\mathcal{E}_0$ *of the model* (4.2.1) *with* $\delta_D = 0$*, is GAS in* $\mathcal{D}$ *whenever* $\mathcal{R}_{0T} \leq 1$ *and unstable whenever* $\mathcal{R}_{1T} = \min\{\mathcal{R}_C, \mathcal{R}_D, \mathcal{R}_{ZT}\} > 1$.

Proof. It is convenient to define the following

$$\lambda^*_{iH} = \frac{\beta_H \theta_i}{N^*_H},\ \lambda^*_{iV} = \frac{\beta_V \theta_i}{N^*_H}\ (i = C,\ D,\ Z),\ \lambda^*_{SH} = \frac{\beta_S}{N^*_H},$$

with $\theta_D = 1$, $g_1 = \gamma_C + \mu_H,\ g_2 = \gamma_D + \mu_H$ and $g_3 = \gamma_Z + \mu_H$. Furthermore, consider the Lyapunov function

$$\begin{aligned}\mathcal{K}_1 =& \mu_H\big(Y_C + Y_D + Y_Z\big) + \frac{\mu_H}{\mu_V}\Big[\lambda^*_{CH}(S^*_H + V^*_H)I_C + \lambda^*_{DH}(S^*_H + \sigma_D V^*_H)I_D \\ &+ \lambda^*_{ZH}(S^*_H + \sigma_Z V^*_H)I_Z\Big].\end{aligned}$$

Thus, the Lyapunov derivative is given by

$$\begin{aligned}\mathcal{K}'_1 &= \mu_H\big(Y'_C + Y'_D + Y'_Z\big) + \frac{\mu_H}{\mu_V}\Big[\lambda^*_{CH}(S^*_H + V^*_H)I'_C + \lambda^*_{DH}(S^*_H + \sigma_D V^*_H)I'_D + \lambda^*_{ZH}(S^*_H \\ &\quad + \sigma_Z V^*_H)I'_Z\Big], \\ &= \mu_H\Big[\lambda^*_{CH}I_C(S_H + V_H + \varphi_C S_{RC} + S_{RD} + S_{RZ}) - g_1 Y_C + \lambda^*_{DH}I_D(S_H + \sigma_D V_H + \\ &\quad S_{RC} + S_{RZ}) - \ g_2 Y_D + \big(\lambda^*_{ZH}I_Z + \lambda^*_{SH}Y_Z\big)(S_H + \sigma_Z V_H + S_{RC} + S_{RD} + \varphi_Z S_{RZ}) \\ &\quad - g_3 Y_Z\Big] + \frac{\mu_H}{\mu_V}\Big[\lambda^*_{CH}(S^*_H + V^*_H)\big(\lambda^*_{CV}S_V Y_C - \mu_V I_C\big) + \lambda^*_{DH}(S^*_H + \sigma_D V^*_H)\big(\lambda^*_{DV}S_V \\ &\quad Y_D - \mu_V I_D\big) + \lambda^*_{ZH}(S^*_H + \sigma_Z V^*_H)\big(\lambda^*_{ZV}S_V Y_Z - \mu_V I_Z\big)\Big].\end{aligned}$$

Since $S_H(t) + V_H(t) + S_{RC}(t) + S_{RD}(t) + S_{RZ}(t) \leq N^*_H = S^*_H + V^*_H$ in $\mathcal{D}$ for all t, then

$$\begin{aligned}\mathcal{K}'_1 &\leq \mu_H\Big[\lambda^*_{CH}I_C(S^*_H + V^*_H) - g_1 Y_C + \lambda^*_{DH}I_D(S^*_H + \sigma_D V^*_H) - g_2 Y_D + \big(\lambda^*_{ZH}I_Z + \lambda^*_{SH}Y_Z\big) \\ &\quad (S^*_H + \sigma_Z V^*_H) - g_3 Y_Z\Big] + \frac{\mu_H}{\mu_V}\Big[\lambda^*_{CH}(S^*_H + V^*_H)\big(\lambda^*_{CV}S_V Y_C - \mu_V I_C\big) + \lambda^*_{DH}(S^*_H + \sigma_D \\ &\quad V^*_H)\big(\lambda^*_{DV}S_V Y_D - \mu_V I_D\big) + \lambda^*_{ZH}(S^*_H + \sigma_Z V^*_H)\big(\lambda^*_{ZV}S_V Y_Z - \mu_V I_Z\big)\Big], \\ &\leq Y_C\Big\{\mu_H g_1\big[\big(\mathcal{R}_C\big)^2 - 1\big]\Big\} + Y_D\Big\{\mu_H g_2\big[\big(\mathcal{R}_D\big)^2 - 1\big]\Big\} + Y_Z\Big\{\mu_H g_3\big[\big(\mathcal{R}_Z\big)^2 - 1\big]\Big\}.\end{aligned}$$

Thus, it follows that, for $\mathcal{R}_{0T} \leq 1$ in $\mathcal{D}$, the Lyapunov derivative $\mathcal{K}'_1 \leq 0$. Furthermore, it follows from the LaSalle's Invariance Principle (LaSalle, 1976) that the maximal invariant set contained in $\big\{(S_H, V_H, S_{RC}, S_{RD}, S_{RZ}, Y_C, Y_D, Y_Z, R_C, R_D, R_Z, S_V,$

$I_C, I_D, I_Z)(t) \in \mathcal{D} : \mathcal{K}_1' = 0\big\}$ is the singleton $\{\mathcal{E}_0\}$. Hence, $\mathcal{E}_0$ is GAS in $\mathcal{D}$ whenever $\mathcal{R}_{0T} \leq 1$. Equivalently, $\mathcal{E}_0$ is GAS in $\mathcal{D}$ whenever $\mathcal{R}_0 \leq 1$. □

Theorem 4.3.4 shows that the three diseases (CHIKV, DENV and ZIKV) will be effectively controlled in (or eliminated from) the community if the associated *basic reproduction threshold*, $\mathcal{R}_{0T}$, can be brought to (and maintained at) a value less than or equal to unity.

It is worth mentioning that persistence results, for the three diseases, can be established for the case when $\mathcal{R}_{1T} > 1$ using the approach in Section 2.5.3.

4.4 Model (Data) Fitting, Simulations and Sensitivity Analysis

4.4.1 Data Fitting and Simulations

The model (4.2.1) is fitted using weekly data (for the three disease), given by the Mexican Health Secretariat Boletin Epidemiologico for 2016 for the period Week 42 of 2015 to Week 33 of 2016 en México (2003), as tabulated in Table 4.3 (see also Figure 4.2). Pearson's Chi-squared and the least square regression method (implemented in the statistical software, R) were used to fit the model (4.2.1) to the data. Figures $4.3 - 4.5$ show reasonably good fit with respect to the cumulative number of new cases for each of the three diseases over the same time period. The model (4.2.1) is further simulated, using parameter values from the ranges given in Table 3.3, to gain insight into some of its qualitative and quantitative properties. A contour plot of the *reproduction number* of CHIKV ($\mathcal{R}_C$) as a function of coverage for DENV vaccine at steady-state (V_H^*/N_H^*) and the modification parameter for the infectiousness of CHIKV in relation to DENV (θ_C) is depicted in Figure 4.6. This contour plot show a marked reduction in the reproduction number with decreasing θ_C since ($\mathcal{R}_C$) is directly proportional to this parameter: a decrease in the first induces a decrease in

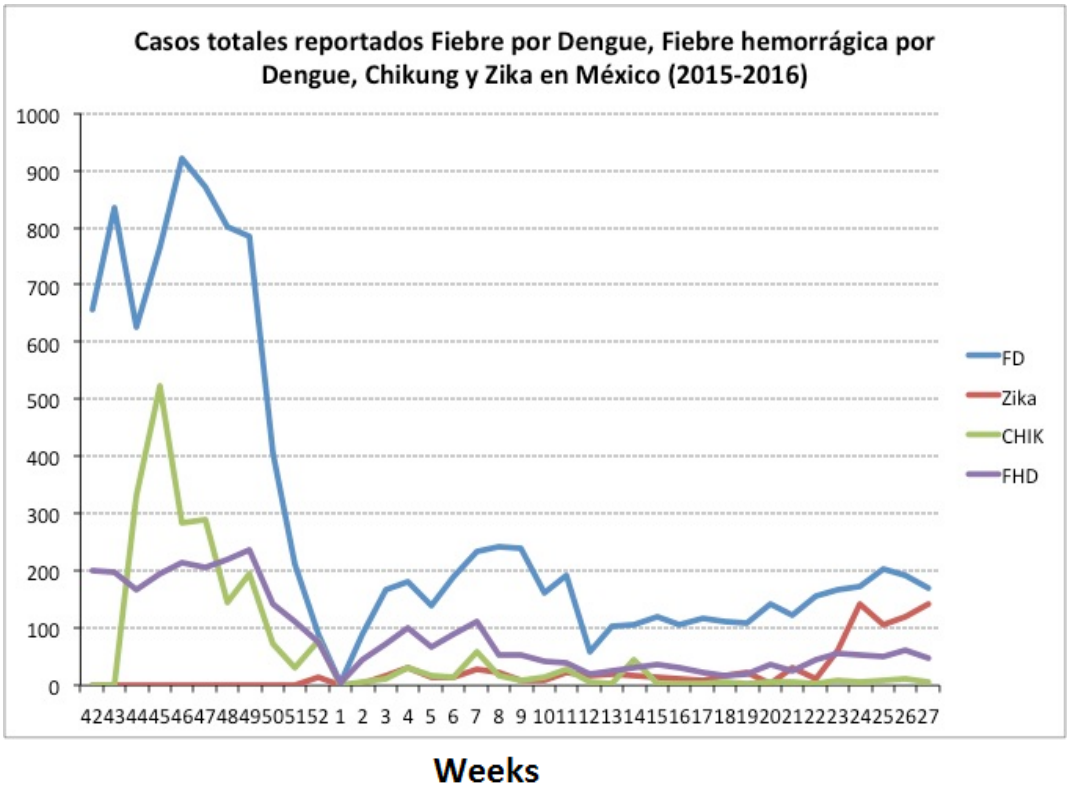

Figure 4.2: Data integrated from the weekly reports in en México (2003). Courtesy of Dr. Andreu Comas-García, Universidad Autónoma de San Luis Potosí

the second.

A similar plot, for the reproduction number of DENV ($\mathcal{R}_D$) as a function of vaccine coverage (V_H^*/N_H^*) and efficacy ($1-\sigma_D$), is depicted in Figure 4.7, from which it follows that $\mathcal{R}_D$ decreases (albeit marginally) with increasing vaccine coverage and efficacy. It is, however, worth noting that, with the parameter values used in the simulations, the DENV vaccine is not adequate enough to lead to effective control (or elimination) of DENV (since they are unable to reduce $\mathcal{R}_D$ to values less than unity). Furthermore, a contour plot of the *reproduction number* of ZIKV ($\mathcal{R}_Z$), as a function of coverage for DENV vaccine at steady-state (V_H^*/N_H^*) and the modification parameter for the infectiousness of ZIKV in relation to DENV (θ_Z), is depicted in Figure 4.8. This

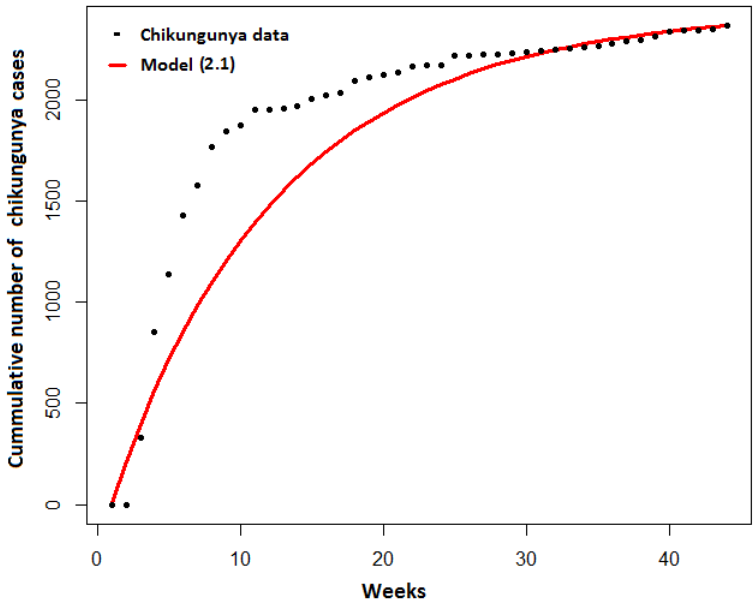

Figure 4.3: Fitting of the model (2.4.1) to CHIKV data given in Table 4.3. Best fit parameter values obtained are $\mu_H = 1/(70 \times 365), \beta_H = 0.79, \beta_S = 0.009, \psi_D = 0.43, \alpha_H = 0.38, \sigma_D = 0.19, \sigma_Z = 0.26, \theta_C = 0.99, \theta_Z = 0.10, \eta_C = 0.14, \eta_D = 0.07, \rho_D = 0.15, \gamma_C = 0.086, \gamma_D = 0.143, \gamma_Z = 0.098, \varphi_C = 0.22, \varphi_Z = 0.51, \xi_C = 0.032, \xi_D = 0.033, \xi_Z = 0.029, \delta_D = 0.001, \Pi_V = 5000, \beta_V = 0.75$ and $\mu_V = 1/12$.

figure shows that $\mathcal{R}_Z$ is only mildly affected by changes in θ_Z even in the region of antibody-dependent enhancement ($\theta_Z > 1$). However, if the modification parameter θ_Z is low (implying a relatively low infectiousness with respect to DENV), then a sufficiently large vaccination coverage can reduce the ZIKV reproduction number. On the other hand, as depicted in Figure 4.9, DENV vaccine efficacy has a very mild impact on ZIKV transmission dynamics. This figure further shows that the vaccine (no matter the high levels of efficacy and coverage) is unable to reduce the ZIKV reproduction number to a value less than unity (implying that the DENV vaccine will have a limited effect on the onset of ZIKV outbreaks). It can be concluded from

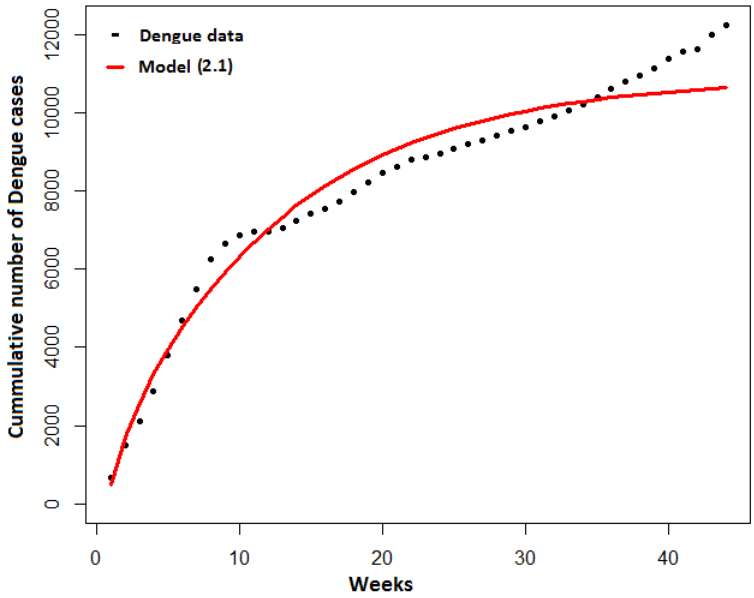

Figure 4.4: Fitting of the model (2.4.1) to DENV (FD strain) data given in Table 4.3. Best fit parameter values obtained are $\mu_H = 1/(70 \times 365), \beta_H = 0.56, \beta_S = 0.009, \psi_D = 0.48, \alpha_H = 0.38, \sigma_D = 0.14, \sigma_Z = 0.12, \theta_C = 0.79, \theta_Z = 0.69, \eta_C = 0.40, \eta_D = 0.35, \rho_D = 0.28, \gamma_C = 0.086, \gamma_D = 0.143, \gamma_Z = 0.10, \varphi_C = 0.18, \varphi_Z = 0.03, \xi_C = 0.045, \xi_D = 0.026, \xi_Z = 0.029, \delta_D = 0.001, \Pi_V = 50000, \beta_V = 0.75$ and $\mu_V = 1/12$.

these simulations that reducing $\mathcal{R}_Z$ to a value below unity depends very much on intrinsic mosquito sensitivity towards the two viruses (DENV and ZIKV), and not on the DENV vaccine properties.

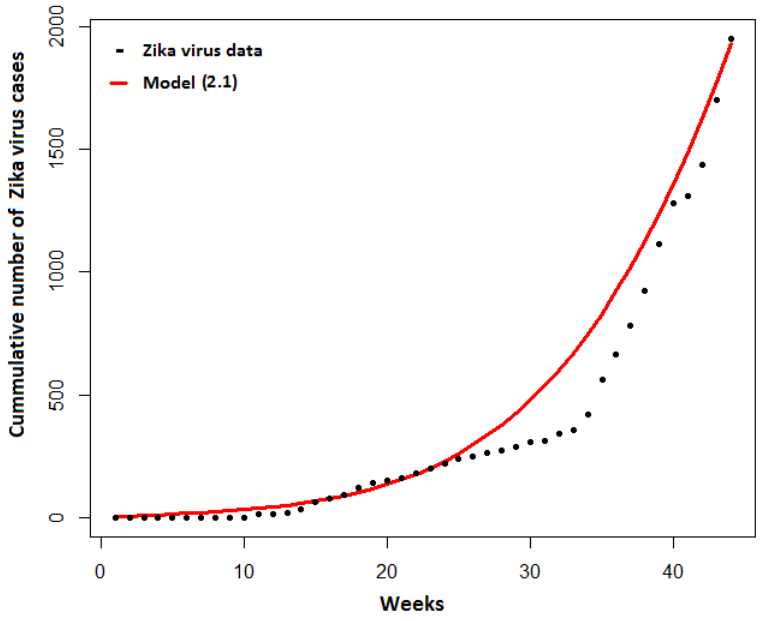

Figure 4.5: Fitting of the model (2.4.1) to ZIKV data given in Table 4.3. Best fit parameter values obtained are $\mu_H = 1/(70 \times 365), \beta_H = 0.43, \beta_S = 0.01, \psi_D = 0.15, \alpha_H = 0.29, \sigma_D = 0.12, \sigma_Z = 0.20, \theta_C = 0.18, \theta_Z = 0.10, \eta_C = 0.19, \eta_D = 0.41, \rho_D = 0.02, \gamma_C = 0.086, \gamma_D = 0.143, \gamma_Z = 0.10, \varphi_C = 0.40, \varphi_Z = 0.36, \xi_C = 0.035, \xi_D = 0.035, \xi_Z = 0.030, \delta_D = 0.001, \Pi_V = 50000, \beta_V = 0.75$ and $\mu_V = 1/12$.

4.4.2 Sensitivity Analysis

As in Section 2.4.5, sensitivity analysis (using LHS-PRCC) is carried out to determine the parameters of the model (4.2.1) that have the greatest influence on the dynamics of the three of the diseases (with respect to a chosen response function), as described below. Ranges and baseline values of the parameters (relevant to the dynamics of the three diseases in Mexico), tabulated in Table 4.2, will be used in these analyses.

Using the population of humans infected with CHIKV (Y_C) as the response function, it is shown in Table 3.4 that the top PRCC-ranked parameters of the autonomous

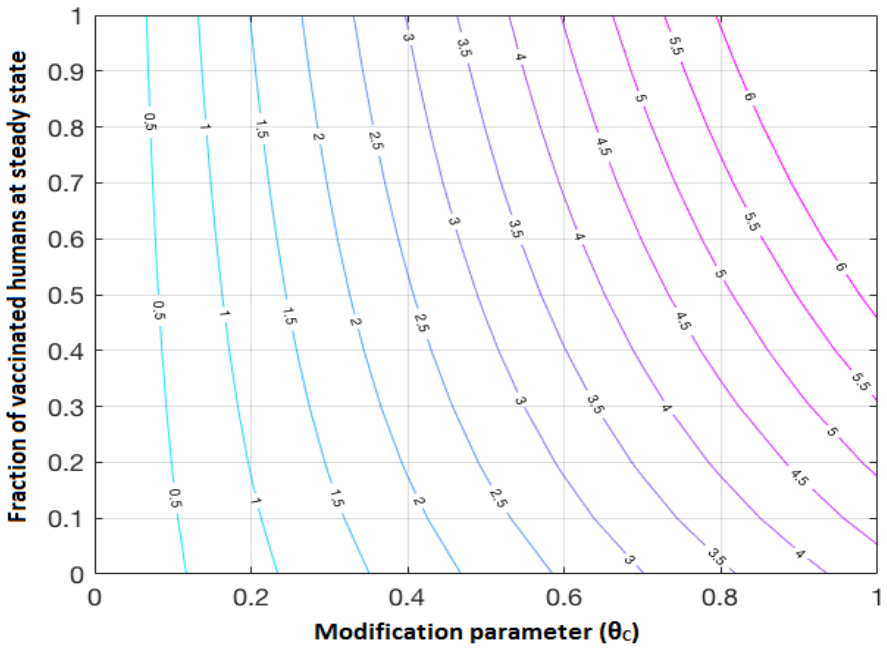

Figure 4.6: Simulations of the model (2.4.1), showing a contour plot of $\mathcal{R}_C$ as a function of the fraction of vaccinated humans at steady-state (V_H^*/N_H^*) and modification parameter for chikungunya infection (θ_C) $\in [0, 1]$. Parameter values used are as given in Figure 4.3.

version of the model are:

(a) the modification parameter accounting for the assumption that a susceptible human is more likely to acquire DENV infection than ZIKV (θ_Z);

(b) the rate at which humans acquire DENV infection (β_H);

(c) the rate of recovery from ZIKV (γ_Z);

(d) the vaccination rate of susceptible humans against DENV disease (ψ_D).

A possible explanation of this observed effect may lie on the assumption that CHIKV is competitively-weaker than DENV, but stronger than ZIKV. In an ecological context, CHIKV is competitively-inferior only to DENV. Therefore, if a vaccine against

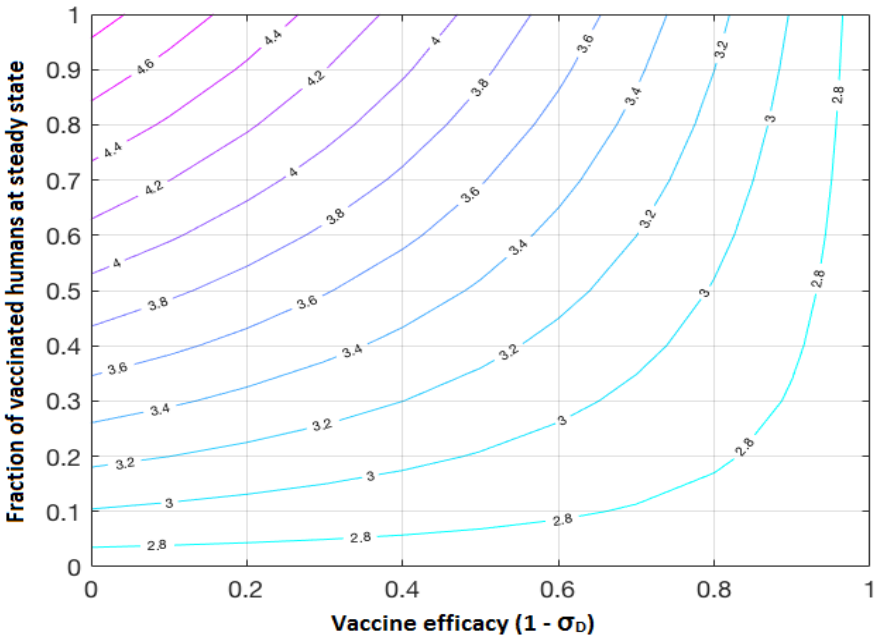

Figure 4.7: Simulations of the model (2.4.1), showing a contour plot of $\mathcal{R}_D$ as a function of the fraction of vaccinated humans at steady-state (V_H^*/N_H^*) and dengue vaccine efficacy $(1-\sigma_D) \in [0,1]$. Parameter values used are as given in Figure 4.4.

DENV is acting it may or may not be very efficient in preventing DENV but it widens the niche that CHIKV can occupy (since the top competitor is being reduced in competitive ability). The effect is that more hosts are available to CHIKV, but not to DENV (thus, generating a net increase in the incidence of the former virus). Similarly, using the population of humans infected with DENV (Y_D) as the response function, the top PRCC-ranked parameters:

(a) the modification parameter accounting for the assumption that a susceptible human is more likely to acquire DENV infection than CHIKV (θ_C);

(b) the rate of acquisition of infection (β_H);

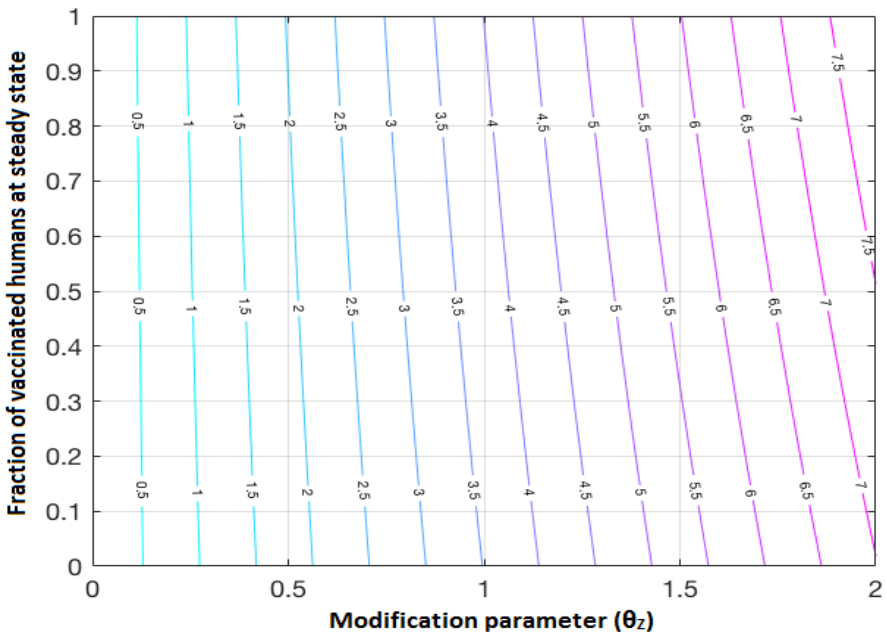

Figure 4.8: Simulations of the model (2.4.1), showing a contour plot of $\mathcal{R}_Z$ as a function of the fraction of vaccinated humans at steady-state (V_H^*/N_H^*) and modification parameter for Zika virus infection $(\theta_Z) \in [0, 2]$. Parameter values used are as given in Figure 4.5.

(c) the rate of recovery from CHIKV (γ_C);

(d) the natural mortality rate of mosquitoes (μ_V).

Furthermore, using the population of individuals with ZIKV (Y_Z) as the response function, the top PRCC-ranked parameters are:

(a) the rate at which susceptible humans acquire DENV infection (β_H);

(b) mosquito recruitment rate (Π_V);

(c) the natural mortality rate of mosquitoes (μ_V);

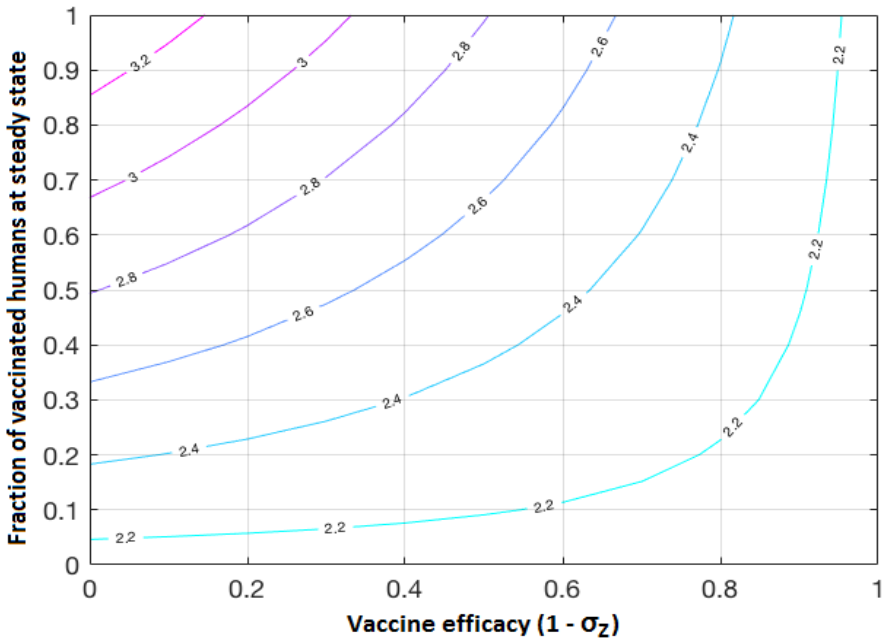

Figure 4.9: Simulations of the model (2.4.1), showing a contour plot of $\mathcal{R}_Z$ as a function of the fraction of vaccinated humans at steady-state (V_H^*/N_H^*) and (dengue) vaccine efficacy on Zika virus $(1-\sigma_D) \in [0,1]$. Parameter values used are as given in Figure 4.5.

(d) the recovery rate from DENV (γ_D);

(e) the vaccination rate of susceptible humans against DENV (ψ_D).

However, using the *basic reproduction number* ($\mathcal{R}_0$) as the response function (i.e., using $\mathcal{R}_C, \mathcal{R}_D$ and $\mathcal{R}_Z$), the top PRCC-ranked parameters are:

(a) the modification parameter accounting for the assumption that a susceptible human is more likely to acquire DENV infection than ZIKV (θ_Z);

(b) the modification parameter accounting for the assumption that a susceptible human is more likely to acquire DENV infection than CHIKV (θ_C);

(c) mosquito birth rate (Π_V) and natural death rate of adult mosquitoes (μ_V);

(d) the rate at which humans acquire DENV infection (β_H).

In summary, this study identifies six highly-ranked parameters that play a crucial role on the transmission dynamics of the three disease, namely:

(a) the rate at which humans acquire DENV infection (β_H);

(b) the modification parameter accounting for the assumption that a susceptible human is more likely to acquire DENV infection than CHIKV (θ_C) and ZIKV (θ_Z);

(c) the recovery rate from CHIKV (γ_C);

(d) the natural mortality rates (μ_V) and recruitment rate of mosquitoes (Π_V).

4.5 Effect of Seasonality and Climate Variability

4.5.1 Thermal Response Functions

To incorporate the effect of seasonal and climate (local weather) variabilities in the model (4.2.1), the weather-related parameters of the model (namely, mosquitoes recruitment rate (Π_V), mosquitoes death rate (μ_V), effective contact rate of susceptible mosquito with an infected human (β_V) and effective contact rate of susceptible humans with an infected mosquito (β_H)) are now expressed as functions of temperature and/or rainfall (with mean monthly temperature chosen to be in the range $16^{\circ}C \leq T(t) \leq 32^{\circ}C$). For simplicity, air and water temperature are assumed to be the same near the surface of the water (so that, as in Chapter 3, $T_W(t) = T_A(t) = T(t)$).

(i) *Natural death rate of mosquitoes* (μ_V): Following Polwiang (2015) and Yang et al. (2009), the temperature-dependent natural death rate of mosquitoes (*Aedes aegypti*) is given by:

$$\mu_V = \mu_V(T) = 0.8692 - 0.159T + 0.01116T^2 - 3.408 \times 10^{-4}T^3 + 3.809 \times 10^{-6}T^4.$$

(ii) *Production (birth) rate of mosquitoes* (Π_V): Following Agusto et al. (2015); Okuneye and Gumel (2017); Parham and Michael (2010); Polwiang (2015) and Tun-Lin et al. (2000), the temperature- and rainfall-dependent recruitment rate of mosquitoes (*Aedes aegypti*) is given by:

$$\Pi_V = \Pi_V(T, R) = \frac{N_A B(T) p_{EA}(T) p_{EA}(R)}{\tau_E + \tau_L(T) + \tau_P},$$

where N_A is the total number of adult female mosquitoes and $B(T)$ is the temperature-dependent number of eggs laid *per*adult *per*oviposition given by

$$B(T) = -15.437 + 1.289T - 0.0163T^2.$$

Furthermore, following Parham and Michael (2010), $p_{EA}(T, R)$ (the temperature- and rainfall-dependent daily probability that an egg survives to become an adult mosquito) is given by:

$$p_{EA}(T, R) = p_{EA}(T) p_{EA}(R),$$

where temperature-dependent daily probability that an egg survives to become an adult mosquito, denoted by $p_{EA}(T)$, is given by:

$$p_{EA}(T) = -0.0000472222T^3 - 0.000622222T^2 + 0.130278T - 1.19333.$$

Following Parham and Michael (2010) (Supplemental Material), the rainfall-dependent daily probability that an egg survives to become an adult mosquito, denoted by $p_{EA}(R)$, is given by:

$$p_{EA}(R) = \prod_{i=E,L,P} (4p_{Mi}/R_M^2)R(R_M - R),$$

where p_{Mi} is the peak daily survival probability of immature mosquitoes in development stage i (where $i = E$ = eggs; $i = L$ = larvae; $i = P$ = pupae) and $R_M > R(t) > 0$, for all t, is the maximum rainfall threshold in the community. It should be stated that, in line with Parham et al. (2012), the definition of $p_{EA}(R,T) = p_{EA}(R)p_{EA}(T)$ emphasizes the assumed independence of temperature and rainfall with each other. Finally, τ_E, $\tau_L(T)$ and τ_P are the development times of eggs, larvae and pupae in the aquatic stages. The development times from eggs to larvae and pupae to adults are approximately independent of temperature, while the development time from larvae to pupae varies with temperature (Parham and Michael, 2010; Waldock et al., 2013). Thus, following Waldock et al. (2013), the temperature dependent development time of larvae is given by,

$$\tau_L(T) = \left(-0.000705544\,T^2 + 0.0355594T - 0.293506\right)^{-1}.$$

(iii) *Effective contact rate of a susceptible mosquito with an infected human* (β_V): Following Lambrechts et al. (2011); Polwiang (2015); Scott et al. (2000), the effective contact rate of susceptible mosquito with an infected human is a temperature-dependent parameter given by:

$$\beta_V = \beta_V(T) = \begin{cases} (0.0943 + 0.0043T)\,(-0.9037 + 0.0729T)\,, & \text{if } 16^{\circ}\text{C} \leq T \leq 26^{\circ}\text{C}, \\ (0.0943 + 0.0043T)\,, & \text{if } 26^{\circ}\text{C} < T \leq 32^{\circ}\text{C}. \end{cases}$$

For the temperature range $16^0\text{C} \leq T \leq 26^0\text{C}$, the first bracket in the definition of the parameter β_V is the temperature-dependent biting rate and the second

bracket represents the temperature-dependent probability of infection *per* bite (Polwiang, 2015). For the temperature range $26^0\text{C} < T \leq 32^0\text{C}$, the probability of infection *per* bite is reported to be 1 (Polwiang, 2015).

(iv) *Effective contact rate of a susceptible human with an infected mosquito* (β_H): Similarly, following Lambrechts et al. (2011); Polwiang (2015); Scott et al. (2000), the effective contact rate of susceptible humans with an infected mosquito is a temperature-dependent parameter given by:

$$\beta_H = \beta_H(T) = (0.0943 + 0.0043T)\, 0.001044T(T - 12.286)\sqrt{32.461 - T}.$$

The terms in the definition of β_H are similarly defined as in β_V.

It is worth mentioning that all of the aforementioned temperature-and/or-rainfall-dependent parameters of the model (4.2.1) are positive for all mean monthly temperature and rainfall in the chosen range $[16, 28]^\circ$C and $[10, 190]$ mm, respectively (see Table 4.6). The chosen mean monthly temperature is for some regions within Mexico (see Tables $4.7 - 4.9$). Furthermore, the maximum rainfall threshold (R_M) is chosen for Mexico to be $R_M = 198$ mm [93].

Numerical Simulations

The model (4.2.1), with the weather-dependent parameters (namely, mosquitoes recruitment rate (Π_V), mosquitoes death rate (μ_V), effective contact rate of susceptible mosquito with an infected human (β_V) and effective contact rate of susceptible humans with an infected mosquito (β_H)) defined in Section 4.5 (now defined as the *non-autonomous model*), is now simulated to assess the effect of variability in local temperature and rainfall on the dynamics of the three diseases in the model. Simulations are carried out for Mexico (and two Mexican states where the three diseases are endemic).

4.5.2 Simulations for Mexico

Mexico, a country in the southern portion of North America, lie in the coordinate 23°N (latitude), 102°W (longitude) and covers about 2 million square kilometers with climate conditions varying from tropical to desert and a total population of approximately 121 million (INEGI, 2013). Mosquito-borne diseases (especially CHIKV, DENV and ZIKV) remain a public health problem in Mexico, despite the efforts to stop and mitigate the impact of epidemics, with 24, 605 confirmed cases of DENV on EW (epidemiological week) 47 of 2015 and 16,835 cases in the same EW of 2016 (and all four DENV serotypes have been reported in Mexico) [5]. The total reported cases of CHIKV exploded in 2015 with the updated confirmed cases reaching 9,952 cases in November 2015 from 155 cases in October 2014 (see Figure 4.2). Similarly, the cases of the ZIKV (first case reported in 2015) have been reported in 23 states with a total number of confirmed cases reaching 6,764 in November, 2016 (Figure 4.2).

The non-autonomous model is now simulated to assess the impact of the aforementioned climate variables on the transmission dynamics of the three diseases in the chosen regions. The first set of simulations are carried out for a fixed mean monthly rainfall value of Mexico (namely, $R(t) = 63.2$ mm [93]). Figure 4.10 (see also Table 4.6 for the values of the temperature-dependent parameters of the model) shows that the total number of new cases of the three diseases increases with increasing mean monthly temperature until a peak of $[27 - 29]$°C is attained, and decreases with increasing temperature thereafter. Similarly, for Mexico's fixed mean monthly temperature ($T(t) = 22$°C), Figure 4.11 shows an increase in the number of cases with increasing rainfall until an initial peak rainfall value (of $R(t) = 100$ mm) is reached, and the number of cases decreases with increasing rainfall thereafter.

It is further evident from Figure 4.10 that (for the fixed mean monthly rainfall

of 63.2 mm for Mexico), maximum disease activity (for all three diseases) occurs for temperature in the range $[27-29]^{\circ}$C. Hence, since the current mean monthly temperature for Mexico is 22°C, projected increase in global temperature could cause a shift (increase in mean monthly temperature) to the high transmission temperature range (thereby making Mexico more vulnerable for the spread of the three mosquito-borne diseases). Furthermore, the combined effect of the mean monthly temperature and rainfall for Mexico is assessed by simulating the model (4.2.1) using various combinations of mean monthly temperature and rainfall values, as tabulated in Table 4.7. The results obtained, depicted in Figure 4.12 show an increase in the number of burden of these diseases with increasing temperature and rainfall until a peak is reached, and a decrease with decreasing mean monthly temperature and (or increasing) rainfall thereafter. These diseases-associated burden are maximized in the whole of Mexico when the mean monthly temperature values are in the $[25-26.4]^{\circ}$C range and the mean monthly rainfall values are in the range $[90-128]$ mm (occurring during the months of June, July and September). Several Mexican states fit, on average, the above climatic conditions. Simulations for two of these states are described below.

4.5.3 Simulations for Mexican States of Oaxaca and Chiapas

Oaxaca and Chiapas are the fifth and sixth largest states in Mexico, respectively (with Oaxaca covering an area of $95,364$ square kilometers and a population of about 3.9 million, while Chiapas covers an area of $75,634$ square kilometers and a population of around 4.8 million people [113]). The Mexican Dirección General de Elidemiología reports Oaxaca and Chiapas as two of Mexicos's 28 states with endemic levels of mosquito-borne viral diseases (particularly DENV, CHIKV and ZIKV) throughout 2015 and 2016 (See Table 4.3 for the epidemiological weeks of years 2015 and 2016 in Mexico [73]). For instance, the two states account for 25.92% of the total number of

confirmed cases of ZIKV infection in pregnant women in Mexico (7.52% in Oaxaca and 18.4% in Chiapas) [257]. Furthermore, data from Pan American Health Organization shows that, since the first local transmission of CHIKV in Chiapas in 2015, the cumulative total confirmed cases reached 11,199 as of mid-December 2015 [3].

To assess the effect of local variabilities in temperature and rainfall in the two states, we run simulations of the non-autonomous model using various combinations of mean monthly temperature and rainfall values for each of the two states (as tabulated in Tables 4.8 and 4.9). The results obtained, depicted in Figures 4.13 and 4.14, show an increase in the burden of these diseases with increasing temperature and rainfall until a peak is reached, and a decrease with decreasing mean monthly temperature and (or increasing) rainfall thereafter. The peak diseases-associated burden for Oaxaca (Figure 4.13) and Chiapas (Figure 4.14) occur when temperature and rainfall values lie in the range $[20 - 22.5]^{\circ}$C, $[51 - 102]$ mm (occurring during the months of May through September) and $[19 - 21]^{\circ}$C, $[85 - 107]$ mm (occurring during the months of May, July, August and October), respectively. Thus, this study suggests that control efforts on these diseases should be intensified for these states during these months.

4.6 Summary of Results

In this chapter, a new SIRS model for the transmission dynamics of (co-existence of) DENV, CHIKV and ZIKV in a population, where a proportion of individuals receive the newly-released *Dengvaxia* vaccine against DENV, is formulated. The model is built based on three main hypotheses, namely:

(a) a competitive DENV-CHIKV-ZIKV superinfection hierarchy;

(b) antibody-dependent enhancement (represented by setting the parameter, θ_Z to

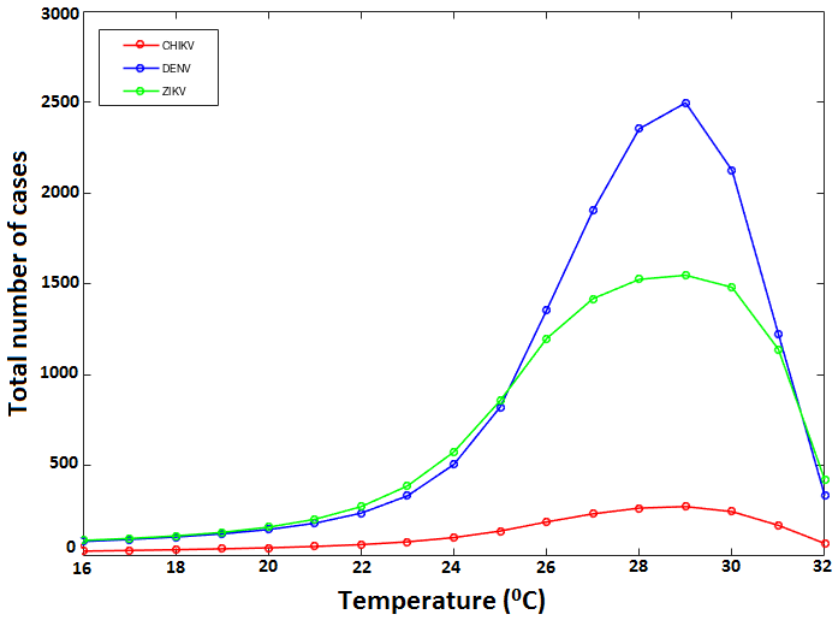

Figure 4.10: Effect of temperature on disease dynamics (for fixed mean monthly rainfall $R(t) = 63.2$ mm). Simulations of the non-autonomous version of the model (2.4.1), showing the total number of new infections as a function of time for various temperature values in the range $[16, 32]^{\circ}$C. Parameter values used in the simulations are as in Tables 3.3 and 4.6.

a value greater than unity);

(c) that the *Dengvaxia* vaccine could reduce susceptibility to ZIKV (represented by setting the parameter σ_Z to a value less than unity).

The main findings in this chapter are summarized below:

(i) The model has a disease-free equilibrium which is locally-asymptotically stable whenever a certain threshold quantity ($\mathcal{R}_0$) is less than unity. This disease-free equilibrium is globally-asymptotically stable, for a special case without dengue-induced mortality in humans, whenever the associated reproduction number is

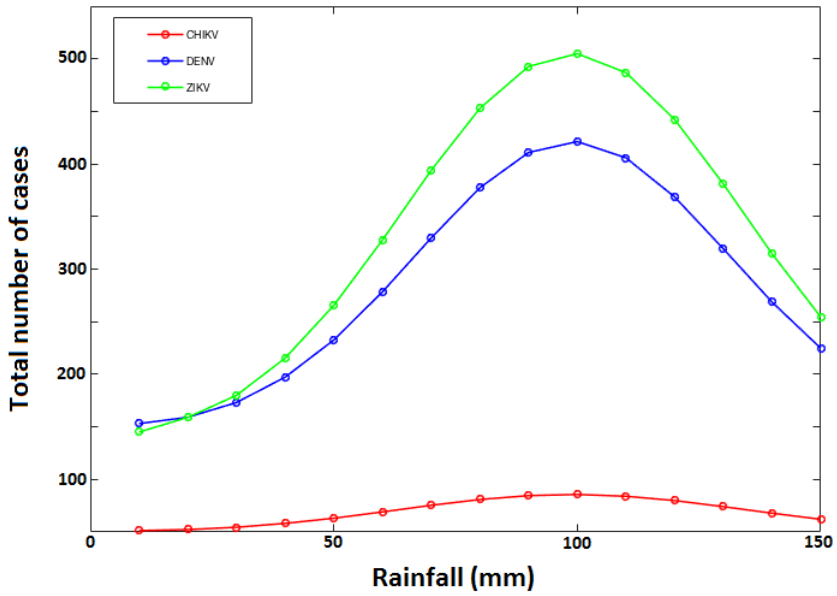

Figure 4.11: Effect of rainfall on disease dynamics (for fixed mean monthly temperature 22°C). Simulations of the non-autonomous version of the model (2.4.1), showing the total number of new infections as a function of time for various levels of rainfall in the range $[10, 150]$ mm. Parameter values used in the simulations are as in Tables 3.3 and 4.6.

less than unity. The diseases persist in the community if a certain threshold quantity ($\mathcal{R}_{1T}$) exceeds unity.

(ii) Uncertainty and sensitivity analysis of the model shows that the top eight parameters that have the most influence on the dynamics of the model (with respect to various response functions) are, the rate at which humans acquire DENV infection (β_H), the modification parameter accounting for the assumption that a susceptible human is more likely to acquire DENV infection than CHIKV (θ_C) and ZIKV (θ_Z), the vaccination rate of susceptible humans against DENV (ψ_D), the recovery rate from CHIKV (γ_C), the natural mortality rates

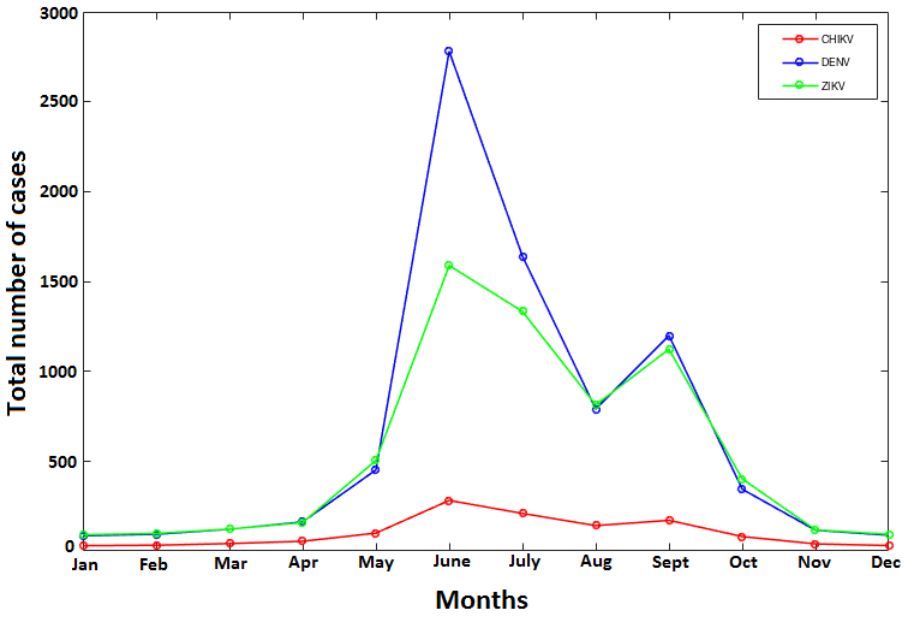

Figure 4.12: Simulations of the non-autonomous version of the model (2.4.1), showing the total number of new infections in Mexico for the various temperature and rainfall values given in Table 4.7. All parameters are as given in Tables 3.3 and 4.6.

of mosquitoes (μ_V), the recruitment rates of mosquitoes (Π_V) and the rate of loss of vaccine-induced immunity (α_H).

Numerical simulations of the model show that:

(a) The ZIKV reproduction number ($\mathcal{R}_Z$) is only mildly affected by changes in the parameter related to the infectiousness of ZIKV in relation to DENV (θ_Z) even in the region where antibody-dependent enhancement ($\theta_Z > 1$) is assumed.

(b) For low values of θ_Z (i.e., a relatively low infectiousness of ZIKV in relation to DENV), a sufficiently large vaccination coverage can reduce the ZIKV reproduction number.

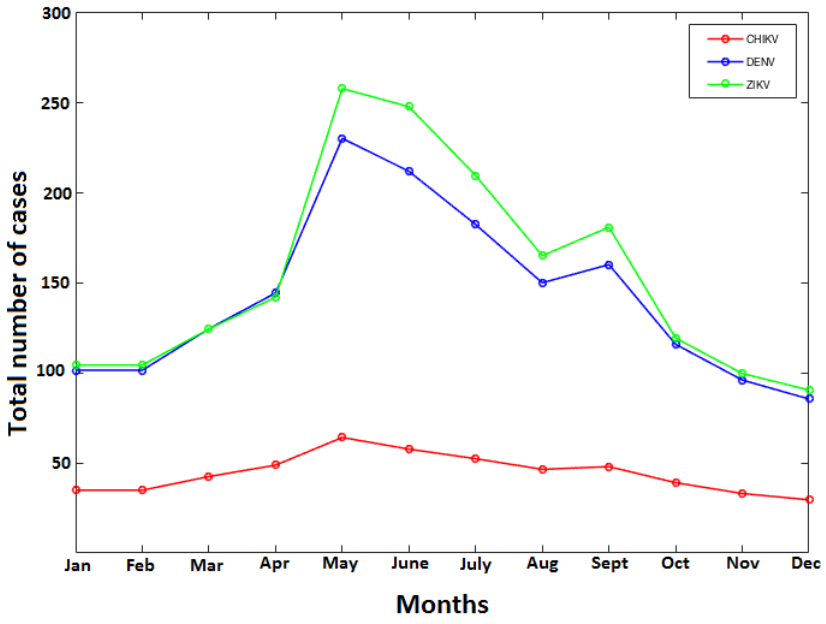

Figure 4.13: Simulations of the non-autonomous version of model (2.4.1), showing the total number of new infections in Oaxaca, Mexico for the various temperature and rainfall values given in Table 4.8. All parameters are as given in Tables 3.3 and 4.6.

(c) The efficacy of the DENV vaccine has a very mild impact on ZIKV transmission dynamics. In particular, the DENV vaccine (no matter the levels of efficacy and coverage) is unable to reduce the ZIKV reproduction number to a value less than unity (implying that the DENV vaccine will have a limited effect on the onset of Zika outbreaks).

(d) Reducing the ZIKV reproduction number ($\mathcal{R}_Z$) to a value below unity depends very much on the intrinsic mosquito sensitivity towards the two viruses (DENV and ZIKV), and not on the DENV vaccine properties.

Furthermore, to understand the effect of seasonality and climate variability on the dy-

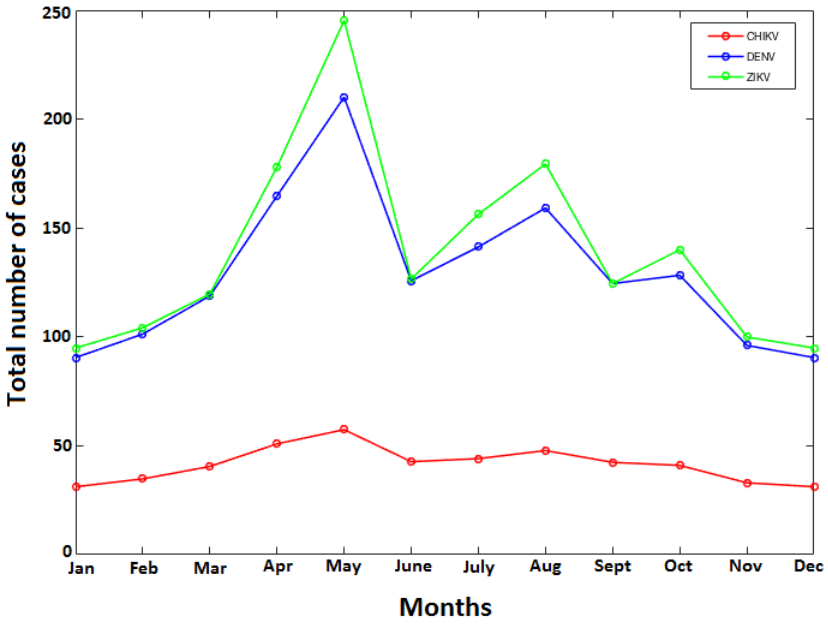

Figure 4.14: Simulations of the non-autonomous version of model (2.4.1), showing the total number of new infections in Chiapas, Mexico for the various temperature and rainfall values given in Table 4.9. All parameters are as given in Tables 3.3 and 4.6.

namics of the model, functional forms of the weather-related parameters of the model (namely, mosquitoes recruitment rate (Π_V), mosquitoes death rate (μ_V), effective contact rate of susceptible mosquito with an infected human (β_V) and effective contact rate of susceptible humans with an infected mosquito (β_H)) are simulated with the model. Numerical simulations of the effect of seasonality and climate variability on the dynamics of the model, using relevant data from Mexico (and the Mexican states of Oaxaca and Chiapas), show the following:

(i) For a fixed mean monthly rainfall value for Mexico (i.e., $R(t) = 63.2$ mm), the burden of the three diseases (measured in terms of the total number of new cases) increases with increasing mean monthly temperature in the range

([16 − 29]°C, and decreases with increasing mean monthly temperature above 29°C.

(ii) For a fixed mean monthly temperature value for Mexico (i.e., $T(t) = 22$°C), the burden of the diseases increases with increasing rainfall value until a threshold of [95 − 100] mm is reached. At higher rainfall values (above the threshold), disease burden decreases. This is as a result of decreases in the maturation rate of immature mosquitoes (above this rainfall threshold) due to the flushing out of the immature mosquitoes from the breeding sites.

(iii) For mean monthly temperature and rainfall data for the whole of Mexico and the Mexican states of Oaxaca and Chiapas (Tables 4.7, 4.8 and 4.9), the peak burden of the diseases for the Mexican states of Oaxaca (Figure 4.13) and Chiapas (Figure 4.14) occur when temperature and rainfall values lie in the range [20 − 22.5]°C, [51 − 102] mm (these occur during the months of May through September) and [19 − 21]°C, [85 − 107] mm (these occur during the months of May, July, August and October), respectively. The burden of the diseases is maximized in the whole of Mexico when the mean monthly temperature values are in the [25 − 26.4]°C range and the mean monthly rainfall values are in the range [90 − 128] mm (which occurs during the months of June, July and September).

(iv) For the fixed mean monthly rainfall of 63.2 mm for Mexico, maximum disease activity (for all three diseases) occur for temperature in the range $[27, 29]$°C (Figure 4.10). Hence, since the current mean monthly temperature for Mexico is 22°C, projected global warming could cause a shift (increase in mean monthly temperature) to the high transmission temperature range (thereby making Mexico more vulnerable for the spread of the three mosquito-borne diseases).

Week	Chikungunya		Dengue		Zika virus	
	cases	cummulative	cases	cummulative	cases	cummulative
1	0	0	658	658	0	0
2	0	0	835	1493	0	0
3	330	330	627	2120	0	0
4	524	854	766	2886	0	0
5	284	1138	920	3806	0	0
6	290	1428	872	4678	0	0
7	146	1574	802	5480	0	0
8	195	1769	784	6264	0	0
9	74	1843	407	6671	0	0
10	30	1873	213	6684	0	0
11	79	1952	89	6973	13	13
12	0	1952	4	6977	0	13
13	7	1959	88	7065	3	16
14	12	1971	167	7232	16	32
15	30	2001	180	7412	31	63
16	18	2019	140	7552	15	78
17	13	2032	189	7741	13	91
18	60	2092	234	7975	28	119
19	18	2110	243	8218	22	141
20	10	2120	239	8457	8	149
21	14	2134	163	8620	9	158
22	29	2163	193	8813	23	181
23	5	2168	60	8873	18	199
24	4	2172	102	8975	21	220
25	44	2216	107	9082	17	237
26	2	2218	120	9202	13	250
27	4	2222	107	9309	12	262
28	3	2225	116	9425	8	270
29	7	2232	113	9538	16	286
30	4	2236	108	9646	22	308
31	7	2243	141	9787	4	312
32	5	2248	123	9910	31	343
33	4	2252	157	10067	12	355
34	9	2261	168	10235	62	417
35	7	2268	173	10408	143	560
36	9	2277	204	10612	105	665
37	12	2289	191	10803	119	784
38	5	2294	169	10972	141	925
39	16	2310	176	11148	188	1113
40	26	2336	234	11382	170	1283
41	4	2340	206	11588	25	1308
42	3	2343	49	11637	129	1437
43	4	2347	354	11991	265	1702
44	18	2365	255	12246	249	1951

Table 4.3: Case data for the three diseases obtained from the weekly Mexican Health Secretariat Boletin Epidemiologico for 2016 [73].

T (°C)	R (mm)	$\mathcal{R}_C$	$\mathcal{R}_D$	$\mathcal{R}_Z$
$16-20$	$16-30$	$0.012-0.111$	$0.018-0.166$	$1.363-1.384$
	$30-60$	$0.027-0.235$	$0.04-0.349$	$1.364-1.451$
	$60-90$	$0.058-0.299$	$0.086-0.444$	$1.369-1.50$
	$90-120$	$0.069-0.303$	$0.103-0.45$	$1.371-1.504$
	$120-150$	$0.047-0.282$	$0.07-0.42$	$1.367-1.487$
$20-24$	$16-30$	$0.079-0.343$	$0.118-0.511$	$1.374-1.54$
	$30-60$	$0.18-0.724$	$0.268-1.076$	$1.416-1.975$
	$60-90$	$0.38-0.920$	$0.565-1.369$	$1.57-2.236$
	$90-120$	$0.456-0.932$	$0.679-1.386$	$1.653-2.252$
	$120-150$	$0.308-0.87$	$0.458-1.293$	$1.508-2.168$
$24-28$	$16-30$	$0.247-0.782$	$0.368-1.162$	$1.46-2.05$
	$30-60$	$0.564-1.646$	$0.839-2.447$	$1.777-3.272$
	$60-90$	$1.188-2.093$	$1.768-3.112$	$2.61-3.931$
	$90-120$	$1.428-2.119$	$2.124-3.151$	$2.955-3.97$
	$120-150$	$0.964-1.978$	$1.433-2.94$	$2.296-3.761$
$28-32$	$16-30$	$0.223-0.662$	$0.332-0.984$	$1.443-1.896$
	$30-60$	$0.507-1.394$	$0.754-2.073$	$1.710-2.906$
	$60-90$	$1.068-1.774$	$1.588-2.637$	$2.441-3.460$
	$90-120$	$1.284-1.795$	$1.909-2.670$	$2.746-3.492$
	$120-150$	$0.866-1.676$	$1.288-2.492$	$2.163-3.316$

Table 4.4: Values of reproduction numbers (for the non-autonomous version of the model (4.2.1)) for the three diseases for various temperature and rainfall values in the range $[16-32]^0$C and $[16-150]$ mm, respectively. Specifically, the maximum reproduction number for each of these diseases is found to be in the temperature and rainfall range of $[27-29]^0$C and $[90-120]$ mm, respectively.

Parameters	Y_C Class	Y_D Class	Y_Z Class	$\mathcal{R}_C$	$\mathcal{R}_D$	$\mathcal{R}_Z$
μ_H	-0.0042	-0.0746	-0.0127	$+0.018$	$+0.041$	-0.059
β_H	**+0.8943**	**+0.8493**	**+0.9546**	**+0.76**	$+0.57$	**+0.44**
β_S	$+0.0587$	-0.0219	$+0.0202$	–	–	$+0.02$
ψ_D	**-0.6364**	-0.0133	**-0.8734**	–	**-0.72**	-0.27
α_H	0.1582	$+0.0231$	$+0.3067$	–	**+0.74**	$+0.053$
σ_D	$+0.0133$	-0.0127	$+0.2582$	–	-0.01	–
σ_Z	$+0.3325$	-0.0596	-0.0334	–	–	$+0.12$
η_C	-0.0234	-0.0180	$+0.0298$	–	–	–
η_D	-0.0134	$+0.0481$	$+0.0109$	–	–	–
ρ_D	$+0.0445$	-0.0208	-0.0707	–	–	–
θ_Z	**+0.9853**	$+0.0781$	$+0.0056$	–	–	**+0.95**
θ_C	$+0.0315$	**+0.9826**	-0.0030	**+0.95**	–	–
γ_C	-0.0046	**-0.8002**	$+0.0246$	-0.48	–	–
γ_D	$+0.0363$	-0.0678	-0.6910	–	-0.32	–
γ_Z	**+0.8160**	-0.1079	-0.0465	–	–	-0.24
φ_C	$+0.0049$	-0.0046	-0.0301	–	–	–
φ_Z	$+0.0881$	-0.0737	$+0.0106$	–	–	–
ξ_C	$+0.0588$	$+0.0776$	$+0.0210$	–	–	–
ξ_D	$+0.0449$	$+0.0521$	-0.0261	–	–	–
ξ_Z	$+0.6024$	-0.0268	-0.0088	–	–	–
Π_V	$+0.2771$	$+0.6615$	**+0.9357**	**+0.89**	**+0.93**	**+0.85**
β_V	$+0.0460$	$+0.2475$	$+0.4247$	$+0.54$	-0.25	$+0.19$
μ_V	-0.5804	**-0.7960**	**-0.9147**	**-0.75**	**+0.79**	**-0.87**
δ_D	$+0.0609$	-0.0063	-0.0001	–	-0.024	–
N_H^*	–	–	–	-0.11	-0.08	-0.054

Table 4.5: PRCC values for the parameters of the model (4.2.1), using the total number of humans with symptoms of CHIKV (Y_C), DENV (Y_D) and ZIKV (Y_Z) as the response functions. The top (most-dominant) parameters that affect the dynamics of the model, with respect to each of the three response functions, are highlighted in bold font. "Notation: a dashed line ($-$) indicates the parameter is not in the expression for the relevant responses $\mathcal{R}_C, \mathcal{R}_D$ and $\mathcal{R}_Z$".

T (°C)	$\mu_V(T)$	$\beta_V(T)$	$\beta_H(T)$	$\Pi_V(T,R)$				
	$(\times 10^{-2})$	$(\times 10^{-2})$	$(\times 10^{-2})$	Rainfall (mm)				
				$16-30$	$30-60$	$60-90$	$90-120$	$120-150$
$16-18$	$3.52-3.59$	$4.0-7.0$	$4.1-7.0$	$0.6-10$	$2.9-46.5$	$13.2-75.3$	$19-77.2$	$8.7-67.2$
$18-20$	$3.53-3.6$	$7.0-10$	$7.0-10$	$2.0-19.7$	$10.5-87.6$	$46.5-141.6$	$67.2-145.2$	$30.6-126.5$
$20-22$	$3.6-3.64$	$10-13$	$10-14$	$3.8-30.1$	$19.7-133.5$	$87.6-216$	$126.5-221.4$	$57.6-192.9$
$22-24$	$3.4-3.6$	$13-17$	$14-17$	$5.8-42.1$	$30.1-187$	$133.5-302.5$	$192.9-310.1$	$87.8-270.2$
$24-26$	$3.0-3.4$	$17-20$	$17-19$	$8.1-56.2$	$42.2-249.3$	$187-403.3$	$270.2-413.4$	$123.0-360.1$
$26-28$	$2.7-3.0$	$20-21$	$19-21$	$10.8-68.8$	$56.2-304.9$	$249.3-493.2$	$360.1-505.5$	$163.9-440.4$
$28-30$	$2.66-2.7$	$21-223$	$19-21$	$13.3-70.8$	$67.5-314.1$	$299.2-508.2$	$432.2-520.8$	$196.9-453.8$
$30-32$	$2.7-3.6$	$22-23$	$10-19$	$8.8-67.5$	$45.5-299.2$	$201.8-484.0$	$291.5-496.1$	$132.7-432.2$

Table 4.6: Temperature- and rainfall-dependent parameters of the model (where T: Temperature and R: Rainfall) for various temperature and rainfall values in the range $[16-32]$°C and $[16-150]$ mm, respectively.

Month	Jan	Feb	Mar	Apr	May	Jun	Jul	Aug	Sept	Oct	Nov	Dec
Temperature (°C)	16.5	17.2	19.7	22.6	24.9	26.4	25.9	26.4	25.0	23.0	19.2	16.7
Rainfall (mm)	18.0	29.2	11.0	15.9	47.9	90.6	127.4	150.0	121.0	65.1	20.2	17.8

Table 4.7: Monthly mean temperature (in °C) and rainfall (in mm) for Mexico [93].

Month	Jan	Feb	Mar	Apr	May	Jun	Jul	Aug	Sept	Oct	Nov	Dec
Temperature (°C)	18	18	20	21.5	22.5	21	20.5	20	20	19	17.5	16.5
Rainfall (mm)	3.0	3.0	3.0	12	51	99	102	69	99	36	9.0	3.0

Table 4.8: Monthly mean temperature (in °C) and rainfall (in mm) for Oaxaca, Mexico [93].

Month	Jan	Feb	Mar	Apr	May	Jun	Jul	Aug	Sept	Oct	Nov	Dec
Temperature (°C)	17	18	19.5	21	21	20	19.5	20	20	19	17.5	17
Rainfall (mm)	4.7	5.6	14.3	50.6	106.1	177.8	87.4	106.5	188.6	106.2	23.4	9

Table 4.9: Monthly mean temperature (in °C) and rainfall (in mm) for Chiapas, Mexico [93].

Chapter 5

CONCLUSION

MBDs continue to inflict severe public health and socio-economic burden on human populations in many parts of the world (particularly the tropical and sub-tropical parts of the world where MBDs are endemic). Although progress has been made, over the decades, on the control of such diseases (due to the use of numerous intervention strategies), these diseases remain major public health burden in affected areas and regions. A major factor responsible for this is climate change, which has been shown to strongly affect the ecology and physiology of the MBD vectors.

Mathematical models have played significant roles in the study of the spread of MBDs, and consequently, contributing to the design of various effective and optimal control strategies. This dissertation is focused on using mathematical approaches to gain insight into the role of climate change on the population biology of the mosquito, and on the dynamics of some of the main diseases they cause. The main contributions of this dissertation can be classified into three main categories, namely:

(a) formulation of new and realistic weather-driven models;

(b) rigorous analyses of these models to gain qualitative insight into the dynamics of these models;

(c) contributions to public health (which includes carrying out sensitivity analysis to suggest control strategies and numerical analysis to determine of suitable range for maximum local mosquito abundance and disease transmission intensity).

The specific contributions of the dissertation are summarized as follows:

5.1 Chapter 2

In Chapter 2, a new weather-driven mathematical model for assessing the impact of two climate variables (rainfall and temperature) on the population biology of the mosquito was designed. Some of the notable ecological features of this model, which extends numerous other models for mosquito population biology in literature, include adding:

(i) four larval instar stages in the aquatic stages;

(ii) density-dependence for egg oviposition process;

(iii) three distinct stages of the gonotrophic cycle of the adults female mosquito.

Detailed qualitative analysis of the autonomous version of the model is carried out (showing the global asymptotic stability of the trivial equilibrium when a certain reproduction threshold ($\mathcal{R}_M$) is less than unity; as well as showing the local asymptotic stability of the non-trivial equilibrium when the threshold exceeds unity; this latter equilibrium bifurcates intoa stable limit cycle *via* a super-critical Hopf bifurcation).

Furthermore, it was shown that the dynamics of the full (non-autonomous) model is governed by the *vectorial reproduction ratio* ($\mathcal{R}_{Mt}$; the spectral radius of a certain linear operator of a function of the next generation matrices of the model which account for the number of new adult female mosquitoes produced by a reproductive adult female mosquito over its reproductive period). The trivial periodic solution of the model is shown to be locally-asymptotically stable, whenever the $\mathcal{R}_{Mt}$ is less than unity. Furthermore, it is shown, using uniform persistence theory, that the model has at least one positive periodic solution whenever $\mathcal{R}_{Mt} > 1$.

Sensitivity analysis of the autonomous version of the model shows that the top five parameters that have the most influence on the dynamics of the model (with

respect to various response functions) are:

(a) the probability that an adult female mosquito questing for bloodmeal successfully take a bloodmeal;

(b) the natural mortality rate of larvae and adult female mosquitoes;

(c) the maturation rate of female larvae from Stage 1 to Stage 2.

Hence, this study suggests that the population of adult mosquito in a community can be effectively-controlled using mosquito-reduction strategies, as well as personal protection against mosquito bites.

In addition, numerical simulations of the non-autonomous model (2.3.1), using relevant functional forms of the temperature- and rainfall-dependent parameters of the model (given in Section 2.3.1) and parameter values associated with the population dynamics of the *Anopheles species* of mosquitoes (which causes malaria in humans), show that for mean monthly temperature and rainfall values in the range $[10, 40]^{\circ}$C and $[90 - 120]$ mm, respectively, peak mosquito abundance is attained when temperature and rainfall values lie in the range $[20 - 25]^{\circ}$C and $[105 - 115]$ mm, respectively.

5.2 Chapter 3

In Chapter 3, a new weather-driven mathematical model (an extension of designed in chapter 2 by including the population dynamics of the human host and the interaction between *Anopheles* mosquitoes and humans) is designed to assess the impact of temperature variability on the transmission dynamics of malaria in a population. Some of the notable additional features of the model include incorporating:

(a) the *Plasmodium's* sporogonic cycle;

(b) disease transmission to vectors by asymptomatically-infectious humans;

(c) reduced malaria susceptibility in humans due to recovery from prior malaria infection;

(d) transition from symptomatic to asymptomatically-infectious stages for malaria-infected humans;

(e) the complete loss of partial immunity in humans;

(f) the effect of daily temperature range (DTR).

It was shown that the autonomous version of the model has a non-trivial disease-free equilibrium (NDFE) which exists whenever the *vectorial reproduction number* ($\mathcal{R}_M$) exceeds unity. The NDFE is shown to be globally-asymptotically stable, in the absence of disease-induced mortalities in humans (i.e., $\delta_H = \delta_{HA} = 0$), whenever the associated reproduction number (denoted by $\mathcal{R}_0$) is less than unity.

Furthermore, this study suggests (using detailed sensitivity analysis of the autonomous version of the model) that effective malaria control entails a multi-faceted approach based on:

(i) minimizing the contact humans have with mosquitoes (i.e., minimizing the *per capita* mosquito biting rate and the transmission probability from infected mosquitoes by using mosquito repellents and insecticide-treated bed nets, and potentially *via* the use of anti-malaria drugs as intermittent preventative therapy);

(ii) reducing the mosquito population (i.e., increasing death rate of mature mosquitoes by insecticide spraying, using insecticide-treated bed nets and removing stagnant waters, to prevent successfully fed adult female mosquitoes from returning close-by breeding sites);

(iii) early diagnosis and treatment of malaria cases.

Numerical simulations of the model indicate that temperature variability is important in determining the optimum temperature ranges for malaria transmission, with increasing DTR shifting the optimum temperature for transmission down from about 29.5 °C when temperature is constant, to 23.5 °C when DTR is 20 °C. In addition, by considering two reduced version of the model (one omitting explicit representation of the gonotrophic cycle and the other omitting the sporogonic cycle), numerical simulations indicate that the mosquito gonotrophic cycle does not seem to have major impact on malaria dynamics, and its explicit inclusion in malaria transmission models can be relaxed. Moreover, the omission of sporogony, significantly affects the model predictions (suggesting that it is crucial to include sporogony in models for malaria transmission dynamics).

5.3 Chapter 4

In Chapter 4, a new mathematical model is designed to gain qualitative and quantitative insight into the transmission dynamics of three disease viruses: DENV, CHIKV and ZIKV, that co-circulate in a given region, owing to the fact that they share the same transmitting vector (*Aedes* mosquito) but have some variations in transmission modes. In the SIRS model designed, a proportion of individuals receive the newly-released *Dengvaxia* vaccine against DENV. The model is built based on three main hypotheses, namely:

(a) a competitive DENV-CHIKV-ZIKV superinfection hierarchy;

(b) antibody-dependent enhancement (represented by setting a parameter, θ_Z to a value greater than unity);

(c) that the *Dengvaxia* vaccine could reduce susceptibility to ZIKV (represented by setting a parameter, σ_Z to a value less than unity).

The model is further extended to incorporate the effect of temperature and rainfall variability on the population biology of *Aedes* mosquitoes, to gain insight into the effect of these climate variables on transmission dynamics of the three diseases in the region of study.

The model has a disease-free equilibrium (DFE) which is locally-asymptotically stable whenever the basic reproduction number ($\mathcal{R}_0$; which is the maximum of the reproduction number of each of the three diseases) is less than unity. Furthermore, this equilibrium is globally-asymptotically stable, for a special case without dengue-induced mortality in humans, whenever the associated reproduction number is less than unity. Furthermore, the diseases are shown to persist in the community if a certain threshold quantity ($\mathcal{R}_{1T}$; which is the minimum of the reproduction number of each of the three diseases) exceeds unity.

Sensitivity analysis of the autonomous model shows that the top parameters that have the most influence on the dynamics of the model (with respect to various response functions) are:

(a) the rate at which humans acquire DENV infection;

(b) the modification parameter accounting for the assumption that a susceptible human is more likely to acquire DENV infection than CHIKV and ZIKV;

(c) the recovery rate from CHIKV;

(d) the natural mortality rates of mosquitoes;

(e) the recruitment rates of mosquitoes;

Numerical simulations of the autonomous model show that the ZIKV reproduction number (denoted by $\mathcal{R}_Z$) is only mildly affected by changes in the parameter related to the infectiousness of ZIKV in relation to DENV (θ_Z) even in the region where antibody-dependent enhancement ($\theta_Z > 1$) is assumed. In addition, the efficacy of the DENV vaccine has a very mild impact on ZIKV transmission dynamics. In particular, the DENV vaccine (no matter the levels of efficacy and coverage) is unable to reduce the ZIKV reproduction number to a value less than unity (implying that the DENV vaccine will have a limited effect on the onset of Zika outbreaks).

The model is further simulated to assess the effect of seasonality and climate variability on the dynamics of the model, using relevant data from Mexico. These simulations show that, for a fixed mean monthly rainfall value for Mexico (i.e., $R(t) = 63.2$ mm), the burden of the three diseases (as measured in terms of the total number of new cases) increases with increasing mean monthly temperature in the range ($[16 - 29]^\circ$C, and decreases with increasing mean monthly temperature thereafter. Moreover, for a fixed mean monthly temperature value for Mexico (i.e., $T(t) = 22^\circ$C), the burden of the diseases increases with increasing rainfall value until a threshold of $[95 - 100]$ mm is reached. At higher rainfall values (above the threshold), disease burden decreases. In addition, for the fixed mean monthly rainfall of 63.2 mm for Mexico, maximum disease activity (for all three diseases) occur for temperature in the range $[27, 29]^\circ$C. Hence, since the current mean monthly temperature for Mexico is 22°C, projected global warming could cause a shift (increase in mean monthly temperature) to the high transmission temperature range (thereby making Mexico more vulnerable for the spread of the three mosquito-borne diseases).

REFERENCES

Kwazulu-natal monthly climate average, south africa. URL https://www.worldweatheronline.com/kwazulu-natal-weather/za.aspx.

Lagos monthly climate average, nigeria. URL https://www.worldweatheronline.com/lagos-weather/lagos/ng.aspx?wwo_r=srch.

Mexico chikungunya, dengue fever and zika virus update. URL http://outbreaknewstoday.com/mexico-chikungunya-dengue-fever-and-zika-virus-update-66022/.

Nairobi monthly climate average, kenya. URL http://www.worldweatheronline.com/nairobi-weather-averages/nairobi-area/ke.aspx.

Panorama epidemiológico de dengue, 2016. dirección general de elidemiología , secretaría de salud, méxico. URL http://www.epidemiologia.salud.gob.mx/doctos/panodengue/PANORAMAS_2016/Pano_dengue_sem_48_2016.pdf.

A. Abdelrazec and A. B. Gumel. Mathematical assessment of the role of temperature and rainfall on mosquito population dynamics. *Journal of mathematical biology*, 74(6):1351–1395, 2017.

E. G. Acosta and R. Bartenschlager. Paradoxical role of antibodies in dengue virus infections: considerations for prophylactic vaccine development. *Expert review of vaccines*, 15(4):467–482, 2016.

Y. A. Afrane, B. W. Lawson, A. K. Githeko, and G. Yan. Effects of microclimatic changes caused by land use and land cover on duration of gonotrophic cycles of anopheles gambiae (diptera: Culicidae) in western kenya highlands. *Journal of medical entomology*, 42(6):974–980, 2005.

F. Agusto, A. Gumel, and P. Parham. Qualitative assessment of the role of temperature variations on malaria transmission dynamics. *Journal of Biological Systems*, 23(04):1550030, 2015.

J. A. Ahumada, D. Lapointe, and M. D. Samuel. Modeling the population dynamics of culex quinquefasciatus (diptera: Culicidae), along an elevational gradient in hawaii. *Journal of medical entomology*, 41(6):1157–1170, 2004.

B. M. Althouse, K. A. Hanley, M. Diallo, A. A. Sall, Y. Ba, O. Faye, D. Diallo, D. M. Watts, S. C. Weaver, and D. A. Cummings. Impact of climate and mosquito vector abundance on sylvatic arbovirus circulation dynamics in senegal. *The American journal of tropical medicine and hygiene*, 92(1):88–97, 2015.

N. M. Anstey, N. M. Douglas, J. R. Poespoprodjo, and R. N. Price. Plasmodium vivax: clinical spectrum, risk factors and pathogenesis. In *Advances in parasitology*, volume 80, pages 151–201. Elsevier, 2012.

N. Bacaér. Approximation of the basic reproduction number r_0 for vector-borne diseases with a periodic vector population. *Bulletin of Mathematical Biology*, 69 (3):1067 – 1091, 2007.

N. Bacaér. Periodic matrix population models: growth rate, basic reproduction number and entropy. *Bulletin of Mathematical Biology*, 71(7):1781 – 1792, 2009.

N. Bacaér. Genealogy with seasonality, the basic reproduction number, and the influenza pandemic. *Journal of Mathematical Biology*, 62(5):741 – 762, 2011.

N. Bacaér and X. Abdurahman. Resonance of the epidemic threshold in a periodic environment. *Journal of Mathematical Biology*, 57(5):649 – 673, 2008.

N. Bacaér and S. Guernaoui. The epidemic threshold of vector-borne diseases with seasonality. *Journal of Mathematical Biology*, 53(3):421 – 436, 2006.

N. Bacaér and R. Ouifki. Growth rate and basic reproduction number for population models with a simple periodic factor. *Mathematical Biosciences*, 210(2):647 – 658, 2007.

J. K. Baird. Neglect of plasmodium vivax malaria. *Trends in parasitology*, 23(11): 533–539, 2007.

D. H. Barouch, S. J. Thomas, and N. L. Michael. Prospects for a zika virus vaccine. *Immunity*, 46(2):176–182, 2017.

M. Bayoh and S. Lindsay. Effect of temperature on the development of the aquatic stages of anopheles gambiae sensu stricto (diptera: Culicidae). *Bulletin of entomological research*, 93(5):375–381, 2003.

M. N. Bayoh. *Studies on the development and survival of Anopheles gambiae sensu stricto at various temperatures and relative humidities*. PhD thesis, Durham University, 2001.

M. N. Bayoh and S. W. Lindsay. Temperature-related duration of aquatic stages of the afrotropical malaria vector mosquito anopheles gambiae in the laboratory. *Medical and veterinary entomology*, 18(2):174–179, 2004.

L. M. Beck-Johnson, W. A. Nelson, K. P. Paaijmans, A. F. Read, M. B. Thomas, and O. N. Bjørnstad. The effect of temperature on anopheles mosquito population dynamics and the potential for malaria transmission. *PLOS one*, 8(11):e79276, 2013.

L. M. Beck-Johnson, W. A. Nelson, K. P. Paaijmans, A. F. Read, M. B. Thomas, and O. N. Bjørnstad. The importance of temperature fluctuations in understanding mosquito population dynamics and malaria risk. *Royal Society open science*, 4(3): 160969, 2017.

M. Belda, E. Holtanová, T. Halenka, and J. Kalvová. Climate classification revisited: from köppen to trewartha. *Climate research*, 59(1):1–13, 2014.

K. Berkelhamer and T. J. Bradley. Mosquito larval development in container habitats: the role of rotting *Scirpus californicus*. *Journal of the American Mosquito Control Association*, 5:258 – 260, 1989.

M. Besnard, S. Lastere, A. Teissier, V. Cao-Lormeau, and D. Musso. Evidence of perinatal transmission of zika virus, french polynesia, december 2013 and february 2014. *Eurosurveillance*, 19(13):20751, 2014.

M. Betancourt-Cravioto, P. Kuri-Morales, J. F. González-Roldán, R. Tapia-Conyer, M. D. E. Group, et al. Introducing a dengue vaccine to mexico: development of a system for evidence-based public policy recommendations. *PLoS neglected tropical diseases*, 8(7):e3009, 2014.

S. Bhattacharya, C. Sharma, R. Dhiman, and A. Mitra. Climate change and malaria in india. *CURRENT SCIENCE-BANGALORE-*, 90(3):369, 2006.

P. Bi, S. Tong, K. Donald, K. A. Parton, and J. Ni. Climatic variables and transmission of malaria: a 12-year data analysis in shuchen county, china. *Public health reports*, 118(1):65, 2003.

S. M. Blower and H. Dowlatabadi. Sensitivity and uncertainty analysis of complex models of disease transmission: an hiv model, as an example. *International Statistical Review/Revue Internationale de Statistique*, pages 229–243, 1994.

T. Boden. Global, regional, and national co2 emissions.

P. Cailly, A. Tranc, T. Balenghiene, C. Totyg, and P. Ezannoa. A climate-driven abundance model to assess mosquito control strategies. *Ecological Modelling*, 227: 7–17, 2012.

C. Caminade, S. Kovats, J. Rocklov, A. M. Tompkins, A. P. Morse, F. J. Colón-González, H. Stenlund, P. Martens, and S. J. Lloyd. Impact of climate change on global malaria distribution. *Proceedings of the National Academy of Sciences*, 111 (9):3286–3291, 2014.

V.-M. Cao-Lormeau, A. Blake, S. Mons, S. Lastère, C. Roche, J. Vanhomwegen, T. Dub, L. Baudouin, A. Teissier, P. Larre, et al. Guillain-barré syndrome outbreak associated with zika virus infection in french polynesia: a case-control study. *The Lancet*, 387(10027):1531–1539, 2016.

C. W. Cardoso, M. Kikuti, A. P. P. Prates, I. A. Paploski, L. B. Tauro, M. M. Silva, P. Santana, M. F. Rego, M. G. Reis, U. Kitron, et al. Unrecognized emergence of chikungunya virus during a zika virus outbreak in salvador, brazil. *PLoS neglected tropical diseases*, 11(1):e0005334, 2017.

G. D. L. R. Cariboni, J. and A. Saltelli. The role of sensitivity analysis in ecological modeling. *Ecological modeling*, 203(1-2):167 – 182, 2007.

E. Carrillo-Valenzo, R. Danis-Lozano, J. X. Velasco-Hernández, G. Sánchez-Burgos, C. Alpuche, I. López, C. Rosales, C. Baronti, X. de Lamballerie, E. C. Holmes, et al. Evolution of dengue virus in mexico is characterized by frequent lineage replacement. *Archives of virology*, 155(9):1401–1412, 2010.

R. Carter and K. N. Mendis. Evolutionary and historical aspects of the burden of malaria. *Clinical microbiology reviews*, 15(4):564–594, 2002.

J. Casals and L. Whitman. Mayaro virus: a new human disease agent. i. relationship to other arbor viruses. *Carib Med J*, 27(1-4):103–10, 1965.

C. Castillo-Chavez and B. Song. Dynamical models of tuberculosis and their applications. *Mathematical Bioscience Engineering*, 1(2):361–404, 2004.

C. Castillo-Chavez and J. X. Velasco-Hernandez. On the relationship between evolution of virulence and host demography. *Journal of theoretical biology*, 192(4): 437–444, 1998.

CDC. Mosquitoes.

CDC. First female-to-male sexual transmission of zika virus infection reported in new york city. july 15, 2016. 2016.

J. Charlwood, T. Smith, P. Billingsley, W. Takken, E. Lyimo, and J. Meuwissen. Survival and infection probabilities of anthropophagic anophelines from an area of high prevalence of plasmodium falciparum in humans. *Bulletin of Entomological Research*, 87(5):445–453, 1997.

R. N. Charrel, X. de Lamballerie, D. Raoult, et al. Chikungunya outbreaks-the globalization of vectorborne diseases. *New England Journal of Medicine*, 356(8): 769, 2007.

N. Chitnis, J. Cushing, and J. Hyman. Bifurcation analysis of a mathematical model for malaria transmission. *SIAM Journal on Applied Mathematics*, 67(1):24–45, 2006.

S. Chow, C. Li, and D. Wang. *Normal Forms and Bifurcation of Planar Vector Fields*. Cambridge University Press, Cambridge, 1994.

C. Christiansen-Jucht, K. Erguler, C. Y. Shek, M.-G. Basáñez, and P. E. Parham. Modelling anopheles gambiae ss population dynamics with temperature-and age-dependent survival. *International journal of environmental research and public health*, 12(6):5975–6005, 2015.

J. Cohen. Q&a with scott halstead: Zika will subside in '5 years, max'. *Science Mar*, 7, 2016.

J. Coleman, J. Juhn, and A. A. James. Dissection of midgut and salivary glands from ae. aegypti mosquitoes. *Journal of visualized experiments: JoVE*, (5), 2007.

W. E. Collins and G. M. Jeffery. Plasmodium ovale: parasite and disease. *Clinical microbiology reviews*, 18(3):570–581, 2005.

F. Corsica. Zika virus transmission from french polynesia to brazil. *Emerg Infect Dis*, 21(10):1887, 2015.

A. F. Cowman, J. Healer, D. Marapana, and K. Marsh. Malaria: biology and disease. *Cell*, 167(3):610–624, 2016.

A. Dao, A. Adamou, J. E. Crawford, J. M. Ribeiro, R. Gwadz, S. F. Traoré, T. Lehmann, et al. The distribution of hatching time in anopheles gambiae. *Malaria journal*, 5(1):19, 2006.

A. Davidson. Suspected female-to-male sexual transmission of zika virus—new york city, 2016. *MMWR. Morbidity and mortality weekly report*, 65, 2016.

W. Dejnirattisai, P. Supasa, W. Wongwiwat, A. Rouvinski, G. Barba-Spaeth, T. Duangchinda, A. Sakuntabhai, V.-M. Cao-Lormeau, P. Malasit, F. A. Rey, et al. Dengue virus sero-cross-reactivity drives antibody-dependent enhancement of infection with zika virus. *Nature immunology*, 17(9):1102, 2016.

H. Delatte, G. Gimonneau, A. Triboire, and D. Fontenille. Influence of temperature on immature development, survival, longevity, fecundity, and gonotrophic cycles of aedes albopictus, vector of chikungunya and dengue in the indian ocean. *Journal of medical entomology*, 46(1):33–41, 2009.

J. Depinay, C. Mbogo, G. Killeen, B. Knols, J. Beier, J. Carlson, J. Dushoff, P. Billingsley, H. Mwambi, J. Githure, and A. Toure. A simulation model of african anopheles ecology and population dynamics for the analysis of malaria transmission. *Malaria Journal*, 3(1):29, 2004.

T. S. Detinova, D. Bertram, W. H. Organization, et al. Age-grouping methods in diptera of medical importance, with special reference to some vectors of malaria. 1962.

M. Diallo, J. Thonnon, M. Traore-Lamizana, and D. Fontenille. Vectors of chikungunya virus in senegal: current data and transmission cycles. *The American journal of tropical medicine and hygiene*, 60(2):281–286, 1999.

G. Dick, S. Kitchen, and A. Haddow. Zika virus (i). isolations and serological specificity. *Transactions of the Royal Society of Tropical Medicine and Hygiene*, 46(5): 509–520, 1952.

O. Diekmann, J. A. P. Heesterbeek, and J. A. Metz. On the definition and the computation of the basic reproduction ratio r 0 in models for infectious diseases in heterogeneous populations. *Journal of mathematical biology*, 28(4):365–382, 1990.

K. Dietz, L. Molineaux, and A. Thomas. A malaria model tested in the african savannah. *Bulletin of the World Health Organization*, 50(3-4):347, 1974.

D. L. Doolan, C. Dobaño, and J. K. Baird. Acquired immunity to malaria. *Clinical microbiology reviews*, 22(1):13–36, 2009.

M. R. Duffy, T.-H. Chen, W. T. Hancock, A. M. Powers, J. L. Kool, R. S. Lanciotti, M. Pretrick, M. Marfel, S. Holzbauer, C. Dubray, et al. Zika virus outbreak on yap island, federated states of micronesia. *New England Journal of Medicine*, 360(24): 2536–2543, 2009.

Y. Dumont and F. Chiroleu. Vector control for the chikungunya disease. *Mathematical biosciences and engineering*, 7(2):313–345, 2010.

M. Dupont-Rouzeyrol, O. O'Connor, E. Calvez, M. Daures, M. John, J.-P. Grangeon, and A.-C. Gourinat. Co-infection with zika and dengue viruses in 2 patients, new caledonia, 2014. *Emerging infectious diseases*, 21(2):381, 2015.

A. P. Durbin. Dengue antibody and zika: Friend or foe? *Trends in immunology*, 37 (10):635–636, 2016.

R. Edelman. Dengue and dengue vaccines, 2005.

S. E. Eikenberry and A. B. Gumel. Mathematical modeling of climate change and malaria transmission dynamics: a historical review. *Journal of mathematical biology*, pages 1–77, 2018.

R. H. d. N. en México. Dirección general de epidemiología, secretaria de salud; méxico, 2003.

M. Enserink. Massive outbreak draws fresh attention to little-known virus, 2006.

V. Ermert, A. H. Fink, A. E. Jones, and A. P. Morse. Development of a new version of the liverpool malaria model. ii. calibration and validation for west africa. *Malaria journal*, 10(1):62, 2011.

D. A. Ewing, C. A. Cobbold, B. Purse, M. Nunn, and S. M. White. Modelling the effect of temperature on the seasonal population dynamics of temperate mosquitoes. *Journal of theoretical biology*, 400:65–79, 2016.

A. Fagbami. Epidemiological investigations on arbovirus infections at igbo-ora, nigeria. *Tropical and geographical medicine*, 29(2):187–191, 1977.

A. S. Fauci and D. M. Morens. Zika virus in the americas—yet another arbovirus threat. *New England Journal of Medicine*, 374(7):601–604, 2016.

F. B. Faye, L. Konaté, C. Rogier, and J.-F. Trape. Plasmodium ovale in a highly malaria endemic area of senegal. *Transactions of the Royal Society of Tropical Medicine and Hygiene*, 92(5):522–525, 1998.

J. A. Filipe, E. M. Riley, C. J. Drakeley, C. J. Sutherland, and A. C. Ghani. Determination of the processes driving the acquisition of immunity to malaria using a mathematical transmission model. *PLoS computational biology*, 3(12):e255, 2007.

F. Forouzannia and A. B. Gumel. Mathematical analysis of an age-structured model for malaria transmission dynamics. *Mathematical biosciences*, 247:80–94, 2014.

B. D. Foy, K. C. Kobylinski, J. L. C. Foy, B. J. Blitvich, A. T. da Rosa, A. D. Haddow, R. S. Lanciotti, and R. B. Tesh. Probable non–vector-borne transmission of zika virus, colorado, usa. *Emerging infectious diseases*, 17(5):880, 2011.

F. E. Fry and K. E. Watt. Yields of year classes of the smallmouth bass hatched in the decade of 1940 in manitoulin island waters. *Transactions of the American Fisheries Society*, 85(1):135–143, 1957.

L. Furuya-Kanamori, S. Liang, G. Milinovich, R. J. S. Magalhaes, A. C. Clements, W. Hu, P. Brasil, F. D. Frentiu, R. Dunning, and L. Yakob. Co-distribution and co-infection of chikungunya and dengue viruses. *BMC infectious diseases*, 16(1): 84, 2016.

S. M. Garba, A. B. Gumel, and M. A. Bakar. Backward bifurcations in dengue transmission dynamics. *Mathematical biosciences*, 215(1):11–25, 2008.

T. G. George. Positive definite matrices and sylvester's criterion. *The American Mathematical Monthly*, 98(1):44 – 46, 1991.

P. W. Gething, D. L. Smith, A. P. Patil, A. J. Tatem, R. W. Snow, and S. I. Hay. Climate change and the global malaria recession. *Nature*, 465(7296):342–346, 2010.

R. V. Gibbons and D. W. Vaughn. Dengue: an escalating problem. *BMJ: British Medical Journal*, 324(7353):1563, 2002.

N. G. Gratz. Emerging and resurging vector-borne diseases. *Annual review of entomology*, 44(1):51–75, 1999.

N. G. Gratz, A. B. Knudsen, W. H. Organization, et al. The rise and spread of dengue, dengue haemorrhagic fever and its vectors: a historical review (up to 1995). 1996.

P. Graves, T. Burkot, A. Saul, R. Hayes, and R. Carter. Estimation of anopheline survival rate, vectorial capacity and mosquito infection probability from malaria vector infection rates in villages near madang, papua new guinea. *Journal of Applied Ecology*, pages 134–147, 1990.

S. M. Gray and N. Banerjee. Mechanisms of arthropod transmission of plant and animal viruses. *Microbiology and Molecular Biology Reviews*, 63(1):128–148, 1999.

T. W. B. Group. Climate change knowledge portal for development practitioners and policy makers.

D. J. Gubler. Aedes aegypti and aedes aegypti-borne disease control in the 1990s: top down or bottom up. *The American journal of tropical medicine and hygiene*, 40(6):571–578, 1989.

D. J. Gubler. Dengue and dengue hemorrhagic fever. *Clinical microbiology reviews*, 11(3):480–496, 1998.

D. J. Gubler and G. G. Clark. Community-based integrated control of aedes aegypti: a brief overview of current programs. *The American journal of tropical medicine and hygiene*, 50(6_Suppl):50–60, 1994.

D. Gyurech, J. Schilling, J. Schmidt-Chanasit, P. Cassinotti, F. Kaeppeli, and M. Dobec. False positive dengue ns1 antigen test in a traveller with an acute zika virus infection imported into switzerland. *Swiss Med Wkly*, 146:w14296, 2016.

S. B. Halstead. Pathogenesis of dengue: challenges to molecular biology. *Science*, 239 (4839):476–481, 1988.

S. B. Halstead. The xxth century dengue pandemic: need for surveillance and research. 1992.

S. B. Halstead. Safety issues from a phase 3 clinical trial of a live-attenuated chimeric yellow fever tetravalent dengue vaccine. *Human vaccines & immunotherapeutics*, (just-accepted):00–00, 2018.

R. Harbach. Mosquito taxonomic inventory, 2013.

S. I. Hay, J. Cox, D. J. Rogers, S. E. Randolph, D. I. Stern, G. D. Shanks, M. F. Myers, and R. W. Snow. Climate change and the resurgence of malaria in the east african highlands. *Nature*, 415(6874):905–909, 2002.

V. Heang, C. Y. Yasuda, L. Sovann, A. D. Haddow, A. P. T. da Rosa, R. B. Tesh, and M. R. Kasper. Zika virus infection, cambodia, 2010. *Emerging infectious diseases*, 18(2):349, 2012.

J. C. Helton and F. J. Davis. Latin hypercube sampling and the propagation of uncertainty in analyses of complex systems. *Reliability Engineering & System Safety*, 81(1):23–69, 2003.

D. Hershkowitz. Recent directions in matrix stability. *Linear Algebra and its Applications*, 171:161–186, 1992.

H. W. Hethcote. The mathematics of infectious diseases. *SIAM review*, 42(4):599–653, 2000.

W. M. Hirsch, H. Hanisch, and J.-P. Gabriel. Differential equation models of some parasitic infections: methods for the study of asymptotic behavior. *Communications on Pure and Applied Mathematics*, 38(6):733–753, 1985.

M. B. Hoshen and A. P. Morse. A weather-driven model of malaria transmission. *Malaria Journal*, 3(1):32, 2004.

J. Huang, E. D. Walker, J. Vulule, and J. R. Miller. Daily temperature profiles in and around western kenyan larval habitats of anopheles gambiae as related to egg mortality. *Malaria Journal*, 5(1):87, 2006.

S. S. Imbahale, K. P. Paaijmans, W. R. Mukabana, R. van Lammeren, A. K. Githeko, and W. Takken. A longitudinal study on anopheles mosquito larval abundance in distinct geographical and environmental settings in western kenya. *Malaria journal*, 10(1):81, 2011.

INEGI. Anuario estadístico y geográfico por entidad federativa 2013, 2013.

B. L. Innis. Dengue and dengue hemorrhagic fever. *Exotic viral infections—1995. Chapman & Hall, London, United Kingdom*, pages 103–146, 1995.

M. Instituto Nacional de Estadśtica y Geografía. URL http://www.beta.inegi.org.mx/app/areasgeograficas/?ag=07.

IPCC. Climate change 2007: impacts, adaptation and vulnerability. *Genebra, Suíça*, 2001.

A. Jacobson. Emerging and re-emerging viruses: an essay, 1997.

P. Jeandel, R. Josse, and J. Durand. Exotic viral arthritis: role of alphavirus. *Medecine tropicale: revue du Corps de sante colonial*, 64(1):81–88, 2004.

G. M. Jeffery and D. E. Eyles. The duration in the human host of infections with a panama strain of plasmodium falciparum. *The American journal of tropical medicine and hygiene*, 3(2):219–224, 1954.

S. Kalayanarooj, D. W. Vaughn, S. Nimmannitya, S. Green, S. Suntayakorn, N. Kunentrasai, W. Viramitrachai, S. Ratanachu-Eke, S. Kiatpolpoj, B. Innis, et al. Early clinical and laboratory indicators of acute dengue illness. *Journal of Infectious Diseases*, 176(2):313–321, 1997.

E. D. Kilbourne. The emergence of" emerging diseases": a lesson in holistic epidemiology. *The Mount Sinai journal of medicine, New York*, 63(3-4):159–166, 1996.

G. F. Killeen and T. A. Smith. Exploring the contributions of bed nets, cattle, insecticides and excitorepellency to malaria control: a deterministic model of mosquito host-seeking behaviour and mortality. *Transactions of the Royal Society of Tropical Medicine and Hygiene*, 101(9):867–880, 2007.

M. K. Kindhauser, T. Allen, V. Frank, R. S. Santhana, and C. Dye. Zika: the origin and spread of a mosquito-borne virus. *Bulletin of the World Health Organization*, 94(9):675, 2016.

S. C. Kliks, A. Nisalak, W. E. Brandt, L. Wahl, and D. S. Burke. Antibody-dependent enhancement of dengue virus growth in human monocytes as a risk factor for dengue hemorrhagic fever. *The American journal of tropical medicine and hygiene*, 40(4): 444–451, 1989.

R. Knowles and A. S. B. D. Gupta. A study of monkey-malaria, and its experimental transmission to man. *The Indian Medical Gazette*, 67(6):301, 1932.

M. H. Kuniholm, N. D. Wolfe, C. Y.-h. Huang, E. Mpoudi-Ngole, U. Tamoufe, D. S. Burke, and D. J. Gubler. Seroprevalence and distribution of flaviviridae, togaviridae, and bunyaviridae arboviral infections in rural cameroonian adults. *The American journal of tropical medicine and hygiene*, 74(6):1078–1083, 2006.

K. D. Lafferty. The ecology of climate change and infectious diseases. *Ecology*, 90(4): 888–900, 2009.

K. D. Lafferty and E. A. Mordecai. The rise and fall of infectious disease in a warmer world. *F1000Research*, 5, 2016.

D. D. Laishram, P. L. Sutton, N. Nanda, V. L. Sharma, R. C. Sobti, J. M. Carlton, and H. Joshi. The complexities of malaria disease manifestations with a focus on asymptomatic malaria. *Malaria journal*, 11(1):29, 2012.

V. Lakshmikantham and S. Leela. *Differential and Integral Inequalities: Theory and Applications: Volume I: Ordinary Differential Equations*. Academic press, 1969.

L. Lambrechts, K. P. Paaijmans, T. Fansiri, L. B. Carrington, L. D. Kramer, M. B. Thomas, and T. W. Scott. Impact of daily temperature fluctuations on dengue virus transmission by aedes aegypti. *Proceedings of the National Academy of Sciences*, 108(18):7460–7465, 2011.

R. M. Lana, T. G. Carneiro, N. A. Honório, and C. T. Codeco. Seasonal and non-seasonal dynamics of aedes aegypti in rio de janeiro, brazil: Fitting mathematical models to trap data. *Acta tropica*, 129:25–32, 2014.

V. Laperriere, K. Brugger, and F. Rubel. Simulation of the seasonal cycles of bird, equine and human west nile virus cases. *Preventive veterinary medicine*, 98(2-3): 99–110, 2011.

F. J. Lardeux, R. H. Tejerina, V. Quispe, and T. K. Chavez. A physiological time analysis of the duration of the gonotrophic cycle of anopheles pseudopunctipennis and its implications for malaria transmission in bolivia. *Malaria journal*, 7(1):141, 2008.

J. P. LaSalle. *The stability of dynamical systems*, volume 25. Siam, 1976.

S. M. Lemon, P. F. Sparling, M. A. Hamburg, D. A. Relman, E. R. Choffnes, A. Mack, et al. Vector-borne diseases: understanding the environmental, human health, and ecological connections. workshop summary. In *Vector-borne diseases: understanding the environmental, human health, and ecological connections. Workshop summary.* National Academies Press, 2008.

S. Levin and D. Pimentel. Selection of intermediate rates of increase in parasite-host systems. *The American Naturalist*, 117(3):308–315, 1981.

B. L. Ligon. Reemergence of an unusual disease: the chikungunya epidemic. In *Seminars in pediatric infectious diseases*, volume 17, pages 99–104. Elsevier, 2006.

S. Lindsay and R. Hutchinson. Malaria and deaths in the english marshes–authors' reply. *The Lancet*, 368(9542):1152, 2006.

J. Lines, T. Wilkes, and E. Lyimo. Human malaria infectiousness measured by age-specific sporozoite rates in anopheles gambiae in tanzania. *Parasitology*, 102(2): 167–177, 1991.

J. Liu-Helmersson, M. Quam, A. Wilder-Smith, H. Stenlund, K. Ebi, E. Massad, and J. Rocklöv. Climate change and aedes vectors: 21st century projections for dengue transmission in europe. *EBioMedicine*, 7:267–277, 2016.

Y. Lou and X.-Q. Zhao. A climate-based malaria transmission model with structured vector population. *SIAM Journal on Applied Mathematics*, 70(6):2023–2044, 2010.

G. Macdonald. Epidemiological basis of malaria control. *Bulletin of the World Health Organization*, 15(3-5):613, 1956.

G. Macdonald et al. The epidemiology and control of malaria. *The Epidemiology and Control of Malaria.*, 1957.

J. Mackenzie, K. Chua, P. Daniels, B. Eaton, H. Field, R. Hall, K. Halpin, C. Johansen, P. Kirkland, S. Lam, et al. Emerging viral diseases of southeast asia and the western pacific. *Emerging infectious diseases*, 7(3 Suppl):497, 2001.

F. Macnamara. Zika virus: a report on three cases of human infection during an epidemic of jaundice in nigeria. *Transactions of the Royal Society of Tropical Medicine and Hygiene*, 48(2):139–145, 1954.

P. Magal and X.-Q. Zhao. Global attractors and steady states for uniformly persistent dynamical systems. *SIAM journal on mathematical analysis*, 37(1):251–275, 2005.

R. Maharaj. Life table characteristics of anopheles arabiensis (diptera: Culicidae) under simulated seasonal conditions. *Journal of medical entomology*, 40(6):737–742, 2003.

A. O. Mala, L. W. Irungu, E. K. Mitaki, J. I. Shililu, C. M. Mbogo, J. K. Njagi, and J. I. Githure. Gonotrophic cycle duration, fecundity and parity of anopheles gambiae complex mosquitoes during an extended period of dry weather in a semi arid area in baringo county, kenya. *Int J Mosq Res*, 1(2):28–34, 2014.

S. Marino, I. B. Hogue, C. J. Ray, and D. E. Kirschner. A methodology for performing global uncertainty and sensitivity analysis in systems biology. *Journal of theoretical biology*, 254(1):178–196, 2008.

P. Martens. Climate change impacts on vector-borne disease transmission in europe. *Climate change and human health. The Royal Society, London, UK*, pages 45–54, 1999.

P. Martens. *Health and climate change: modelling the impacts of global warming and ozone depletion.* Routledge, 2013.

W. Martens, L. W. Niessen, J. Rotmans, T. H. Jetten, and A. J. McMichael. Potential impact of global climate change on malaria risk. *Environmental health perspectives*, 103(5):458, 1995.

A. McCombie. Some relations between air temperatures and the surface water temperatures of lakes. *Limnology and Oceanography*, 4(3):252–258, 1959.

M. D. McKay, R. J. Beckman, and W. J. Conover. Comparison of three methods for selecting values of input variables in the analysis of output from a computer code. *Technometrics*, 21(2):239–245, 1979.

R. G. McLeod, J. F. Brewster, A. B. Gumel, and A. Slonowsky. Sensitivity and uncertainty analyses for a sars model with time-varying inputs and outputs. *Mathematical Biosciences and Engineering*, 3(3):527–544, 2006.

J. Mena-Lorca, J. X. Velasco-Hernández, and P. A. Marquet. Coexistence in metacommunities: A tree-species model. *Mathematical Biosciences*, 202(1):42–56, 2006.

L. H. Miller, M. F. Good, and G. Milon. Malaria pathogenesis. *Science*, 264(5167): 1878–1883, 1994.

D. Moore, S. Reddy, F. Akinkugbe, V. Lee, T. David-West, O. Causey, and D. Carey. An epidemic of chikungunya fever at ibadan, nigeria, 1969. *Annals of Tropical Medicine & Parasitology*, 68(1):59–68, 1974.

E. A. Mordecai, K. P. Paaijmans, L. R. Johnson, C. Balzer, T. Ben-Horin, E. Moor, A. McNally, S. Pawar, S. J. Ryan, T. C. Smith, et al. Optimal temperature for malaria transmission is dramatically lower than previously predicted. *Ecology letters*, 16(1):22–30, 2013.

D. M. Morens, G. K. Folkers, and A. S. Fauci. The challenge of emerging and reemerging infectious diseases. *Nature*, 430(6996):242, 2004.

S. S. Morse. Factors in the emergence of infectious diseases. In *Plagues and politics*, pages 8–26. Springer, 2001.

P. Mulatti, H. M. Ferguson, L. Bonfanti, F. Montarsi, G. Capelli, and S. Marangon. Determinants of the population growth of the west nile virus mosquito vector culex pipiens in a repeatedly affected area in italy. *Parasites & vectors*, 7(1):26, 2014.

D. Musso, E. Nilles, and V.-M. Cao-Lormeau. Rapid spread of emerging zika virus in the pacific area. *Clinical Microbiology and Infection*, 20(10), 2014.

J. Muyembe-Tamfum, C. Peyrefitte, R. Yogolelo, E. B. Mathina, D. Koyange, E. Pukuta, M. Mashako, H. Tolou, and J. Durand. Epidemic of chikungunya virus in 1999 and 200 in the democratic republic of the congo. *Medecine tropicale: revue du Corps de sante colonial*, 63(6):637–638, 2003.

M. Negev, S. Paz, A. Clermont, N. G. Pri-Or, U. Shalom, T. Yeger, and M. S. Green. Impacts of climate change on vector borne diseases in the mediterranean basin—implications for preparedness and adaptation policy. *International journal of environmental research and public health*, 12(6):6745–6770, 2015.

C. N. Ngonghala, G. A. Ngwa, and M. I. Teboh-Ewungkem. Periodic oscillations and backward bifurcation in a model for the dynamics of malaria transmission. *Mathematical biosciences*, 240(1):45–62, 2012.

G. A. Ngwa. On the population dynamics of the malaria vector. *Bulletin of mathematical biology*, 68(8):2161–2189, 2006.

G. A. Ngwa, A. M. Niger, and A. B. Gumel. Mathematical assessment of the role of non-linear birth and maturation delay in the population dynamics of the malaria vector. *Applied Mathematics and Computation*, 217(7):3286–3313, 2010.

A. M. Niger and A. B. Gumel. Mathematical analysis of the role of repeated exposure on malaria transmission dynamics. *Differential Equations and Dynamical Systems*, 16(3):251–287, 2008.

M. A. Nowak and R. M. May. Superinfection and the evolution of parasite virulence. *Proc. R. Soc. Lond. B*, 255(1342):81–89, 1994.

E. Oehler, L. Watrin, P. Larre, I. Leparc-Goffart, S. Lastere, F. Valour, L. Baudouin, H. Mallet, D. Musso, and F. Ghawche. Zika virus infection complicated by guillain-barre syndrome–case report, french polynesia, december 2013. *Eurosurveillance*, 19 (9):20720, 2014.

N. H. Ogden and L. R. Lindsay. Effects of climate and climate change on vectors and vector-borne diseases: ticks are different. *Trends in parasitology*, 32(8):646–656, 2016.

K. Okuneye and A. B. Gumel. Analysis of a temperature-and rainfall-dependent model for malaria transmission dynamics. *Mathematical biosciences*, 287:72–92, 2017.

K. Okuneye, A. Abdelrazec, and A. B. Gumel. Mathematical analysis of a weather-driven model for the population ecology of mosquitoes. *Mathematical Biosciences & Engineering*, 15(1):57–93, 2018a.

K. Okuneye, S. Eikenberry, and A. B. Gumel. Weather-driven malaria transmission model with gonotrophic and sporogonic cycles. *Submitted*, 2018b.

K. O. Okuneye, J. X. Velasco-Hernandez, and A. B. Gumel. The "unholy" chikungunya–dengue–zika trinity: A theoretical analysis. *Journal of Biological Systems*, 25(04):545–585, 2017.

W. H. Organization et al. Immunization, vaccines and biologicals: 2002-2003 highlights. 2005.

W. H. Organization et al. Cumulative zika suspected and confirmed cases reported by countries and territories in the americas, 2015-2016, 2016.

K. Paaijmans, A. Jacobs, W. Takken, B. Heusinkveld, A. Githeko, M. Dicke, and A. Holtslag. Observations and model estimates of diurnal water temperature dynamics in mosquito breeding sites in western kenya. *Hydrological Processes*, 22(24): 4789–4801, 2008a.

K. P. Paaijmans, M. O. Wandago, A. K. Githeko, and W. Takken. Unexpected high losses of anopheles gambiae larvae due to rainfall. *PLoS One*, 2(11):e1146, 2007.

K. P. Paaijmans, B. G. Heusinkveld, and A. F. Jacobs. A simplified model to predict diurnal water temperature dynamics in a shallow tropical water pool. *International journal of biometeorology*, 52(8):797–803, 2008b.

K. P. Paaijmans, S. Blanford, A. S. Bell, J. I. Blanford, A. F. Read, and M. B. Thomas. Influence of climate on malaria transmission depends on daily temperature variation. *Proceedings of the National Academy of Sciences*, 107(34):15135–15139, 2010a.

K. P. Paaijmans, S. Blanford, A. S. Bell, J. I. Blanford, A. F. Read, and M. B. Thomas. Influence of climate on malaria transmission depends on daily temperature variation. *Proceedings of the National Academy of Sciences*, 107(34):15135–15139, 2010b.

K. P. Paaijmans, S. S. Imbahale, M. B. Thomas, and W. Takken. Relevant microclimate for determining the development rate of malaria mosquitoes and possible implications of climate change. *Malaria journal*, 9(1):196, 2010c.

R. M. Packard. The fielding h. garrison lecture:"break-bone" fever in philadelphia, 1780: Reflections on the history of disease. *Bulletin of the History of Medicine*, 90 (2):193, 2016.

P. E. Parham and E. Michael. Modeling the effects of weather and climate change on malaria transmission. *Environmental health perspectives*, 118(5):620–626, 2010.

P. E. Parham, D. Pople, C. Christiansen-Jucht, S. Lindsay, W. Hinsley, and E. Michael. Modeling the role of environmental variables on the population dynamics of the malaria vector anopheles gambiae sensu stricto. *Malaria Journal*, 11 (1):271, 2012.

P. Parks. A new proof of hermite's stability criterion and a generalization of orlando's formula. *International Journal of Control*, 26(2):197–206, 1977.

C. Parmesan and G. Yohe. A globally coherent fingerprint of climate change impacts across natural systems. *Nature*, 421(6918):37, 2003.

M. Pascual and M. J. Bouma. Do rising temperatures matter? *Ecology*, 90(4): 906–912, 2009.

J. A. Patz, P. R. Epstein, T. A. Burke, and J. M. Balbus. Global climate change and emerging infectious diseases. *Jama*, 275(3):217–223, 1996.

J. A. Patz, W. Martens, D. A. Focks, and T. H. Jetten. Dengue fever epidemic potential as projected by general circulation models of global climate change. *Environmental health perspectives*, 106(3):147, 1998.

L. Paul, E. Carlin, M. Jenkins, A. Tan, C. Barcellona, C. Nicholson, L. Trautmann, S. Michael, and S. Isern. Dengue virus antibodies enhance zika virus infection. biorxiv. *preprint. doi: http://dx. doi. org/10.1101/050112*, 2016.

E. E. Petersen. Update: interim guidance for preconception counseling and prevention of sexual transmission of zika virus for persons with possible zika virus exposure—united states, september 2016. *MMWR. Morbidity and mortality weekly report*, 65, 2016.

G. Pialoux, B.-A. Gaüzère, S. Jauréguiberry, and M. Strobel. Chikungunya, an epidemic arbovirosis. *The Lancet infectious diseases*, 7(5):319–327, 2007.

S. Polwiang. The seasonal reproduction number of dengue fever: impacts of climate on transmission. *PeerJ*, 3:e1069, 2015.

T. Porphyre, D. Bicout, and P. Sabatier. Modelling the abundance of mosquito vectors versus flooding dynamics. *Ecological modelling*, 183(2-3):173–181, 2005.

A. M. Powers and C. H. Logue. Changing patterns of chikungunya virus: re-emergence of a zoonotic arbovirus. *Journal of General Virology*, 88(9):2363–2377, 2007.

J. Pull and B. Grab. A simple epidemiological model for evaluating the malaria inoculation rate and the risk of infection in infants. *Bulletin of the World Health Organization*, 51(5):507, 1974.

A. T. Pyke, M. T. Daly, J. N. Cameron, P. R. Moore, C. T. Taylor, G. R. Hewitson, J. L. Humphreys, and R. Gair. Imported zika virus infection from the cook islands into australia, 2014. *PLoS currents*, 6, 2014.

I. A. Rather, S. Kumar, V. K. Bajpai, J. Lim, and Y.-H. Park. Prevention and control strategies to counter zika epidemic. *Frontiers in microbiology*, 8:305, 2017.

V. Ravi. Re-emergence of chikungunya virus in india. *Indian journal of medical microbiology*, 24(2):83, 2006.

P. Reiter. Climate change and mosquito-borne disease. *Environmental health perspectives*, 109(Suppl 1):141, 2001.

P. Reiter, C. J. Thomas, P. M. Atkinson, S. I. Hay, S. E. Randolph, D. J. Rogers, G. D. Shanks, R. W. Snow, and A. Spielman. Global warming and malaria: a call for accuracy. *The lancet Infectious diseases*, 4(6):323, 2004.

L. S. Rickman, T. R. Jones, G. W. Long, S. Paparello, I. Schneider, C. F. Paul, R. L. Beaudoin, and S. L. Hoffman. Plasmodium falciparum-infected anopheles stephensi inconsistently transmit malaria to humans. *The American journal of tropical medicine and hygiene*, 43(5):441–445, 1990.

J. G. Rigau-Pérez, G. G. Clark, D. J. Gubler, P. Reiter, E. J. Sanders, and A. V. Vorndam. Dengue and dengue haemorrhagic fever. *The Lancet*, 352(9132):971–977, 1998.

M. C. Robinson. An epidemic of virus disease in southern province, tanganyika territory, in 1952–1953. *Transactions of the Royal Society of Tropical Medicine and Hygiene*, 49(1):28–32, 1955.

D. J. Rogers and S. E. Randolph. The global spread of malaria in a future, warmer world. *Science*, 289(5485):1763–1766, 2000.

T. L. Root, D. P. MacMynowski, M. D. Mastrandrea, and S. H. Schneider. Human-modified temperatures induce species changes: joint attribution. *Proceedings of the National Academy of Sciences of the United States of America*, 102(21):7465–7469, 2005.

J. Rosenbaum, M. B. Nathan, R. Ragoonanansingh, S. Rawlins, C. Gayle, D. D. Chadee, and L. S. Lloyd. Community participation in dengue prevention and control: a survey of knowledge, attitudes, and practice in trinidad and tobago. *The American journal of tropical medicine and hygiene*, 53(2):111–117, 1995.

L.-C. S. R. Ross et al. An application of the theory of probabilities to the study of a priori pathometry.—part i. *Proceedings of the Royal Society A*, 92(638):204–230, 1916.

R. Ross. The newala epidemic: Iii. the virus: isolation, pathogenic properties and relationship to the epidemic. *Epidemiology & Infection*, 54(2):177–191, 1956.

A. Roth, A. Mercier, C. Lepers, D. Hoy, S. Duituturaga, E. Benyon, L. Guillaumot, and Y. Souares. Concurrent outbreaks of dengue, chikungunya and zika virus infections-an unprecedented epidemic wave of mosquito-borne viruses in the pacific 2012-2014. *Euro surveillance: bulletin Europeen sur les maladies transmissibles= European communicable disease bulletin*, 19(41), 2014.

F. Rubel, K. Brugger, M. Hantel, S. Chvala-Mannsberger, T. Bakonyi, H. Weissenböck, and N. Nowotny. Explaining usutu virus dynamics in austria: model development and calibration. *Preventive veterinary medicine*, 85(3-4):166–186, 2008.

A. B. Sabin. Research on dengue during world war ii1. *The American journal of tropical medicine and hygiene*, 1(1):30–50, 1952.

M. A. Safi, M. Imran, and A. B. Gumel. Threshold dynamics of a non-autonomous seirs model with quarantine and isolation. *Theory in Biosciences*, 131(1):19–30, 2012.

W. Sama, G. Killeen, and T. Smith. Estimating the duration of plasmodium falciparum infection from trials of indoor residual spraying. *The American journal of tropical medicine and hygiene*, 70(6):625–634, 2004.

S. Saxena, M. Singh, N. Mishra, and V. Lakshmi. Resurgence of chikungunya virus in india: an emerging threat. *Weekly releases (1997–2007)*, 11(32):3019, 2006.

L. Schofield and G. E. Grau. Immunological processes in malaria pathogenesis. *Nature Reviews Immunology*, 5(9):722, 2005.

T. W. Scott, P. H. Amerasinghe, A. C. Morrison, L. H. Lorenz, G. G. Clark, D. Strickman, P. Kittayapong, and J. D. Edman. Longitudinal studies of aedes aegypti (diptera: Culicidae) in thailand and puerto rico: blood feeding frequency. *Journal of medical entomology*, 37(1):89–101, 2000.

Z. Shuai, J. Heesterbeek, and P. van den Driessche. Extending the type reproduction number to infectious disease control targeting contacts between types. *Journal of mathematical biology*, 67(5):1067–1082, 2013.

U. Siegenthaler, T. F. Stocker, E. Monnin, D. Lüthi, J. Schwander, B. Stauffer, D. Raynaud, J.-M. Barnola, H. Fischer, V. Masson-Delmotte, et al. Stable carbon cycle–climate relationship during the late pleistocene. *Science*, 310(5752):1313–1317, 2005.

C. P. Simmons, J. J. Farrar, N. van Vinh Chau, and B. Wills. Dengue. *New England Journal of Medicine*, 366(15):1423–1432, 2012.

D. Simpson. Zika virus infection in man. *Transactions of the Royal Society of Tropical Medicine and Hygiene*, 58(4):335–338, 1964.

R. K. Singh, K. Dhama, R. Khandia, A. Munjal, K. Karthik, R. Tiwari, S. Chakraborty, Y. S. Malik, and R. Bueno-Marí. Prevention and control strategies to counter zika virus, a special focus on intervention approaches against vector mosquitoes-current updates. *Frontiers in Microbiology*, 9:87, 2018.

D. Smith, J. Dushoff, R. Snow, and S. Hay. The entomological inoculation rate and plasmodium falciparum infection in african children. *Nature*, 438(7067):492–495, 2005.

H. L. Smith. Competing subcommunities of mutualists and a generalized kamke theorem. *SIAM Journal on Applied Mathematics*, 46(5):856–874, 1986.

H. L. Smith. Monotone dynamical systems: an introduction to the theory of competitive and cooperative systems. *Bulletin (New Series) of the American Mathematical Society*, 33:203–209, 1996.

J. D. Smith, A. G. Craig, N. Kriek, D. Hudson-Taylor, S. Kyes, T. Fagen, R. Pinches, D. I. Baruch, C. I. Newbold, and L. H. Miller. Identification of a plasmodium falciparum intercellular adhesion molecule-1 binding domain: a parasite adhesion trait implicated in cerebral malaria. *Proceedings of the National Academy of Sciences*, 97(4):1766–1771, 2000.

T. Smith, N. Maire, K. Dietz, G. F. Killeen, P. Vounatsou, L. Molineaux, and M. Tanner. Relationship between the entomologic inoculation rate and the force of infection for plasmodium falciparum malaria. *The American journal of tropical medicine and hygiene*, 75(2_suppl):11–18, 2006.

T. Solomon, M. Baylis, and D. Brown. Zika virus and neurological disease—approaches to the unknown. *The Lancet Infectious diseases*, 16(4):402–404, 2016.

L. Spence and L. Thomas. Application of haemagglutination and complement-fixation techniques to the identification and serological classification of arthropod-borne viruses. *Transactions of the Royal Society of Tropical Medicine and Hygiene*, 53 (3):248–255, 1959.

N. Stern. Stern review report on the economics of climate change. 2006.

N. Sullivan. Antibody-mediated enhancement of viral disease. *Current topics in microbiology and immunology*, 260:145–169, 2001.

W. Takken, M. Klowden, and G. Chambers. Effect of body size on host seeking and blood meal utilization in anopheles gambiae sensu stricto (diptera: Culicidae): the disadvantage of being small. *Journal of medical entomology*, 35(5):639–645, 1998.

B. Tang, Y. Xiao, and J. Wu. Implication of vaccination against dengue for zika outbreak. *Scientific reports*, 6:35623, 2016.

F. C. Tanser, B. Sharp, and D. Le Sueur. Potential effect of climate change on malaria transmission in africa. *The Lancet*, 362(9398):1792–1798, 2003.

H. R. Thieme. Convergence results and a poincaré-bendixson trichotomy for asymptotically autonomous differential equations. *Journal of mathematical biology*, 30 (7):755–763, 1992.

H. R. Thieme. Persistence under relaxed point-dissipativity (with application to an endemic model). *SIAM Journal on Mathematical Analysis*, 24(2):407–435, 1993.

H. R. Thieme. *Mathematics in population biology*. Princeton University Press, 2003.

D. Tilman. Competition and biodiversity in spatially structured habitats. *Ecology*, 75(1):2–16, 1994.

A. Tran, G. L'Ambert, G. Lacour, R. Benoît, M. Demarchi, M. Cros, P. Cailly, M. Aubry-Kientz, T. Balenghien, and P. Ezanno. A rainfall-and temperature-driven abundance model for aedes albopictus populations. *International journal of environmental research and public health*, 10(5):1698–1719, 2013.

K. A. Tsetsarkin, D. L. Vanlandingham, C. E. McGee, and S. Higgs. A single mutation in chikungunya virus affects vector specificity and epidemic potential. *PLoS pathogens*, 3(12):e201, 2007.

W. Tun-Lin, T. Burkot, and B. Kay. Effects of temperature and larval diet on development rates and survival of the dengue vector aedes aegypti in north queensland, australia. *Medical and veterinary entomology*, 14(1):31–37, 2000.

E. A. Undurraga, F. E. Edillo, J. N. V. Erasmo, M. T. P. Alera, I.-K. Yoon, F. M. Largo, and D. S. Shepard. Disease burden of dengue in the philippines: Adjusting for underreporting by comparing active and passive dengue surveillance in punta princesa, cebu city. *The American journal of tropical medicine and hygiene*, 96(4): 887–898, 2017.

P. van den Driessche and J. Watmough. Reproduction numbers and sub-threshold endemic equilibria for compartmental models of disease transmission. *Mathematical biosciences*, 180(1-2):29–48, 2002.

E. Van Handel. Nutrient accumulation in three mosquitoes during larval development and its effect on young adults. *Journal of the American Mosquito Control Association*, 4(3):374–376, 1988.

K. S. Vannice, A. Durbin, and J. Hombach. Status of vaccine research and development of vaccines for dengue. *Vaccine*, 34(26):2934–2938, 2016.

G. Vogel. The forgotten malaria, 2013.

J. Waldock, N. L. Chandra, J. Lelieveld, Y. Proestos, E. Michael, G. Christophides, and P. E. Parham. The role of environmental variables on aedes albopictus biology and chikungunya epidemiology. *Pathogens and global health*, 107(5):224–241, 2013.

J. Wang, N. H. Ogden, and H. Zhu. The impact of weather conditions on culex pipiens and culex restuans (diptera: Culicidae) abundance: a case study in peel region. *Journal of medical entomology*, 48(2):468–475, 2011.

W. Wang and X.-Q. Zhao. Threshold dynamics for compartmental epidemic models in periodic environments. *Journal of Dynamics and Differential Equations*, 20(3): 699–717, 2008.

R. T. Watson, M. C. Zinyowera, and R. H. Moss. *Climate change 1995. Impacts, adaptations and mitigation of climate change: scientific-technical analyses*. 1996.

J. Westling, C. A. Yowell, P. Majer, J. W. Erickson, J. B. Dame, and B. M. Dunn. Plasmodium falciparum, p. vivax, andp. malariae: A comparison of the active site properties of plasmepsins cloned and expressed from three different species of the malaria parasite. *Experimental parasitology*, 87(3):185–193, 1997.

N. White. Plasmodium knowlesi: the fifth human malaria parasite, 2008.

M. Whitten, S.-H. Shiao, and E. Levashina. Mosquito midguts and malaria: cell biology, compartmentalization and immunology. *Parasite immunology*, 28(4):121–130, 2006.

WHO. Answers on dengue vaccines. 2017., a.

WHO. Zika - epidemiological report. mexico, b.

WHO. Dengue and dengue hemorrhagic fever in the americas: Guidelines for prevention and control. *Pan American Health Organization, Washington, DC, Scientific Publication*, 548, 1994.

WHO. Dengue guidelines for diagnosis, treatment, prevention and control: new edition. 2009.

WHO. *Guidelines for the treatment of malaria*. World Health Organization, 2015.

WHO. *World malaria report 2015*. World Health Organization, 2016.

P. Winch, C. Kendall, and D. Gubler. Effectiveness of community participation in vector-borne disease control. *Health policy and planning*, 7(4):342–351, 1992.

J. Wu, R. Dhingra, M. Gambhir, and J. V. Remais. Sensitivity analysis of infectious disease models: methods, advances and their application. *Journal of The Royal Society Interface*, 10(86):20121018, 2013.

L. Yakob and A. C. Clements. A mathematical model of chikungunya dynamics and control: the major epidemic on réunion island. *PloS one*, 8(3):e57448, 2013.

L. Yakob and T. Walker. Zika virus outbreak in the americas: the need for novel mosquito control methods. *The Lancet Global Health*, 4(3):e148–e149, 2016.

H. Yang, M. Macoris, K. Galvani, M. Andrighetti, and D. Wanderley. Assessing the effects of temperature on the population of aedes aegypti, the vector of dengue. *Epidemiology & Infection*, 137(8):1188–1202, 2009.

H. M. Yang, M. d. L. da Graça Macoris, K. C. Galvani, and M. T. M. Andrighetti. Follow up estimation of aedes aegypti entomological parameters and mathematical modellings. *Biosystems*, 103(3):360–371, 2011.

P. N. Yergolkar, B. V. Tandale, V. A. Arankalle, P. S. Sathe, S. AB, S. S. Gandhe, M. D. Gokhle, G. P. Jacob, S. L. Hundekar, and A. C. Mishra. Chikungunya outbreaks caused by african genotype, india. *Emerging infectious diseases*, 12(10): 1580, 2006.

H. Zeller. Dengue, arbovirus and migrations in the indian ocean. *Bull Soc Pathol Exot*, 91(1):56–60, 1998.

F. Zhang and X.-Q. Zhao. A periodic epidemic model in a patchy environment. *Journal of Mathematical Analysis and Applications*, 325(1):496–516, 2007.

X.-Q. Zhao. Uniform persistence and periodic coexistence states in infinite-dimensional periodic semiflows with applications. *Canad. Appl. Math. Quart*, 3 (4):473–495, 1995.

X.-Q. Zhao. Permanence implies the existence of interior periodic solutions for fdes. *Qualitative theory of Differential Equations and Applications*, 2:125–137, 2008.

X.-Q. Zhao, J. Borwein, and P. Borwein. *Dynamical systems in population biology*. Springer, 2017.

Z. Zhi-Fen, D. Tong-Ren, H. Wen-Zao, and D. Zhen-Xi. *Qualitative theory of differential equations*, volume 101. American Mathematical Soc., 2006.

Chapter A

APPENDIX A

COEFFICIENT OF EQUATIONS (2.4.12) AND (2.4.14)

A.1 COEFFICIENT OF EQUATION (2.4.12)

The coefficients $(b_i, i = 0, 1, \ldots, 7)$ of Equation (2.4.12) in Section 2.4.2 are given by:

$$
\begin{aligned}
b_0 &= \Big(\frac{1}{\mathcal{R}_M} - 1\Big) Q_1 X_6, \\
b_1 &= \bigg[\Big(\frac{1}{\mathcal{R}_M} - 1\Big) Q_1 X_3 + Q_2 X_5 X_6\bigg] \delta_L + 1, \\
b_2 &= \bigg[\Big(\frac{1}{\mathcal{R}_M} - 1\Big) Q_1 X_2 + Q_2 \big(X_5 X_3 + X_4 X_6\big)\bigg] \delta_L^2, \\
b_3 &= \bigg[\Big(\frac{1}{\mathcal{R}_M} - 1\Big) Q_1 + Q_2 \big(X_1 X_6 + X_2 X_4 + X_3 X_4\big)\bigg] \delta_L^3, \\
b_4 &= Q_2 \big(X_1 X_3 + X_2 X_4 + X_5 + X_6\big) \delta_L^4, \\
b_5 &= Q_2 \big(X_1 X_2 + X_3 + X_4\big) \delta_L^5, \\
b_6 &= Q_2 \left(X_1 + X_2\right) \delta_L^6, \\
b_7 &= Q_2 \delta_L^7,
\end{aligned}
\tag{A.1.1}
$$

where,

$$
\begin{aligned}
&Q_1 = \frac{\sigma_E C_P D K_U}{\alpha \tau_W^* \eta_V^* B}, \quad Q_2 = \frac{K_U (C_P D)^2 \sigma_E C_E}{(\alpha \tau_W^* \eta_V^* B)^2 \psi_U}, \quad X_1 = C_1 + C_2 + C_3 + C_4, \\
&X_2 = C_2 + C_3 + C_4 + \xi_1, \quad X_3 = C_2 C_3 + C_2 C_4 + C_3 C_4 + C_3 \xi_1 + C_4 \xi_1 + \xi_1 \sigma_{L_2}, \\
&X_4 = C_1 C_2 + C_1 C_3 + C_1 C_4 + C_2 C_3 + C_2 C_4 + C_3 C_4, \quad X_5 = C_1 C_2 C_3 + C_1 C_2 C_4 \\
&+ C_1 C_3 C_4 + C_2 C_3 C_4, \quad X_6 = C_2 C_3 C_4 + C_3 C_4 \xi_1 + C_4 \xi_1 \sigma_{L_2} + \xi_1 \sigma_{L_2} \sigma_{L_3},
\end{aligned}
$$

A.2 COEFFICIENT OF EQUATION (2.4.14)

$$
\begin{aligned}
A_1 &= D\big(C_1C_2C_3C_4C_E + C_1C_2C_3C_4C_P + C_1C_2C_3C_EC_P + C_1C_2C_4C_EC_P + C_1C_3C_4C_EC_P \\
&\quad + C_2C_3C_4C_EC_P\big) + C\big(C_5C_6 + C_5C_7 + C_6C_7\big) > 0, \\
A_2 &= \sum_{i=1}^{2} C_i \sum_{j=i+1}^{3} C_j \sum_{k=j+1}^{4} C_j \sum_{l=k+1}^{5} C_l \sum_{m=l+1}^{6} C_m \sum_{n=m+1}^{7} C_n \left(C_E + C_P + \sum_{q=n+1}^{7} C_q \right) \\
&\quad + C_EC_P \left(\sum_{i=1}^{3} C_i \sum_{j=i+1}^{4} C_j \sum_{k=j+1}^{5} C_k \sum_{l=k+1}^{6} C_l \sum_{m=l+1}^{7} C_m - \alpha\tau_W^*\eta_V^*\gamma_U \sum_{i}^{3} C_i \sum_{j=i+1}^{4} C_j \right) \\
&\quad - \alpha\tau_W^*\eta_V^*\gamma_U \sum_{i=1}^{2} C_i \sum_{j=i+1}^{3} C_j \sum_{k=j+1}^{4} C_k \left(\sum_{l=k+1}^{4} C_l + C_E + C_P \right) > 0, \\
A_3 &= \sum_{i=1}^{3} C_i \sum_{j=i+1}^{4} C_j \sum_{k=j+1}^{5} C_j \sum_{l=k+1}^{6} C_l \sum_{m=l+1}^{7} C_m \left(C_E + C_P + \sum_{n=m+1}^{7} C_n \right) \\
&\quad + C_EC_P \left(\sum_{i=1}^{4} C_i \sum_{j=i+1}^{5} C_j \sum_{k=j+1}^{6} C_k \sum_{l=k+1}^{7} C_l - \alpha\tau_W^*\eta_V^*\gamma_U \sum_{i}^{4} C_i \right) \\
&\quad - \alpha\tau_W^*\eta_V^*\gamma_U \sum_{i=1}^{3} C_i \sum_{j=i+1}^{4} C_j \left(\sum_{k=j+1}^{4} C_k + C_E + C_P \right) > 0, \\
A_4 &= \sum_{i=1}^{4} C_i \sum_{j=i+1}^{5} C_j \sum_{k=j+1}^{6} C_j \sum_{l=k+1}^{7} C_l \left(C_E + C_P + \sum_{m=l+1}^{7} C_m \right) \\
&\quad + C_EC_P \left(\sum_{i=1}^{5} C_i \sum_{j=i+1}^{6} C_j \sum_{k=j+1}^{7} C_k - \alpha\tau_W^*\eta_V^*\gamma_U \right) \qquad \text{(A.2.1)} \\
&\quad - \alpha\tau_W^*\eta_V^*\gamma_U \sum_{i=1}^{3} C_i \left(\sum_{j=i+1}^{4} C_j + C_E + C_P \right) > 0, \\
A_5 &= \sum_{i=1}^{5} C_i \sum_{j=i+1}^{6} C_j \sum_{k=j+1}^{7} C_j \left(C_E + C_P + \sum_{l=k+1}^{7} C_l \right) + C_EC_P \sum_{i=1}^{6} C_i \sum_{j=i+1}^{7} C_j \\
&\quad - \alpha\tau_W^*\eta_V^*\gamma_U C > 0, \\
A_6 &= \sum_{i=1}^{6} C_i \sum_{j=i+1}^{7} C_j \left(C_E + C_P + \sum_{k=j+1}^{7} C_k \right) + C_EC_P \sum_{i=1}^{7} C_i - \alpha\tau_W^*\eta_V^*\gamma_U > 0, \\
A_7 &= \sum_{i=1}^{7} C_i \left(C_E + C_P + \sum_{j=i+1}^{7} C_j \right) > 0, \\
A_8 &= C_E + C_P + \sum_{i=1}^{7} C_i > 0,
\end{aligned}
$$

where, $C_E = \sigma_E + \mu_E, C_P = \sigma_P + \mu_P, C_i = \sigma_{L_i} + \mu_L$ (for $i = 1, 2, 3, 4$), $C_5 = \eta_V^* + \mu_A, C_6 = \tau_W^* + \mu_A, C_7 = \gamma_U + \mu_A$, $C = C_E C_P \prod_{j=1}^{4} C_j$, $D = C_5 C_6 C_7 - \alpha \tau_W^* \eta_V^* \gamma_U > 0$ and A_i $(i = 1, \ldots, 8)$.

Chapter B

APPENDIX B

B.1 PROOF OF LEMMA 2.5.1

Proof. Model (2.3.1) can be written as

$$\frac{dx}{dt} = \mathcal{F}(x,t) - \mathcal{V}(x,t) = f(t,x)$$

where $x = (E, L_1, L_2, L_3, L_4, P, V, W, U)^T$,

$$\mathcal{F} = \Big(\psi_U\Big(1 - \frac{U}{K_U}\Big)U, 0, 0, 0, 0, 0, 0, 0, 0\Big)^T$$

$$\mathcal{V} = \Big(C_E(t)E, C_1(t)L_1 - \sigma_E(t)E, C_2(t)L_2 - \sigma_{L_1}(t)L_1, C_3(t)L_3 - \sigma_{L_2}(t)L_2, C_4(t)L_4$$
$$- \sigma_{L_3}(t)L_3, C_P(t)L_P - \sigma_{L_4}(t)L_4, C_5(t) - \sigma_P(t)P - \gamma_U U, C_6(t) - \eta_V^*, C_7(t) - \alpha\tau_W^*\Big)^T.$$

The function $\mathcal{V}$ can further be expressed as $\mathcal{V} = \mathcal{V}^- - \mathcal{V}^+$ where

$$\mathcal{V}^+ = \Big(0, \sigma_E(t)E, \sigma_{L_1}(t)L_1, \sigma_{L_2}(t)L_2, \sigma_{L_3}(t)L_3, \sigma_{L_4}(t)L_4, \sigma_P(t)P + \gamma_U U, \eta^* V, \alpha\tau^* W\Big)^T,$$

$$\mathcal{V}^- = \Big(C_E(t)E, C_1(t)L_1, C_2(t)L_2, C_3(t)L_3, C_4(t)L_4, C_P(t)L_P, C_5(t), C_6(t), C_7(t)\Big)^T.$$

The functions $\mathcal{F}$, $\mathcal{V}^+$, and $\mathcal{V}^-$ satisfy the following:

(A1) For each $1 \leq i \leq 9$, the functions $\mathcal{F}_i(t,x)$, $\mathcal{V}_i^+(t,x)$, and $\mathcal{V}_i^-(t,x)$ are non-negative, continuous on $\mathbb{R} \times \mathbb{R}_+^9$ and continuously differential with respect to x.

(A2) Since some of the model parameters are ω-periodic functions, there exists a real number $\omega > 0$, such that $\mathcal{F}_i(t,x)$, $\mathcal{V}_i^+(t,x)$, and $\mathcal{V}_i^-(t,x)$ are ω-periodic in t.

(A3) If $x_i = 0$, then clearly, $\mathcal{V}^-(t,x) = 0$.

(A4) $\mathcal{F}_i = 0$ for $2 \leq i < 9$.

(A5) If $x_i = 0\ \forall i$, $\mathcal{F}_i(x) = \mathcal{V}_i^+(x) = 0$.

(A6) Since the trivial solution for the model is given by $x^0(t) = (0,0,0,0,0,0,0,0,0)$, then for

$$M(t) = \Big(\frac{\partial f_i(t, x^0(t))}{\partial x_j}\Big)_{1 \leq i,j \leq 9},$$

$\rho(\Phi_M(\omega)) = 0 < 1$, where $\Phi_M(\omega)$ is the monodromy matrix of the linear ω-periodic system $\dfrac{dz}{dt} = M(t)z$.

(A7) Similarly, for

$$V(t) = \Big(\frac{\partial \mathcal{V}_i(t, x^0(t))}{\partial x_j}\Big)_{1 \leq i,j \leq 9},$$

$\rho(\Phi_{-V}(\omega)) = 0 < 1$.

□

Chapter C

APPENDIX C

C.1 PROOF OF THEOREM 3.4.1

Proof. Let $\mathcal{R}_{MP} \leq 1$. Consider, first of all, the mosquito-only system of the model (3.4.1):

$$\begin{aligned}
\frac{dE}{dt} &= \psi_E \varphi_Z \left(1 - \frac{E}{K_E}\right)_+ (S_Z + E_Z + I_Z) - (\sigma_E + \eta_E + \mu_E)E, \\
\frac{dL_1}{dt} &= \sigma_E E - (\sigma_{L_1} + \eta_L + k_L L + \mu_L)L_1, \\
\frac{dL_j}{dt} &= \sigma_{L_{(j-1)}} L_{j-1} - (\sigma_{Lj} + \eta_L + k_L L + \mu_L)L_j,\ j = 2, 3, 4, \\
\frac{dP}{dt} &= \sigma_{L_4} L_4 - (\sigma_P + \eta_P + \mu_P)P, \\
\frac{dS_X}{dt} &= f\sigma_P P + \varphi_Z S_Z - (b_H p_H + \eta_M + \mu_M)S_X, \\
\frac{dE_X}{dt} &= \varphi_Z E_Z - (b_H p_H + \kappa_M + \eta_M + \mu_M)E_X, \\
\frac{dI_X}{dt} &= \varphi_Z I_Z + \kappa_M E_X - (b_H p_H + \eta_M + \mu_M)I_X, \\
\frac{dS_Y}{dt} &= b_H p_H (1 - \beta_V)\mathcal{G}_H S_X + b_H p_H (1 - \mathcal{G}_H)S_X - (\theta_Y + \eta_M + \mu_M)S_Y, \\
\frac{dE_Y}{dt} &= b_H p_H \beta_V \mathcal{G}_H S_X + b_H p_H E_X - (\theta_Y + \kappa_M + \eta_M + \mu_M)E_Y, \\
\frac{dI_Y}{dt} &= \kappa_M E_Y + b_H p_H I_X - (\theta_Y + \eta_M + \mu_M)I_Y, \\
\frac{dS_Z}{dt} &= \theta_Y S_Y - (\varphi_Z + \eta_M + \mu_M)S_Z, \\
\frac{dE_Z}{dt} &= \theta_Y E_Y - (\varphi_Z + \kappa_M + \eta_M + \mu_M)E_Z, \\
\frac{dI_Z}{dt} &= \theta_Y I_Y + \kappa_M E_Z - (\varphi_Z + \eta_M + \mu_M)I_Z,
\end{aligned} \tag{C.1.1}$$

The system (C.1.1) has a unique trivial equilibrium (whenever $\mathcal{R}_{MP} \leq 1$), given by

$$\mathcal{T}_{01} = \big(0, 0, 0, 0, 0, 0, 0, 0, 0, 0, 0, 0, 0, 0, 0\big), \tag{C.1.2}$$

in the invariant region

$$\begin{aligned}
\Omega_1 = \big\{\big(E, L_1, L_2, L_3, L_4, P, S_X, E_X, I_X, S_Y, E_Y, I_Y, S_Z, E_Z, I_Z\big)(t) \in \mathbb{R}_+^{15} : 0 \leq E(t), \\
0 \leq L_j(t)\,(j = 1, 2, 3, 4), 0 \leq P(t), 0 \leq S_X(t), 0 \leq E_X(t), 0 \leq I_X(t), 0 \leq S_Y(t), \\
0 \leq E_Y(t), 0 \leq I_Y(t), 0 \leq S_Z(t), 0 \leq E_Z(t), 0 \leq I_Z(t)\big\},
\end{aligned}$$

Further, consider the following Lyapunov function for the system (C.1.1):

$$\begin{aligned}
\mathcal{K}_1 = a_0\Big[a_1 E + a_2 L_1 + a_3 L_2 + a_4 L_3 + a_5 L_4\Big] + C_E \prod_{j=1}^{4} C_{Lj}\Big[a_6 P + C_P \theta_Y b_H p_H (S_X \\
+ E_X + I_X) + C_P C_X \theta_Y (S_Y + E_Y + I_Y) + C_P C_X C_Y (S_Z + E_Z + I_Z)\Big].
\end{aligned}$$

where

$$a_0 = \theta_Y b_H p_H \sigma_{L4} f \sigma_P, a_1 = \sigma_E \sigma_{L1} \sigma_{L_2} \sigma_{L3}, a_2 = C_E \sigma_{L1} \sigma_{L_2} \sigma_{L3},$$
$$a_3 = C_{L1} C_E \sigma_{L2} \sigma_{L3}, a_4 = C_{L1} C_{L2} C_E \sigma_{L_3}, a_5 = C_{L1} C_{L2} C_{L3} C_E,$$
$$a_6 = f \sigma_P \theta_Y b_H p_H.$$

The Lyapunov derivative is given by (where a dot represents differentiation with respect to time t)

$$\begin{aligned}
\dot{\mathcal{K}}_1 =& a_0 \Big[a_1 \dot{E} + a_2 \dot{L}_1 + a_3 \dot{L}_2 + a_4 \dot{L}_3 + a_5 \dot{L}_4 \Big] + C_E \prod_{j=1}^{4} C_{Lj} \Big[a_6 \dot{P} + C_P \theta_Y b_H p_H (\dot{S}_X \\
&+ \dot{E}_X + \dot{I}_X) + C_P C_X \theta_Y (\dot{S}_Y + \dot{E}_Y + \dot{I}_Y) + C_P C_X C_Y (\dot{S}_Z + \dot{E}_Z + \dot{I}_Z) \Big], \\
=& a_0 \prod_{j=1}^{4} \sigma_{Lj} \left[\psi_E \varphi_Z \left(1 - \frac{E}{K_E} \right) (S_Z + E_Z + I_Z) \right] - C_E C_P \mathcal{D}_1 \prod_{j=1}^{4} C_{Lj} (S_Z + E_Z + I_Z) \\
&- k_L L S, \\
=& \left[C_E C_P \mathcal{D}_1 \prod_{j=1}^{4} C_{Lj} (\mathcal{R}_{MP} - 1) - \mathcal{D}_2 \frac{E}{K_E} \right] (S_Z + E_Z + I_Z) - k_L L S,
\end{aligned}$$

where $C_E = \sigma_E + \eta_E + \mu_L$, $C_{Lj} = \sigma_{Lj} + \eta_L + \mu_L \, (j = 1, 2, 3, 4)$, $C_P = \sigma_P + \eta_P + \mu_P$, $C_X = b_H p_H + \eta_M + \mu_M$, $C_Y = \theta_Y + \eta_M + \mu_M$, $C_Z = \varphi_Z + \eta_M + \mu_M$, $\mathcal{D}_1 = C_X C_Y C_Z - \theta_Y b_H p_H \varphi_Z = \big(\eta_M + \mu_M\big) \big[C_Z (C_X + \theta_Y) + b_H p_H \theta_Y \big] > 0$ and $\mathcal{D}_2 = \theta_Y b_H p_H f \sigma_E \sigma_P \prod_{j=1}^{4} \sigma_{Lj} \psi_E \varphi_Z$ and $S = a_0 \big[a_2 L_1 + a_3 L_2 + a_4 L_3 + a_5 L_4 \big]$.

Thus, it follows, for $\mathcal{R}_{MP} \leq 1$ in Ω_1, that the Lyapunov derivative $\dot{\mathcal{K}}_1 \leq 0$. Furthermore, it follows from the Theorem 6.4 in LaSalle (1976) (LaSalle's Invariant Principle) that the maximal invariant set contained in

$$\Big\{ \big(E, L_1, L_2, L_3, L_4, P, S_X, E_X, I_X, S_Y, E_Y, I_Y, S_Z, E_Z, I_Z \big) \in \Omega_1 : \dot{\mathcal{K}}_1 = 0 \Big\}$$

is the singleton $\{\mathcal{T}_{01}\}$ (as shown in proof of Theorem 2.4.2). Hence, the unique trivial equilibrium ($\mathcal{T}_{01}$) of the system (C.1.1) is GAS in Ω_1 whenever $\mathcal{R}_{MP} \leq 1$. Thus, for $\mathcal{R}_{MP} \leq 1$,

$$\big(E, L_1, L_2, L_3, L_4, P, S_X, E_X, I_X, S_Y, E_Y, I_Y, S_Z, E_Z, I_Z \big)(t) \to (0, 0, \ldots, 0), \text{ as } t \to \infty. \tag{C.1.3}$$

Since the model (3.4.1) is Type K Smith (1986), it follows, by substituting (C.1.3) into (3.4.1), that

$$\big(S_H, W_H, E_{HN}, E_{HR}, I_H, A_H, R_H \big)(t) \to \left(\frac{\Pi_H}{\mu_H}, 0, 0, 0, 0, 0, 0 \right), \text{ as } t \to \infty. \tag{C.1.4}$$

Thus, by combining (C.1.3) and (C.1.4), it follows that the TDFE ($\mathcal{T}_0$) of the model (3.4.1) is GAS in Ω whenever $\mathcal{R}_{MP} \leq 1$. □

Chapter D

APPENDIX D

D.1 DERIVATION OF $\mathcal{R}_{V1H}, \mathcal{R}_{V2H}$ AND $\mathcal{R}_{V3H}$ IN SECTION 3.4.2

Consider the expression for $\mathcal{R}_{VH}$ given by Equation (3.4.5),

$$\mathcal{R}_{VH} = b_H\beta_H\frac{S_H^{\diamond}}{N_H^*}\frac{\kappa_M\varphi_Z\theta_Y(C_YC_Z + C_Yg_X + g_Xg_Z)}{(C_XC_YC_Z - b_Hp_H\varphi_Z\theta_Y)(g_Xg_Yg_Z - b_Hp_H\varphi_Z\theta_Y)},$$

$$= b_H\beta_H\frac{S_H^{\diamond}}{N_H^*}\kappa_M\varphi_Z\theta_Y \times \frac{C_YC_Z + C_Yg_X + g_Xg_Z}{C_XC_YC_Zg_Xg_Yg_Z} \times \left[1 - \frac{b_Hp_H\varphi_Z\theta_Y}{C_XC_YC_Z}\right]^{-1}$$
$$\times \left[1 - \frac{b_Hp_H\varphi_Z\theta_Y}{g_Xg_Yg_Z}\right]^{-1},$$

$$= b_H\beta_H\frac{S_H^{\diamond}}{N_H^*}\frac{1}{C_X}\left[\frac{\kappa_M\varphi_Z\theta_Y}{g_Xg_Yg_Z} + \frac{\kappa_M\varphi_Z\theta_Y}{C_Zg_Yg_Z} + \frac{\kappa_M\varphi_Z\theta_Y}{C_YC_Zg_Y}\right]\sum_{j=0}^{n}\left(\frac{b_Hp_H}{g_X}\frac{\theta_Y}{g_Y}\frac{\varphi_Z}{g_Z}\right)^j$$
$$\sum_{k=0}^{m}\left(\frac{b_Hp_H}{C_X}\frac{\theta_Y}{C_Y}\frac{\varphi_Z}{C_Z}\right)^k,$$

where $n, m \to \infty$ It can further be expressed as

$$\mathcal{R}_{VH} = b_H\beta_H\frac{S_H^{\diamond}}{N_H^*}\frac{1}{C_X}\big(\mathcal{R}_{V1H} + \mathcal{R}_{V2H} + \mathcal{R}_{V3H}\big),$$

where

$$\mathcal{R}_{V1H} = \frac{\theta_Y}{g_Y}\frac{\varphi_Z}{g_Z}\frac{\kappa_M}{g_X}\sum_{j=0}^{n}\left(\frac{b_Hp_H}{g_X}\frac{\theta_Y}{g_Y}\frac{\varphi_Z}{g_Z}\right)^j\sum_{k=0}^{m}\left(\frac{b_Hp_H}{C_X}\frac{\theta_Y}{C_Y}\frac{\varphi_Z}{C_Z}\right)^k,$$
$$\mathcal{R}_{V2H} = \frac{\theta_Y}{g_Y}\frac{\kappa_M}{g_Z}\frac{\varphi_Z}{C_Z}\sum_{j=0}^{n}\left(\frac{b_Hp_H}{g_X}\frac{\theta_Y}{g_Y}\frac{\varphi_Z}{g_Z}\right)^j\sum_{k=0}^{m}\left(\frac{b_Hp_H}{C_X}\frac{\theta_Y}{C_Y}\frac{\varphi_Z}{C_Z}\right)^k,$$
$$\mathcal{R}_{V3H} = \frac{\kappa_M}{g_Y}\frac{\theta_Y}{C_Y}\frac{\varphi_Z}{C_Z}\sum_{j=0}^{n}\left(\frac{b_Hp_H}{g_X}\frac{\theta_Y}{g_Y}\frac{\varphi_Z}{g_Z}\right)^j\sum_{k=0}^{m}\left(\frac{b_Hp_H}{C_X}\frac{\theta_Y}{C_Y}\frac{\varphi_Z}{C_Z}\right)^k.$$

Chapter E

APPENDIX E

E.1 REDUCED MODELS

E.1.1 GONOTROPHIC CYCLE OMITTED

Adult female model equations without explicit modeling of the gonotrophic cycle.

$$\begin{aligned}
\frac{dS_X}{dt} &= f\sigma_P P - \big[\Gamma p_H \beta_V \mathcal{G}_H + \eta_M + \mu_M(t)\big] S_X, \\
\frac{dE_X}{dt} &= \Gamma p_H \beta_V \mathcal{G}_H S_X - \big[\kappa_M(t) + \eta_M + \mu_M(t)\big] E_X, \\
\frac{dI_X}{dt} &= \kappa_M(t) E_X - \big[\eta_M + \mu_M(t)\big] I_X,
\end{aligned} \tag{E.1.1}$$

where

$$\Gamma = \left(\frac{1}{b_H} + \frac{1}{\varphi_Z} + \frac{1}{\theta_Y}\right)^{-1}.$$

The egg production term in the resulting model is given by

$$\psi_E \Gamma \left(1 - \frac{E}{K_E}\right)(S_X + E_X + I_X),$$

and the force of infection is given by

$$\lambda_H = \Gamma \beta_H \frac{I_X}{N_H}.$$

E.1.2 SPOROGONIC CYCLE OMITTED

Adult female compartments in the absence of the *Plasmodium's* sporogonic cycle

$$\begin{aligned}
\frac{dS_X}{dt} &= f\sigma_P P + \varphi_Z S_Z - \big[b_H p_H + \eta_M + \mu_M(t)\big] S_X, \\
\frac{dI_X}{dt} &= \varphi_Z I_Z - \big[b_H p_H + \eta_M + \mu_M(t)\big] I_X, \\
\frac{dS_Y}{dt} &= b_H p_H (1 - \beta_V) \mathcal{G}_H S_X + b_H p_H (1 - \mathcal{G}_H) S_X - \big[\theta_Y(t) + \eta_M + \mu_M(t)\big] S_Y, \\
\frac{dI_Y}{dt} &= b_H p_H \beta_V \mathcal{G}_H S_X + b_H p_H I_X - \big[\theta_Y(t) + \eta_M + \mu_M(t)\big] I_Y, \\
\frac{dS_Z}{dt} &= \theta_Y(t) S_Y - \big[\varphi_Z + \eta_M + \mu_M(t)\big] S_Z, \\
\frac{dI_Z}{dt} &= \theta_Y(t) I_Y - \big[\varphi_Z + \eta_M + \mu_M(t)\big] I_Z,
\end{aligned} \tag{E.1.2}$$